Epigenetic Regulation of Hematopoiesis in Zebrafish

Dissertation Advisor: Leonard I. Zon Hsuan-Ting Huang

Epigenetic Regulation of Hematopoiesis in Zebrafish

The initiation of the hematopoietic program is orchestrated by key transcription factors that recruit chromatin regulators in order to activate or inhibit blood target gene expression. To generate a complete compendium of chromatin factors that establish the genetic code during developmental hematopoiesis, we conducted a large-scale reverse genetic screen targeting 425 chromatin factors in zebrafish and identified over 30 novel chromatin regulators that function at distinct steps of embryonic hematopoiesis.

In vertebrates, developmental hematopoiesis occurs in two waves. During the first and primitive wave, mainly erythrocytes are produced, and we identified at least 15 chromatin factors that decrease or increase formation of *scl*$^{+}$, *gata1*$^{+}$, and β-*globin e3*$^{+}$ erythroid progenitors. In the definitive wave, HSCs capable of self-renewal and differentiation into multiple lineages are induced, and we identified at least 18 chromatin factors that decrease or increase the formation of *c-myb*$^{+}$ and *runx1*$^{+}$ stem and progenitor cells in the aorta gonad mesonephros (AGM) region, without disruption of vascular development. The

majority of the chromatin factors identified from the screen are involved in histone acetylation, histone methylation, and nucleosome remodeling, the same modifications that are hypothesized to have the most functional impact on the transcriptional status of a gene. Moreover, these factors can be mapped to subunits of chromatin complexes that modify these marks, such as HBO/HAT, HDAC/NuRD, SET1A/MLL, ISWI, and SWI/SNF.

One of the strongest phenotypes identified from the screen came from knockdown of chromodomain helicase DNA binding domain 7 (*chd7*). Morpholino knockdown of *chd7* resulted in increased primitive and definitive blood production from the induction of stem and progenitor cells to the differentiation of myeloid and erythroid lineages. This expansion of the blood lineage is cell autonomous as determined by blastula transplantation experiments.

Though chromatin factors are believed to function broadly and are often expressed ubiquitously, the combined results of the screen and *chd7* analysis show that individual factors have very tissue specific functions. These studies implicate chromatin factors as playing a major role in establishing the programs of gene expression for self-renewal and differentiation of hematopoietic cells.

Contents

Acknowledgments

This dissertation would not have been possible without the contributions of many people over the past six years. First and foremost, I would like to thank my advisor, Len, for all of his support and mentoring in the past six years. I still find it hard to believe that Len had let me, a brand new graduate student, take on such a large and potentially very expensive project. My favorite part about Len is that he is always optimistic and encouraging, always willing to try something new. I admire how he works hard to make sure all of us in the lab are happy and successful. I feel very fortunate to have met Len, as I have gained many different kinds of experiences during my time here in the lab, and I can only hope that some day, I can be as good of a PI as he is.

I would like to thank the members of my Dissertation Advisory Committee, Alan Cantor, Fred Winston, Alan Davidson, and Stuart Orkin. They have been very encouraging througout these years, and I really did enjoy all of my DAC meetings. I'm very happy that Alan C. was my Chair. I can feel that he is looking out for me and wants me to be successful. He was always very organized and took very good notes for the DAC reports. Fred is such a nice person, and I felt safe knowing that Fred, with all of his experiences in BBS, would know if any part of the project was going to be too much work me. I really appreciated Alan

D. for all of his insightful comments. I owe him a big extra thanks because even after moving to New Zealand, he continued to attend my DAC meetings via Skype. I have to thank Stu for taking the extra time to fill in for Alan D. after he left. I would also like to thank the members of my Dissertation Exam Committee, Alan Cantor, Fernando Camargo, Stirling Churchman, and Nancy Speck for taking the time to read my dissertation and being part of the exam.

There are so many people in the lab that I would like to thank. First, I need to thank all the members of Team Chromo (= chromatin morpholino). The chromodomains also happen to be the first chromatin factor family that we screened. Yi Zhou, Peter Song, Tony Dibiase, and more recently Tom Ward have provided extensive bioinformatic support to all of my projects, especially for the screen. Yi was always ready to share his advice everytime I needed his help. I have to thank Katie Kathrein for all of her support in the screen project. It is nice to have someone to bounce ideas off of, and she was always very nice, generous, and patient when working with me. I really do appreciate it. The screen project would have been impossible without the help of Abby Barton, Zach Gitlin, and Yue-Hua Huang, who never got tired of doing the same thing every week, injecting, staging, and scoring embryos. Yue-Hua was the most meticulous microinjector I have ever known. Abby goes above and beyond her duties in the

lab is always looking after me.

I would like to thank my past and present baymates, Dave Langenau, Yariv Houvras, Elizabeth Paik, Pulin Li, and Tony Xu. Dave and Yariv are really fun to interact with, and they're both brilliant scientists that I look up to. They will always make time if I ever needed their help, which I did. Elizabeth, Pulin, and Tony are like family to me. We've done so many things together inside and out of the lab. Having Elizabeth and Pulin in the bay means that Tony and I will never miss a deadline or forget about some important event. Tony's enthusiasm is very contagious. Elizabeth, Pulin, and I get distracted easily with anything that has to do with shopping or fashion. One of my favorite things is when we all laugh out loud at the same time. They have made my time here in the lab so much more special. I also need to thank the other grad students Xiuning Le, Narie Storer, Colleen Albacker, Alison Taylor, Jared Ganis, Ellen Durand, Justin Tang, and Kristin Rose, who are wonderful friends and make the graduate student bunch in the Zon lab look cool, especially during the annual departmental Halloween competition.

I hope I have become a better mentor thanks to all the summer students who have worked with me. Hudson Duan was my first summer student, and even though he always had to leave at the end of the day to play basketball, he still

managed to get some pretty cool in situs done. Then Zach Gitlin and Julia Tchen came the next summer. Zach did an excellent job characterizing one of the screen hits that summer. Julia was always paying attention and eager to learn. I was very impressed with her maturity level for someone her age. I guess I didn't give Zach enough work to do because he came back again the following summer and even ended up getting a position in the lab to help us finish the screen. I think we're even. I had gotten used to having a student around, so I decided to volunteer to take a summer student again, except I got two instead of one. Joe Festa worked hard during the time he was here and helped me characterize some mutant fish. Emmanuel Mendoza came throught the HHMI program, so needless to say, he was a hard working and talented student. We managed to finish a chromatin overexpression screen last summer.

Then there are all the talented post-docs in the lab who were always willing to share their experiences with me and give me feedback when I needed it. I learned the basics from Xiaoying Bai, microinjections and *in situs*. Craig Ceol taught me blastula transplantation. Michelle Lin, Eirini Trompouki, Teresa Bowman, and Owen Tamplin helped me with all things protein, tissue culture, mouse work, and confocal imaging, respectively. Dave showed me how to work with zinc finger nucleases. I owe a big thank you to Teresa, Chuck Kaufman, and

Marlies Rossman for helping me prepare my thesis in such a short amount of time, as well as Vera Binder and Pulin. Their encouragement really kept me going in the last few weeks of writing.

I would also like to thank my classmates for their support and friendship throughout the past couple of years of grad school, especially Melissa Wu, Ariya Lapan, Xun Wang, Cynthia Hsu, Angela Chen, and Nihal Terzi. I never thought that I would have the chance to meet new friends who liked anime as much as I do after leaving college, and I love how we all make the effort to get together once a month for afternoon tea or for a nice homemade dinner. It's so much fun to talk to them about science, grad school, life, and seeing how we've influenced each other to try new things. I will miss them so much if I leave Boston.

Finally, I have to thank my parents and my sister for their love and support throughout my graduate career. My parents never asked me to do anything except to be happy and call home once in a while to let them know that I am doing well. One of the highlights of my time in grad school is that I got to travel a lot and visit new places because we were all living in different countries. I cannot wait to go home again.

This dissertation is dedicated to

my mom, Shu-Zong Wang, and

my dad, Kwang-Chun Huang,

for their constant

love and support.

Chapter 1

Introduction

The development of multicellular organisms from a single cell is a highly regulated process involving the formation of tissue specific stem cells that are capable of self-renewal and progressive differentiation into the various specialized cell types of an organ. These principles are illustrated in the blood system, where self-renewing hematopoietic stem cells (HSCs) are needed to maintain a constant pool of progenitors committed to the various blood lineages in order to replenish the mature blood cells that turn over. Because the various cell types at different stages of blood differentiation have been largely elucidated, hematopoiesis has been widely used as a model for the study of stem cell biology and the regulation of lineage commitment and differentiation. One of the major questions in developmental biology is the molecular mechanism that drives this process.

Hematopoietic development

The ontogeny of hematopoietic cells is a complex process that is spatiotemporally regulated. Whereas the specific anatomical sites in which hematopoiesis occurs varies between species, it can be divided into two major waves. The first and primitive wave produces mainly a transient population of erythroid and myeloid cells. The definitive wave generates *bona fide* HSCs that

will sustain hematopoiesis throughout the lifetime of the organism. Understanding how these processes occur provides insights into the mechanisms of how tissues develop and function.

Primitive hematopoiesis

The primitive wave is characterized by the production of hematopoietic cells with limited lineage potential. In mice, the first blood cells in the early embryo arise in the yolk sac at embryonic day E7.5 (Sabin 1920). These cells originate from hemangioblasts in the primitive streak, which migrate into the yolk sac and differentiate into committed endothelial and hematopoietic progenitors (Choi et al 1998, Fehling et al 2003, Huber et al 2004, Ueno et al 2006). Primitive macrophages and other myeloid progenitors also arise in the yolk sac at E8.25 (Palis et al 1999, Ferkowicz et al 2003). Primitive blood formation is important for generating erythroid cells that deliver oxygen to the embryo proper.

In zebrafish, primitive hematopoiesis occurs intraembryonically from the lateral mesoderm. Erythroid progenitors arise from the posterior lateral mesoderm whereas myeloid progenitors arise in the anterior lateral mesoderm (Bennett et al. 2001, Detrich et al. 1995, Herbomel et al. 1999). The lateral

mesoderm converges in the midline of the trunk prior to the onset of the heartbeat at 24 hours post-fertilization (hpf), forming the intermediate cell mass (ICM) region. There, the primitive red cells continue to mature as they gradually enter the cirulation.

Through the characterization of various zebrafish mutants, several molecular pathways that regulate the production of primitive blood have been identified. First, proper patterning and specification of the ventral mesoderm is required to induce primitive blood formation. This process is initiated during gastrulation with cells in the marginal zone that can give rise to a variety of tissues, including notochord, somites, pronephros, and blood. Several lines of evidence point to bone morphogenic proteins (BMPs) for instructing ventral mesoderm, among others. Zebrafish mutants for genes in the BMP pathway become dorsalized while overexpression of *bmp4* ventralizes the embryo, resulting in decreased or increased expression domains of hematopoietic markers, respectively (Amatruda and Zon 1999, Hammerschmidt and Mullins 2002, Neave et al 1997). In addition, *spadetail* (*spt*) mutants, which are defective in the convergence of paraxial mesoderm, also lose *gata1*$^{+}$ erythroid cells.

The primitive blood cells are then believed to arise from the hemangioblast, a common precursor for blood and endothelial cells. This

hypothesis is supported by the zebrafish *cloche* (*clo*) mutant, which lacks all blood and endothelial lineages (Stainier et al 1995). The transcription factor *scl* is believed to regulate these cells as overexpression of *scl* resulted in increased vascular *flk* and erythroid *gata1* expression and can rescue their expression in *clo* mutants (Gering et al 1998, Liao et al 1998). The earliest hematopoietic markers expressed are *gata2* and *scl* in the bilateral stripes of the lateral plate mesoderm starting 11 hpf (Crosier et al 2002). Induction of *gata1* at 14 hpf in the posterior lateral mesoderm marks the commitment of these cells to the erythroid fate, and by 16 hpf, expression of embryonic globin genes such as *β-globin e3* signals the beginning of the differentiation of these erythroid progenitors down the red cell lineage. Similarly, *pu.1*$^{+}$ macrophages arise from the anterior lateral mesoderm that also expresses *scl* (Lieschke et al 2002). The entry of primitive blood into circulation completes the first wave of hematopoiesis.

During the transition from primitive to definitive hematopoiesis, additional sites of blood formation can be found in the allantois, placenta, and the prospective aorta-gonad-mesonephros (AGM) region in mice by E9.0 (Corbel et al 2007, Cumano et al 1996, Zeigler et al 2006). These blood cells mainly have erythroid-myeloid potential, but under the right conditions, lymphoid potential

could be elicited from the prospective AGM region with ability for multilineage reconstitution in adult mice, albeit a low levels (Cumano et al 1996, Cumano et al 2001). Additionally, populations of c-Kit$^+$CD34$^+$ cells from neonatal yolk sac and AGM were able to show multilineage engraftment of neonatal recipient mice but not adult mice (Yoder et al 1997). In zebrafish, a distinct population of erythromyeloid progenitor cells emerges from the posterior blood island (PBI) of 24 hpf embryos (Bertrand et al 2007). Overall, primitive hematopoiesis is largely restricted to myeloid and erythroid lineages, with certain populations exhibiting more definitive phenotypes as the embryo matures.

Definitive hematopoiesis

The definitive wave is initiated soon after the onset of circulation. It is defined by the emergence of HSCs capable of long-term lineage reconstitution and self-renewal. HSCs are believed to derive from the endothelium, specifically from the ventral wall of the aorta. Observations in various species show hematopoietic clusters adhering to the endothelium of the dorsal aorta, as well as vitelline and umbilical arteries (Jaffredo et al 2005). Hematopoietic cells from the AGM were shown to be functional HSCs by their ability to reconstitute the adult hematopoietic system of irradiated mice (Medvinsky and Dzierzak 1996,

Muller et al 1994). Tracing experiments also provide evidence for an endothelial origin of HSCs (Zovein et al 2008). These observations do not exclude the possibility that HSCs arise in the sub-aortic mesenchyme and migrate through the endothelial layer to form the hematopoietic clusters as transplantable cells can be found in this region (Bertrand et al 2005). Recently, imaging of zebrafish and mouse AGM confirmed the budding of hematopoietic cells from the aortic endothelium (Bertrand et al 2010, Boisset et al 2010, Kissa and Herbomel 2010). In zebrafish, these cells bud off, migrate towards the vein, and enter the circulation to seed additional hematopoietic sites.

Several transcription factors regulating HSC formation, self-renewal, and differentiation have been found. In addition to primitive blood, SCL is also required for definitive blood formation. Knockout Scl mice demonstrated complete loss of stem and progenitor cells as well as downstream blood lineages (Robb et al 1995, Shivdasani et al 1995). Expression of CD41, one of the markers expressed in HSCs, is also lost in $Scl^{-/-}$ mice (Mikkola et al 2002). Runx1 is required for the induction of HSCs from the AGM and differentiation of adult megakaryocytic and lymphoid populations (Li et al 2006, Okuda et al 1996). Although the endothelium is not affected in $Runx1^{-/-}$ embryos, RUNX1 is required for the emergence of HSCs from the hemogenic endothelium (Kissa et al 2010,

Lancrin et al 2009, North et al 1999, Yokomizo et al 2001). C-myb is important for HSC self-renewal and multilineage differentiation (Lieu and Reddy 2009, Mucenski et al 1991). Several other factors such as Bmi1, cMyc, Gfi1, Gata2, Mll, Evi1, and Prdm16 also regulate HSC self-renewal and function (Aguilo et al 2011, Chuikov et al 2010, Hock et al 2004, Laurenti et al 2008, Lessard and Sauvageau 2003, Macmahon et al 2007, Park et al 2003, Rodrigues et al 2005, Yuasa et al 2005).

Studies in zebrafish have elucidated several pathways important for HSC induction in the AGM. At 36 hpf, *c-myb* expression is lost in both *clo* and *spt* mutants (Thompson et al 1998). Disruption of signaling pathways that affect vascular development also affected the formation of HSCs. The *plcg1* mutant in the vascular endothelial growth factors (VEGF) pathway lose *ephrinB2* arterial gene expression and disrupt intersomitic vessel formation, which coincides with the loss of *runx1*$^{+}$ cells in the AGM (Gering and Patient 2005, Lawson et al 2003). Overexpression of *vegf* could rescue *c-myb*$^{+}$ cells and improves to a certain extent the defects in *flk*$^{+}$ vascular cells of *spt* mutants (Burns et al 2009). These studies suggest a hierarchical pathway in which proper formation of the vessel followed by arterial fate specification is required for HSCs to emerge from the dorsal aorta.

Definitive hematopoietic stem and progenitor cells (HSPCs) in the AGM can be identified with expression of *runx1*, *c-myb, ikaros*, *lmo2*, *scl,* and *cd41* along the ventral wall of the dorsal aorta (Bertrand et al 2007, Liao et al. 1998; Thompson et al. 1998; Willett et al. 2001; Kalev-Zylinska et al. 2002; Kissa et al. 2008; Bertrand et al. 2008). *runx1* overexpression causes HSC expansion in embryos while morpholino knockdown causes defects in definitive hematopoiesis and vasculoangiogenesis (Burns et al. 2005). Furthermore, *c-myb* and *cd41* expression is reduced in *runx1* morphants (Kalev-Zylinska et al. 2002, Kissa et al 2008). Although *c-myb* is also expressed in primitive erythroid cells, it is not required for their development (Thompson et al. 1998).

After exiting the AGM, the HSCs proliferate and undergo further maturation at different anatomical sites until the adult marrow niche is established. In mice, the HSCs are believed to colonize the fetal liver first, followed by the spleen and thymus until finally they reach the bone marrow (Dzierzack and Speck 2008, Morrison et al 1995, Sánchez et al 1996, Yokota et al 2006). In zebrafish, the AGM HSCs migrate to the caudal hematopoietic tissue (CHT) and then to the kidney marrow and thymus after between 3 to 5 dpf (Murayama et al. 2006; Jin et al. 2007; Kissa et al. 2008). Additional sites

harboring HSCs in mice include the umbilical artery and placenta (de Bruijn et al 2000, Geckas et al 2005, Ottersbach et al 2005).

Expression of lineage specific transcription factors direct the differentiation of HSCs into each of the specific blood lineages. GATA1 is required for erythroid development as Gata1 deficient cells never gave rise to red cells and hemizygous knockout mice die during mid-gestation from severe anemia (Fujiwara et al 1996, Pevny et al 1991). Ikaros is important for differentiation of HSCs down the lymphoid lineage (Yoshida et al 2006). Several transcription factors are important for myeloid lineage specification. PU.1 is a regulator of both multipotent progenitors and myeloid lineages. Knockout mice die late in gestation, failing to develop granulocytic and monocytic lineages (Scott et al 1994). cMYB functions in multipotent progenitors as well, and it regulates various myeloid genes (Ness et al 1993, Shapiro 1995). cMyb knockout mice are also embryonic lethal with severe reductions in granulocytes and monocytes (Mucenski et al 1991). In zebrafish, the developing lymphoid and myeloid cells in the CHT can be identified by the expression of *c-myb*, *scl*, *runx1*, and *ikaros* (Murayama et al. 2006; Zhang and Rodaway 2007). Differentiating definitive erythroid cells begin to express adult globin genes, and thymic immigrants

differentiate into *rag1*$^{+}$ lymphoid cells (Murayama et al. 2006; Jin et al. 2007; Kissa et al. 2008).

Regulation of cell fate

The balance of the various transcription factors is important for lineage determination and controlling multipotency versus differentiation. Overexpression of *scl* and *lmo2* in the early embryo expands the formation of *gata1*$^{+}$ erythroid and *flk*$^{+}$ vascular progenitors by converting non-axial mesoderm to the hematopoietic and endothelial cell fates (Dooley et al. 2005, Gering et al. 2003). Loss of *gata1* did not affect the expression of upstream genes *scl, lmo2*, and *gata2*. Instead, there was a fate switch of erythroid cells to myeloid cells (Galloway et al 2005). *pu.1* was found to be expressed in cells that normally develop into erythroid cells, and subsequent increased formation of *mpo*$^{+}$ granulocytes and *l-plastin*$^{+}$ macrophages in the *gata1* morphants confirmed the differentiation of these precursors down the myeloid lineage.

As a result, proper levels of hematopoietic transcription factor expression are required for specification and differentiation of the different hematopoietic cell types. The activity of the transcription factors on its targets, however, is dependent on its ability to access the DNA. To achieve this, transcription factors

often recruit additional co-factors that includes chromatin modifying factors in order to effect activation or repression of their target genes.

Chromatin regulation

Because DNA is packaged into chromatin, transcriptional complexes need to be able to alter the chromatin conformation in order to activate or inhibit gene expression. The DNA contains all the genetic information required for development, and it is compacted into chromatin in order to contain 3 billion base pairs of information inside a 5-micrometer nucleus (Avery et al 1944). The basic structure of chromatin is the nucleosome, which is composed of 147 base pairs of DNA wrapped around an octamer of specialized histone proteins (Kornberg and Thomas 1974, Luger et al 1997). Changes to chromatin conformation can be achieved by covalent modifications to both the cytosine bases in the DNA and histone proteins (Fisher-Adams and Grunstein 1995, Holliday and Pugh 1975, Lenfant et al 1996, Megee et al 1995, Riggs 1975). In addition, nucleosomes can be mobilized (Varga-Weisz and Becker 1998). These kinds of modifications that do not alter the DNA sequence are considered part of the epigenetic regulatory mechanisms. Consequently, the activation of a gene not

only depends on the presence of transcription factors but also on the chromatin environment.

Histone modifications and nucleosome remodeling

Specific changes in chromatin conformation have been associated with specific gene functions. Condensation of nucleosomes results in a repressive chromatin structure that prevents gene transcription. Conversely, decondensation of nucleosomes facilitates gene transcription. Because DNA is bound to histone proteins, the nucleosomes themselves act as inhibitors of transcription. Mobilizing nucleosomes is important not only in the promoters regions for transcription factor binding but also for transcriptional elongation by RNA polymerase. These processes are greatly facilitated in the presence of nucleosome remodelers and are regulated in part by histone modifications (Orphanides et al 1998).

Histone modifications are an essential part of the epigenetic mechanism that regulates both chromatin and nonhistone protein interactions. The modification of N-terminal histone tails have been characterized the most. These covalent modifications include acetylation, methylation, phosphorylation, ubiquitylation, sumoylation, ADP ribosylation, deimination, proline

isomerization, and more recently hydroxylation and crotonylation (Kouzarides 2007, Tan et al 2011). All these modification play a role in regulating gene transcription. Histone lysine acetylation is generally correlated with decondensed chromatin and active transcription. The acetylation mark facilitates binding of transcriptional factors to chromatin (Lee et al 1993, Lefebvre et al 1998, Vettese-Dadey et al 1996), reducing the stability of the histone-DNA interaction (Hong et al 1993, Puig et al 1998), or by disrupting higher order histone structures (Baneres et al 1997, Garcia-Ramirez et al 1995, Tse et al 1998). Histone phosphorylation is believed to function in a similar manner to histone acetylation by changing nucleosome conformation or higher order structures, best exemplified by the induction of global levels of H3S10 phosphorylation during mitosis (Chen and Allfrey 1987, Chen et al 1990, Hendzel et al 1997). Ubiquitin is a relatively large modification that can alter nucleosome conformation, yet it can promote either transcriptional initiation and elongation or repression (Kim et al 2009, Pavri et al 2006, Usachenko et al 1996, Varshavsky et al 1983, Wang et al 2004). Sumoylation occurs on all four histones and antagonizes both lysine acetylations and ubiquitylations, and this modification has been found to be repressive in yeast (Nathan et al 2006). ADP-ribosylation has been implicated in transcription via the association with

enzymes that catalyze it with the transcriptional complex (Ju et al 2006). Deimination is believed to antagonize the activating effects of arginine methylation (Cuthbert et al 2004). Isomerization of H3P38 is likely involved in the regulation of a nearby mark, H3K36, discussed below (Nelson et al 2006, Chen et al 2006). One of the newest marks discovered, histone crotonylation, is associated with enhancers and transcriptional start sites (Tan et al 2011).

Histone methylation is more complex, reflecting different states of transcription depending on the residue that is modified. Lysines may be mono-, di-, or tri-methylated. Arginines can be mono-, symmetrically or asymmetrically di-methylated. H3K4, H3K36, and H3K79 are implicated in transcriptional activation. H3K4me3 localizes to the 5' end of active genes, but H3K4me1 and –me2 are associated more with enhancer regions than transcriptional start sites (Bernstein et al 2005, Kim et al 2005, Schübeler et al 2004). H3K36me3 is found throughout the body of active genes but inhibits transcription initiation if methylated in the promoter region (Keogh et al 2005). Little is known about the function of H3K79. On the opposite end, H3K9, H3K27, and H4K20 are associated with transcriptional repression. Both H3K9me and H3K27me have well known roles in heterchromatin formation (Cao 2002, Schotta et al 2002). Very little is known about H4K20 methylation except that it is also found in

heterochromatin (Schotta et al 2004). However, these repressive marks can be activating too when monomethylated (Barski et al 2007). Like lysine methylation, arginine methylation can be both activating and repressive (Lee at al 2005). Overall, specific histone marks generally associated with either transcription activation or repression, but as in the case of lysine methylation, their function can be highly context dependent.

Interactions among histone modifications provide another layer of epigenetic regulation. Lysines can be acetylated, methylated, or ubiquitinated, thus competitive antagonism can occur between different modification pathways. Modification of one residue can be dependent on another within the same or different histone tails. For example, H3K4 and H3K79 methylations are dependent on H2BK123 ubiquitination (Lee et al 2007). The binding of nonhistone proteins or the catalytic activity of enzymes can also be regulated by the histone marks. PHF8 binding to H3K4me3 is enhanced when H3K9 and H3K14 are also acetylated (Vermeulen et al 2010). In yeast, the isomerization of H3P38 regulates the ability of Set2 enzyme to methylate H3K36 (Nelson et al 2006). The combined effect of histone modifications helps to establish chromatin domains that not only functions to regulate chromatin structure but also allows for gene specific regulation.

Histone modifying factors

Histone modifications are dynamic, with modifications appearing and disappearing within minutes, thus identification of the enzymes that catalyze these modifications would help identify important regulators of gene transcription. Specific protein domains that can catalyze ('writers'), bind ('readers'), and remove ('erasers') histone modifications are found on chromatin modifying factors. The cloning and identification of histone acetyltransferase Gcn5 was the first study to link directly a chromatin factor to gene regulation, and it also contains a conserved bromodomain that is now known to bind acetylated histone tails, allowing the protein to be targeted to the chromatin (Brownell et al 1996, Owen et al 2000). Subsequent studies have identified a wide array of chromatin factor families that can recognize or modify histone marks.

The acetyltransferases, which have the ability to acetylate histones, have long been known to be integral components of transcriptional complexes. There are three main families of histone acetyltransferases (HATs), GNAT, MYST, and CBP/P300, and these enzymes can modify multiple lysine residues *in vitro*. Histone deacetylases (HDACs) remove the acetyl mark. Like HATs, they also do not show specific activities towards a particular acetyl group either, but are

often associated with repressive chromatin complexes (Sterner and Berger 2000). Many HATs contain bromodomains, which recognize and bind acetylated histone marks.

In contrast to HATs, histone lysine methyltransferases (HKMTs) have relatively more specific activity towards methylating histones at particular residues. The first HKMT identified, SUV39H1, targets H3K9 methylation (Rea et al 2000). MLL and SET1 catalyze methylation of H3K4 (Wang et al 2009). The catalytic activity is mediated by the SET domain of these proteins. The removal of the mark is accomplished by lysine-specific demethylases (LSD1) and JmjC jumonji (JMJ) domain containing demethylases (Shi et al 2004, Tsukada et al 2006). The LSD1 family demethylates H3K4me1 and –me2, whereas JMJC proteins can demethylate H3K4me3 and H3K36me3. These methyl marks are recognized by chromodomains. Kinases have also been shown to have specific activity towards specific histone residues, but are more difficult to study as signaling pathways need to be activated in order to observe the modifications (Kouzarides 2007). Enzymes that catalyze the ubiquitination, sumoylation, ADP-ribosylation, deimination, and proline isomerization of histone marks have also been identified (Cuthbert et al 2004, Hassa et al 2006, Nathan et al 2006, Nowak and Corces 2004, Shilatifard 2006, Wang et al 2004).

The individual chromatin factors can assemble into multisubunit complexes including those that can catalyze ATP-dependent chromatin remodeling. This class of remodelers is important to displace nucleosomes to allow the transcriptional machinery to bind to the DNA. For example, the SWI/SNF chromatin remodeling complex was found to facilitate GAL4 and TBP transcription factor bindings to DNA and transcription initiation by disrupting nucleosomal DNA (Imbalzano et al 1994, Kwon et al 1994). Mutating one of the SWI/SNF subunits abolished GAL4 binding (Côté et al 1994). Several chromatin remodelling complexes have been identified thus far, including INO80, ISWI, and CHD. They can be recruited by transcription factors to facilitate their binding to chromatin to help activate or repress target genes. RUNX1 has been shown to interact directly with BRG1 and INI1 of the SWI/SNF complex in Jurkat cells, a human T lymphoblast like cell line. In addition, they colocalize to the promoters of RUNX1 target genes GMCSF and IL3. siRNA knockdown of RUNX1 reduced the association of BRG1 and INI1 at these promoters, indicating that RUNX1 recruits components of the SWI/SNF complex to its target genes. These promoters were associated with active histone marks H3K4me2 and H4-ac but not the repressive mark H3K27me2, implicating that association of RUNX1 and SWI/SNF promotes gene expression (Bakshi et al 2010).

Chromatin remodeling in development.

Evidence is accumulating that chromatin remodeling have essential functions in development. SWI/SNF has been shown to be required for the development of all organisms studied so far. BRG1 and BRM are the catalytic subunits of SWI/SNF, and they assemble with various BAF subunits to form the SWI/SNF complex (Kasten et al 2011). Loss of BRG1 or several of the other BAF subunits in knockout mice result in early lethality during the peri-implantation stage (Ho and Crabtree 2010). These phenotypes are consistent with a role for BAF complex in embryonic stem (ES) cell pluripotency and self-renewal (Ho et al 2009). The SWI/SNF complex was again required for ES cells to exit the stem cell state as two subunits BAF57 or BAF155 were required in Nanog repression (Schaniel et al 2009). SWI/SNF was required again at multiple steps during the ES cell differentiation into neuronal progenitors then into neurons (Lessard et al 2007). In BRG1 deficient neuronal cells, components of the NOTCH and sonic-hedgehog pathway expression were dysregulated, contributing to the differentiation defects. Subunit switching of the different BAF subunits occurred at the different transition stages, suggesting tissue specific BAF complex formation at each stage of development depending on the BAF components that are present. Thus chromatin factors can have a wide variety of possible functions

depending on the developmental context.

Depletion of members of other remodeling families also result in developmental defects. The CHD family is composed of nine proteins, CHD1-9, that contain tandem chromodomains preceding the ATPase domain. CHD1 was believed to be a crucial factor for transcription, but *Chd1* mutant *Drosophila* zygotes are viable. It is expressed broadly throughout embryogenesis and in the imaginal discs, but the mutants only showed defects in wing development and gametogenesis (McDaniel et al 2008). How such tissue specific defects arise from a broadly expressing factor is not completely understood.

CHD7 in development

Of all the CHD factors, CHD7 is the most extensively studied. De novo mutations of *CHD7* in humans account for 67% of CHARGE syndrome patients (Zentner et al 2010). CHARGE stands for an association of multiple anomalies including Coloboma of the eyes, Heart defects, Atresia of the choanae, Retarded growth and development, and Genital and Ear abnormalities (Pagon et al 1982). Identifying the mechanism of CHD7 function will help elucidate its role in the pathogenesis of CHARGE syndrome.

CHARGE syndrome

The birth incidence for CHARGE defects is relatively rare, about 1 in 10,000. In addition to the CHARGE syndrome, additional anomalies including hyposmia, cleft lip/palate, and tracheoesophageal fistula can be found in CHARGE syndrome patients. In fact, many features of CHARGE syndrome overlap with other syndromes, including Treacher Collins. Treacher Collins syndrome is caused by a mutation in TCOF1 that affects craniofacial development (Dixon et al 2007). Both TCOF1 and CHD7 function in ribosomal biogenesis in the nucleolus, thus the overlap in developmental defects is not so surprising (Zentner et al 2010a). The most consistent features of CHARGE are temporal bone abnormalities (98%), external ear malformations (91%), and hearing loss (89%) (Zentner et al 2010b).

Additionally, CHD7 may be associated with T cell immunodeficiency. In one study of a cohort of 25 children diagnosed with CHARGE syndrome, 60% of the children exhibited some degree of lymphopenia (Jyonouchi et al 2009). CHARGE syndrome patients exhibiting T-cell deficiency were often reported to be athymic, suggesting the possibility that the immunodeficiency is not due to hematopoietic defects in the bone marrow (Gennery et al 2008, Hoover-Fong et al 2009, Inoue et al 2010). Thus the overall developmental defects that are

potentially caused by CHD7 are broad.

Since the discovery that *CHD7* was a causative gene of CHARGE (Vissers et al 2004), many attempts were made to uncover the mechanism by which haploinsufficiency for *CHD7* causes CHARGE syndrome. Most mutations occur *de novo*. The majority of the mutations result in nonsense or frameshift mutation (72%), the remaining are either splice (13%) or missense (10%). These mutations appear throughout the body of the gene. Consequently, *CHD7* mutations are thought to be haploinsufficient.

Mouse models of CHARGE

Mouse models delineate an important function for Chd7 in ear formation. One study characterized nine mutant alleles for Chd7 generated by ENU mutagenesis (Bosman et al 2005). Similar to human patients, mutant mice displayed semicircular canal truncations of the inner ear. Chd7 was found to be expressed in the canal pouches of the vestibular system, vestibulo-cochlear ganglion, the cochlea, and the cartilage primordium, consistent with the inner ear defects observed in heterozygous mice. Chd7 was also expressed in multiple tissues such as the tongue, facial mesenchyme, brain ventricles, olfactory and lung epithelium. Interestingly, Chd7 was found to be expressed weakly in yolk

sac vessels at E12.5. The *Whirligig* (*Whi*) allele contains a nonsense mutation in Chd7, and a third of these mice had palatal and choanal defects like the human patients. Additionally, some of the heterozygous mice showed defects in interventricular septum, thus some of the animals showed hemorrhaging. Overall, Chd7 was expressed in multiple tissues that are affected by CHARGE syndrome, and the mice can be used as a model to study the pathology of CHARGE given the overlapping defects with human CHARGE patients (Bosman et al 2005).

Full targeted knockdown was achieved using gene-trapped reporter mice, $Chd7^{Gt}$ (Hurd et al 2007). Homozygous mutants were lethal by E11. Heterozygous mice display a head bobbing and circling behavior consistent with inner ear defects. Both heterozygous and homozygous mice showed developmental delay, suggesting Chd7 was important for the proliferation and development. There is a specific requirement for Chd7 in olfactory epithelium proliferation and differentiation partly by regulating pro-neural gene expression of Fgf10, Ngn1, NeuroD, and Isl1 (Hurd et al 2010, Layman et al 2009). Comparison between $Chd7^{flox/+}$, $Chd7^{Gt/Gt}$, and $Chd7^{Gt}$ mice showed dose dependent changes in the inner ear, with $Chd7^{Gt/Gt}$ mice showing the highest reduction in neuroblasts and cell proliferation (Hurd et al 2010). Thus one of the

functions of CHD7 in development appears to be the regulation of cell proliferation.

Molecular functions of CHD7

CHD7 is a member of the chromodomain (CHD) family for chromatin remodelers. It is a large protein of 300 kDa that contains two tandem chromodomains in its N-terminus and a SNF2 helicase domain, characteristic of CHD family members (Woodage et al 2007). The *Drosophila* ortholog *kismet* functions in promoting RNA polymerase II transcriptional elongation downstream of P-TEFB recruitment. *kismet* also functions to antagonize heterochromatin spreading mediated by Polycomb group proteins (Srinivasan et al 2008). Genome-wide localization studies of CHD7 in cancer cell lines and ES cells collectively showed that CHD7 binds to enhancer regions (Schnetz et al 2009, Schnetz et al 2010). These binding sites are DNase I hypersensitive and overlap with P300 binding. A direct interaction was even detected between CHD7 and P300. CHD7 binding also correlates with histone H3K4me1 and me2 marks, which are typically found in enhancer regions. More recently, CHD7 has been found to regulate RNA biogenesis in the nucleolus and that it was required for neural crest development formation from ES cells (Bajpai et al 2010, Zentner

et al 2010). Knockdown of *Chd7* in *Xenopus* reduced neural crest gene expression and cell migration, and CHD7 interacts with components of the PBAF complex to regulate the expression of neural crest transcription factors. In ES cells, there was co-localization of CHD7 with ES cell pluripotency genes OCT4, SOX2, and NANOG at these sites. However, there was an interesting observation that the most highly expressed embryonic stem cell genes were modestly upregulated when CHD7 was depleted, though such a small change in expression might not have any significant impact on the cells. There has also been only one other report of CHD7 acting as a negative regulator, which is its recruitment by SETDB1 to repress PPAR γ in mesenchymal stem cells (Takada et al 2007). Thus CHD7 not only has broad roles in development, but it also has broad molecular functions.

Summary

Evidence has been accumulating demonstrating the importance of chromatin regulating various developmental transitions (Ho and Crabtree 2010). There are over 400 proteins that contain chromatin binding or chromatin modifying domains in humans, and how they function together to achieve target and tissue specifity is not well understood. As discussed earlier, combinatorial

assembly of chromatin factor complexes is believed to be part of the mechanism, exemplified by SWI/SNF complex. It has been postulated that the specific subunits of each complex can be expressed differentially in different tissues to achieve specifity. Although they may be interchangeable, BRG1 and BRM mouse knockouts showed completely different phenotypes (Bultman et al 2000, Reyes et al 1998). Thus the function of chromatin regulators *in vivo* is much more specific and may be more dynamic than previously thought.

There are now over 120 different residues and at least 10 different kinds of post-translational modifications that can be found on histone proteins (Strahl and Allis 2000, Tan et al 2011, Wolffe and Hayes 1999). To study the role of all the chromatin factors in a specific developmental process would require a significant amount of time to generate knockouts for all 400 chromatin factors. The zebrafish provides an excellent model system for such a study for several reasons. They have a short developmental time and high fecundity make them amenable for large-scale screening. Their relatively small size allows a large number of them to be maintained in a facility. The embryos are transparent and develop *ex utero*, facilitating visualization of embryonic processes under a dissecting microscope or by *in situ* hybridizations for gene expression analysis (Patton and Zon). Furthermore, targeted gene knockdowns can be achieved in

zebrafish by the use of morpholinos, which are chemically modified antisense oligonucleotides that inhibit translation or disrupt splicing (Nasevicius and Ekker). Most importantly, the molecular pathways involved in hematopoiesis are well conserved between teleosts and mammals (Davidson and Zon), as are the chromatin factors. Thus screening using a morpholino-based approach provides a rapid way to assess the function of chromatin factors within the hematopoietic system.

In this dissertation, we have attempted to systematically identify chromatin factors that regulate developmental hematopoiesis by a reverse genetic approach. We curated a list of 425 human chromatin modifying factors encompassing most of the known chromatin regulators. Then we annotated 487 zebrafish homologs corresponding to these chromatin factors and designed morpholinos to knock them down. We conducted two simultaneous screens for primitive and definitive blood formation. In the primitive blood screen, we scored for changes in globin gene expression. In the definitive screen, we scored for changes in stem and progenitor gene expression. Knockdown of many chromatin factors resulted in decreased or increased hematopoietic gene expression in both primitive and definitive screens. We identified very specific hematopoietic phenotypes for *smarca1* and *chd7*, and found that different

chromatin factors function at different steps of hematopoiesis. Our analysis of the screen hits indicated that histone methylation and acetylation and nucleosome remodeling were important processes in regulating hematopoietic gene expression. Furthermore, we found that multiple subunits of chromatin modifying complexes were represented in our screen hit list, indicating the possibility that theses chromatin complexes regulate blood development. Follow-up work of *chd7* confirmed that chromatin factors identified in the screen can have very tissue specific functions. Knockdown of *chd7* resulted in increased primitive and definitive blood formation, suggesting that it functions as a repressor of hematopoiesis. Other chromatin factors, for example *unk* and *jmjd2b*, were found to have important roles in both hematopoiesis and development of other tissues. The concerted action of both transcription factors and chromatin factors result in the proper specification and differentiation of blood lineages, as illustrated in the movie. The resource that we have established in this dissertation will be valuable for future studies of chromatin factors in development.

Chapter 2

Identification of epigenetic regulators of hematopoiesis

Attributions

This chapter was written in preparation for manuscript submission to the journal Nature Cell Biology as a Resource article. Dr. Zon encouraged me to use this style as it would facilitate the submission.

I have performed all the experiments described in this chapter. This included the design of the screen, curation of the gene list, bioinformatic analysis of the chromatin factors in zebrafish, microinjection of morpholinos, WISH, and analysis of the data. Katie Kathrein assisted with curation of the gene list, bioinformatic analysis of the chromatin factors in zebrafish, microinjection of morpholinos, and data analysis. Abby Barton and Zachary Gitlin assisted with microinjection of morpholinos, WISH, and data collection. Yue-Hua Huang assisted with microinjections of morpholinos. Yi Zhou collected and curated the preliminary list of human chromatin factors from public databases and assisted with bioinformatic analysis of the chromatin factors. Anhua Song assisted by Anthony DiBiase constructed the chromatin factor database and uploaded results from the screen.

Introduction

The programs of gene expression required for maintenance and differentiation of a cell type are tightly regulated by a network of transcription factors and associated complexes that include chromatin modifying factors. To orchestrate the correct sequence of events required, transcription factors recruit chromatin modifying factors to facilitate or inhibit gene expression. The epigenetic information consists of chemical modifications to cytosine bases in the DNA and histone proteins that fold the DNA into nucleosomes, and the nucleosomes themselves can then be repositioned, dissociated, and/or reconstituted (Li et al 2007). All these chromatin alterations are carried out by a specific set of conserved domains found on chromatin factors. Mouse knockout models and zebrafish mutants of several chromatin factors have been used to investigate the role of chromatin factors in vertebrate development, but the majority of the chromatin factors have not been characterized in this manner.

Hematopoiesis is a well characterized process encompassing the formation of hematopoietic stem cells (HSCs) and their subsequent specialization to become multilineage progenitors that generate terminally differentiated cells of all the peripheral blood lineages. The blood program is initiated during the early stages of embryonic development, and the master transcriptional regulators

controlling hematopoiesis have been identified. Genes known to be required for stem cell production, survival, or self-renewal of HSCs include Runx1, Scl, Lmo2, Mll, and Bmi1. Upon formation, the quiescent HSCs begin to differentiate into lineage restricted progenitors. GATA1, PU.1, and Ikaros are among key transcription factors required for commitment to the erythroid, myeloid, and lymphoid lineages, respectively (Orkin and Zon 2008). In contrast to transcriptional regulators, few chromatin factors have been studied for their role in hematopoiesis, but several have been identified as leukemic translocation partners, underscoring the importance they have in normal development of the tissue (Rice et al 2007).

In order to generate a comprehensive list of chromatin factors with a role in hematopoiesis, we have undertaken a large-scale *in vivo* reverse genetic screen targeting zebrafish homologs of 425 human chromatin factors to identify epigenetic regulators of developmental hematopoiesis. The zebrafish provides a suitable platform for rapid high-throughput screening to assay the function of chromatin factors in blood development due to their high fecundity, rapid development, conservation of hematopoiesis, and ease of genetic knockdowns using morpholinos. We have identified at least 47 factors that affect hematopoietic development of primitive and definitive blood, including 28 new

factors that have yet to be associated with blood formation. We have also characterized the distinct stages of hematopoiesis at which these factors play a role, the majority of which function at the stem and progenitor level. Furthermore, we provide an example of a chromatin factor combination that can greatly increased expression of stem and progenitor genes *c-myb* and *runx1*, providing evidence for functional protein complex associations based on known protein interaction data. Taken together, our screen provides a valuable resource for elucidating the network of chromatin regulators of hematopoietic development.

Results

Screen overview

To generate a complete compendium of factors that establish the epigenetic code during developmental hematopoiesis, we have undertaken the first large-scale *in vivo* reverse genetic screen targeting chromatin factors (Figure 2-1A). We designed antisense oligonucleotide morpholinos to knock down expression of 487 zebrafish homologs of 425 human chromatin factors. Our gene list comprises most of the known human factors containing chromatin binding, modifying, or remodeling domains curated from several public databases: CREMOFAC, SMART domain by NRDB, CDD at NCBI, Pfam, and ChromDB. Using comparative genomics, homologous genes in zebrafish were retrieved by BLAST search of the unique human protein sequences into the zebrafish genome.

Morpholinos for each chromatin factor were injected into single cell embryos, and a portion of the embryos collected were set aside as uninjected wild-type controls. Each morpholino was injected at three concentrations. In a series of pilot experiments knocking down the eight known zebrafish DNA methyltransferase genes with ATG and splicing morpholinos, we have determined the optimal dose range for ATG morpholinos to be 2, 4, and 6 ng and for splicing morpholinos to be 4, 8, and 12 ng (Shimoda et al 2005). These doses

typically give a range of phenotypes from a hypomorph to a complete knockdown for most mRNA products, similar to an allelic series. For morpholinos that induced severe morphological effects at this dose range, appropriate dilutions were made and the morpholino was rescreened at a lower dose (see Methods).

Post-injection, the embryos were grown to the proper developmental stage and collected to assay for hematopoietic defects by whole-mount *in situ* hybridization (WISH). We conducted two screens simultaneously for primitive and definitive blood formation. For the primitive screen, developing erythrocytes were assayed by *β-globin e3* expression at the 16 somite stage (ss), or 17 hours post-fertilization (hpf), in the posterior tail of the embryo. For the definitive screen, the establishment of hematopoietic stem and progenitor cells (HSPCs) in the aorta, gonad, mesonephros (AGM) region was detected with *c-myb* and *runx1* expression at 36 hpf (Figure 2-1B). Changes in gene expression were evaluated by comparing morphants, embryos injected with morpholinos, to their corresponding uninjected wild-type controls, and the results for each injection were determined based on a minimum of 65% of the embryos exhibiting the same phenotype.

Classification of screen results.

According to the expression phenotypes observed, the morphants were divided into three major categories: no change, decrease, or increase. Due to the range of decreased staining from subtle reduction to complete absence of staining, we further subdivided the decrease category into mild, intermediate, and strong (Figure 2-2). Morphants with developmental abnormalities were listed separately (Supplementary Figure 2-1). Any morphant showing changes in blood marker expression were considered screen hits. We reasoned that morphologically normal morphants that showed the strongest decrease or increase in blood formation represented genes that were most likely to be specific to blood development. The 25 and 47 morphants from the primitive and definitive primary screen hits, respectively, that met these critieria were selected for further analysis.

Chromatin factors regulate primitive blood development from the mesoderm.

To confirm the phenotype from the primary screen and characterize additional blood defects, morpholinos were reinjected and screened for changes in *β-globin e3, scl,* and *gata1* expression. Of the 25 primary hits, knockdown of 13

chromatin factors reduced *β-globin e3* expression while depletion of another 12 factors increased *β-globin e3* expression at 17 hpf. 18 of the 25 primary hits were verified in which knockdown of 7 factors resulted in a strong reduction of *β-globin e3* expression while knockdown of the other 11 factors increased *β-globin e3* expression (Supplementary Table 1).

To determine the earliest step in blood development that is affected in the primitive wave morphants, we examined *scl* and *gata1* expression changes at 10-12 ss (14 hpf) for formation of mesodermal precursor and erythroid progenitors, respectively (Figure 2-3). 15 morphants showed changes in *scl* and *gata1* expression consistent with the changes in *β-globin e3*, such as *smarca1* and *cicl*, suggesting that most of the factors categorized in the strong decrease or increase categories play a role in the formation of mesodermal precursors competent to make blood. The remaining 3, *chrac1, actr2b*, and *hdac9b*, had normal *scl* expression but reduced *gata1* and *β-globin e3* expression, indicating that these factors function at the next step in regulating the formation of erythroid progenitors from the mesoderm. Most of the factors represent novel regulators of erythroid development since only Zfat, *HDAC9*, and *ASH2L* have been shown previously to be required for globin gene expression or erythroid development (Kim et al 2007, Muralidhar et al 2011, Tsunoda et al 2010).

Chromatin factors regulate the induction of HSPCs.

As in the primitive screen, we re-screened 47 definitive primary screen hits to confirm and characterize additional HSPC phenotypes. Injection of 41 and 6 morpholinos resulted in decreased and increased *c-myb* and *runx1* staining, respectively, in the AGM at 36 hpf. Of the 29 morpholinos that were validated, 24 were strongly reduced and 5 increased *c-myb* and *runx1* expression (Supplementary Table 2).

Previous work has shown that proper vessel development and establishment of artery identity are important for AGM stem cell induction (Burns et al 2009, Lawson et al 2003). Thus the expression of the vascular marker *flk* and the arterial identity marker *ephrinB2* were analyzed for the 29 verified hits. 22 morphants, the majority of those examined, showed normal *flk* and *ephrinB2* expression, indicating that the chromatin factors identified in the strong decrease and increase categories function in the specification or maintenance of HSPCs from the hemogenic endothelium (Figure 2-4). Some of these factors have been shown to regulate HSC self-renewal, like Prdm16 and HDACs (MacMahon et al 2007, Chuikov et al 2010, Aguilo et al 2011, Young et al 2004). This indicates the possibility that other factors in this same phenotypic category represent potential new candidates required for HSC maintenance, of

which few are known.

The remaining 7 chromatin factors were found to function at earlier stages of HSPC specification based on their vascular defects. There were 4 factors, *hdac4l, mier1b, phf21a,* and *suv39h1*, with normal *flk* but *ephrinB2* expression was reduced, suggesting that they function at an earlier step in the establishment of aorta identity required for proper HSPC formation. SUV39H1 has been shown to be recruited by multiple hematopoietic transcription factors, such as RUNX1 and PU.1, to repress target genes, and our results indicate that it is also required at the earlier hemogenic endothelium stage as well (Chakraborty et al 2003, Stopka et al 2005). Finally, 3 morphants, *mier1*, *jhdm1bb*, and *rbbp7*, lost both intersomitic *flk* and arterial *ephrinB2* expression, hence the loss of HSPCs in these morphants is likely due to the absence of a hemogenic endothelium. These results are consistent with data showing an interaction between RBBP7 and TAL1/SCL via the LSD1 histone demethylase complex, and *scl* is required for both endothelial and blood formation, hence the loss of HSPCs in the morphants may be related to loss of *scl* function in the absence of *rbbp7* (Hu et al 2009, Patterson et al 2005). Of the 47 factors that we characterized, this class of morphants was surprisingly rare given how broadly chromatin factors are believed to function. This suggests that the chromatin factors identified in our

screen have very specific effects on the formation of HSPCs. Overall, our definitive chromatin factor screen identified many new potential regulators specifically involved in the development of HSPCs from the AGM.

ISWI chromatin remodeling is essential for hematopoiesis.

One of the most striking phenotypes we observed came from knockdown of *smarca1* in the primitive screen. *smarca1*, or *snf2l*, is the catalytic subunit of ISWI complex and had the most reduction in *β-globin e3* expression of all the factors examined in the primitive blood analysis. We found that high levels of *smarca1* knockdown abolished all *scl* expression at 10 ss (14 hpf), consistent with the loss of *gata1*$^{+}$ and *β-globin e3*$^{+}$ cells in these morphants. The loss of primitive *scl* expression would also impair definitive blood formation since these early *scl*$^{+}$ cells have been shown to contribute to definitive hematopoiesis as well (Supplementary Figure 2-2A) (Dooley et al 2005). Because loss of *smarca1* also impairs embryonic development, we injected *smarca1* at lower doses to allow embryos to develop to 36 hpf and were able to confirm loss of *c-myb* and *runx1* expression in the AGM (Supplementary Figure 2-2B). These results are consistent with a study in which depletion of SMARCA5 (SNF2H), the other catalytic subunit that forms distinct ISWI complexes from SNF2L, prevents

erythroid differentiation of $CD34^+$ human hematopoietic progenitors and results in embryonic lethality by E7.5 (Stopka and Skoultchi 2003). In addition, 2 other genes associated with ISWI chromatin remodeling, *chrac1* and *rsf1b,* were also identified as a primitive screen in the same category as *smarca1*, suggesting a possible interaction between the 3 factors as part of the ISWI chromatin remodeling complex in primitive blood. Taken together, our study suggests that zebrafish *smarca1* is the functional homolog of SMARCA5 in mice, and it is essential for hematopoietic development.

Chromatin factor complex subunits are conserved.

Given that chromatin factors often function in multisubunit complexes, we hypothesized that we could identify chromatin complexes important for hematopoietic development by mapping known protein interactions between the different chromatin factors found in our screen hits. We used the 18 and 29 strongest hits from the primitive and definitive screens, respectively, as the center of a "hub" and added additional subunits that were also found as hits in other phenotypic categories of our screen (Figure 2-5). The results confirmed that multiple subunits of the same complex are represented in our gene list. The definitive chromatin factor hits encompass a wide range of chromatin factor

complexes, BAF/PBAF, SET1, NuRD/SIN3A/HDAC, NuA4/HAT, P300/CBP, and PRC1/PRC2. In contrast, a smaller number of complexes was represented in the primitive list, most of them overlapping with the ones identified from the definitive list such as BAF/PBAF and SET1. A different HAT1 complex HBO1 was present in the primitive list, but it still functions in acetylation. Moreover, fewer of the subunits in the primitive complexes were also identified as hits in the primitive screen. This comparison suggests that primitive hematopoiesis employs only a subset of the chromatin factor complexes used during definitive hematopoiesis. This may reflect an increased complexity in the regulation of definitive stem cells given their ability to self-renew and generate all the blood lineages.

We tested whether knockdown of multiple subunits reportedly in the same complex could enhance the hematopoietic phenotype when combined. CHD7 and ARID2 have been shown to participate in the PBAF chromatin remodeling complex in human neural crest stem cells, and both *chd7* and *arid4b* were definitive screen hits that increased HSPC formation (Bajpai et al 2010). *arid2* and *arid4b* belong to the same family of AT-rich interacting domain (ARID) containing factors, thus we tested whether knockdown of both *chd7* and *arid4b* could enhance the individual morphant phenotypes. Indeed, there was a

dramatic increase of *c-myb*$^{+}$ and *runx1*$^{+}$ cells in the AGM at the expense of *flk* expression in the double morphants (Supplementary Figure 2-3). Given the staining patterns with normal *flk* in the head, it is likely that all the vascular cells in the tail competent to produce blood have been induced to express hematopoietic genes. Although we cannot exclude the possibility that *chd7* and *arid4b* function in parallel, our results suggest the possibility that chromatin factors identified in our screen reported to function in the same complex in mammalian systems synergize to enhance the blood phenotype in our morphants, providing *in vivo* evidence for the role of these chromatin complexes in regulating distinct steps of hematopoietic development.

Other categories of screen hits with milder phenotypes also function in blood development.

In addition to the chromatin factors with strong decrease or increase phenotypes, primitive screen hits with milder reductions in *β-globin e3* expression were also found to function at different stages of erythroid differentiation. We characterized the 7 chromatin factors from the primitive screen that were not verified because they showed only an intermediate decrease in *β-globin e3* expression upon reinjection, and we observed that 6

morphants had normal *scl* but reduced *gata1* expression. These results suggests that the 6 chromatin factors likely function at the erythroid specification stage. CHD4 and CBX8, 2 of the 6 factors, have already been shown to be associated with the FOG1/GATA1 transcriptional complex and the TIF1-γ elongation complex, respectively, that are known key regulators of erythroid development (Bai et al 2010, Hong et al 2005). The last one of the 7 factors tested, *kat5*, showed only a decrease in *β-globin e3* without loss of *scl* and *gata1* expression, indicating that it plays a role in erythroid cell differentiation. In comparison to the 18 strong hits, the remaining chromatin factors likely function at later stages of erythropoiesis after induction of the scl^{+} mesoderm.

Given that most of the strongest definitive hits did not show any vascular defects, morphants in other categories with milder reductions in *c-myb* and *runx1* expression would have normal vasculature as well. As predicted, of the 11 morphants tested in the intermediate decrease category, we did not observe any defects in *flk* and *ephrinB2* expression. Collectively, we have identified a large number of new chromatin factors that regulate different steps of primitive and definitive hematopoiesis.

Discussion

Hematopoietic stem cells undergo proliferation and differentiation under the control of cell-specific transcription factors whose function is facilitated by chromatin factors. These factors establish an epigenetic landscape that controls self-renewal at the same time as providing lineage priming to drive differentiation. In an effort to better understand the epigenetic regulation of blood stem cells, we undertook a genetic approach to define the function of most of the chromatin factors in the zebrafish genome. A library of zebrafish genes homologous 425 human chromatin factors were identified, and these genes were targeted by morpholinos to suppress gene expression. Our library contains canonical 'readers,' 'writers,' and 'erasers' of chromatin as well as less characterized domain families. The large numbers of zebrafish embryos produced allowed the screening of such a large number of genes. We identified a cohort of 18 factors that directly regulate primitive hematopoiesis and 29 factors that are essential for definitive hematopoiesis, and they include both known and novel regulators of hematopoiesis.

In our investigation of the primitive wave of hematopoiesis, we analyzed expression of the embryonic globin gene, *β-e3*, upon chromatin factor knockdown. From this work, we identified 7 genes that resulted in nearly

complete loss of globin staining and 11 that caused an increase. Only 3 genes from either category have defined roles in hematopoiesis. Most of these chromatin factors regulate the formation of hematopoietic precursors from the mesoderm since 15 of the 18 factors showed changes in both *scl* and *gata1* expression consistent with the *β-globin e3* phenotype. All other primitive screen hits likely function at later stages of erythroid progenitor specification and differentiation given that only *gata1*$^{+}$ and/or *β-globin e3*$^{+}$ cells were affected. In a recent study investigating the histone modifications on differentiating erythroid cells in mouse fetal liver, five histone marks were induced during this transition, H3K4me2, H3K4me3, H3K9Ac, H4K16Ac, and H3K79me2 (Wong et al 2011). Our strongest primitive hits is composed of chromatin factors involved in methylation and acetylation of histones, including H3K4 methylation, consistent with the mouse findings. These data support the current model that methylation and acetylation marks have the most functional impact on transcription.

For our study of definitive hematopoiesis, we examined expression of HSPC markers *c-myb* and *runx1* after knockdown of chromatin factors. We identified 24 genes that greatly reduced and 5 that increased the number of *c-myb*$^{+}$ and *runx1*$^{+}$ cells in the AGM. A number of these genes have been shown previously to regulate HSC function, including *prdm16, p300, crebbp*, *jhdm1b,* and *hdacs*. Still,

over half of the gene list represents putative novel chromatin factors important for HSPC regulation and includes includes interesting factors such as the nucleosome remodeler *nap1l4* and components of the SET1 chromatin complex, *cxxc1l* and *setd1ba*, which has been shown to interact with MLL complexes. Although a similar study characterizing changes in histone marks during various stages of definitive HSC formation has not been done, we predict that they will include histone modifications such as methylation of H3K4, H3K9, and H3K36, and acetylation as well based on the chromatin factors identified from the screen.

Interestingly, disruption of both positive and negative regulators of chromatin frequently resulted in the same reduced marker expression phenotype in our screen. For example, knockdown of *p300*, which functions in a complex to acetylate histones, and *hdac6*, which deacetylates histones, each resulted in loss of *c-myb*$^{+}$ and *runx1*$^{+}$ cells in the AGM. While these genes encode proteins that likely serve opposing roles in regulation of their respective target genes, their functions are both required for proper HSC specification. These data are in concordance with more recent discoveries that transcription factors recruit both positive and negative regulators to activate and repress target genes, respectively, which has been shown for GATA1 (Blobel et al 1998, Hong et

al 2005, Kadam and Emerson 2003, Rodriguez et al 2005).

Another interesting observation from our screen is that two factors with similar functions, namely *p300* and *crebbp*, showed opposing phenotypes. P300 and CBP are homologous proteins that share a bromodomain and histone acetyltransferase domain (Ogryzko et al 1996, Bannister and Kouzarides 1996). They interact with a wide variety of transcription factors, regulate different cellular functions, and are targets of leukemic chromosomal translocations (Blobel 2000, Rice et al 2007). Mouse knockouts of P300 and Cbp exhibit similar phenotypes (Yao et al 1998). Despite their largely overlapping roles, evidence of differential regulation has been accumulating (Kalkhoven 2004). In HSCs, Cbp plays an important role in HSC self-renewal whereas P300 regulates HSC differentiation, and these results are supported by recent ChIP-seq results indentifying distinct binding sites between the two factors (Ramos et al 2010, Rebel et al 2002). Taken together, our results suggest that the effect chromatin factors have *in vivo* cannot be predicted based solely on their domain function, thus future studies of chromatin factors in the context of development would be important for our understanding of chromatin regulation and gene expression.

Of the 47 genes that we characterized for primitive and definitive blood formation, the majority could be mapped to known chromatin modifying

complexes: histone methylation/demethylation (SET1A/MLL and PRC complexes, Jmj proteins), histone acetylation/deacetylation (HDAC/NuRD/Sin3A and NuA4 complexes), and nucleosome remodeling (SWI/SNF and ISWI complexes). For other chromatin factors that could not be mapped because of the lack of protein interaction data, it is still possible that they may also be associated with these complexes. Based on genome-wide histone mark and nucleosome localization studies, these modifications are highly correlated with the transcriptional status of a gene (Mikkelsen et al 2007, Schones et al 2008, Schübeler et al 2004). Though this does not exclude the possibility that other marks such as histone phosphorylation may be important for the development of other tissues, our findings provide *in vivo* evidence that these chromatin modifications have the most important functional impact on hematopoiesis.

Although a number of chromatin factors identified in both primitive and definitive blood screens have no known function in hematopoiesis, new hypotheses regarding the subunit composition of the chromatin factor complexes can be generated. One of the most striking results from our primitive screen was the knockdown of *smarca1,* which nearly abolishes all *scl*, *gata1*, and *β-globin e3* expression in the embryo. *chrac1* and *rsf1b*, other components that form the ISWI complex, were also identified in the screen though according to

mammalian data, they normally complex with the other homolog, *smaraca5*. Our data suggest that ISWI chromatin remodeling is important for primitive and definitive hematopoiesis and that the complex involves *smarca1*, *chrac1*, and *rsf1b*. In combining our screen results with currently available protein interaction data, an epigenetic network regulating the different stages of embryonic hematopoiesis could be generated.

The mechanism by which ubiquitously expressed chromatin factor subunits have tissue specific function is not known. Moreover, members of the same chromatin domain family could compensate for each other, yet individual knockdown of many of these factors still resulted in a hematopoietic phenotype, suggesting that their functions are not entirely redundant. A study in neural stem cells identified changes in BAF subunit composition as they transitioned to a more committed neuronal lineage (Lessard et al 2007). Our screen results would indicate a similar model given that the predicted chromatin complexes important for primitive blood overlapped with those for definitive blood, but the screen hits that mapped to these complexes were not all the same. This model for combinatorial assembly is one type of mechanism that would allow chromatin factors in vertebrates to achieve stage specific and tissue specific epigenetic regulation.

In addition to validating the remainder of our gene list, new studies focusing on the interaction between hematopoietic transcription factors and our chromatin factor list would provide a more complete transcriptional network of gene regulation in blood development. To facilitate these and other studies, we have generated a searchable database in which the screen data can be accessed as a resource. All information about experimental design, methods, screen results, and characterization data presented here are included in the database. Most importantly, the database provides a collection of morpholino sequences that result in an embryonic phenotype. These effects can be deduced based on the morphological defects or abnormal staining pattern of the blood markers in the embryo. For example, we observed morphants with abnormal patterning of globin expressing cells in morphants such as *sirt1*, *dbf4*, and *setd6* that may be related to cell migration defects in the mesoderm. Live images for morphants with interesting phenotypes can also be found in the database.

Overall, we have identified a set of genes involved in the regulation of developmental hematopoiesis, including specification of HSCs and primitive erythropoiesis. Through our verification of morphant phenotypes, we have also found a subset of chromatin factors that regulate mesoderm, artery, and vessel formation, with implications for the role of these factors outside of

hematopoiesis. These data provide a resource for the identification and characterization of novel regulators in blood development as well as for the assembly of chromatin factor complex associations in blood. The epigenetic changes can only be achieved by a network of chromatin factor complexes that can recognize, interpret, and catalyze additional modifications on chromatin. In combination with other genetic and biochemical studies, our screen helps to unravel the epigenetic code that establishes the programs of gene expression for self-renewal and differentiation in hematopoietic cells.

Zebrafish maintenance and microinjection

Zebrafish (*Danio rerio*) Tüebingen strain were bred and maintained according to Animal Research guidelines at Children's Hospital Boston. Embryos were developed at 25°C and staged according to hours post-fertilization and morphological features (Kimmel et al 1995). Microinjection of morpholinos were performed at the 1-2 cell stage. Injection volumes were measured using a stage micrometer to a diameter of ~91 μm (0.4 nl) and injected one to three times into the same embryo to achieve a 3 dose range.

Morpholino design and synthesis

Due to the occurrence of a whole genome duplication event in zebrafish evolution, there are several human genes that have two homologous sequences that can be found in the zebrafish genome. For these genes, we have designated with *a* and *b* suffix according to standard zebrafish nomenclature guidelines.

For each zebrafish homolog, the sequences were analyzed to identify the most suitable target sites for morpholino knockdown. Translation blocking, or ATG, morpholinos were designed if the transcriptional start site was well annotated. Otherwise, splice blocking morpholinos were designed in which

exons were prioritized based on the proximity to the 5' end of the gene and their non-divisibility by 3, increasing the likelihood of a frameshift mutation after exon excision. All splicing morpholinos targeted exons prior to or within the chromatin domain of interest. Once the target site was selected, morpholino oligos were designed and synthesized (Gene-Tools).

Whole-mount in situ hybridization and imaging

WISH on zebrafish embryos fixed in 4% paraformaldehyde were performed as described previously using the Biolane HTI *in situ* robot (Intavis) (Thisse and Thisse 2008). Probes used were *c-myb* (Thompson et al 1998), *runx1* (Kalev-Zylinska et al 2002), *gata1* (Liao et al 1998), *scl* (Gering et al 1998), *β-globin e3* (Brownlie et al 2003), *flk* (Thompson et al 1998), and *ephrinB2* (Lawson et al 2002). Stained embryos were imaged using a Nikon stereoscope with a Nikon Coolpix 4500 camera or Zeiss Axiocam camera. Embryos mounted in glycerol were imaged on a Nikon E600 compound microscope.

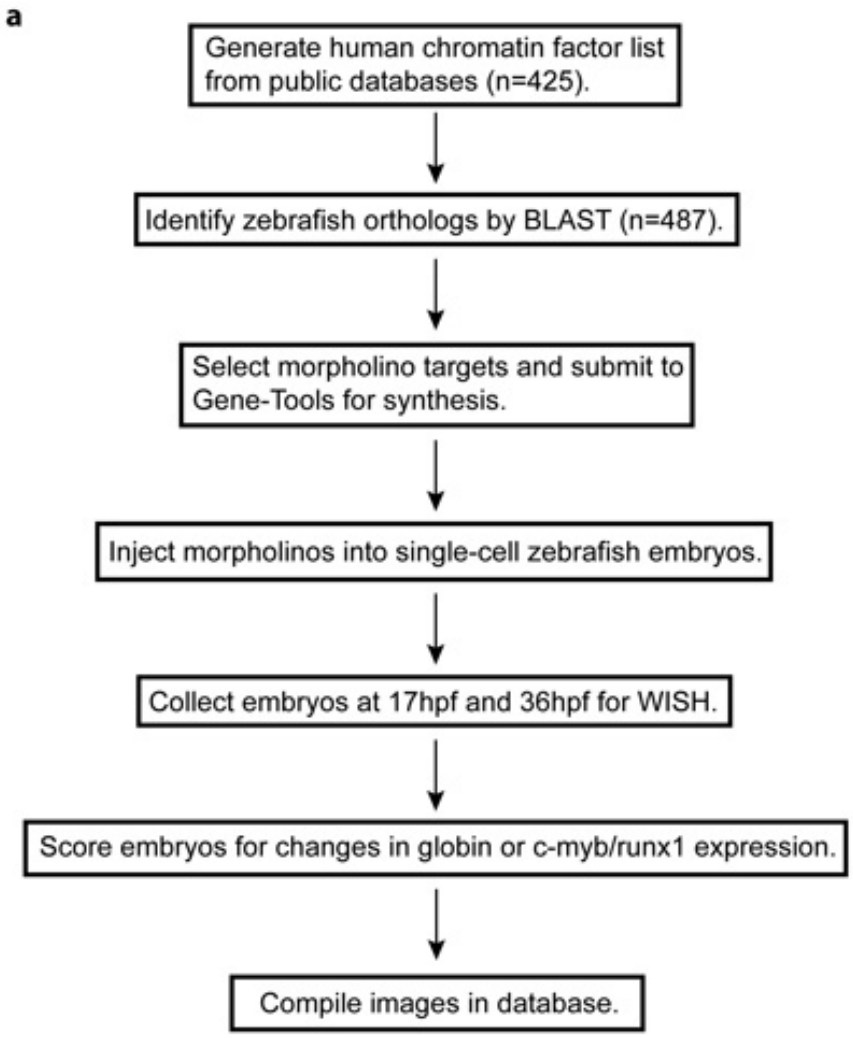

Figure 2-1. Chromatin factor screen design.
(A) Schematic of screen procedure.

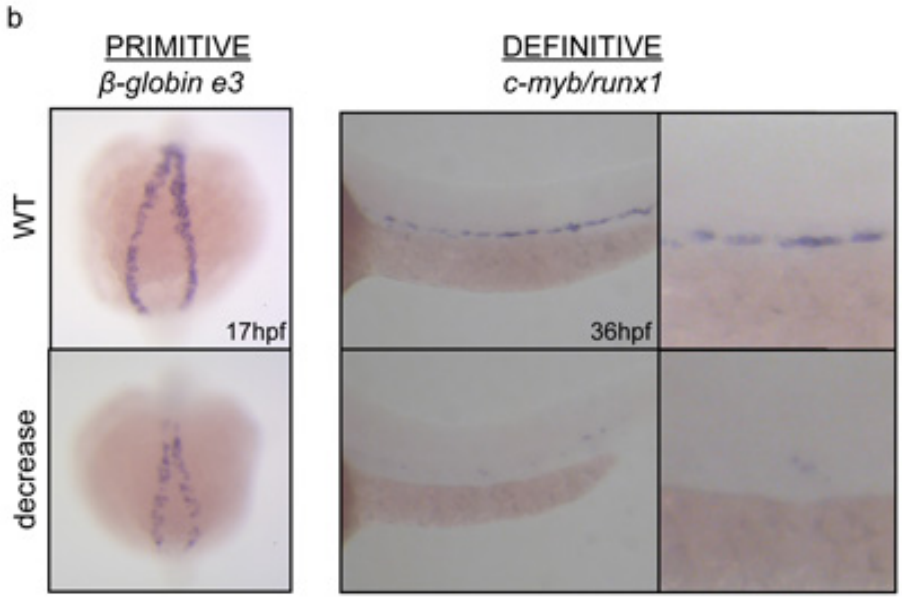

Figure 2-1. Continued.

(B) Example of screen phenotypes observed for reduced β-*globin e3* expression and *c-myb/runx1* in 17 hpf and 36 hpf embryos, respectively.

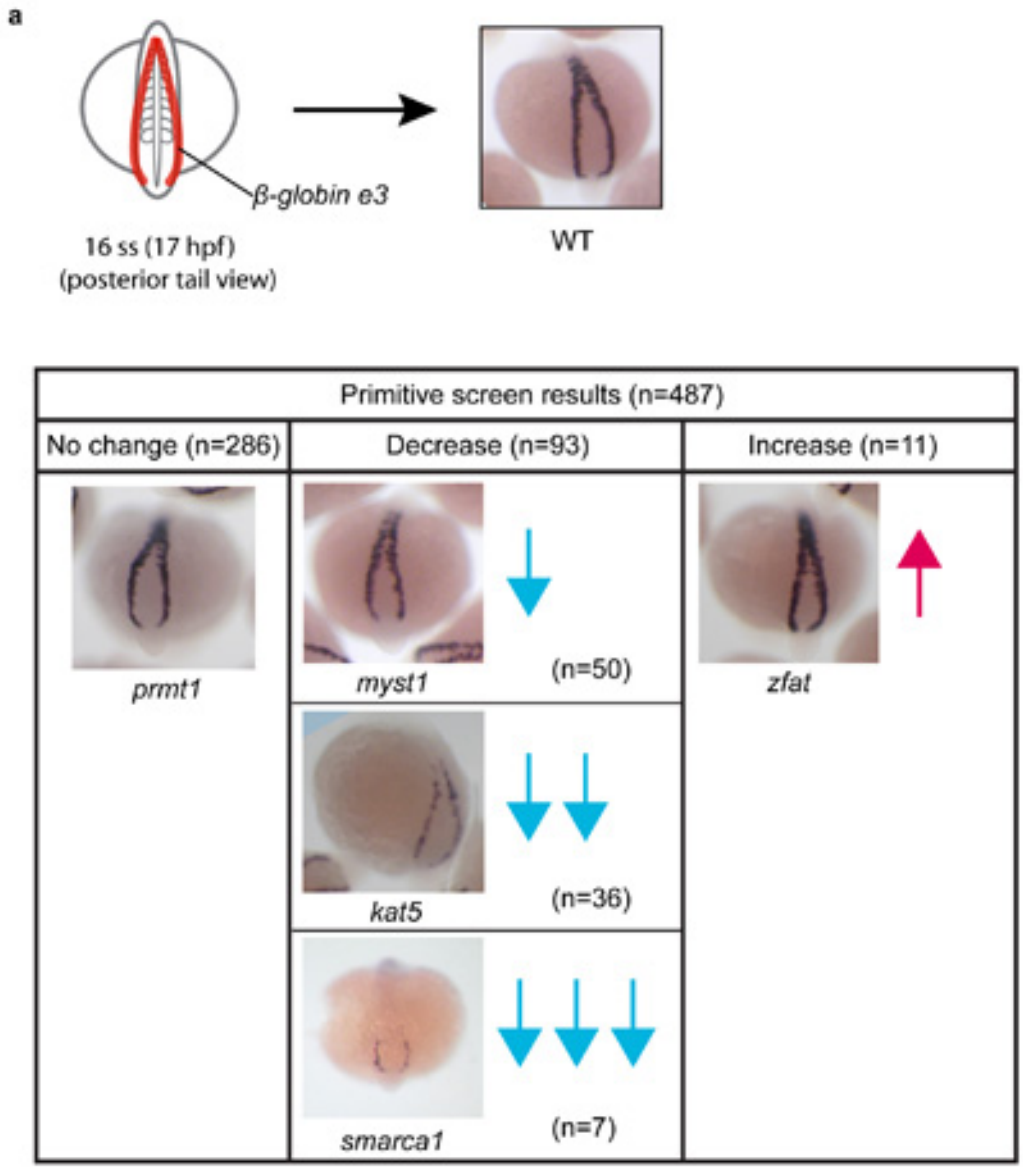

Figure 2-2. Summary of screen results.

(A) Primitive screen results.

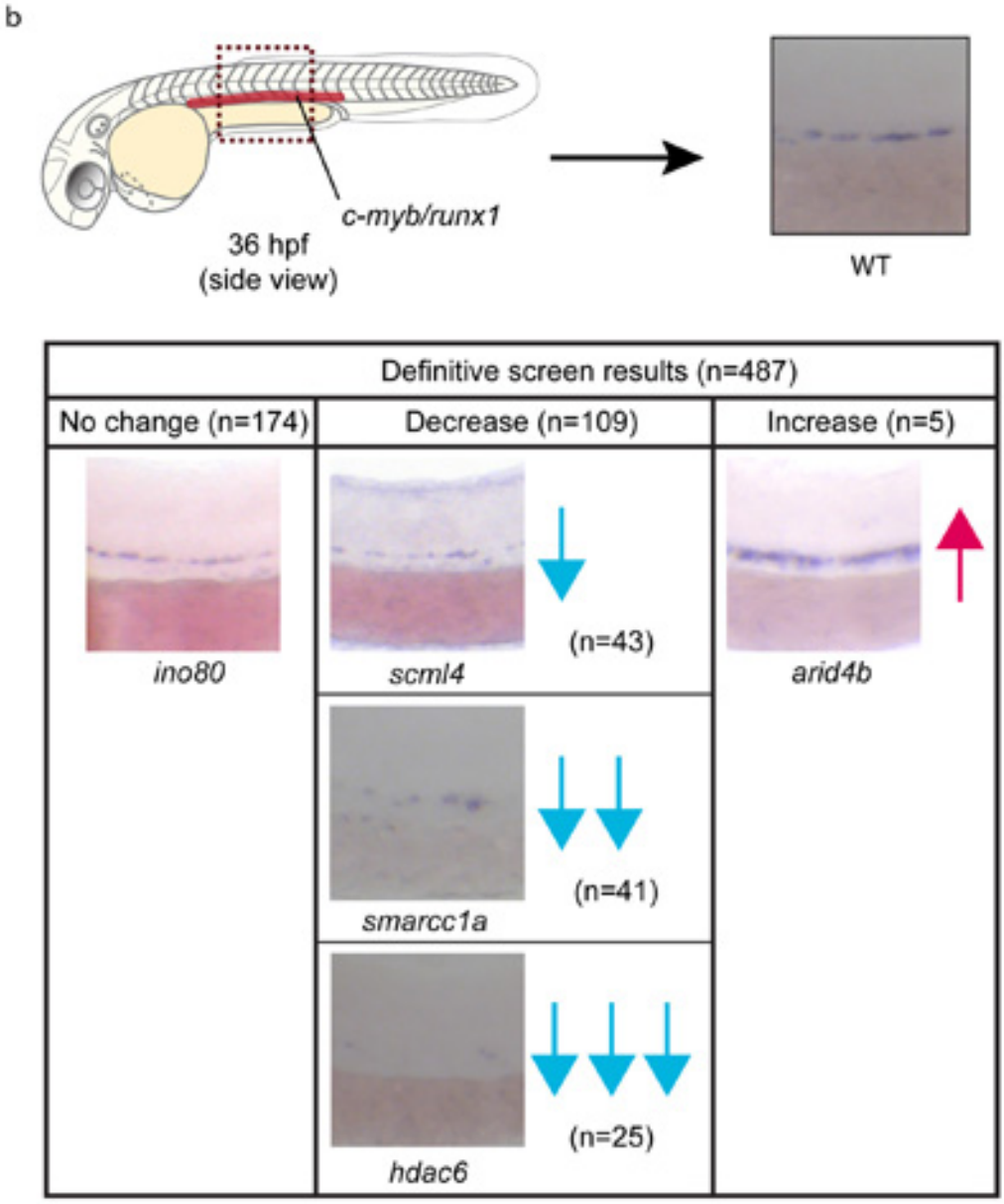

Figure 2-2. Continued.

(B) Definitive screen results. Blue downward arrows represent reduced expression of the marker, with three arrows representing the strongest reduction. Red upward arrows represent increase in marker expression.

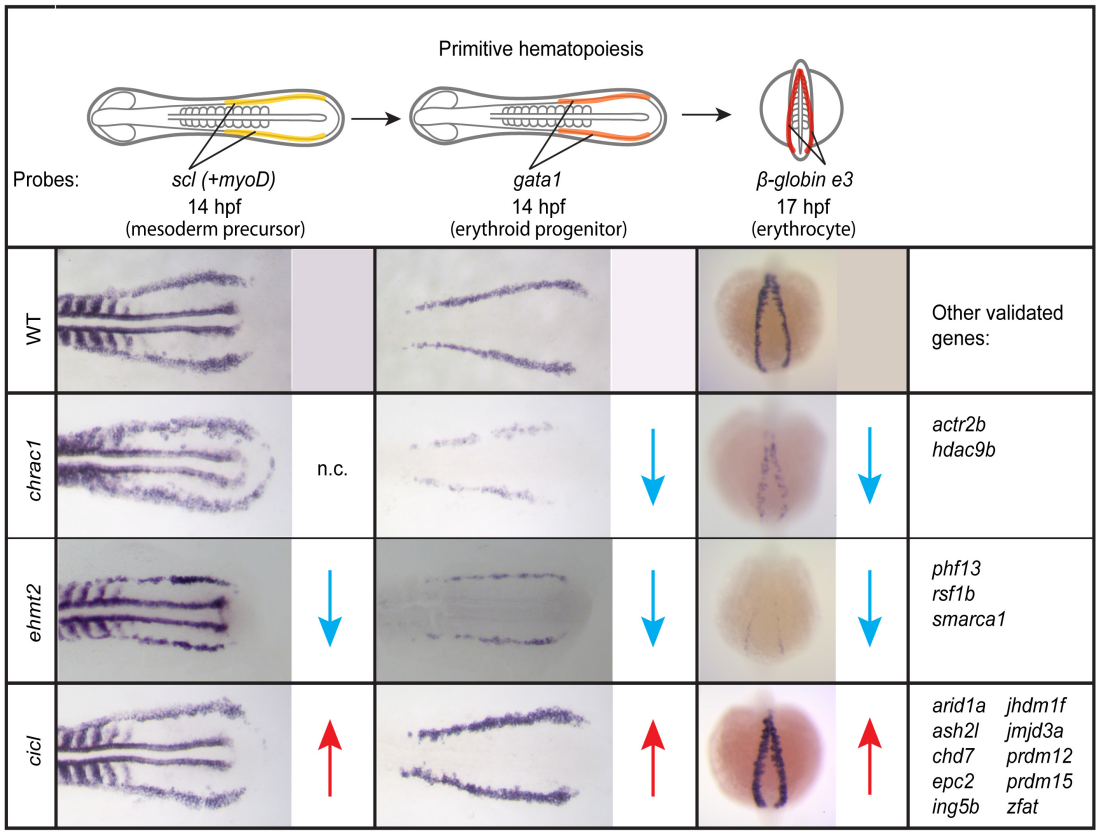

Figure 2-3. Chromatin factors regulate distinct steps of primitive hematopoiesis. Blue downward arrows mean decreased expression. Red upward arrows mean increased expression. n.c. means no change in marker expression.

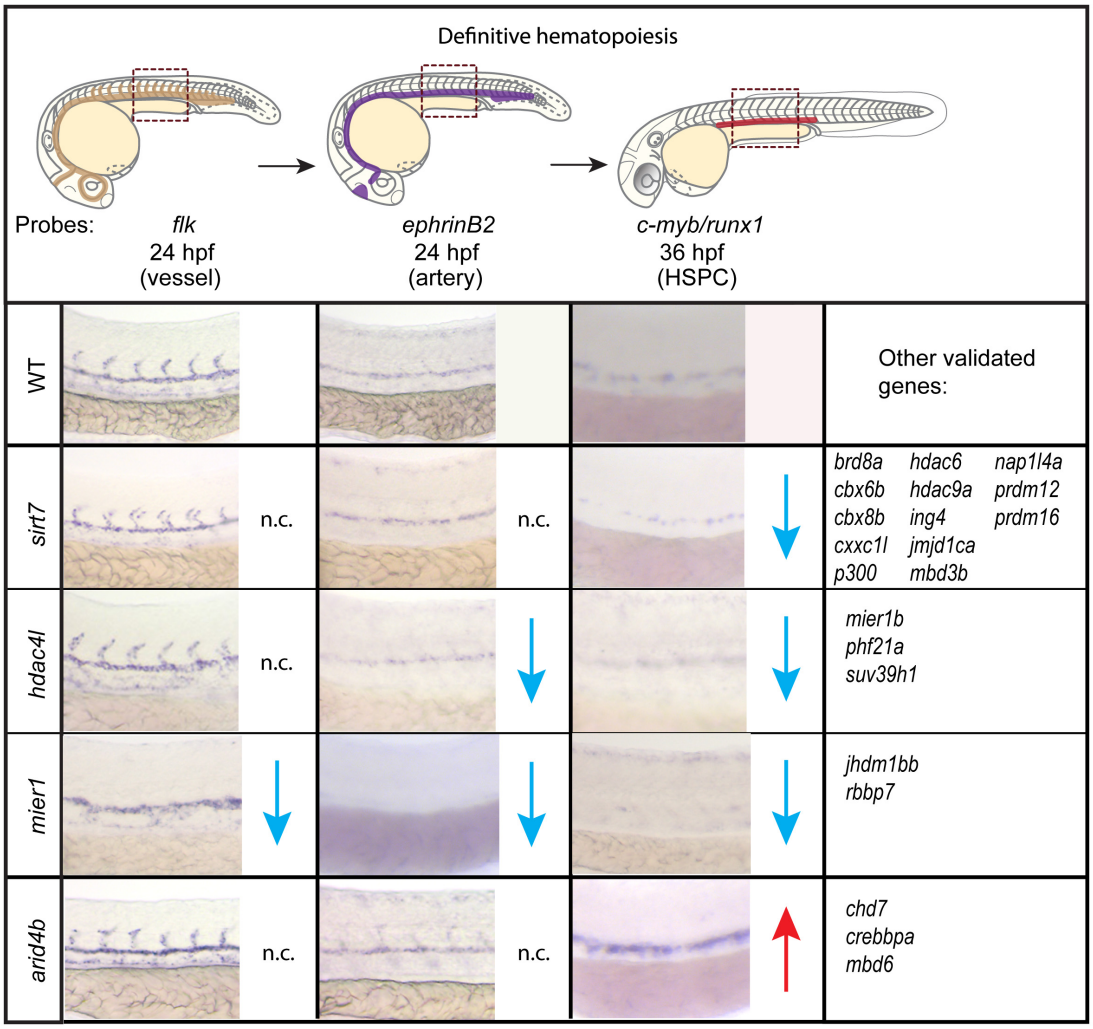

Figure 2-4. Chromatin factors regulate HSPC induction. Blue downward arrows mean decreased expression. Red upward arrows mean increased expression. n.c. means no change in marker expression.

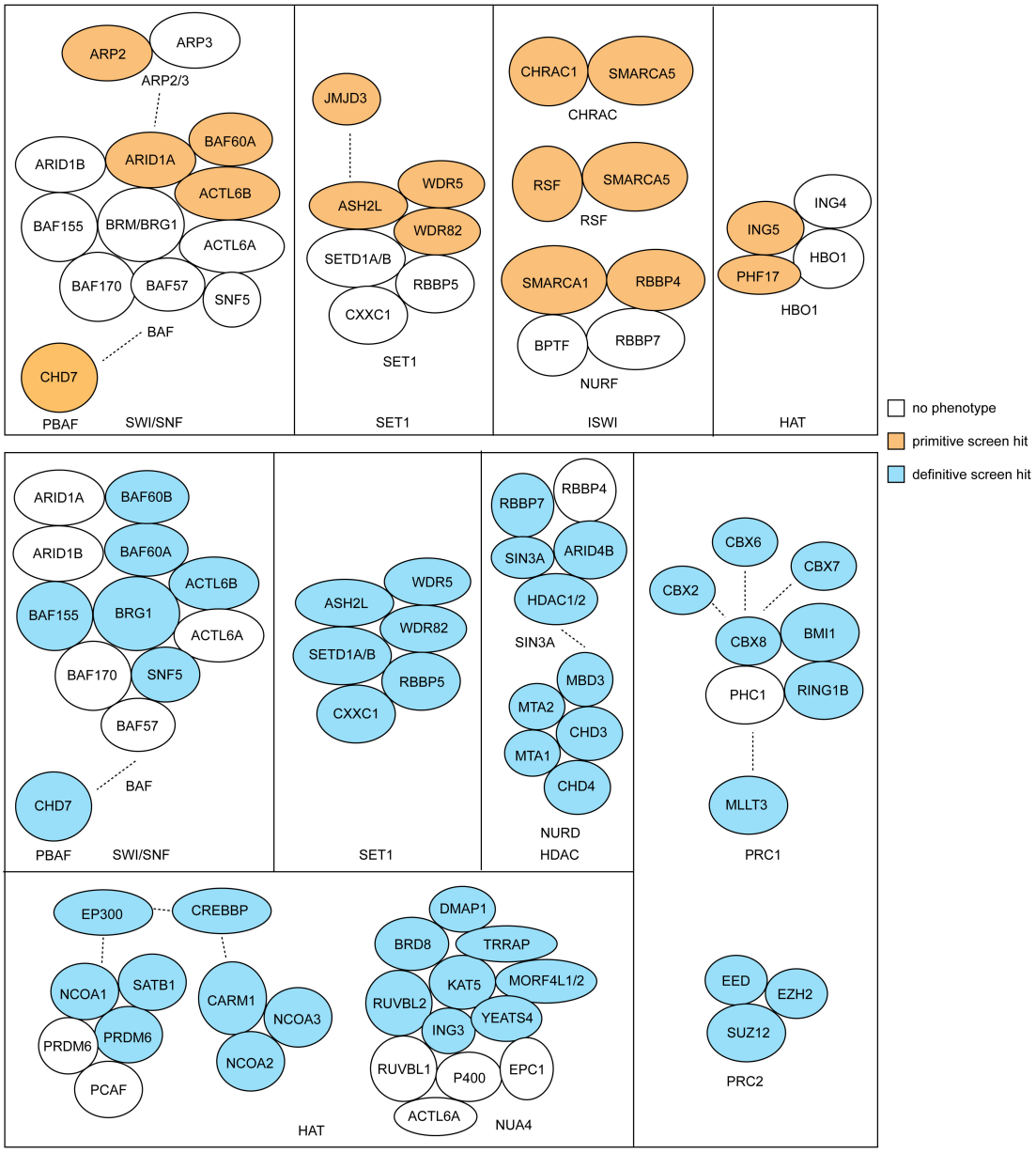

Figure 2-5. Screen hits map to known chromatin modifying complexes. Filled in circles represent chromatin factors that were called as screen hits.

Chapter 3

The chromatin factor *chd7* is a cell autonomous regulator of hematopoiesis

Attributions

I performed all the experiments described in this chapter. CHD7 ChIP-seq data was obtained from the Bernstein lab (Ram et al 2011). Anthony Dibiase helped generate peak files used for MEME motif and GREAT analysis. Jian Xu generated the Flag-cMYB K562 cell line that was used for co-immunoprecipitation experiments (Orkin lab). Andrew Woo performed gel filtration of K562 protein extracts (Cantor lab). Full length human CHD7 construct was obtained from Wysocka lab (Bajpai et al 2010).

Introduction

Gene regulation involves the changing of chromatin structure to control access of cellular factors to DNA. The different mechanisms that regulate chromatin structure include DNA methylation, histone modifications, and nucleosome remodeling, and these modifications are catalyzed by specific protein domains of chromatin modifying factors. For example, histone lysine methylation can be catalyzed by SET domain containing enzymes such as MLL while histone lysine acetylation is catalyzed by HAT domain containing enzymes such as MOF (Li et al 2007). These modifications are then recognized by additional factors containing specific modules like PHD and bromodomain domains that can bind the methylation and acetylation marks, respectively. These modifications can act combinatorially to regulate gene transcription.

Unlike histone lysine acetylation which almost always correlates with active transcription, lysine methylation can be either activating or inhibitory depending on the histone residue that is modified. H3K4 methylation correlates with active transcription whereas methylated H3K27 is a repressive mark. Thus chromatin factors that recognize these methylation marks would be important subunits of transcriptional complexes to help 'read' the chromatin state of a gene locus. One such group of chromatin factors is the chromodomain (CHD) family of proteins.

In vertebrates, there are nine factors that belong to the CHD family, and they are characterized by tandem chromodomains, which bind methylated histone tails, followed by a catalytic Snf2 helicase domain. The family is subdivided into three groups, CHD1-2, CHD3-5, and CHD6-9, and most of them have been shown to play important roles in transcriptional regulation. CHD1 regulates embryonic stem (ES) cell pluripotency genes (Gaspar-Maia et al 2009). CHD3 and CHD4 are subunits of the repressive NuRD chromatin remodeling complex (Xue et al 1998). CHD5 is a tumor suppressor that regulates p53 target genes (Bagchi et al 2007). CHD8 regulates cell cycle and β-catenin target genes (Rodriguez-Paredes et al 2009, Thompson et al 2008).

Among the nine CHD proteins, CHD7 is of particular interest. *De novo* mutations of CHD7 are found in 67% of CHARGE (Coloboma of the eye, Heart malformations, Atresia of the choanae, Retardation of growth, Genital hypoplasia and Ear abnormalities and deafness) syndrome patients (Zentner et al 2010). Several studies have been conducted to study the function of CHD7 during development to help understand the pathological basis of CHARGE syndrome. Chd7 mutant mice display many features of CHARGE syndrome, including postnatal growth retardation, inner ear malformations, genital hypoplasia, and olfactory defects (Bosman et al 2005, Bergman et al 2010, Hurd et al 2010).

Genome-wide localization studies revealed CHD7 binding predominantly at enhancer sites (Schnetz et al 2009, Schnetz et al 2010). Biochemical purification of CHD7 revealed associations with PBAF complex to regulate human neural crest stem cells development (Bajpai et al 2010). Taken together, CHD7 has broad functions throughout development, though much remains unknown about its precise mechanism of action.

In our reverse genetic chromatin modifying factor screen in zebrafish, we identified *chd7* as a novel and potent regulator of hematopoiesis. During early embryonic development in vertebrates, two waves of hematopoiesis establish blood formation in the embryo. The first and primitive wave produces mainly red cells whereas the definitive wave produces all the hematopoietic cell types required to sustain the organism for the remainder of its life, most importantly the hematopoietic stem cell (HSC). Knockdown of *chd7* increased both primitive and definitive blood formation, suggesting that *chd7* acts as a repressor of hematopoiesis. Blastula transplantation experiments demonstrated that this effect is cell autonomous. To identify gene targets of CHD7, ChIP-seq performed in K562 human erythroleukemia cells revealed an underlying MYB motif, and gel filtration analysis showed co-elution of CHD7 and MYB, suggesting an interaction between the two factors in the regulation of the hematopoietic transcriptional

program.

Results

Knockdown of chd7 results in increased HSPC formation.

For the chromatin factor knockdown screen described in detail in Chapter 2, a morpholino targeting exon 4 of *chd7* was used. *chd7* is a large gene composed of 40 exons encoding a transcript nearly 10kb in size, and exon 4 lies just before the sequences that encode the chromodomains (Figure 3-1A). The morpholino was injected into 1-cell stage zebrafish embryos, and the injected embryos, or morphants, and uninjected controls were subsequently collected at 36hpf and stained for the combination of hematopoietic stem and progenitor cell (HSPC) markers *c-myb* and *runx1* by whole-mount *in situ* hybridization (WISH). The stainings showed an expansion of HSPC markers in the aorta gonado mesonephros (AGM) region in the morphants compared to uninjected wild-type control embryos, suggesting *chd7* functions as a repressor. To verify the phenotype, knockdown of *chd7* using a second morpholino targeting exon 3 of the gene resulted in the same phenotype. By qPCR, the morphants have a 1.5-2 fold increase in *c-myb* and *runx1* expression (Figure 3-1D). Injection of both morpholinos resulted in the most robust phenotype, thus all subsequent experiments were performed with co-injections of exon 3 and 4 morpholinos (Figure 3-1C).

To determine whether the splice blocking activities of the morpholinos would result in a knockdown of *chd7*, RT-PCR was performed to test for the presence of splice variants in the morphants (Figure 3-1B). The PCR products were subsequently cloned, and sequencing revealed that exon 3 splicing morpholino results in the deletion of 276 bp of that exon whereas exon 4 splicing morpholino resulted in a 31 bp insertion at the end of exon 4. Both splicing defects resulted in a frameshift that introduced stop codons immediately following the splice junctions, indicating that Chd7 should be truncated after amino acid 656, deleting all annotated functional domains of this protein.

The increase in *c-myb* and *runx1* expression in *chd7* morphants reflects increased hematopoietic cell production. *chd7* morpholinos were injected into *Tg(c-myb:GFP)* embryos, and confocal imaging of transgenic embryos revealed an increase in GFP-positive cells both in the AGM and in the caudal hematopoietic tissue (CHT). (Figure 3-1E). Quantification revealed a near 50% increase of GFP-positive cells in the morphants. Given that *c-myb* is expressed in various cell types, including the spinal cord and pronephric cells, the experiment was repeated in *Tg(cd41:GFP)* embryos with similar results (data not shown). Conversely, overexpression of full length human CHD7 by mRNA injection into the single-cell of *Tg(c-myb:GFP)* and *Tg(lmo2:dsRed)* double transgenic embryos

suppressed the formation of GFP positive cells in the AGM (Figure 3-1F). In summary, knockdown of *chd7* results not only in increased hematopoietic gene expression but also in hematopoietic cell expansion.

Loss of chd7 enhances all stages embryonic hematopoiesis.

Given that knockdown of *chd7* leads to increased formation of HSPCs, we examined whether other hematopoietic cell types were also expanded over the course of embryonic development. The first and primitive wave begins with the formation of *scl*$^{+}$ mesodermal precursors that differentiate into *gata1*$^{+}$ erythroid progenitor cells which subsequently begin to express *β-globin e3* as they differentiate into red cells. All these cell types were expanded in *chd7* morphants (Figure 3-2A). The primitive myeloid lineage was also expanded as can be seen by the increase in the number of *pu.1*$^{+}$ and *mpo*$^{+}$ cells. Given that *scl* was expanded as early as 5 ss (12 hpf), we examined mesodermal markers *eve1* and *brachyury* but did not observe an expansion of the mesoderm during gastrulation at 6 hpf. Consequently, *chd7* not only functions in hematopoietic cells but also in early mesodermal precursors competent to undergo hematopoiesis.

Enhanced blood formation in *chd7* morphants extends beyond the formation

of HSPCs in the AGM during the definitive wave (Figure 3-2B). At 5 dpf, hematopoiesis has shifted to the CHT in the tail, the equivalent of fetal placenta/liver hematopoiesis in mammals. HSPC and myeloid marker c-*myb* was upregulated in *chd7* morphants, as well as larval erythroid*β-globin e1* expression. Increased number of circulating thrombocytes could be seen in *Tg(cd41:GFP)* morphant embryos. The lymphoid marker *rag1* was expressed normally, although at times the size of the thymus can be smaller than that of wild-type embryos. Patients with CHARGE syndrome have been described with a defective thymus, suggesting that CHD7 is involved in thymic development, and thus, the *rag1* phenotype may be due to impaired formation of the thymus and not due to defects in the hematopoietic lineage.

chd7 acts cell autonomously to regulate stem cell formation.

Because morpholino knockdown occurs throughout the entire embryo, other mesodermal tissues were examined for changes in gene expression in *chd7* morphants. *myoD* expression in the developing somites and *flk* in the developing vasculature appeared normal. *nkx2.5* is reduced in cardiomyocytes. Like blood, pronephric ducts expressing *pax2a* was increased in *chd7* morphants (Figure 3-3A). Overall, *chd7* morphants appeared normal with a normal beating heart, and

thus these changes in gene expression do not seem to have significant functional effects on tissue development at these early embryonic stages.

Blastula transplantation experiments were performed to test the cell autonomy of the expansion of HSPCs. *Tg(c-myb:GFP)* embryos were first injected with a standard control or *chd7* morpholino. Dextran blue was included to trace the donor cells. Once embryos reached the blastula stage (3-4hpf), approximately 30 to 40 pluripotent blastula cells were transplanted into *Tg(lmo2:dsRed)* embryos at the equivalent stage and examined for the ability to form GFP positive *c-myb* cells located within the red fluorescent vasculature of the hosts at 36 hpf (Figure 3-3B). In three sets of transplantation experiments, there were more chimeric embryos transplanted with *chd7* morphant cells compared to controls (Figure 3-3C). Consequently, although knockdown of *chd7* affects multiple tissues, the expansion of blood in the morphants is a cell autonomous event.

chd7 is expressed ubiquitously during development.

To understand how *chd7* can have such a specific hematopoietic effect, we examined its gene expression pattern. Given the large size of the gene, three different probes encompassing the 5', middle, and 3' end of the gene were made.

The expression pattern detected by all three probes were identical. c*hd7* is maternally deposited and remains ubiquitously expressed until 2 dpf, when expression becomes restricted to the head and brain (Fiure 4).

Knockdown of *chd7* does not increase cell proliferation or cell death in the early embryo.

To determine whether the hematopoietic cell expansion is the result of increased cell proliferation or reduced apoptosis, phospho-histone H3 (pH3) staining and terminal deoxynucleotidyl transferase dUTP nick end labeling (TUNEL) assay was performed. As before, *chd7* morpholino was injected into 1-cell stage embryos and collected at different timepoints ranging from somitogenesis to 36 hpf. Mitotic cells were detected using an anti-phospho histone H3 antibody, and apoptotic cells were assayed by TUNEL staining for fragmentation of DNA. No significant differences were observed for both assays in the hematopoietic regions between wild-type uninjected and *chd7* morphant embryos at different stages (Figure 3-5A,B). However, at 5 dpf, an increase in cell proliferation was observed in the CHT by BrdU incorporation (Figure 3-5C). It is possible that cell proliferation is enhanced during the earlier stages, but that the pH3 antibody is not sensitive enough to detect it.

CHD7 is a potential regulator of cMYB.

To search for target genes that could cause the blood expansion phenotype observed in zebrafish *chd7* morphants, CHD7 ChIP-seq data from human erythroleukemic K562 cells was analyzed. The data was obtained from a large scale ChIP-seq study of human chromatin regulators in K562 and ES cells published previously (Ram et al 2011). Using a significance cutoff of 10^{-9}, 8,348 peaks were identified. Using the Genomic Regions Enrichment of Annotations Tool, the majority of CHD7 binding sites were distal to the transcriptional start site, consistent with previous studies (Schnetz et al 2009, Schnetz et al 2010). Binding peaks were found at the promoters of several hematopoietic genes including SCL, LMO2, NFE2, HBB, and RUNX1. Peaks were also found at the MYC locus as well as 119 MYC target genes, an important regulator of cell proliferation.

In a motif search of CHD7 binding sites using Multiple Em for Motif Elicitation (MEME) analysis, an underlying MYB motif was identified (Figure 3-6A). Western blot of K562 nuclear extracts after gel filtration showed co-elution of CHD7 and MYB in the same protein fraction corresponding to a size of 1.4 MDa, a size much larger than either MYB (75kDa) or CHD7 (~300kDa) alone

(Figure 3-6B). However, no direct interaction between MYB and CHD7 was detected by co-immunoprecipitation. It remains possible that they may still be present in the same complex.

To test for genetic interaction between *chd7* and *c-myb*, *chd7* morpholinos were injected into *cmyb*^{t25127} mutant zebrafish embryos. The mutant allele contains a missense mutation in the DNA binding domain of *c-myb,* and the mutants progressively lose all definitive hematopoietic lineages starting from 2 dpf (Soza-Reid et al 2010). Embryos were grown to 36 hpf and collected for WISH to examine the patterns of *c-myb* and *runx1* expression. None of the genotyped embryos in the initial experiment were homozygous mutant for *c-myb*, thus the experiment will be repeated.

Discussion

In this study, *chd7* was found to be a potent repressor of embryonic hematopoietic cell development. Knockdown of *chd7* resulted in increased primitive and definitive hematopoiesis from the earliest stage of *scl*$^{+}$ mesodermal precursor formation at 12 hpf up to the formation of definitive blood lineages at 5 dpf. Given the early hematopoietic phenotype, *chd7* likely functions at the stem and progenitor level. Gene expression of Chd7 from sorted blood populations in mice show high expression of Chd7 in various cell types such as granulocytes and neutrophils in the myeloid lineage and natural killer, T, and B cells from the lymphoid lineages, suggesting that CHD7 may also regulate later stages of HSC differentiation (Beerman et al 2010).

It is not surprising that knockdown of *chd7* affects multiple tissues given its ubiquitous expression during embryonic development and the range of defects exhibited by knockout mice and human CHARGE syndrome patients. Although embryos injected with *chd7* exon 3 and 4 splice blocking morpholinos appeared relatively normal, contrary to the embryonic lethal phenotype of knockout mouse embryos, this is likely due to preservation of maternal transcript required during the earliest stages of embryonic development. Indeed, translation blocking morpholinos targeted against *chd7* mRNA in zebrafish embryos

resulted in general malformations such as defective retinal differentiation, reduced number of motor neurons, loss of bone mineralization, and improper vascular segmentation (Patten et al 2012). It is also possible that the remaining 656 amino acids in the N-terminus after morpholino induced splice blocking may have residual activity, although no annotated domains exist within that region to allow prediction of possible functions it may have. Whole mount immunohistochemistry for Chd7 using the available mouse CHD7 antibody to help verify the knockdown is ongoing. Nevertheless, the exon 3 and 4 splice blocking morpholinos worked to elucidate the role that *chd7* has in hematopoiesis, and it is cell autonomous.

There are multiple ways by which the blood expansion phenotype caused by loss of *chd7* might have occurred. Although increased cell proliferation was the most likely mechanism, no increase in mitosis was observed by pH3 staining. However, CHD7 binding to MYC and MYC target genes were found in K562 cells, suggesting that CHD7 may be involved in regulating cell proliferation. BrDU remains to be tested at the earlier stages to verify this phenotype. Another possible mechanism would be a fate change from other tissues to blood. Given the lack of mesoderm expansion during gastrulation and the preservation of other posterior mesodermal tissues tested (somites, vasculature, pronephros),

this is not likely the case. An interesting alternative would be enhanced self-renewal of the HSPCs. However, this hypothesis would require the use of other systems such as Chd7 conditional knockout mice in which established assays are available to answer this question. Thus *chd7* may not only regulate proliferation of hematopoietic cells but also the self-renewal of HSPCs.

The identification of the MYB motif from CHD7 ChIP-seq binding sites in K562 cells hinted towards a potential interaction that could account for the hematopoietic expansion phenotype observed in *chd7* morphants. Overexpression of c-Myb in ES cells has been shown to increase multilineage colony formation and self-renewal in culture whereas conditional knockout of the gene in mouse bone marrow resulted in defective self-renewal and multilineage differentiation of adult HSCs (Dai et al 2006, Lieu and Reddy 2009). Although CHD7 is generally associated with active transcription, the results in zebrafish suggest a model in which Chd7 limits the ability of *c-myb* to activate the hematopoietic program, and thus, knockdown of *chd7* leads to enhanced hematopoiesis. Although no direct interaction was observed by co-immunoprecipiation in K562 cells, the co-elution of both proteins by gel filtration is consistent with CHD7 and MYB being present in the sample complex. A protein pull-down with CHD7 may be able to identify MYB as an interacting

protein and provide additional clues about the mechanism of CHD7 function.

No specific hematopoietic defects have been identified in CHARGE patients with confirmed mutations in *CHD7*. A small number of patients have been shown to exhibit T cell deficiencies, but they also exhibit thymic aplasia, hence the T cell deficiency is probably non-cell autonomous. Bone marrow analysis would be required to determine whether there are any changes in hematopoiesis of in CHARGE syndrome patients.

Future studies addressing the mechanism of how CHD7 functions in HSPCs and multilineage differentiation are important for our understanding of hematopoiesis. Very few genes are known to regulate self-renewal of stem cells, and the studies presented here implicate *CHD7* as a strong candidate. It is an integral regulator of the hematopoietic program because all cell types within the hematopoietic lineage examined have been affected, which may be useful as a therapeutic target.

[Note added in proof. Recently, a direct interaction between CHD7 and the transactivation domain of RUNX1 was reported. Conditional deletion of Chd7 using Vav-Cre did not cause any lineage specific defects, but Chd7 deficient bone marrow cells had a competitive advantage in T cell reconstitution. Runx1 is

required for the emergence of HSCs, thus these results are consistent with those in the zebrafish. This presents another potential mechanism for the blood expansion observed in *chd7* morphants, namely loss of Chd7 releases the transactivation domain of RUNX1 resulting in increased RUNX1 activity.**]**

Materials and Methods

Zebrafish maintenance and microinjection.

Zebrafish (*Danio rerio*) Tüebingen strain were bred and maintained according to Animal Research guidelines at Children's Hospital Boston. Other lines used were *Tg(c-myb:EGFP)* (North et al 2007), *Tg(cd41:EGFP)* (Traver et al 2003), *Tg(lmo2:dsRed)* (North et al 2007), and *Tg(kdrl:RFP)* (Huang et al 2005). Embryos were developed at 25˚C or 28.5˚C and staged according to hours post fertilization (hpf) and morphological features (Kimmel et al 1995). Morpholinos were injected into the yolk, and mRNA was injected into the cell of 1-cell stage embryos. Injection volumes were measured using a stage micrometer to a droplet size of 1 nl (~124 μm in diameter).

Morpholino design and synthesis.

The FASTA sequence for the predicted *chd7* gene in zebrafish was downloaded from NCBI (XM_692864) and input into UCSC zebrafish genome browser to extract exon intron structure of the gene. 25 bps of exon and intron sequence was copied from exons 3 and 4 exon-intron junctions and submitted to Gene-Tools for morpholino oligo design and synthesis. Morpholinos were diluted in nuclease free water and concentrations measured in 0.1 N hydrochloric acid

on a Nanodrop following instructions provided by Gene-Tools. Morpholinos were heated briefly at 65˚C for five minutes prior to embryo injections to disrupt any secondary structures. Morpholino sequences were:

chd7 exon 3: ACTCGTTTATACTCTACACGTACCT

chd7 exon 4: TTACAAGCAAGTTTACCTGAACACC.

Whole-mount in situ hybridization and imaging

WISH on zebrafish embryos fixed in 4% paraformaldehyde was performed as described previously (Thisse and Thisse 2008). Digoxigenin (DIG)-labeled antisense RNAs were transcribed from linearized plasmid templates or PCR products with T7 or SP6 RNA polymerase according to the manufacturer's protocol (Roche). Antisense riboprobes used were *c-myb, runx1* (Kalev-Zylinska et al 2002), *gata1, scl* (Liao et al 1998), *β-globin e3* (Brownlie et al 2003), *β-globin e1, flk* (Thompson et al 1998), *ephrinB2* (Lawson et al 2002), *myoD, pax2a, nkx2.5, pu.1* (Lieschke et al 2002), and *mpo* (Bennett et al 2001).

Probes to detect *chd7* embryonic expression were generated from partial clones EDR1052-99603877 (*chd7* N-terminus), EXELIXIS4269886 (*chd7* Internal), and EDR1052-98884484 (*chd7* C-terminus) (Open Biosystems). Primers used were:

chd7-N-SP6(F) 5'-TAATTTAGGTGACACTATAGAAGAAGCTTGGCTGCACAGCAG-3'

chd7-N-T7(R) 5'-TATAATACGACTCACTATAGGGCCACCCATCACTTGCTGCTG-3'

chd7-I-SP6(F) 5'-TAATTTAGGTGACACTATAGAAGGCAGACTGGCTTGCTGACT-3'

chd7-I-T7(R) 5'-TATAATACGACTCACTATAGGGATAGGCTGTGATGAGGCGGC-3'

chd7-C-SP6(F) 5'-AATTTAGGTGACACTATAGAAGTCCGGATTCCCGGGATCTG-3'

chd7-C-T7(R) 5'- TATAATACGACTCACTATAGGGGGACCAGCGCGCACATCTTA-3'

Stained embryos were imaged using a Nikon stereoscope with a Nikon Coolpix 4500 camera or Zeiss camera. Embryos mounted in glycerol were imaged on a Nikon E600 compound microscope. Confocal imaging was performed on a Zeiss spinning disk confocal microscope using Volocity software for image acquisition.

RT- and qPCR

Pools of 20-50 embryos were collected in 500µl of TRIzol, and RNA extracts were prepared according to the manufacturer's protocol (Invitrogen). cDNA was prepared using the SuperScript III First Strand synthesis kit according to the manufacturer's protocol (Invitrogen). Primers used for RT-PCR were: *chd7ex2* forward: 5'-GGGCACCTACTCACCAATCA-3', *chd7ex4* reverse: 5'-GCCTCTTTCTTGGTGCTGTT-3', *chd7ex3* forward: 5'-TCCCAAGACACCCAAAGAAC-

3', *chd7ex5* reverse: 5'-GCCTCTTTCTTGGTGCTGTT-3', *ef1α* forward: 5'-ATCTACAAATGCGGTGGAAT-3', and *ef1α* reverse: 5'-ATACCAGCCTCAAACTCACC-3'.

qPCR was performed using SsoFast EvaGreen Supermix on the BioRad C1000 CFX-384 real-time PCR machine (BioRad). qPCR primers used were: *c-myb* forward: 5'-CCGACAGAAGCCGGATGA-3', *c-myb* reverse: 5'-TGGCACTTCGCCTCAACTG-3', *runx1* forward: 5'-CGTCTTCACAAACCCTCCTCAA-3', *runx1* reverse: 5'-GCTTTACTGCTTCATCCGGCT-3'. $^{\Delta\Delta}$Ct values were calculated using *ef1α* as the control gene.

Phospho-histone H3, TUNEL, and BrdU assays

The phospho-histone H3 and TUNEL assays were performed as described previously (Shepard et al 2005), followed by staining with diaminobenzidine/H_2O_2 (Invitrogen). For BrdU incorporation assays, live embryos were soaked for 20 minutes in 10mM BrdU/15% DMSO/E3 medium on ice. The solution was rinsed off three times with E3 and embryos were allowed to develop for another 15 minutes prior to fixation with 4% paraformaldehyde (PFA) overnight at 4°C. Embryos were subsequently dehydrated in methanol, rehydrated in PBT, treated with proteinase K, and re-fixed with 4% PFA. After

removal of PFA, embryos were rinsed with water and treated with 2N HCl for one hour before starting immunohistochemistry staining of whole embryos using mouse anti-BrdU and anti-mouse IgG-Alexa546 antibodies.

Blastula transplantation

Blastula transplantation was performed as described previously using an analog microinjector to transfer cells in 2% methylcellulose (Kemp et al 2009).

Co-immunoprecipitation.

Nuclear extracts were prepared from K562 cells expressing Flag-MYB. Immunoprecipitation was performed with anti-MYB (Millipore), anti-CHD7 (Abcam), or IgG (Santa Cruz), followed by Western blotting.

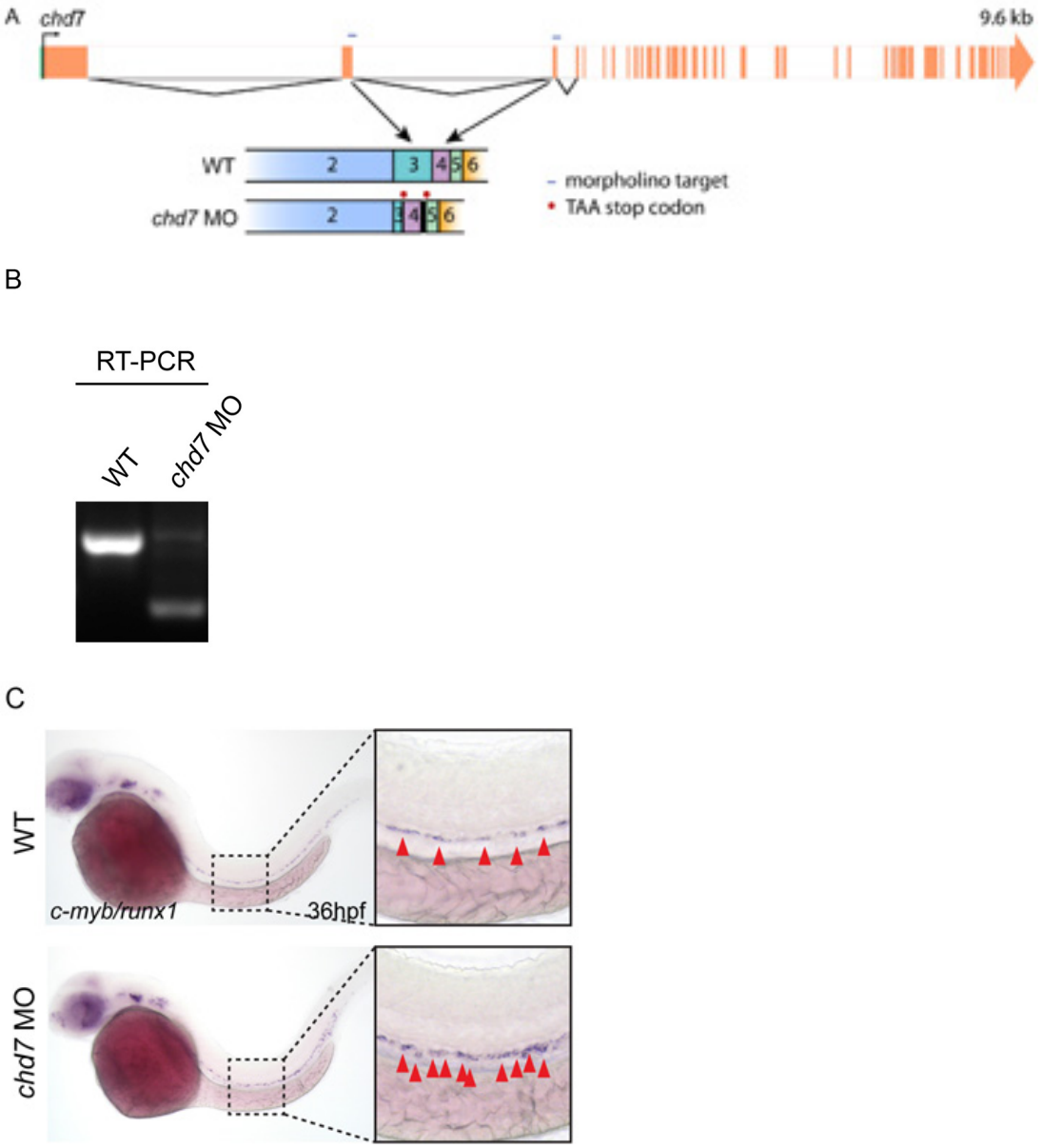

Figure 3-1. *chd7* regulates *c-myb*⁺ and *runx1*⁺ expression.

(A) Gene structure of zebrafish *chd7* with magnified view of exons 2-6 in wild-type uninjected controls and *chd7* morpholino injected embryos. Exon 3 and 4 splicing morpholinos induce a 276 bp deletion and 31 bp insertion, respectively, both resulting in the introduction of downstream stop codons.

(B) RT-PCR of wild-type control and *chd7* morphants show a smaller spliced product in the morphants.

(C) WISH of wild-type and *chd7* morphant embryos for combined expression of *c-myb* and *runx1*. The morphants show increased staining in the AGM. Red arrowheads point to stained cells.

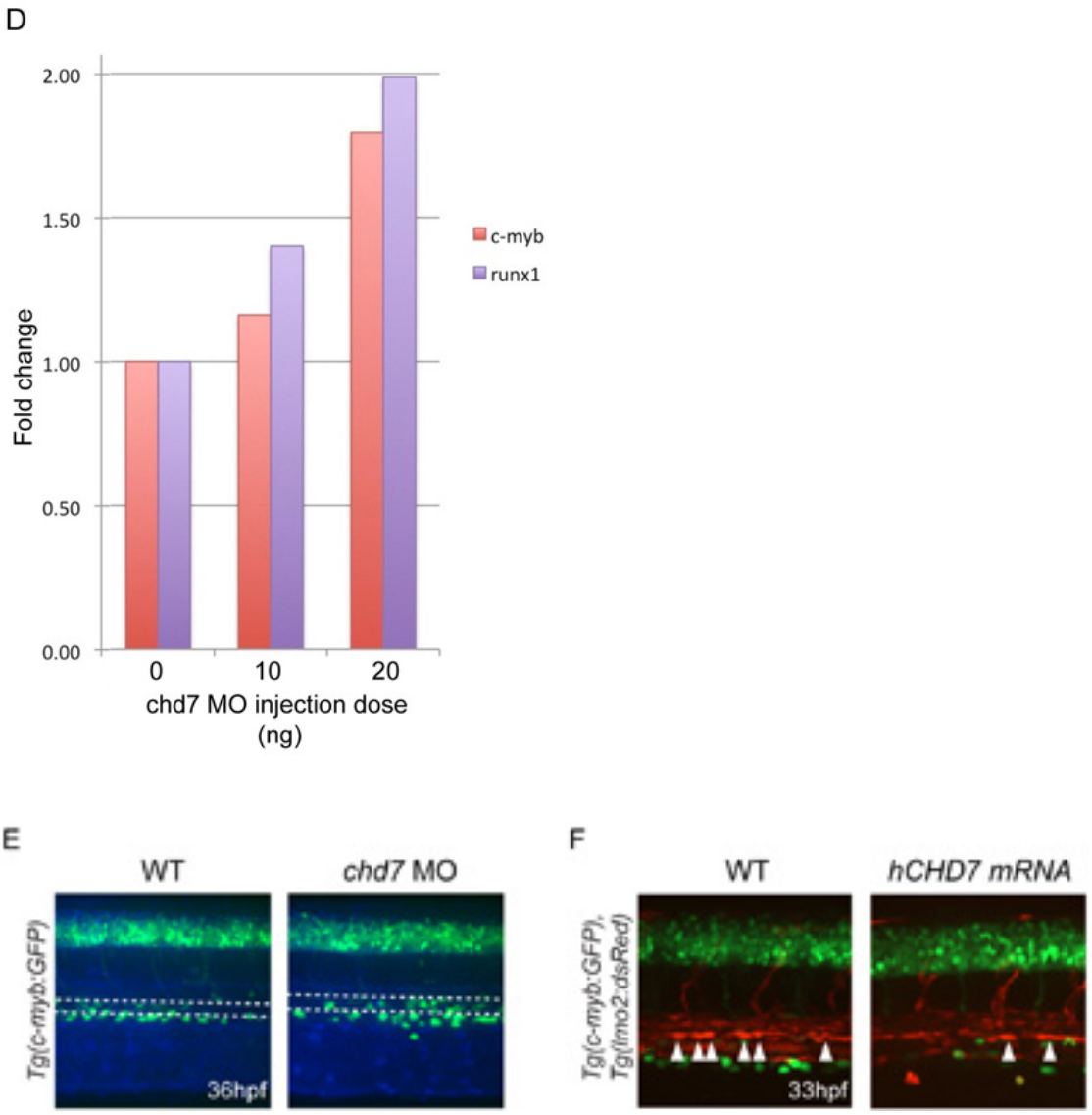

Figure 3-1. Continued.

(D) Quantification of *c-myb* and *runx1* by qPCR. Knockdown of *chd7* results in 1.5-2 fold increase in *c-myb* and *runx1* expression. EF1α was used as control gene.

(E) *Tg(c-myb:EGFP)* morphants show increase in GFP^{+} cells in the AGM region. White dotted lines mark the position of the aorta.

(F) Overexpression of human CHD7 by mRNA injection suppresses formation of *lmo2*$^{+}$ and *c-myb*$^{+}$ cells in the AGM region. White arrowheads point to hemogenic endothelial cells. Embryos are double transgenic for *Tg(c-myb:EGFP)* and *Tg(lmo2:dsRed)*.

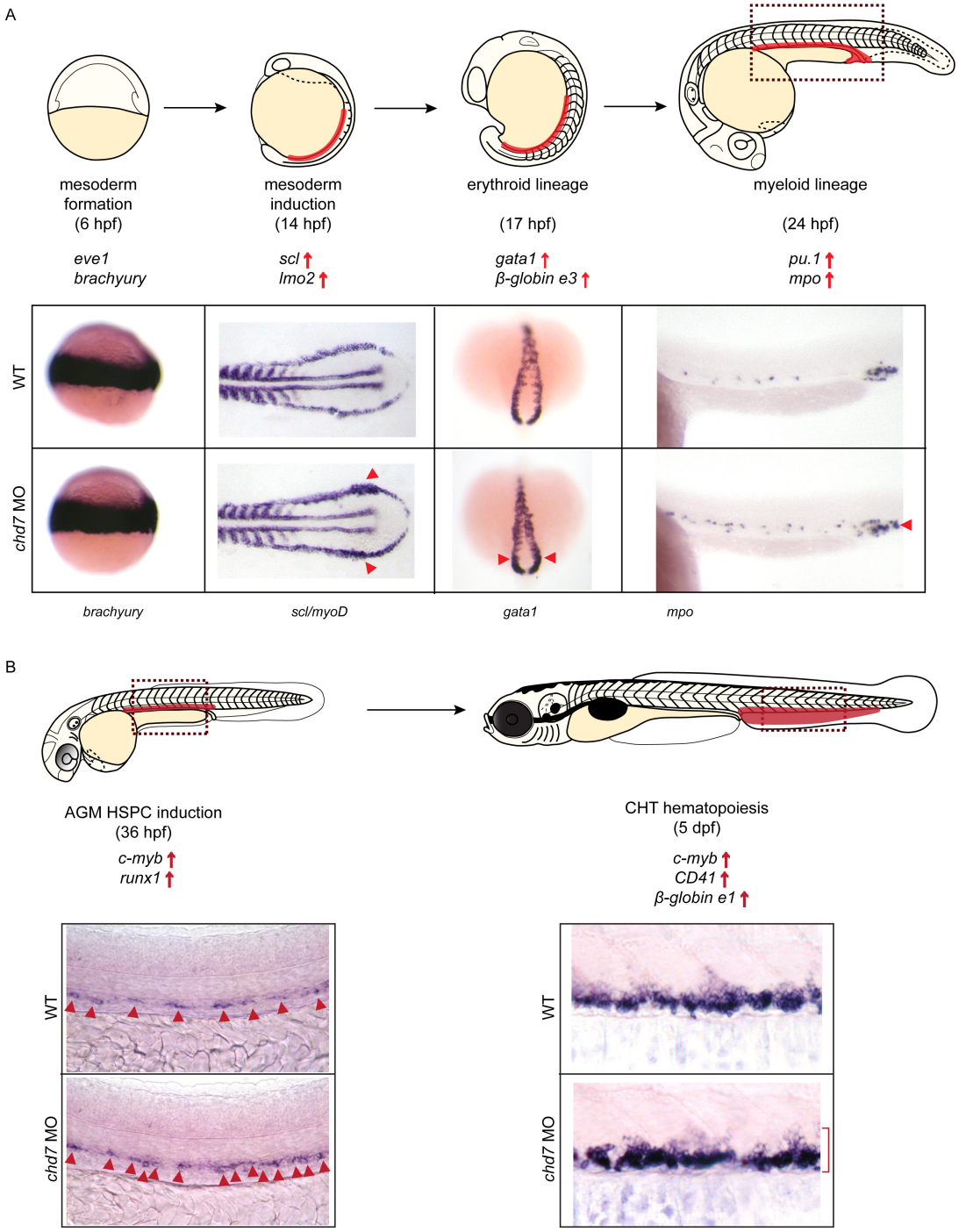

Figure 3-2. *chd7* regulates all stages of embryonic hematopoiesis.

(A) Knockdown of *chd7* increased primitive hematopoiesis, including hematopoietic mesoderm precursors, erythroid progenitors, and myeloid progenitors.

(B) *chd7* morphants also show increased definitive hematopoiesis, from the formation of HSPCs to later differentiation of myeloid progenitors, red blood cells, and thrombocytes. Red arrowheads and bracket indicate increased staining.

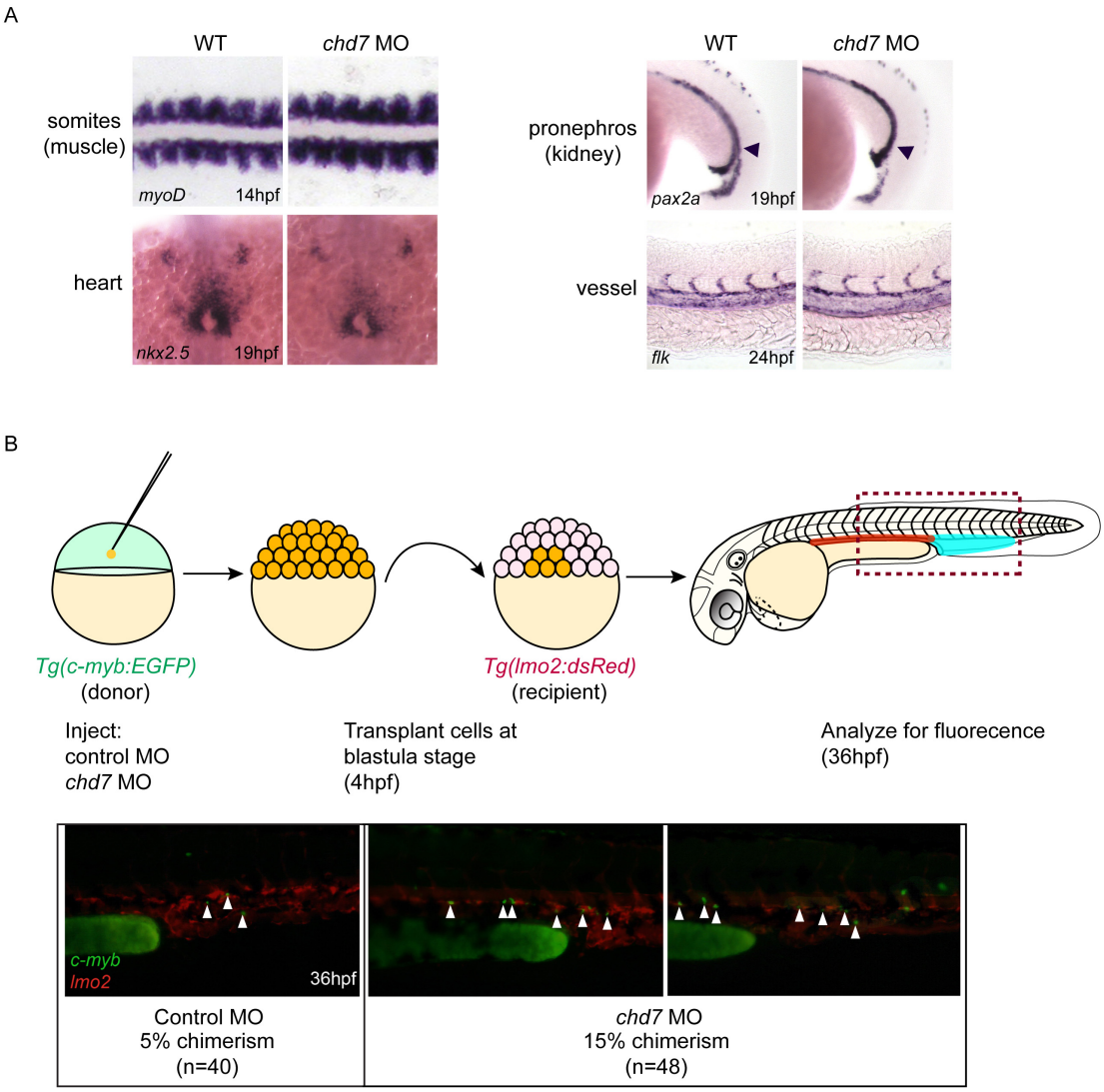

Figure 3-3. *chd7* regulates gene expression in multiple tissues but acts cell autonomously in blood.

(A) Gene expression of non-hematopoietic mesodermal tissues in *chd7* morphants. The heart domain marked by *nkx2.5* was reduced, but pronephric ducts showed increased *pax2a* expression in *chd7* morphants. Somites and vasculature were relatively unaffected. Black arrowhead points to pronephric ducts.

(B) Blastula transplantation experiments demonstrate cell autonomy of *chd7*. Control or *chd7* morpholino was injected in *Tg(c-myb:EGFP)* donor embryos, and blastula cells were subsequently transplanted into *Tg(lmo2:dsRed)* hosts. Chimeric embryos were scored for the number of GFP$^+$ cells in the AGM and CHT. Results of 1 of 3 experiments are shown. White arrowheads point to GFP$^+$ hematopoietic cells.

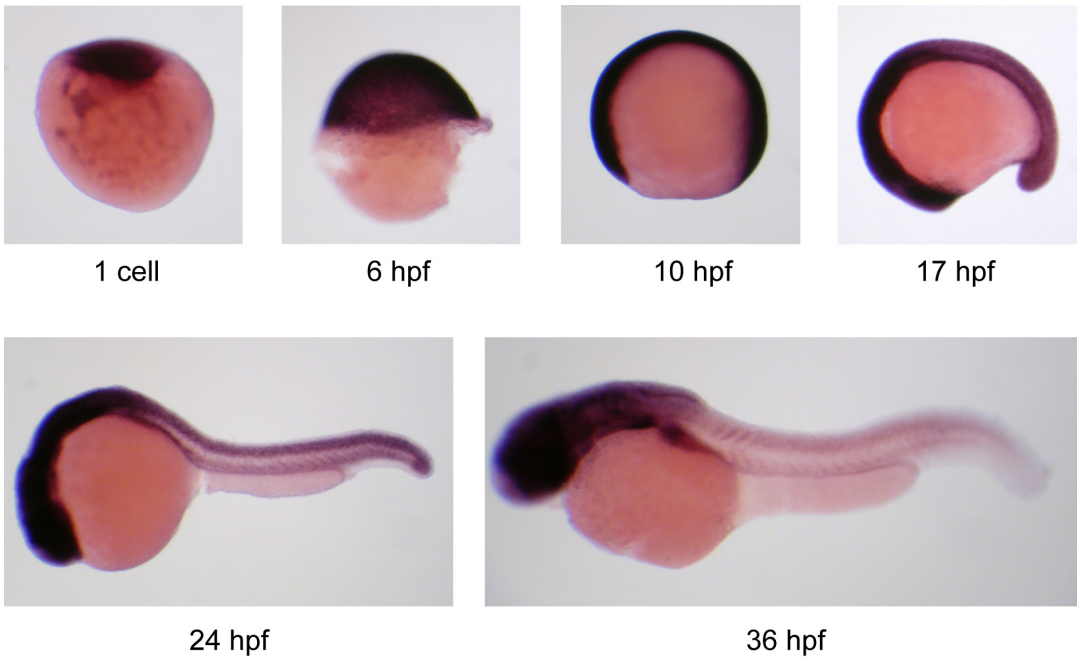

Figure 3-4. *chd7* is expressed ubiquitously during embryonic development. *chd7* mRNA is deposited maternally and is ubiquitously expressed until 24 hpf. Expression becomes highly restricted to the head by 36 hpf. A probe detecting the N-terminus of *chd7* was used.

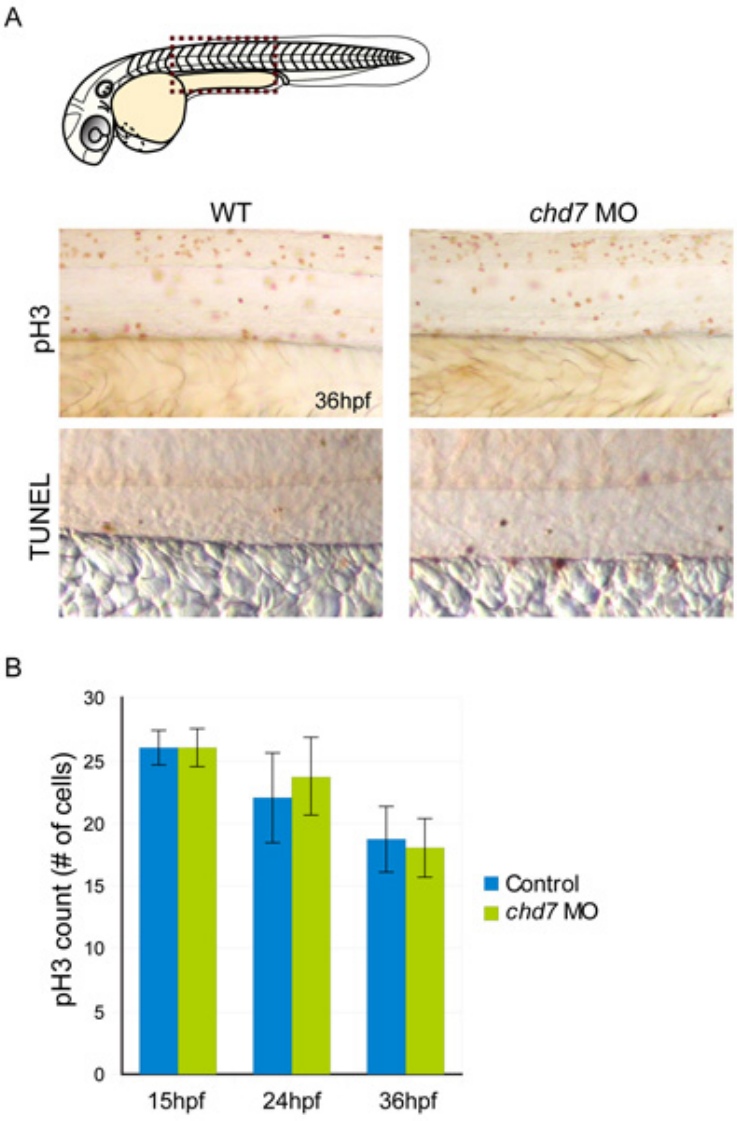

Figure 3-5. No major changes in cell proliferation or apoptosis during early stages of hematopoiesis in *chd7* morphants.

(A) Representative images of pH3 and TUNEL stained embryos in wild-type and *chd7* morphant embryos at 36 hpf showing comparable levels of staining.

(B) Quantification of pH3 at three different stages did not reveal significant differences in proliferation between wild-type and *chd7* morphant embryos.

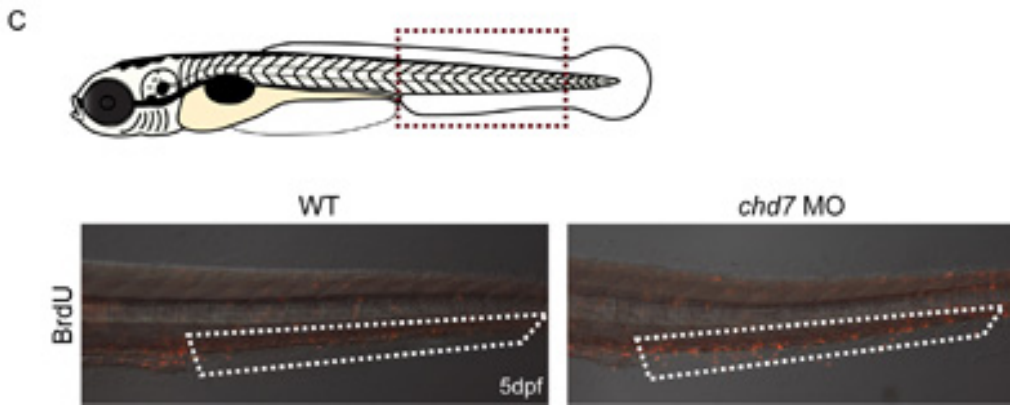

Figure 3-5. Continued.
(C) BrdU staining revealed increased cell proliferation was observed in the CHT at 5 dpf.

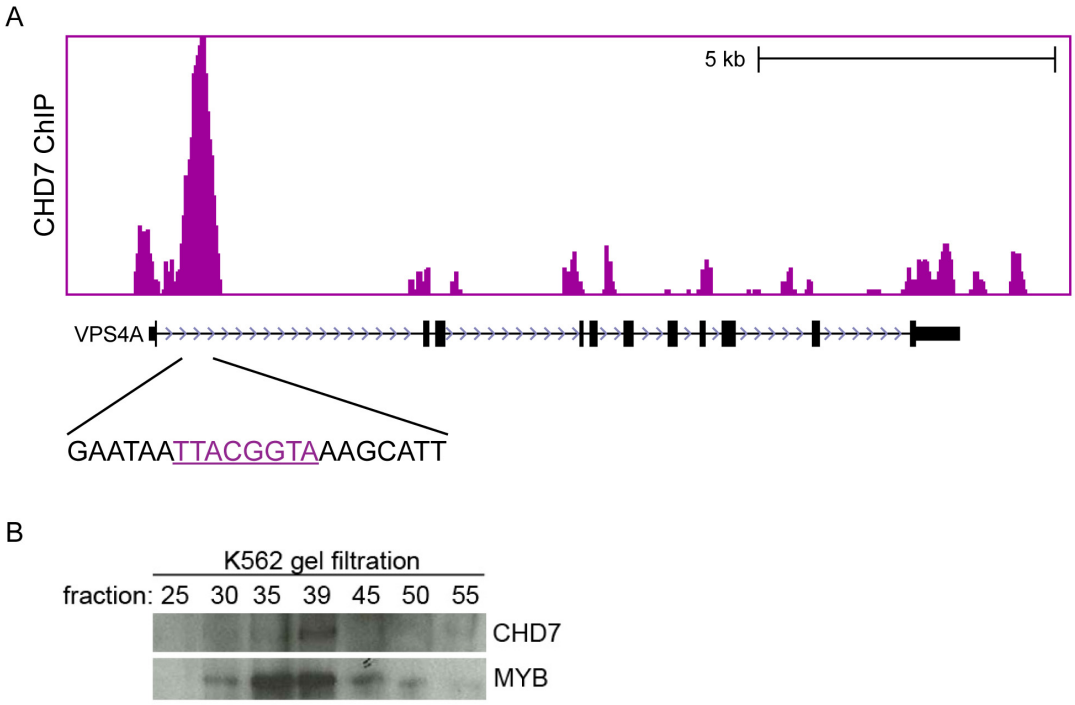

Figure 3-6. Identification of MYB as a putative CHD7 interacting factor.
(A) Over 200 peaks with an underlying MYB motif were identified. VPS4A as a representative gene is shown with peaks indicating CHD7 binding the MYB motif sequence. Peak height is 33.
(B) Western blot for CHD7 and MYB in several protein fractions eluted from a gel filtration column loaded with nuclear extract from K562 cells. Both proteins are present in fraction 39 corresponding to a molecular weight of 1.4 MDa.

Chapter 4

Chromatin factors *unk* and *jmjd2b* are critical regulators of embryonic development and hematopoiesis

Attributions

The *unk* studies were performed in collaboration with Jernej Murn from the laboratory of Yang Shi. I designed morpholino sequences to knockdown *unk* in zebrafish embryos, injected morpholinos, performed acridine orange staining, whole-mount immunohistochemistry stainings, and confocal imaging. Katie Kathrein assisted with embryo injections, acridine orange stainings, and performed the *unk* mRNA rescue experiment.

The *jmjd2b* studies were performed in collaboration with Partha Das from the laboratory of Dr. Stuart Orkin. I designed *jmjd2b* morpholinos, performed injections, and WISH. Katie Kathrein assisted with embryo injections. Cong Xu assisted with WISH.

Introduction

Regulating the structure of chromatin is essential to compact 1.7 meters of DNA into a 5 micrometer nucleus inside a mammalian cell. This is achieved by wrapping DNA around specialized histone proteins to form nucleosomes, which can subsequently be compacted into higher order structures. In addition, chromatin must remain malleable enough to allow the cell to change its conformation in order to adjust gene expression programs in response to diverse stimuli (Bernstein et al 2007).

Many different types of chemical modifications executed by specific protein domains of chromatin modifiers can be used to alter the structure of chromatin. These include cytosine methylation on the DNA and lysine and arginine methylation, lysine acetylation, serine phosphorylation, and lysine ubiquitination on the histone proteins (Li et al 2007). The majority of the enzymes that catalyze these modifications have been identified.

The radical S-adenosylmethionine (SAM) domain was identified computationally a decade ago and subsequently mapped to over 600 proteins. The proteins of this large superfamily catalyze diverse chemical reactions via a conserved domain of cysteine residues (CxxxCxxC) that harbor an iron cluster $[4Fe\text{-}4S]^{1+}$, a strong reducing agent, that is used to generate a radical, 5'-

deoxyadenoxyl, by cleavage of SAM (Sofia et al 2001). This reaction has been implicated in DNA repair and demethylation (Chandor-Proust et al 2008, Okada et al 2010). *Elp3,* an important catalytic subunit of the transcriptional elongation complex, also contains a radical SAM domain (Wittschieben et al 1999). Because of the diverse and large number of proteins found in this family, many radical SAM domain containing factors have not been well characterized. Of the radical SAM factors included in our chromatin factor screen, we identified a putative role for *unkempt (unk)* in the induction of definitive hematopoietic stem cells (HSCs) since *unk* morphants lose *c-myb* and *runx1* expression in the aorta gonad mesonephros (AGM) region at 36 hours post fertilization (hpf). Furthermore, we discovered that *unk* is essential for proper nervous system development as early degeneration of the entire neuroectodermal tissue occurs in the absence of *unk*.

Although the occurrence of histone methylation marks have been known for a long time, histone demethylating enzymes,Lsd1 and Jumonji (JmjC) domain-containing proteins have only been identified recently (Shi et al 2004, Tsukada et al 2006). Ample evidence has accumulated about the importance of these factors in development (Takeuchi et al 2006). In our chromatin factor screen, we discovered that one of the less characterized Jumonji proteins, *jmjd2b,* not only is a regulator of hematopoietic stem and progenitor cells but may also be one of the

critical factors required for the onset of gastrulation in the zebrafish embryo.

Results

Knockdown of *unk* results in widespread neural degeneration.

To characterize the neural defects observed in *unk* morphants, we co-injected *unk* morpholino with acridine orange to determine the degree of neural degeneration observed in the morphants at 28 hours post-fertilization (hpf). Wild-type uninjected embryos from the same clutch were used as controls. As expected, *unk* injected embryos showed a dramatic increase in green fluorescence, indicating cell death. They showed increased apoptosis throughout the entire central nervous system (CNS) including forebrain, midbrain, hindbrain, and the spinal cord (Figure 4-1A). This defect is specific to the depletion of *unk* and not due to general toxicity from the morpholino because the morphants can be rescued with co-injection of mouse Unk mRNA (data not shown).

unk expression is not initiated until after gastrulation. Once expressed, *unk* is ubiquitious, but after 24 hpf, its expression becomes highly restricted to the head and nervous system, consistent with the expression seen in *Drosophila* (Thisse et al 2004, Mohler et al 1992). Whole-mount immunohistochemistry using mouse UNK antibody detected Unk protein expression beginning after the onset of definitive neural formation in the brain at 24 hpf, marking only a few

neurons if any. By 28 hpf, the number of Unk^{+} neurons have increased dramatically, scattered throughout the head region and the spinal cord. This expression pattern was abolished in *unk* morphants (Figure 4-1B).

Both the apoptosis and loss of Unk^{+} cells in the morphants suggested severe defects in the formation of the CNS. In vertebrate development, the nervous system forms from neurons and radial glial cells, which are considered the neural stem cells since they are able to generate more neuronal and glial cell types (Barresi et al 2010). *gfap* is one of the genes expressed by radial glial cells, and confocal imaging of *unk* injected *Tg(gfap:EGFP)* embryos revealed that the neural tube was severely underdeveloped with significant loss of *gfap* expression (Figure 4-1C). Taken together, these data suggest that *unk* expression is required for maintenance and differentiation of neural stem and progenitor cells.

***jmjd2b* is required for zygotic transcription in zebrafish.**

Full knockdown of *jmjd2b* never resulted in live embryos the following day (data not shown). To determine when death occurred, the embryos were observed intermittently after morpholino injection. Embryonic development proceeded normally until ~4 hpf during the onset of the mid-blastula transition

stage (MBT) in which zygotic transcription is initiated. *jmjd2b* morphants did not develop beyond this point when an otherwise normal embryo would undergo epiboly as blastula cells begin to migrate and envelop the yolk. The morphants subsequently underwent a yolk burst phenotype characteristic of embryos that fail to undergo epiboly (Figure 4-2A).

No embryonic transcripts for the zebrafish equivalent of early mammalian trophectoderm (*krt4*), primitive endoderm (*gata6, slc26a),* endoderm (*sox17*), and mesoderm (*brachyury*) were detected after the MBT stage in *jmjd2b* morphants, suggesting zygotic transcription was not initiated or severely delayed (Figure 4-2B). Co-injection of *jmjd2b* morpholino with mouse mRNA ameliorated the phenotype, suggesting that the defects were caused by depletion of *jmjd2b* transcripts (Figure 4-2C). To test the hypothesis that the lack of embryonic gene expression is due to failure to activate zygotic gene transcription, we knocked down *jmjd2b* in *Tg(ubiquitin:EGFP)* embryos and as postulated, did not observe GFP expression in morphant embryos (Figure 4-2D).

Discussion

In addition to having a role in hematopoiesis, we identified distinct functions of *unk* and *jmjd2b* in other tissues during zebrafish development. *unk* is required for maintenance and differentiation of the developing neuroepithelium. Regardless of functional class, only 9 mutants in zebrafish have been described that share a similar neural degeneration phenotype observed in *unk* morphants (Abdelilah et al 1996, Furutani-Seiki et al 1996). Recently, UNK was found to play a role in the ubiquitination of BAF60b subunit of the BAF chromatin remodeling complex in response to Rac activation, and the BAF complex has been shown to be essential for neural development in mice (Lessard et al 2007, Lorès et al 2010). Collectively, the data implicate *unk* as a critical regulator of early neural development.

The evidence presented here for *jmjd2b'*s requirement to initiate zygotic transcription in blastula cells has never been described before. Our current understanding of the genetic regulation of MBT is limited. By gene expression analysis, factors involved in transcription, cell cycle, and embryonic patterning are among the first zygotic genes to be activated while *miR-430* targets maternal mRNA for degradation (Giraldez et al 2006, O'Boyle et al 2007). It is unclear whether depletion of any of these zygotic transcripts would result in a similar

phenotype. Finally, loss of either *mapkapk2* or *nanog* results in a yolk burst phenotype due to defects in yolk syncytial layer, the driver of morphogenic movements during epiboly, which might be the case in *jmjd2b* morphants (Holloway et al 2009, Xu et al 2012). Thus, further characterization of *jmjd2b* in zebrafish would provide important clues to the mechanism of zygotic gene activation.

Evidence of the tissue specific roles of chromatin factors has been accumulating, but the mechanisms by which they achieve this function remains unclear. Differential combinatorial assembly of chromatin complexes is one elucidated mechanism (Lessard et al 2007). Whether this is the only mechanism by which tissue specificity is achieved remains to be determined. Further studies on the function of individual chromatin factors such as *unk* or *jmjd2b* will help answer this question.

Materials and Methods

Zebrafish maintenance and microinjection.

Zebrafish (*Danio rerio*) were bred and maintained according to Animal Research guidelines at Children's Hospital Boston. Embryos were developed at 28.5°C and staged according to hours post fertilization and morphological features (Kimmel et al 1995). Wild-type Tüebingen, *Tg(ubiquitin:EGFP),* and *Tg(gfap:EGFP)* fish were used (Mosimann et al 2011, Bernardos and Raymond 2006). Microinjections were performed into the cell at the 1-cell stage. For mRNA rescue experiments, 200ng of mRNA was co-injected with the morpholino. For the apoptosis assay, 0.1 mg/ml acridine orange was co-injected with morpholino.

Morpholino design.

Morpholinos targeting the ATG start codon of *unk* and *jmjd2b* were synthesized by Gene-Tools. Morpholinos sequences are as follows:

unk: GATGGTGCTTTCGACATGATTTATC

jmjd2b: GGCTCGTTTTGTGCTCTTTTGTCGT

Whole-mount in situ hybridization and immunohistonchemistry.

WISH on zebrafish embryos fixed in 4% paraformaldehyde were performed as described previously (Thisse and Thisse 2008). Immunohistochemistry was performed as described previously (Shepard et al 2005). Stained embryos were imaged using a Nikon stereoscope with a Nikon Coolpix 4500 camera. Fluorescent images were imaged on a Zeiss stereoscope with Zeiss Axiocam camera or by confocal imaging on a Zeiss spinning disk confocal microscope using Volocity software for image acquisition.

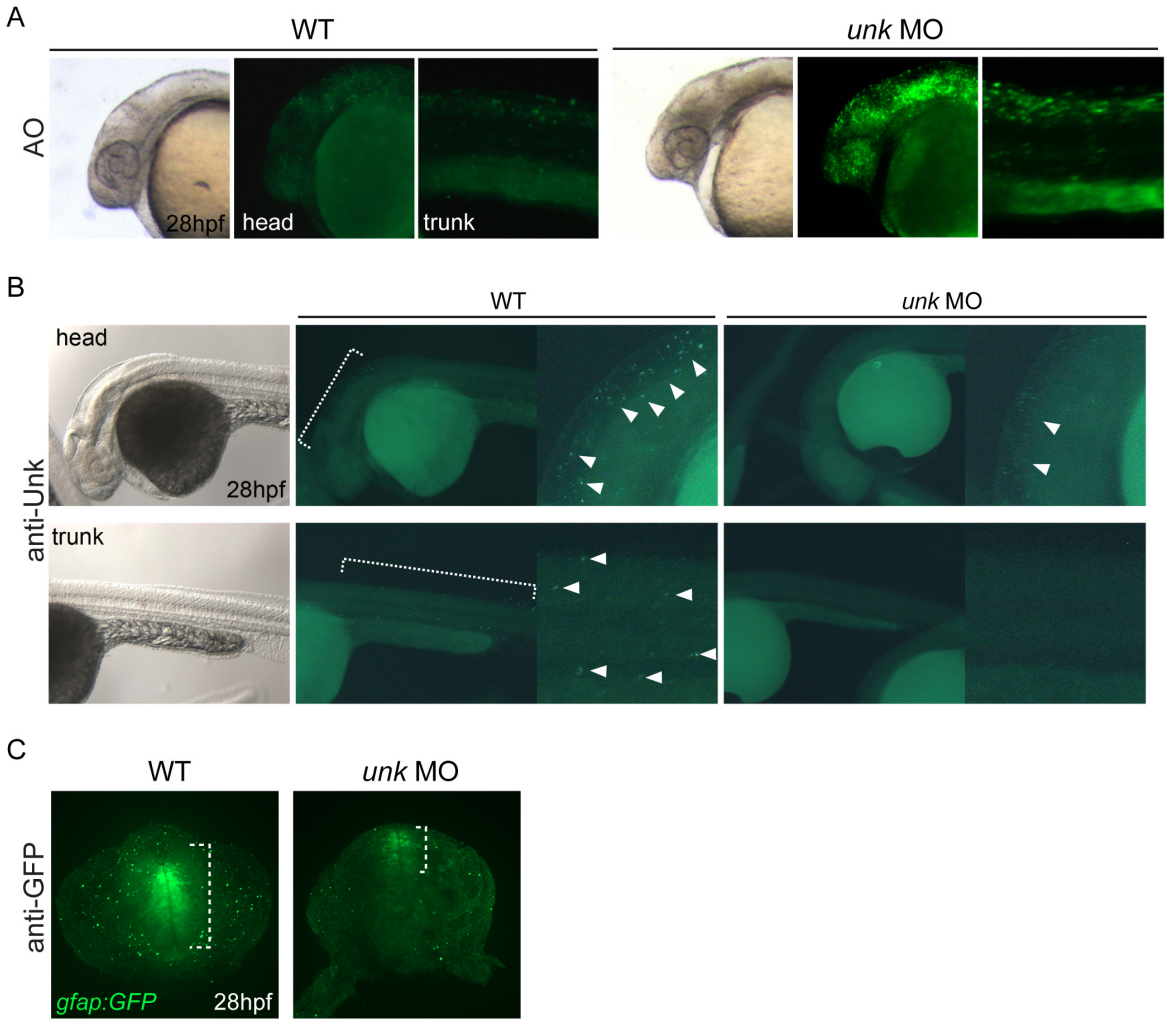

Figure 4-1. *unk* is essential for central nervous system development.
(A) *unk* morphants showed high levels of green fluorescence compared to wild-type uninjected control embryos, indicating widespread neural degeneration of the central nervous system in the brain and spinal cord. Acridine orange staining for apoptosis.
(B) Unk levels are markedly reduced in *unk* morphants. Immunohistochemistry using a mouse anti-UNK antibody.
(C) *Tg(gfap:EGFP)* morpholino injected embryos showed significant loss of GFAP expression, a marker for radial glial cells.

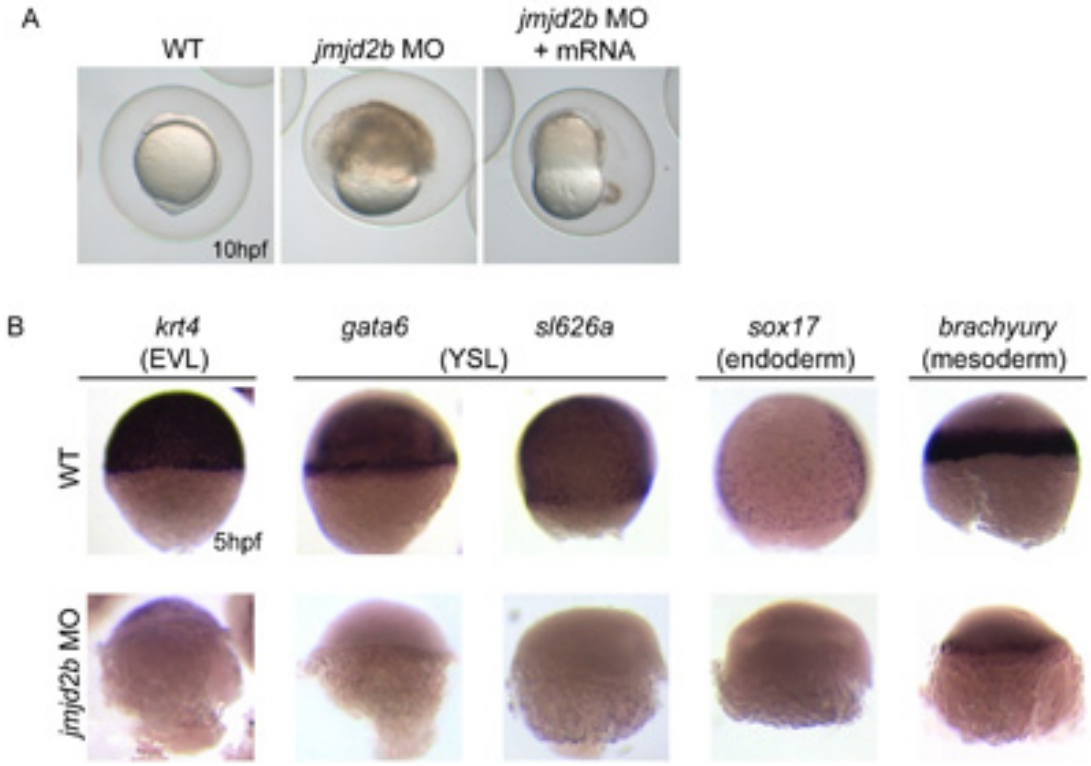

Figure 4-2. *jmjd2b* is required for zygotic transcription.

(A) *jmjd2b* morphants begin to die by 10 hpf and exhibit yolk burst phenotype. Co-injection of *jmjd2b* mRNA allowed embryos to survive to 10 hpf.

(B) Zebrafish markers for enveloping layer (EVL) (*krt4)*, yolk syncytial layer (YSL) (*gata6, slc26a*), endoderm (*sox17)*, and mesoderm (*brachyury*) were not detected in *jmjd2b* morphant embryos by WISH.

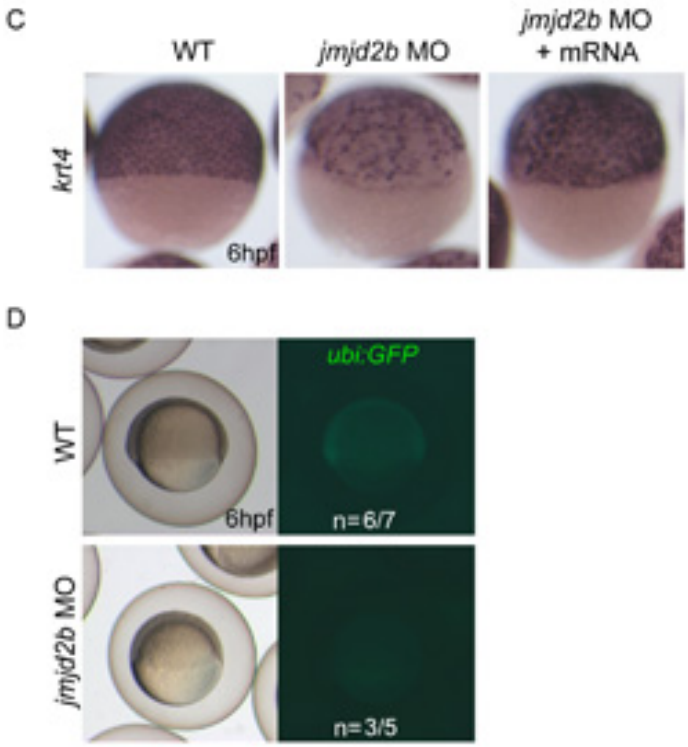

Figure 4-2. Continued.

(C) Embryonic expression of *krt4* can be rescued with mRNA injection.

(D) Loss of *jmjd2b* in *Tg(ubiquitin:EGFP)* leads to lack of GFP exprsesion during gastrulation.

Chapter 5

3D visualization of hematopoiesis in zebrafish

Attributions

I performed all the animation work described in this chapter. Gaël McGill provided technical assistance.

Introduction

The ontogeny of hematopoiesis in vertebrates is a highly dynamic process involving multiple sites of blood formation and movement of these cells at different stages of embryonic development. At least two waves of hematopoiesis occur during development. The first and primitive wave produces erythrocytes and macrophages in the posterior and anterior lateral mesoderm in zebrafish (Detrich et al 1995, Herbomel 1999). This is equivalent to mouse yolk sac hematopoiesis (Palis et al 1999). Primitive blood enters the circulation at 24 hours post-fertilization (hpf), soon after the onset of the heartbeat. At the same time, a transient population of erythroid myeloid progenitors (EMPs) is induced in the posterior blood island in the tail (Bertrand et al 2007). Meanwhile, the aorta gonad mesonephros (AGM) becomes competent to give rise to hematopoietic stem cells (HSCs), which are capable of self-renewal and differentiation into all hematopoietic lineages. The definitive wave is defined by the formation of HSCs. They develop from the ventral wall of the dorsal aorta in the AGM region by 36 hpf and enter the circulation through the caudal vein, migrating to the caudal hematopoietic tissue (CHT) in the tail and subsequently to the kidney, the zebrafish adult hematopoietic organ (Jin et al 2007, Kissa and Herbomel 2010, Kissa et al 2007, Murayama et al 2006, Thompson et al 1998,

Zhang and Rodaway 2007). Similarly, in mammals, the HSCs transition from the AGM to the fetal liver, and finally to the adult bone marrow (Boisset et al 2010, Dzierzak and Speck 2008).

Depicting the process of hematopoietic development using traditional diagrams is difficult given the spatiotemporal regulation of HSCs. To improve visualization of HSC development, a three-dimensional (3D) animation was created based on our current understanding of this process in zebrafish using Autodesk Maya. Maya is a 3D software that can be used for creating 3D animations, visual effects, game development, and post production projects. Multiple programs are embedded within Maya, including 3D modeling, 3D animation, dynamics and effects, rendering and imaging, and Maya Embedded Language (MEL), Maya's own scripting program. The program is highly versatile and can be used for many different kinds of purposes, including animation of 3D protein structures.

Once created, the zebrafish animation can be updated rapidly upon the release of new discoveries using the scene files that have been created for this animation. Actual experimental data such as confocal images can also be incorporated into the movie to present new models of HSC regulation. Overall, this movie provides a clear and simple illustration of the process of HSC

development that can be presented to investigators within or outside the blood field or even to the general public to illustrate the process of hematopoiesis.

Results

Modeling

Six scenes were created for the animation (Figure 2). The first scene involves creating a model of a 36 hpf embryo, the timepoint when HSCs first appear in the AGM. The embryo was created with multiple objects, specifically a Polygon cube for the embryo proper, the eyes, neural tube, and otoliths, the major features observed at this timepoint. A Polygon sphere was used to create the yolk sac. Using reference images of zebrafish embryos, each polygon object was extruded to match the shape of the embryo, and Subdivision lines were increased at the end to smooth the mesh (Figure 5-1A). Finally, the embryo, the eyes, the neural tube, otoliths, and yolk sac objects were then grouped together to generate the final model for the embryo. The same modeling procedure was used to create a 5 day embryo for the final scene.

The second, third, and fourth scenes involve closeups of the HSCs and vasculature. The shape of HSCs are generally described as large round cells, thus a NURBS sphere was created to represent the HSC. For the vasculature, a Subdivision cube was flattened to resemble a flat square-shaped endothelial cell. The cube was then duplicated to generate a long rectangular sheet of "endothelial cells" to create a full (scene 2) or half (scene 3) of a vessel using the

Nonlinear Bend Deformer. For the red cells circulating through the vessel, a NURBS sphere was adjusted to look like a human red cell but more oval in shape as zebrafish red cells are.

For the fifth scene, which involves a lower magnification view of the zebrafish kidney region, a Polygon cube was used to generate objects representing the kidney, including two randomly extruded cubes placed inside the kidney to emulate the nephrons. Circles were used to extrude from a Curve to generate three large vessels that run through the region. One object representing the swim bladder was placed next to the kidney and a large randomly shaped object was placed behind these structures to fill in surrounding space.

Texturing and Lighting

The zebrafish embryo is transparent, thus very little texturing was required. A Blinn shade and transparency was used for all texturing. The yolk was tinted yellow, and a of Bump mapping using an image of the yolk surface was applied to simulate the appearance of globular yolk cells. For the embryo, a Rock texture was colored off-white and Bump mapping was created using Brownian noise to give a cellular look to the surface of the embryo. An image of

the zebrafish eye was used to texture the eyes. A light color was applied to the neural tube to help make it more visible through the other objects covering it (Figure 5-1B). The same textures were applied to the 5 day embryo model.

Since blood is associated with red color, the HSC, red cells, and kidney were textured in that shade, with the red cell being lighter and HSC darker and the kidney in between. Brownian noise was used again for bump mapping and for the transparency attribute of the HSC texture. A camel color was used for the endothelial cells. Brownian noise was also applied to the transparency attribute and leather was used for bump mapping create a more textured surface.

Directional light was used in every scene. Spot lights or Point lights were added where needed. Every scene was enclosed inside a large sphere for lighting purposes. The sphere was textured white, and a hint of yellow was added to the lighting to mimic real life observation of these embryos under a dissecting microscope.

Dynamics

To create circulating blood cells, a Curve Flow was created from the Dynamics effects in which particles flow from one end of the Curve to the other with their movement constrained by circles placed along the length of the curve.

The Curve was drawn following the models of the vessels or embryo, and the scale and location of the circles were adjusted to fit inside these objects. Next, the model of the red cell was Instanced onto the flow particles to create the circulating red cells (Figure 5-1C). Finally, the number of particles emitted was adjusted to the appropriate number to fill the vessel.

Animation

Simple animation was used to model the migration of the HSCs. This involves moving the HSC sphere and setting key frames at each position. To animate the HSCs squeezing through a vessel, a Lattice deformer was placed at the site of extrusion. To animate the budding of the HSC from the endothelium, 3 objects were created to model the different shapes of the HSC during the budding process and blended together using the Blend shape deformer. At the final stage, the endothelial cell was removed by applying full transparency to its texture and replaced with a NURBS sphere representing the HSC that enters into the circulation. The Blend shape deformer was also used to animate the beating heart of the 5 day embryo.

In the final scene when the embryo swims off the scene, the embryo was animated using key frames, and a Bend deformer was applied to the tail so that it

can flip back and forth in a swimming motion. Cameras were also key framed to zoom in, zoom out, and follow the migration of the HSCs.

Rendering and Compositing

Each scene was batch rendered into an image sequence. Scenes were rendered in multiple parts when necessary. For example, to avoid overlapping multiple curve flows in a scene such as the CHT, each curve flow was rendered separately. All image sequences were subsequently composited in After Effects (Figure 5-1D). Title, wording, and scene transitions were added at this step. The selected music was cropped to match the duration of the animation in SoundBooth and also composited in After Effects.

Discussion

The animated video presentation of the ontogeny of HSCs during hematopoietic development provides a concise review of this process that is easily understood. Developmental hematopoiesis is a dynamic process that is spatiotemporally regulated. Studies of embryonic hematopoiesis involve whole-mount *in situ* hybridization (WISH) or imaging of fluorescent transgenic lines of various blood markers at different stages of development to examine the formation of erythroid, myeloid, or lymphoid cells, all of which develop at distinct anatomical sites throughout the embryo. This animation provides the audience with a clear depiction of the zebrafish embryo and the key anatomical sites that would facilitate the understanding of the *in situ* data being presented during a scientific talk (Figure 5-2).

The first version of the movie, titled "Induction of hematopoietic stem cells in zebrafish," was submitted as an introduction to a Cell article that can now be found in Cell Press journal's YouTube channel (www.youtube.com/watch?v=tngFCgcrZ74) (Goessling et al 2009). Given that a wide audience was targeted, short sentences were added to the composition to summarize the process animated in each scene, a very quick and easy task. Over 8,500 views of the animation have occurred over the course of two years,

supporting the usefulness of such visualizations. New evidence regarding the budding process of HSCs from the endothelium has emerged since the creation of the movie, and the animation was updated by adding a new AGM scene, using the same techniques as before. Thus this animation can be rapidly modified to show the latest developments in our understanding of hematopoiesis in zebrafish.

Besides creating Hollywood movies or TV commercials, one of the most valuable aspects about 3D animation is the ability to incorporate real data into it. A method has been described to import confocal images into Maya, thus real AGM and CHT structures, for example, can be imported into Maya and used for the animation (Biological Visualization Interest Group) (Figure 5-3). This and other methods of animating scientific data are more prominent in the field of cell biology to help visualize protein structures or chemical reactions. Because the biology of any system being studied can be complex, the combined presentation of experimental data and the model derived from the data facilitates our understanding of the science being presented. Thus the use of 3D animation in science will only grow in the future.

Materials and Methods

Reference images

Reference images for modeling were taken from wild-type Tüebingen zebrafish embryos at 36 hpf and 5 days using a Nikon stereoscope with a Nikon Coolpix 4500 camera. Confocal imaging was performed on a Zeiss spinning disk confocal microscope of a double 36 hpf transgenic embryo for *Tg(cd41:EGFP)* and *Tg(kdrl:RFP)* (Huang et al 2005, Traver et al 2003).

Softwares and music.

Autodesk Maya 2008 was used for the animation. Adobe After Effects CS4 was used for compositing. Adobe Soundbooth CS5 was used to edit the music. Imaris (BitPlane), a scientific visualization and analysis software, and Blender, a 3D animation freeware, were used to create the object file for the confocal z-stacks of the AGM to import into Maya. The music “Beneath the Lights” by The Kiss was used in the animation.

A. Modeling

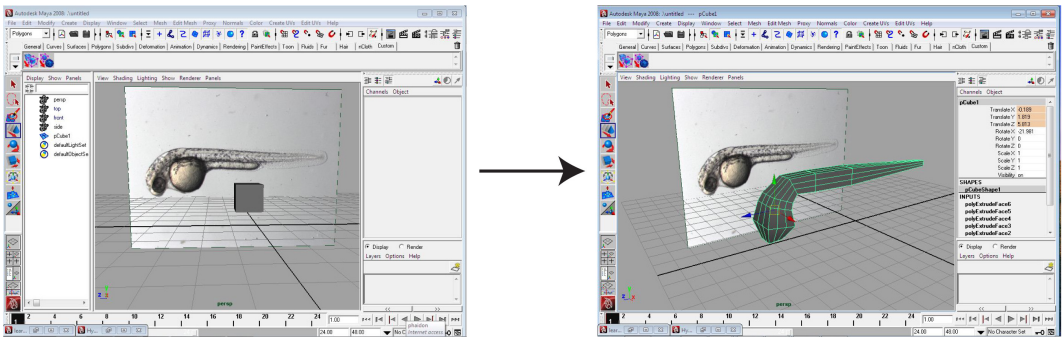

B. Texturing and Lighting

C. Dynamics and Animation

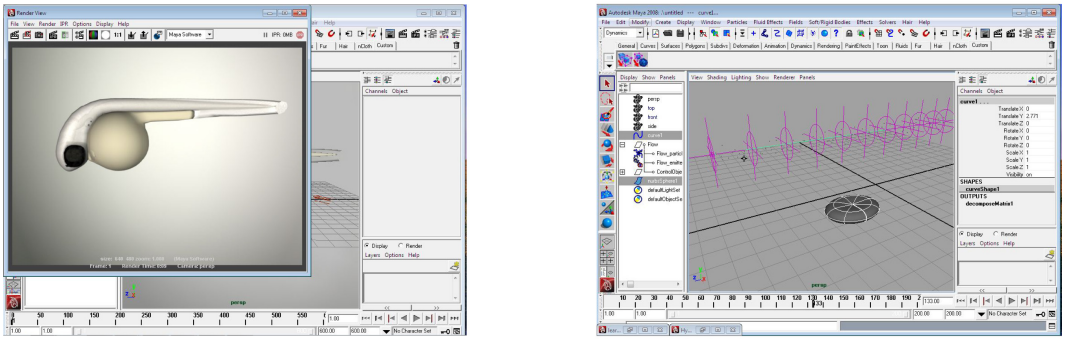

D. Compositing

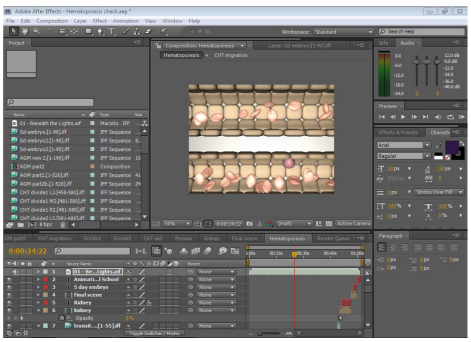

Figure 5-1. The process of 3D animation.

(A) A polygon cube is modeled into a zebrafish embryo in Maya.

(B) Textures and lighting applied to the models finish the look.

(C) Animation of the embryo and HSCs together with curve flow of red cells complete the scenes for rendering.

(D) All scenes are composited together in After Effects.

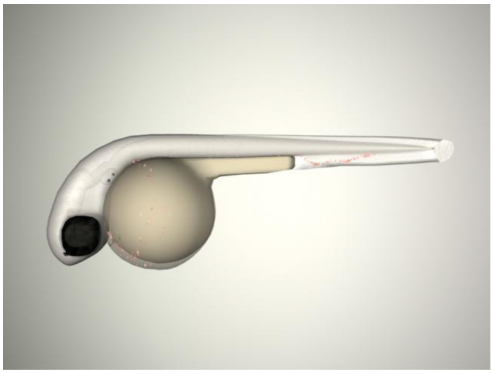

Scene 1:
36 hpf embryo

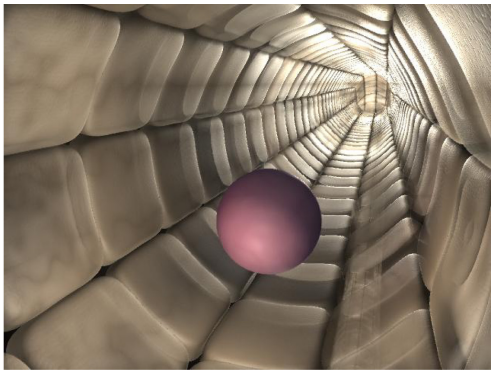

Scene 2:
hemogenic endothelium

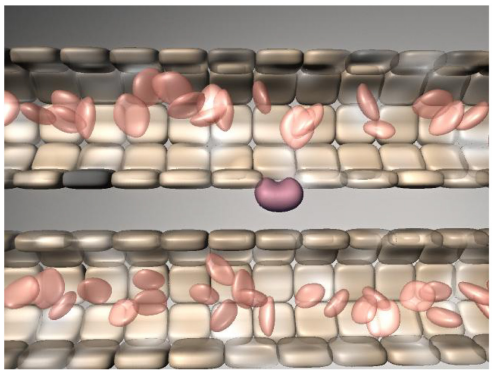

Scene 3:
budding of HSC

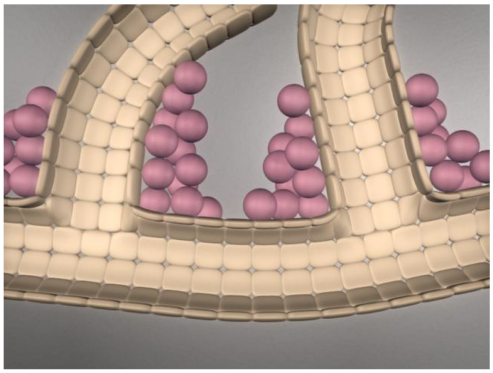

Scene 4:
caudal hematopoietic tissue

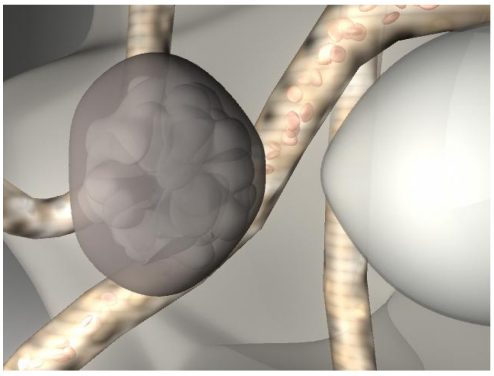

Scene 5:
kidney region

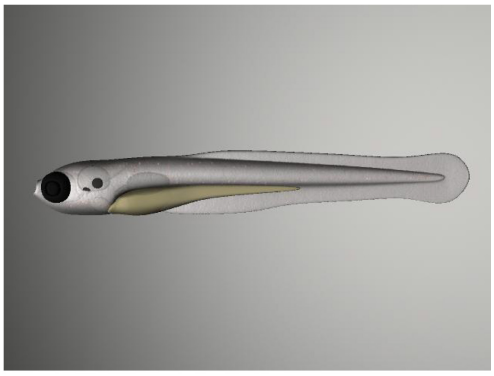

Scene 6:
5 day embryo

Figure 5-2. Scenes for the animation.

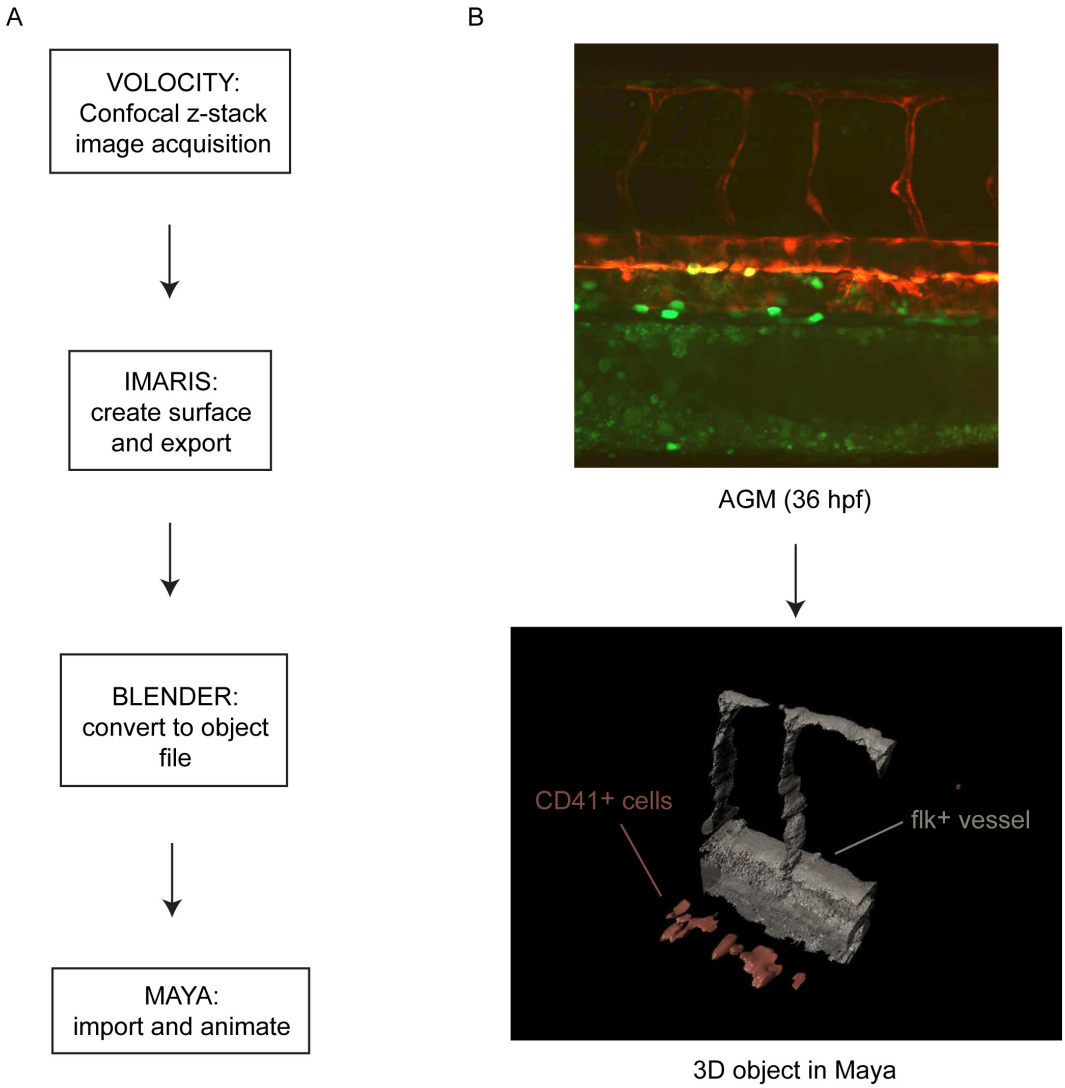

Figure 5-3. 3D reconstruction of confocal data in Maya.

(A) Confocal z-stacks are acquired for example using Volocity software. The confocal data was then transferred to Imaris in which 3D surfaces are generated. The surfaces were imported into Blender, a 3D program, to convert the surfaces into an object file that can be read by Maya.

(B) High resolution z-stacks of a 36 hpf AGM in a double transgenic embryo for *Tg(cd41:EGFP)* and *Tg(flk:RFP)*. Following the procedure, two objects were created, the *cd41*$^{+}$ hematopoietic cells (green channel) and the *kdrl*$^{+}$ vascular cells (red channel) and imported into Maya.

Chapter 6

Discussion

To understand the role of chromatin regulation in hematopoiesis, we conducted a reverse genetic screen knocking down most of the known chromatin factors in zebrafish embryos searching for factors that could alter hematopoietic gene expression during the process of primitive and definitive hematopoiesis. We identified a cohort of 47 factors that regulated distinct stages of primitive and definitive hematopoiesis, from the induction of the mesoderm to generate erythroid cells to the formation of hematopoietic stem and progenitor cells (HSPCs) from the hemogenic endothelium. These chromatin factors function in histone methylation, histone acetylation, and nucleosome remodeling. Characterization of individual factors revealed important tissue specific functions. For example, knockdown of *chd7* resulted in a cell autonomous increase in blood production in both primitive and definitive hematopoiesis. Loss of *unk* and *jmjd2b* reduced definitive hematopoiesis but they were also required for the development of the central nervous system and initiation of zygotic transcription during mid-blastula transition (MBT) stage, respectively. Collectively, these results demonstrate the important role of chromatin factors in establishing the programs of gene expression for specification and differentiation in hematopoiesis and other tissues.

Morpholinos as a powerful tool for studying epigenetics.

Morpholinos have been used widely to knockdown expression of specific genes and have been a valuable tool for developmental studies in zebrafish. They inhibit gene expression by steric blocking of translation initiation or of exon splicing. Delivery can be easily accomplished via microinjection into single cell embryos, and the concentration of the morpholinos can be adjusted to achieve different levels of knockdown in the injected embryos, or morphants, similar to an allelic series. Using our screening method of analyzing morphant phenotypes at three different doses for each morpholino, we were able to elucidate hematopoietic specific phenotypes, if any, for the knockdown of each chromatin factor. Because knockdown of some chromatin factors result in severe developmental abnormalities, which would subsequently affect blood development, we were able to adjust the dosing to reduce these morphological defects in order to determine whether the particular chromatin factor plays a role in blood formation. This is best exemplified by knockdown of *jmjd2b*. The histone demethylase *jmjd2b* is a critical factor for MBT, but at lower levels of knockdown, the embryo is able to develop relatively normally except for the formation of HSPCs at 36 hpf, revealing a requirement for *jmjd2b* in hematopoiesis. This type of manipulation is currently difficult to do for developmental studies in other organisms such as mice. All knockout models would result in complete knockdown of the gene of interest. Furthermore, the development of zebrafish embryos *ex utero* allows for

visualization of developmental processes otherwise difficult in mammalian systems. Defects in morphogenic movements, anterior-posterior patterning, or organ formation can all be scored just by looking at the embryos. Putative factors involved in cardiac function, such as *smarcd2*, and melanocyte development, such as *suv39h1*, have been uncovered in the chromatin factor screen. As a result, zebrafish will continue to be a valuable model for the study of epigenetics in development.

Non-redundant roles of chromatin factors in modulating hematopoietic gene expression.

Chromatin modifying factors are needed to recognize and interpret the various chromatin modifications in order to execute the epigenetic program. With over 11 post-translational modifications that can occur at 60 different histone residues, a reasonably large number of chromatin modifying factors would be needed. We curated a list of 425 chromatin factors encompassing most of the known chromatin factors to screen for epigenetic regulators of hematopoiesis. Perhaps because of the variety of histone methylation marks, with each one having differential functions depending on the chromatin context, a large number of chromatin modifying factors in our gene list are associated with methylation, with nearly 60 SET domain methyltransferases that catalyze the methylation reaction, about 30 demethylases that

can remove the mark, and over 60 binding factors that can be recruited by a methyl mark in zebrafish.

Although there are a large number of related chromatin factors, we observed that loss of individual chromatin factors results in a noticeable hematopoietic phenotype. This implies that they have very tissue specific functions that cannot be compensated by other members of the same family. For example, within the SET domain family, the *mixed-lineage leukemia* (*mll*) gene and other family members *mll3a, mll4a,* and *mll4b* are all expressed ubiquitously in the early embryo, yet only knockdown of *mll* in the screen resulted in a loss of *c-myb* and *runx1* expression in definitive HSPCs (Sun et al 2008). Mll is part of the trithorax proteins that catalyze and maintain the methylation of H3K4 and has been shown to be essential for HSC self-renewal, consistent with our screen results (Jude et al 2007, Macmahon et al 2007). Thus the function of individual chromatin factors *in vivo* is largely distinct, even when they have overlapping expression patterns.

There is also tissue specificity in terms of the level of knockdown required to change the expression of the hematopoietic transcription factors. Because of the three dose screening method, we were able to observe and distinguish between gross developmental phenotypes and blood specific phenotypes. High levels of *smarca1* knockdown resulted in developmental delay, but at lower doses, when the

developmental delay was milder, primitive erythroid cell formation was completely inhibited as shown by lack of *scl*$^{+}$, *gata1*$^{+}$ and *β-globin e3*$^{+}$ cells in morphant embryos. At much lower doses, when embryos developed relatively normally until 36 hpf, we could observe the loss of *c-myb*$^{+}$ and *runx1*$^{+}$ cells in the morphants. Thus the blood cells are more sensitive to levels of *smarca1* compared to other tissues within the embryo. In comparing between the primitive and definitive screens, the 14 hpf embryos seemed to tolerate much higher doses of morpholinos than 36 hpf embryos. It may be because of residual maternal RNA remaining at the earlier timepoint or because the defects arise slightly later in development, but it could also be because of different sensitivities between primitive erythroid cells and definitive HSPCs. Due to the variety of factors that could contribute to the blood phenotype in the morphants, the morpholino dose curve allowed us to distinguish more hematopoietic specific defects by comparing the changes in blood phenotype with respect to the changes in embryonic development.

Differential requirement of chromatin factors in hematopoietic development.

Tissue differentiation is thought to be largely an instructive process directed by lineage specific transcription factors. The concept that gene repression plays an important role in lineage determination has also been proposed with some evidence to

support it. DNA methyltransferase 1 (Dnmt1) catalyzes DNA methylation, which is usually associated with gene repression. Loss of Dnmt1 not only resulted in loss of HSC self-renewal but also skewing towards the myeloid lineage (Bröske et al 2009, Trowbridge et al 2009). Bmi1, a component of the Polycomb repressive complex, was found to be required for repression of the B cell lineage regulators Ebf1 and Pax5 in HSCs, which were activated prematurely in Bmi1 knockout mice (Oguro et al 2010). Our screen results support both models in which chromatin factors participate in lineage specification and differentiation through activating and inhibitory functions.

Based on the primitive screen, depletion of one chromatin factor is sufficient to alter gene expression of *scl, gata1,* and *βH1-globin e3,* which subsequently disrupts normal development of erythroid cells. Reduced *scl* expression always coincided with loss of *gata1* and *βH1-globin e3* expression. Even though *scl* expression was not fully abrogated in morphant embryos, it was sufficient to impair the formation of red cells, demonstrating the critical role that chromatin factors have in maintaining proper gene expression levels that in turn affect cell fate decisions.

In analyzing the screen hits to determine which chromatin modifications were important for the regulation of hematopoietic genes, mainly chromatin factors involved in the processes of histone methylation, histone acetylation, and nucleosome remodeling were found. Based on whole genome mapping of histone modifications,

histone acetylation is generally associated with active transcription. In contrast, the effect of histone methylation depends on the residue that is modified. H3K4 methylation is relatively specific to active gene promoters and H3K36 methylation marks chromatin domains that are actively transcribed. Methylation of H3K9 and H3K27, on the other hand, generally correlate with repression. Finally, nucleosome remodeling is important for mobilizing nucleosomes to make the DNA accessible to transcription factors and other cellular proteins (Bernstein et al 2007).

Overall, the chromatin factor hits from the definitive screen support the model in which activating marks promote HSPC formation. The 29 definitive chromatin factors that were characterized are involved in the processes of H3K4 methylation, H3K9 methylation, H3K36 methylation, and histone acetylation, suggesting that these modifications are important for the induction of HSPCs. Loss of *setd1ba, ash2l, cxxc1l, rbbp4,* and *rbbp7*, components of the SET1 complex known to methylate H3K4, resulted in loss of HSPC formation. Knockdown of *jmjd1ca*, which demethylates H3K9, also resulted in loss of HSPCs. Thus these chromatin factors are needed presumably to activate genes required for the formation of HSPCs, including *c-myb* and *runx1*, via methylation of H3K4 and demethylation of H3K9. However, loss of some other factors, such as the H3K36 demethylase *jhdm1bb*, also resulted in loss *c-myb* or *runx1* expression in the AGM even though retention of active marks

should have enhanced *c-myb* and *runx1* expression instead. This indicates that repression also plays a role during lineage specification.

Consistent with this idea, we observed increased erythroid differentiation in morphants that had more overall transcriptional repression. Knockdown of two thirds of the 18 chromatin factors characterized in the primitive screen resulted in increased globin expression and not a reduction. Depletion of these chromatin factors should have resulted in an accumulation of repressive marks, thus supporting the model that gene repression is critical for differentiation. Loss of *ash2l* would reduce levels of active H3K4 methylation, whereas loss of *jhdm1f* and *jmjd3* would each result in preservation of repressive H3K9 and H3K27 methylation, respectively. Furthermore, loss of *ing5b*, which participates in a histone acetyltransferase complex, should lead to reduced acetylation levels, promoting a more repressive environment. Generally, repressive histone marks inhibit transcription and therefore should have inhibited *scl* and *gata1* expression in the morphants, but our screen results suggest that this is not the case. These observations could mean that repression is required to suppress gene expression of the earlier cell fate or alternative cell fates, especially since scl^{+} cells in the posterior lateral mesoderm also give rise to angioblasts, and perturbing this balance is what results in increased primitive hematopoiesis. Another possible explanation is that the function of either the histone marks or the chromatin factors *in*

vivo are more diverse than currently thought. One example is the Tip60 acetyltransferase, which in ES cells has been found to repress target genes when in complex with p400 (Fazzio et al 2008). Thus the cellular context is an important determining factor in how the epigenetic code is deciphered.

One method to characterize the effects of these chromatin factors on lineage decisions in hematopoiesis is to study the gene expression changes in the morphants. The primary screen provides a targeted list of chromatin factors that can be re-screened for lineage skewing either by WISH or by expression array to identify additional hematopoietic genes that are affected. The primary hit list could then be subdivided into groups that regulate different lineages. For example, neutrophils and thrombocytes are among other lineages that are produced in concert with erythrocytes during the primitive wave, and loss of *gata1* converts erythropoiesis to myelopoiesis (Galloway et al 2005, Warga et al 2009). Taken together, our screen results are consistent with the overall concept that both positive and negative regulation is required for proper specification and differentiation of hematopoietic cells.

Stages of chromatin modification in hematopoietic development.

Based on the characterization of the screen hits, a map can be generated delineating the chromatin modifications important for different steps of blood

development. The screen results suggest that ISWI chromatin remodeling is among the first steps required to initiate the blood program given the severity of the *scl* phenotype. Subsequently, Polycomb and NuRD factors are important for the formation of *gata1*$^{+}$ progenitors given that only *gata1* and *β-globin e3* expression are affected in the *cbx8* and *chd4* morphants, respectively. Then, the NuA4 acetyltransferase is required during the differentiation of erythroid cells since only *β-globin e3* expression was reduced in *kat5* morphants. Furthermore, histone modifications exist in combinatorial patterns (Latham and Dent 2007), and our screen results indicate the possibility that patterns of H3K4, H3K9, and H3K27 methylation plays a role in the transition between the stages of primitive blood formation. It may be possible to use transgenic fish expressing *draculin-GFP,* which is expressed in primitive blood precursors in the lateral mesoderm at 11 hpf all the way to maturing erythroid cells at 24 hpf, to sort GFP-positive cells for mapping these histone marks across the different stages of erythroid development (Herbomel et al 1999). Our screen complements other efforts such as the characterization of histone marks in mouse fetal liver erythropoiesis by providing a list of chromatin factors and chromatin modifications implicated at these different stages of blood development (Wong et al 2011).

Primitive and definitive hematopoiesis utilize the same chromatin complexes.

Many of the primitive and definitive screen hits can be organized into known chromatin complexes, including SWI/SNF, SET1, Sin3A/HDAC, HBO/NuA4/HAT, and PRC1. The SWI/SNF, SET1, and HBO/HAT complexes are important for both primitive and definitive blood formation while Sin3A/HDAC, NuA4/HAT, and PRC1 are required more for definitive blood formation. Despite the large overlap in complexes utilized, fewer components of each complex were needed in the primitive wave. This may reflect the more complex regulation of HSCs, in which they must balance self-renewal with differentiation, whereas primitive blood progenitors only need to produce red cells.

One of the mechanisms by which chromatin factors are believed to achieve tissue specificity is through combinatorial assembly of chromatin modifying complexes. Given that primitive and definitive complexes overlap in terms of their function, the individual components that makeup these complexes are largely distinct. Thus the subunits likely provide tissue and stage specificity for these overlapping chromatin complexes. It would be valuable to test whether screen hits within the same category in various combinations with each other can all enhance the hematopoietic phenotype. This can be tested by injecting combinations of morpholinos at suboptimal doses to determine whether they phenocopy the individual morphants. This was the

case for the combined knockdown of the ISWI related factors *smarca1, chrac1,* and *rsf1b* and the PBAF associated factors *chd7* and *arid4b*. Whether this indicates that these chromatin factors participate in the same chromatin complexes or function in parallel pathways would require protein interaction assays such as co-immunoprecipitations or protein pulldowns to distinguish between the two possibilities. A recent study comparing the localization of 29 chromatin factors between embryonic stem (ES) and K562 cells revealed that the association between groups of chromatin regulators appear to be preserved between the two different cell types, suggesting that chromatin complex associations discovered in our screen could be conserved in other tissues as well (Ram et al 2011).

One interesting observation from the screen was that both enzymes, i.e. 'writers' and 'erasers,' and binding factors, i.e. 'readers,' were found to be equally important for regulating hematopoiesis. Counting the 47 chromatin factors having the greatest decrease or increase blood phenotypes characterized in the screen, the number of enzymes and binding factors in the primitive and definitive lists were roughly equal. Within the enzymatic group, there was even representation of 'writers' and 'erasers.' Thus all three processes are important for maintaining the proper balance of gene expression pattern in the embryo, regardless of whether they form a chromatin complex together or not.

Screen resource for the future.

In order to record the wealth of phenotypes observed in the screen, a database was created to catalog all the results and facilitate future studies of chromatin factor regulation in hematopoiesis and other developmental biology. The database contains all the zebrafish and human annotations for the 425 chromatin factors screened, all the experimental details including methods, all the *in situ* data results for each chromatin factor screened, and is searchable by gene of interest. Most importantly, it provides a collection of morpholino sequences that result in an embryonic phenotype, which will be of interest to the broader community.

The database can be used to identify putative chromatin regulators of a specific developmental process other than hematopoiesis. In zebrafish, histone methylation of H3K4, H3K36, and H3K27 occurs only after the onset of zygotic transcription during MBT stage (Sun et al 2008, Vastenhouw et al 2010). Multiple histone methyltransferases, demethylases, and methyl mark binding proteins might be required at this time, and some of these chromatin factors were probably included in our screen. *phf3* and *phf6,* PHD domain containing factors that can bind methylated histone marks, and *prdm1a, setd4, setd6,* and *setdb1b*, SET domain methyltransferases, are all potential regulators given their early developmental defects.

The mechanisms of chromatin regulation in embryonic development remains largely unknown. The majority of the studies focused on histone modifications have been on the N-terminal tail modifications, yet histones can also be modified within their globular domain. With advances in the development of new antibodies and improvements in mass spectrometry, new histone modifications are being discovered. Most recently, over 67 novel histone modifications were identified, and lysine crotonylation was discovered as a new mark that correlates strongly with active promoters like H3K4 methylation (Tan et al 2011). Thus the identification of new protein domains that can catalyze the crotonylation of histone proteins are likely in progress. Whether these domains will be uncovered in a new class of histone modifying factors or as additional domains in currently known chromatin factors remains to be determined. Even within our current list of 425 chromatin factors, the function of many of those factors containing chromatin modifying domains is unknown. Consequently, our screen database will continue to serve as a valuable resource for the study of chromatin factors and their effects on development.

Individual chromatin factors have essential developmental and tissue specific roles.

Characterization of individual chromatin factors, e.g. *chd7*, from the screen

has already provided insights into the mechanisms of how each regulates development and provides additional clues about how tissue specificity is achieved. Expanding the analysis to other individual factors should yield such insights. *unk*, a radical SAM domain containing protein, not only regulates HSPC formation but is also required for central nervous system development. *jmjd2b*, a histone demethylase, is required for both the initiation of zygotic transcription and induction of HSPCs later in development. One of the factors with the most robust phenotype identified from the screen was *chd7*.

Although expressed ubiquitiously, knockdown of *chd7* resulted in a specific enhancement of primitive and definitive hematopoiesis. The expression of *scl* marks one of the first steps in developmental hematopoiesis, the induction of the lateral mesoderm. By the 5 somite stage (ss), roughly 11.6 hpf, the scl^{+} cells in the posterior tail have already started to expand in *chd7* morphants, and by 24 hpf, primitive erythroid and myeloid lineages are also increased. The same pattern is observed with the formation of definitive $c\text{-}myb^{+}$ and $runx1^{+}$ HSPCs in the aorta gonad mesonephros (AGM) region at 36 hpf and in the erythroid, thrombocytic, and myeloid lineages in the caudal hematopoietic tissue (CHT) at 5 days. It was surprising to see the phenotype persist this long because the morpholinos generally lose their effect by 5 days as they have already been diluted in the embryo through so many cell

divisions. More importantly, the blood expansion is cell autonomous as determined by blastula transplantation experiments. Collectively, these results suggest that *chd7* is as a potent repressor of embryonic hematopoiesis.

Elucidating the molecular mechanism of Chd7 in blood.

One of the major future directions resulting from the chromatin factor screen is to elucidate the mechanism by which the chromatin factors identified regulate hematopoiesis, and *chd7* is a great candidate for initiating such studies. The blood expansion observed in *chd7* morphants could be the result of several mechanisms. One possible model is that hematopoietic transcription factors such as *scl*, *c-myb*, and *runx1* are transcriptional targets of *chd7*, which can be assayed by chromatin immunoprecipitation (ChIP) followed by sequencing to map Chd7 binding sites across the genome. ChIP-seq data of CHD7 in K562 cells, a human erythroleukemic cell line, is available, and initial analysis revealed CHD7 binding at important hematopoietic genes such as SCL, RUNX1, and MYB (Ram et al 2011). This is consistent with an interesting observation in zebrafish embryos in which knockdown of *chd7* in *Tg(cmyb:EGFP)*, *Tg(lmo2:dsRed)*, and *Tg(cd41:gfp)* embryos not only increased the number of fluorescently labeled blood cells but the intensity of the fluorescence was also significantly higher, indicating direct repression by Chd7 at

these hematopoietic promoters. Correlating the CHD7 ChIP binding sites to genome-wide histone marks from the ENCODE database and expression data from K562 cells will help determine whether CHD7 binding associates with repression or not in this context. With the exception of one study so far, CHD7 is generally associated with transcriptional activation, and thus the role for *chd7* in blood appears to be opposite of its function in other tissues, with preliminary evidence to support the case discussed later in this chapter.

A MYB motif was identified from a subset of the CHD7 binding sites, suggesting a potential interaction between CHD7 and MYB. Previous work has shown the essential role for cMyb in regulating multipotent progenitors. Overexpression of c-Myb in ES cells increased multilineage colony formation and self-renewal in culture whereas conditional knockout of the gene in mouse bone marrow resulted in defective self-renewal and multilineage differentiation of adult HSCs (Dai et al 2006, Lieu and Reddy 2009). Thus overexpression of *c-myb* in the context of *chd7* knockdown may be the cause of increased stem cell and blood formation. To determine whether CHD7 and MYB bind to the same set of target genes, ChIP-seq of MYB in K562 cells were initiated. CHD7 can also be knocked down in the K562 cells to determine whether MYB binding changes. If CHD7 inhibits MYB by competing for MYB binding sites, then under normal conditions,

target genes may be occupied by CHD7 whereas in the CHD7 knockdown, MYB would occupy those same sites. If MYB binding was independent of CHD7, then knockdown of CHD7 will probably not cause any changes in MYB binding. The only difference would be in the expression of the target genes. In the presence of CHD7, there would be low to no expression of MYB targets whereas their expression should increase upon depletion of CHD7. Thus analyzing the expression of MYB target genes in the presence or absence of CHD7 will help determine the role of CHD7 in regulating MYB function.

Given that *chd7* is widely expressed but has hematopoietic specific functions, a protein pulldown with mass spectrometry of CHD7 in blood cells will help identify its hematopoietic specific interacting factors. Co-elution of MYB and CHD7 from K562 gel filtration analysis indicated a potential interaction between the two factors, thus the pulldown will also help verify whether MYB and CHD7 interact in the same complex given that a direct interaction was not detected by co-immunoprecipitation. Since multiple hematopoietic genes are affected by *chd7* knockdown, additional hematopoietic transcription factors may be identified in the pulldown. Subunits of repressive chromatin complexes such as SETDB1 may also be pulled down with CHD7 given its negative regulatory function on hematopoietic gene expression. One previous study revealed that SETDB1 can recruit CHD7 to repress target genes in

mesenchymal stem cells (Takada et al 2007). Although expressed at low levels in K562 cells, a direct interaction has been shown for RUNX1 and CHD7 via the transactivation domain of RUNX1 in T cells (see Chapter 3, note added in proof). Runx1 is required for the induction of HSCs from the AGM and differentiation of certain adult lineages, which may also account for the expansion of stem and progenitor cells in *chd7* morphants (Li et al 2006, Okuda et al 1996). Thus identifying the interacting proteins of CHD7 will be important for understanding its function in blood cells.

The next question would be which protein domains of Chd7 are important for its function in hematopoiesis. Mutational truncation analysis to identify the MYB or RUNX1 interacting domains of CHD7 will help determine whether CHD7 represses both MYB and RUNX1 together via two different interacting domains or by competition for the same binding site. In the latter case, a possible model for CHD7 function is that binding to RUNX1 renders it inactive or inefficient in transcriptional activation, but when CHD7 is knocked down, RUNX1 activity is regained and can activate downstream hematopoietic genes such as MYB. Furthermore, it would be interesting to determine whether the chromatin modifying domains of CHD7 are required for suppression of MYB and RUNX1. In a preliminary experiment, overexpression of human *CHD7* suppressed formation of *c-myb*$^{+}$ cells in

Tg(cmyb:EGFP) embryos, and a catalytic mutant *CHD7*^{K998R} can be tested to determine whether suppression of *c-myb*$^{+}$ cells is lost. Overall, understanding the mechanism of CHD7 function will provide much insight into the regulation of hematopoiesis.

Genetic interaction between *chd7* and other proteins identified from the pulldown can be verified in zebrafish. Double morpholino knockdown of *chd7* and the candidate factors can be done to test whether *chd7* morphants are rescued to identify regulators of Chd7 function. Mutants for *c-myb* and *runx1* are available and can be used to test for interaction with *chd7*. The *cmyb*^{t25127} allele results in an amino acid substitution that abrogates its DNA binding domain, and homozygous mutant embryos progressively lose definitive hematopoietic cells after 24 hpf (Soza-Reid et al 2010). However, *c-myb* transcripts accumulate in the ICM of 24 hpf mutants as seen by WISH and then gradually disappear. It is unknown at this point whether *runx1* expression is affected in the mutants. On the other hand homozygous *runx1*^{hg1} mutants lose all *c-myb* expression in the AGM and in the CHT. The mutant allele results in a truncation of the protein starting from within the runt domain (Jin et al 2009). *chd7* morpholino can be injected into embryos from an incross of *cmyb*^{t25127} or *runx1*^{hg1} heterozygous fish to determine whether increased *c-myb* or *runx1* expression is retained in the homozygous mutant embryos. If *chd7* works through *c-myb* and

runx1, mutation of either gene should suppress the expansion of blood induced by loss of *chd7*. One potential caveat to the *c-myb* experiment is that there may be compensation by *b-myb*, thus a double knockdown of *b-myb* and *chd7* may be required to see the suppression. Collectively, these experiments will help elucidate a mechanism for CHD7 function by identifying interacting partners and the target genes that regulate blood development.

Identifying signaling pathways that interact with *chd7*.

Various transgenic fish expressing activators or inhibitors of known signaling pathways important for blood development could be used to rapidly screen for upstream regulators of *chd7*. Heat-shock lines overexpressing activators and inhibitors of Wnt, BMP, and Notch can be injected with *chd7* morpholinos to determine whether *c-myb* or *runx1* expression is affected. Enhancement of bone morphogenic protein (BMP) signaling pathway by overexpressing *bmp2b* increased posterior blood island formation, demonstrating a role for BMP signaling in the induction of primitive hematopoietic cells (Lengerke et al 2008). To test whether inhibition of BMP signaling could suppress the blood expansion of *chd7* morphants, *chd7* morpholino was injected into embryos expressing the BMP inhibitor *chordin* under the control of a heat-shock promoter, *Tg(hsp70l:chd)*. Embryos were

heatshocked briefly after the onset of gastrulation and developed until 36 hpf to examine *c-myb* and *runx1* expression in the AGM. It was interesting to observe that *chd7* overall synergized with BMP pathway because heat-shocked *chordin chd7* morphants displayed a more severe phenotype than uninjected *chordin* embryos, consistent with previous studies (Hurd et al 2010, Layman et al 2009, Patten et al 2012). For example, the tail of the morphants was much shorter, and heart development was severely inhibited. However, *chordin chd7* morphants still had more *c-myb*$^{+}$/*runx1*$^{+}$ cells in the trunk compared to uninjected controls, thus *chd7* does not appear to interact with the BMP pathway in blood, further supporting the differential role of Chd7 in hematopoiesis distinct from other tissues.

***chd7* regulation in adult hematopoiesis.**

Given that knockdown of *chd7* increased most of the hematopoietic lineages tested, one of the questions that arises is whether *chd7* is also required for the differentiation of individual hematopoietic lineages. Specific knockouts of *chd7* in each hematopoietic lineage would have to be generated in order to address this question, which is possible in mice by breeding existing Chd7^{flox} lines to tissue specific Cre recombinase lines. In one initial study, Vav-Cre driven knockout of Chd7 in all hematopoietic lineages in the mouse embryo did not result in specific lineage

defects, but there was an expansion of T cells after competitive transplantation, consistent with the zebrafish phenotype and suggesting functional conservation of CHD7 in mice (see Chapter 3, note added in proof). The role of Chd7 in adult hematopoietic cells can be studied by conitionally deleting Chd7 using Mx1-Cre.

In addition to embryonic hematopoiesis, *chd7* may also have a role in adult hematopoiesis. To date, a zebrafish mutant for *chd7* has not been identified, but a mutant can be generated relatively quickly using engineered zinc finger nucleases (ZFN). Zinc finger nucleases are chimeric proteins containing zinc finger proteins, which provide DNA binding specificity, fused to a FokI endonuclease domain. Dimerization of zinc finger nucleases is required for endonuclease activity, which ultimately results in the introduction of mutations during the repair of double stranded DNA breaks induced at the target sites (Meng et al 2008). Using the context-dependent assembly (CoDA) program, sequences within *chd7* suitable for zinc finger targeting can be rapidly identified (Sander et al 2008). Recently, I have generated three pairs of zinc fingers that target the coding regions of *chd7,* of which two appear to have activity *in vivo*. Screening is in progress to identify founder fish harboring mutations in *chd7*. Although homozygous mutant fish may not survive to adulthood given the crucial role of *chd7* in development, they may still be able to survive to the larval stages to allow for additional blood analysis. The study of globin switching

would be possible with such a mutant. Although still in the process of being analyzed, the microarray results showed an increase in adult globin expression in *chd7* morphants at 36 hpf. Any changes in embryonic or adult globin expression can be assayed by quantitative PCR for the specific globin genes.

With a viable zebrafish *chd7* mutant, the effects of losing *chd7* in the development and maintenance of adult kidney marrow blood populations could be studied. Even the loss of one allele may result in a phenotype given that human CHARGE patients are haploinsufficient for CHD7. Fluorescence activated cell sorting (FACS) can be used to visualize the lymphoid, myeloid, and precursor populations in the kidney marrow. Based on the embryonic phenotype, there may be a higher percentage of blood populations in *chd7* deficient marrow compared to wild-type. Skewing towards the myeloid lineage is possible given the strong upregulation of *c-myb* in the embryo.

Whether upregulation of hematopoietic genes in *chd7* deficient cells correlates with improved regenerative functions can be tested by kidney marrow irradiation and transplantation assays. For the irradiation recovery assay, *chd7* mutant, heterozygous, and wild-type adult zebrafish are sublethaly irradiated, and recovery of lymphoid, myeloid, and precursor populations is measured by FACS over a time course (Trompouki et al 2011). Competitive kidney marrow transplantation experiments can

be performed to determine whether loss of *chd7* improves the transplantability of marrow cells using FACS again to measure marrow populations after transplantation. Some hematopoietic genes have been found to improve self-renewal and engraftment ability of HSCs, notably HoxB4, thus *chd7* deficient cells may also show improved reconstitution given the broad upregulation of hematopoietic genes. These experiments will also help determine whether Chd7 is valuable as a therapeutic target (Antonchuck et al 2001).

Some evidence in mice already suggests a function for *chd7* in adulthood. Chd7 is expressed at low levels in bone marrow HSCs but at very high levels in monocytes and granulocytes of the myeloid lineage and B and T cells of the lymphoid lineage, among others (Beerman et al 2010). Consistent with the high expression in lymphoid cells, Chd7 deficient bone marrow showed a competitive advantage in T cell reconstitution (see Chapter 3, note added in proof). These experiments can be extended to secondary and tertiary transplants to determine whether *chd7* deficient stem cells show enhanced self-renewal capabilities. Collectively, the use of zebrafish mutants and conditional mice will help elucidate the function of Chd7 in regulating adult hematopoiesis.

CHD7 as a therapeutic target.

If indeed the inhibition of CHD7 results in activation of the entire hematopoietic program, it would be a valuable target to manipulate for *ex vivo* generation of blood cells or for therapies such as cord blood transplantation that require cells to reconstitute the entire hematopoietic system. A transgenic fish line expressing GFP under the *chd7* promoter can be generated and used for chemical screening for factors that suppress *chd7*. Any upstream signaling pathway found to interact with *chd7* can be verified with chemicals as part of the screen. The fluorescent readout should be robust given the high levels of ubiquitous expression of *chd7* in the early embryo as determined by whole mount *in situ* hybridization (WISH). As this is not a tissue specific assay, any potential candidates can be retested in *Tg(cmyb:EGFP)* embryos or by WISH for various blood markers.

Chemicals that regulate *chd7* can then be tested for their ability to enhance blood formation in therapeutic cell types such as human embryonic stem (ES) cells and mobilized bone marrow CD34+ cells. Knockdown of *CHD7* will have to be tested first to characterize its function in these systems. Given that $CD34^{+}$ cells are hematopoietic, we would expect that depletion of CHD7 would expand these cells. Transplantation into mice can be used to determine if it enhances engraftment or transplantability. ES cells are pluripotent cell types that can be instructed to form various adult tissue types. Reduction of *CHD7* may relieve repression of

hematopoietic transcription factors and improve directed differentiation of ES cells into blood *ex vivo.* Various efforts are underway to uncover epigenetic drugs that alter the epigenetic state of cells for therapeutic uses. With the use of zebrafish genetics, we have identified *chd7* and other chromatin factors as a putative therapeutic targets for hematopoietic reconstitution in humans.

Concluding remarks.

The work described in this thesis provides a platform for understanding the epigenetic code that directs the specification and differentiation of hematopoietic cells. The hematopoietic system has been used widely to study the molecular mechanism regulating developmental processes. Earlier studies focused on the role of transcription factors in determining cell fate, and current efforts are focused on the epigenetic contributions to this process. Our chromatin factor screen identified a non-redundant and tissue specific role for chromatin factors regulating various stages of developmental hematopoiesis *in vivo* using zebrafish. The workup of *chd7* supports a possible model in which chromatin factors act as gatekeepers of lineage commitment and differentiation given as disruption of *chd7* and other chromatin factors characterized in this thesis appear to regulate development of an entire organ. Elucidating the function of *chd7* and other chromatin factors identified from the

screen will likely reveal new mechanisms into how changes in chromatin structure provides instructive roles for development and how they might contribute to disease.

Appendix I

Chapter 2: Supplementary Figures and Addendum

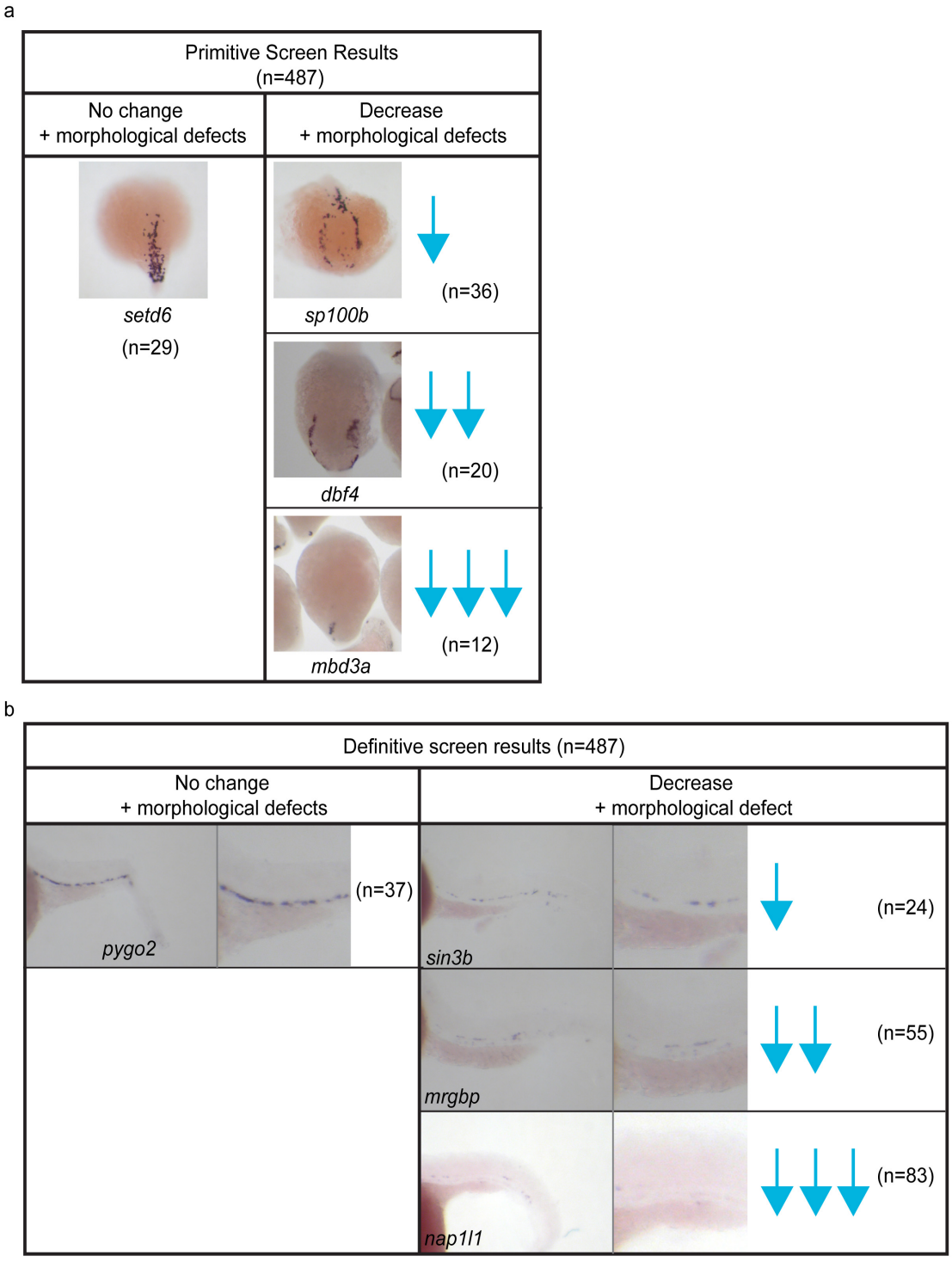

Supplementary Figure 2-1. Screen hits with morphological defects. Blue downward arrows represent reduced expression of the marker, with three arrows representing the strongest reduction.

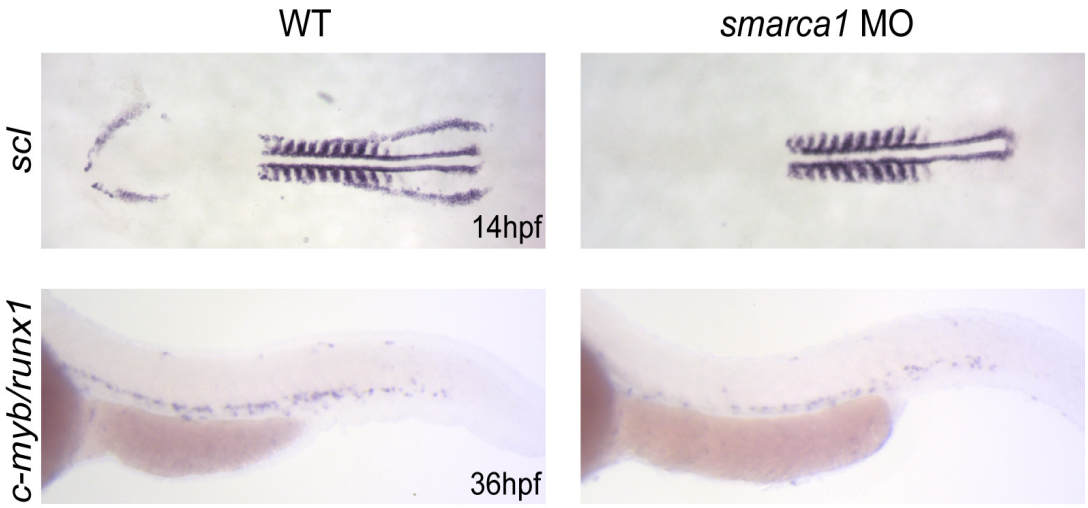

Supplementary Figure 2-2. *smarca1* is required for primitive and definitive hematopoiesis. Knockdown of *smarca1* ablates early embryonic anterior and posterior *scl* expression. Lower levels of *smarca1* knockdown, allowing the embryos to develop to 36 hpf, results in loss of *c-myb*$^{+}$ and *runx1*$^{+}$ cells in the AGM.

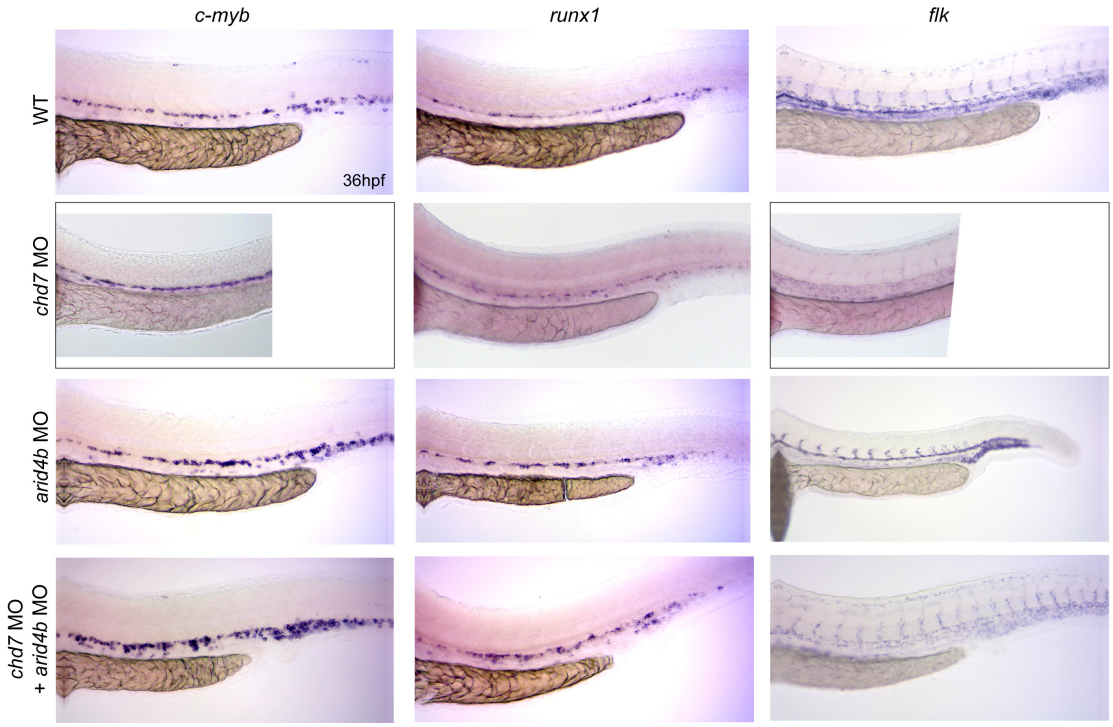

Supplementary Figure 2-3. Combinatorial loss of chromatin factors enhances hematopoiesis. Knockdown of *arid4b* results in increased *c-myb* and *runx1* expression without disrupting vasculature as determined by *flk* staining. Knockdown of *chd7* also results in increased *c-myb* and *runx1* staining, but *flk* expression is reduced. Combined *chd7* and *arid4b* knockdown resulted in higher increase of *c-myb*$^{+}$ and *runx1*$^{+}$ cells with significant loss of *flk* staining.

Decrease	Domain/ Family	Associated Complex
actr2b	Actin	Arp2/3
chrac1	Histone	ISWI
ehmt2	SET	-
hdac9b	HDAC	-
phf13l	PHD	-
rsf1b	PHD	ISWI
smarca1	SNF2	ISWI
Increase		
ash2l	Trithorax	SET1/MLL
arid1a	ARID	SWI/SNF
chd7	Chromodomain	PBAF
cicl	HMG box	-
epc2	EPC	-
ing5b	ING	HBO1
jhdm1f	JmjC	SETD1A
jmjd3a	JmjC	MLL4/ASH2L
prdm12	SET	-
prdm15	SET	-
zfat	Zinc finger	-

Supplementary Table 1. Primitive strong decrease and increase hits.

Decrease	Domain/ Family	Associated Complex
ash2l	TrxG	SET1/MLL
brd8b	bromodomain	NuA4
cbx6b	chromodomain	PRC1
cbx8b	chromodomain	PRC1
cxxc1l	PHD	SET1/MLL
ep300	HAT	NCOA
hdac4l	HDAC	-
hdac6	HDAC	-
hdac9a	HDAC	-
ing4	ING	HBO/HAT
jhdm1bb	Jmj	-
jmjd1ca	Jmj	-
mbd3b	MBD	NuRD, MeCP1
mier1	SANT	HDAC1
mier1b	SANT	HDAC1
mll	SET	SET1/MLL
nap1l4a	NAP	-
phf21a	PHD	HDAC1
prdm12	SET	-
prdm16	SET	-
rbbp7	WD40	HAT1
sirt7	HDAC	-
smarcd1	SWI	BAF
smarcd2	SWI	BAF
suv39h1	SET	HDAC1
Increase		
arid4b	ARID	Sin3A/HDAC
cecr2	bromodomain	CERF
chd7	chromodomain	PBAF
crebbpa	HAT	NCOA
mbd6	MBD	-
setd1ba	SET	SET1/MLL

Supplementary Table 2. Definitive strong decrease and increase hits.

Addendum

To further categorize and analyze our dataset, we are generating a protein-protein interaction map of all 425 chromatin factors screened and mapping our screen hits with no morphological defects onto this network to help identify additional complexes or subunits important for blood development. This work is being done in collaboration with the Winston Hide lab.

We are also developing Fluidigm technology of high-throughput qPCR to analyze changes in gene expression in blood and other tissues, including vessel, heart, kidney, liver, eye, skin, pancreas, muscle, and nervous system, to verify the blood defects of the morphants and to provide clues about the function of these chromatin factors during development. RNA was collected from all 47 morphants that were characterized with additional markers, and we have run 1 plate of each primitive and definitive samples through Fluidigm. We are currently analyzing the results to determine the proper normalization method and whether it accurately reflects the phenotypes observed in the morphants by WISH.

Appendix II

Chapter 3: Addendum

Addendum

To investigate the mechanism by which knockdown of *chd7* causes a hematopoietic expansion phenotype, a BrDU remains to be tested at the earlier stages to verify this phenotype microarray was recently performed to examine global changes in gene expression. RNA was collected from wild-type uninjected controls and *chd7* morpholino injected embryos at 5 ss (12 hpf), the earliest timepoint at which *scl* expression was increased, and at 36 hpf, when definitive HSPCs have formed in the AGM. The experiment was conducted in triplicate, and samples were hybridized to an Affymetrix zebrafish chip. 500 genes were significantly up- or downregulated at the 36 hpf timepoint. Among the hematopoietic genes identified from these arrays are *nfe2* and *β-globin a1*. However, the zebrafish annotations must be converted to human gene annotations for further analysis, such as conducting an Integrated Pathway Analysis (IPA) to identify biological processes potentially involved in the mechanism of *chd7* function in blood. This will be done after my thesis defense.

chd7 morpholinos were re-injected into embryos derived from genotyped *cmyb*^{t25127} heterozygous mutant fish and collected at 36 hpf for WISH of *runx1* and *c-myb*. The embryos will be scored and genotyped after my thesis defense.

Appendix III

Regulation of stem cells in the zebra fish hematopoietic system

Attributions

This article was reprinted with copyright permission from Cold Spring Harbor Library Press.

Huang, H. T., & Zon, L. (2008). Regulation of stem cells in the zebra fish hematopoietic system. *Cold Spring Harbor symposia on quantitative biology, 73*: 111-118.

Regulation of Stem Cells in the Zebra Fish Hematopoietic System

H.-T. Huang and L.I. Zon

Cold Spring Harb Symp Quant Biol 2008 73: 111-118 originally published online November 6, 2008
Access the most recent version at doi:10.1101/sqb.2008.73.029

Regulation of Stem Cells in the Zebra Fish Hematopoietic System

H.-T. Huang and L.I. Zon

Harvard Medical School, Stem Cell Program and Division of Hematology/Oncology, Children's Hospital and Dana Farber Cancer Institute, Howard Hughes Medical Institute, Harvard Stem Cell Institute, Boston, Massachusetts 02115

Hematopoietic stem cells (HSCs) have been used extensively as a model for stem cell biology. Stem cells share the ability to self-renew and differentiate into multiple cell types, making them ideal candidates for tissue regeneration or replacement therapies. Current applications of stem cell technology are limited by our knowledge of the molecular mechanisms that control their proliferation and differentiation, and various model organisms have been used to fill these gaps. This chapter focuses on the contributions of the zebra fish model to our understanding of stem cell regulation within the hematopoietic system. Studies in zebra fish have been valuable for identifying new genetic and signaling factors that affect HSC formation and development with important implications for humans, and new advances in the zebra fish toolbox will allow other aspects of HSC behavior to be investigated as well, including migration, homing, and engraftment.

Stem cells and early progenitors are important for organ formation during development and support tissue function throughout an organism's lifetime. These principles are illustrated in the blood system, where HSCs are needed to maintain a constant pool of progenitors committed to the various blood lineages to replenish the mature blood cells that turn over. Consequently, HSCs, like other stem cells, have the ability to self-renew in order to generate more HSCs and to differentiate along multiple lineage pathways to make erythrocytes, megakaryocytes, monocytes/macrophages, neutrophils, or lymphocytes. Because of their potential therapeutic value, HSCs have been the subject of intense study for many years, but methods for maintaining them in vitro and differentiating them into specific cell types are limited. In addition, HSCs remain difficult to study because their ontogeny is tightly regulated in a spatial and temporal manner, with progenitors of varying potentials arising from different sites.

Research using the zebra fish (*Danio rerio*) model has provided new insights into some of the major issues regarding the regulation and function of HSCs (Davidson and Zon 2004; Carradice and Lieschke 2008; Orkin and Zon 2008). The advantages of using zebra fish include its high fecundity, rapid growth, and external development of transparent embryos, which facilitates visualization of early embryonic processes. Most importantly, the genes controlling hematopoiesis are highly conserved in fish and mammals. Many blood mutants have been isolated from large-scale genetic screens (Ransom et al. 1996; Weinstein et al. 1996), thereby providing powerful tools for dissecting the molecular aspects of HSC control.

EMBRYONIC HEMATOPOIESIS: PRIMITIVE AND DEFINITIVE WAVES

The onset of hematopoiesis in the early embryo is characterized by the induction of distinct progenitors at various anatomical sites. Hematopoiesis subsequently shifts location during the course of development, as depicted in Figure 1. Blood formation occurs in two major waves. In zebra fish, the primitive wave consists of the formation of primitive erythrocytes (*gata1*$^{+}$) in the intermediate cell

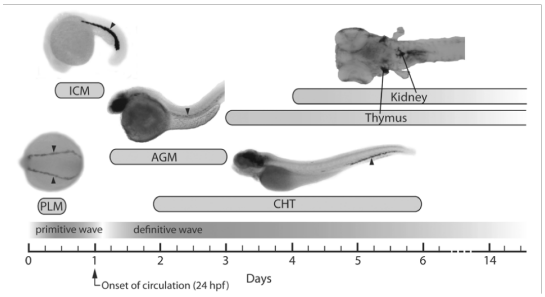

Figure 1. Embryonic hematopoiesis in zebra fish. Hematopoiesis occurs in two waves. In zebra fish, the primitive wave begins with the induction of precursors in the bilateral stripes of the posterior lateral mesoderm (PLM), which converge medially to form the intermediate cell mass (ICM) region where primitive erythrocytes are formed. After the onset of circulation (about 24 hours postfertilization [hpf]), definitive HSCs appear in the aorta-gonad mesonephros (AGM) region. These cells subsequently migrate and colonize the caudal hematopoietic tissue (CHT), thymus, and kidney. Each hematopoietic site is identified by in situ hybridization for *gata1* at 14 hpf (PLM), *gata1* at 20 hpf (ICM), c-*myb* at 36 hpf (AGM), *scl* at day 4 (CHT), and c-*myb* at day 6 (thymus and kidney). (Photos courtesy of X. Bai and T.V. Bowman.)

mass (ICM) region from posterior lateral mesoderm (PLM) (Detrich et al. 1995) and the emergence of primitive myeloid cells (*pu.1*$^+$) from anterior lateral mesoderm (ALM) (Herbomel et al. 1999; Bennett et al. 2001). This initial wave of blood production is equivalent to blood formation on the extraembryonic yolk sac of other vertebrates. The primary function of primitive hematopoiesis is to provide red blood cells to deliver oxygen within the rapidly developing embryo. Although dispensable in zebra fish, this property allows primitive blood mutants to be studied in the fish because early blood defects in most other vertebrates are embryonic-lethal.

Soon after the formation of the ICM, erythromyeloid progenitor cells (*lmo2-gata1*$^+$) appear in the posterior blood island (PBI) located in the tail region (Bertrand et al. 2007), and a wave of definitive HSC (*runx1*$^+$, c-*myb*$^+$, *ikaros*$^+$, *lmo2*$^+$, *scl*$^+$, and *CD41*$^+$) production ensues in the aorta-gonad-mesonephros (AGM) region along the ventral wall of the dorsal aorta (Liao et al. 1998; Thompson et al. 1998; Willett et al. 2001; Kalev-Zylinska et al. 2002; Bertrand et al. 2008; Kissa et al. 2008). These AGM cells subsequently colonize the caudal hematopoietic tissue (CHT), an expansion of the PBI, as well as the thymus and kidney (Murayama et al. 2006; Jin et al. 2007; Kissa et al. 2008).

These secondary hematopoietic tissues provide a niche for blood progenitors to expand and begin to differentiate. The CHT is similar to mouse placenta or fetal liver, and developing lymphoid and myeloid cells in this region can be identified by markers such as c-*myb*, *scl*, *runx1*, and *ikaros* (Murayama et al. 2006; Zhang and Rodaway 2007). Thymic immigrants differentiate into *rag1*$^+$ lymphoid cells (Murayama et al. 2006; Jin et al. 2007; Kissa et al. 2008). The kidney is the adult hematopoietic organ in zebra fish equivalent to mammalian bone marrow, and like the CHT, c-*myb*, *scl*, *runx1*, and *ikaros* are expressed in this region (Murayama et al. 2006; Jin et al. 2007). Within the kidney marrow, HSCs reside adjacent to renal tubule epithelial cells (Kobayashi et al. 2008).

ORIGIN OF BLOOD CELLS: HEMANGIOBLASTS AND HEMOGENIC ENDOTHELIUM

Currently, it is thought that blood and vascular cells derive from a common progenitor based on shared marker expression and physical proximity between the two cell types during development. The lack of blood and vascular markers in developing zebra fish *cloche* (*clo*) mutants provides evidence for the existence of hemangioblasts (Strainier et al. 1995; Thompson et al. 1998), further supported by recent fate-mapping experiments in the early embryo. Photoactivation of fluorescein dextran in single cells within the ventral mesoderm at shield stage (6 hours postfertilization [hpf]) labeled blood and vascular cells later at 30 hpf (Vogeli et al. 2006).

Definitive HSCs are believed to arise from the hemogenic endothelium (Jaffredo et al. 1998; de Brujin et al. 2002) and are transplantable and capable of multilineage differentiation (Cumano et al. 1996; Medvinsky and Dzierzak 1996). In addition, other data suggest that mesenchymal cells ventral to the dorsal aorta have HSC potential (North et al. 2002). By analogy, HSCs produced within the zebra fish AGM region are believed to be equivalent to those found in the same region in mice, supported by expression of homologous markers and lineage-tracing data. Furthermore, hematopoietic mutants such as *clo* and *spadetail* (*spt*) that disrupt formation of the dorsal aorta show loss of HSC induction (Thompson et al. 1998).

TRANSCRIPTIONAL REGULATORS OF HSC FORMATION

Specification of hematopoietic cells involves both the action of master blood transcriptional regulators and signaling molecules from the surrounding tissues. The transcription factors important for hematopoiesis in zebra fish are listed in Table 1. Many of them have been implicated in blood development by the blood-specific roles these factors have in other vertebrates or by genetic analysis of mutants isolated from large-scale screens (Fig. 2). Together, they

Table 1. Hematopoietic transcription factors in zebra fish

Gene	Family	Loss of function	Reference
scl	basic helix loop helix	morphant	Dooley et al. (2005)
c/ebp1	bZIP	morphant	Su et al. (2007)
c/ebpa	bZIP	–	Lyons et al. (2001)
c/ebpb	bZIP	–	Lyons et al. (2001)
tif1y	B box, PHD, Bromo	*moonshine*	Ransom et al. (2004)
cbfb	core-binding factor	–	Blake et al. (2000)
ets1	ETS	–	Zhu et al. (2005)
etsrp	ETS	*y11*	Pham et al. (2007)
mef	ETS	–	Zhu et al. (2005)
pu.1	ETS	morphant	Rhodes et al. (2005)
fli1a	ETS	–	Brown et al. (2000)
cdx1a	homeobox	morphant	Davidson and Zan (2006)
cdx4	homeobox	*kugelig*	Davidson et al. (2003)
hhex	homeobox	deletion b16	Liao et al. (2000)
ldb1	LIM domain binding	–	Toyama et al. (1998)
lmo2	LIM domain	morphant	Patterson et al. (2007)
runx1	runt	morphant	Kalev-Zylinska et al. (2002)
runx3	runt	morphant	Kalev-Zylinska et al. (2003)
stat5	STAT	morphant	Paffett-Lugassy et al. (2007)
tbx16	T box	*spadetail*	Thompson et al. (1998)
trf3	TBP	morphant	Hart et al. (2007)
c-*myb*	zinc finger	deletion b316	Thompson et al. (1998)
draculin	zinc finger	–	Herbomel et al. (1999)
fog1	zinc finger	–	Nishikawa et al. (2003)
gata1	zinc finger	*vlad tepes*	Detrich et al. (1995)
gata2	zinc finger	morphant	Galloway et al. (2005)
gfi1.1	zinc finger	morphant	Wei et al. (2008)
ikaros	zinc finger	–	Willett et al. (2001)
klfd	zinc finger	–	Oates et al. (2001)
klf4	zinc finger	morphant	Gardiner et al. (2007)
klf12	zinc finger	–	Oates et al. (2001)
nfe2	zinc finger	–	Pratt et al. (2002)
ZBP-89	zinc finger	morphant	Li et al. (2006)

Adapted from Davidson and Zon (2004).

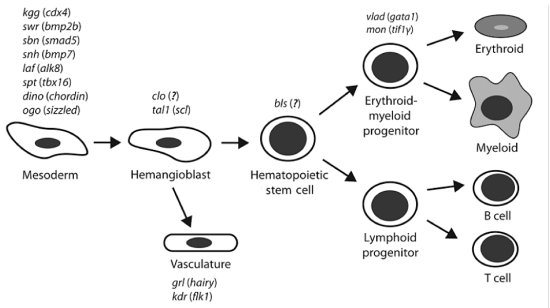

Figure 2. Mutants affecting blood development in zebra fish. Corresponding genes are in parenthesis.

form a transcriptional network that directs various aspects of the blood program from specification to differentiation.

scl and *lmo2* are expressed in hematopoietic progenitors and endothelial cells, possibly acting together to specify the hemangioblast (Patterson et al. 2007). *scl* encodes a basic helix-loop-helix transcription factor, whereas *lmo2* is a LIM-domain transcription factor. *scl* expression is initiated at 10 hpf and is coexpressed with *lmo2*, *gata2*, and *flk1* in the ALM and PLM (Gering et al. 1998; Thompson et al. 1998). A subset of these scl^+ cells in the PLM becomes $gata1^+$, committing to the erythroid lineage, whereas the $scl^+/gata1^-$ population is believed to form endothelial cells (Gering et al. 1998). In the ALM, *pu.1* expression is initiated with the differentiation of myeloid cells (Bennett et al. 2001). Overexpression of *scl* and *lmo2* expands the formation of blood and vascular progenitors along the anteroposterior (AP) axis (Gering et al. 2003), although *scl* itself is capable of activating hematopoietic genes independently of *lmo2* (Dooley et al. 2005). Once primitive erythroblasts from the ICM enter the circulation, additional markers appear that define the definitive wave.

Targeted disruption of *runx1* in mice has demonstrated its requirement for HSC induction in the AGM (Okuda et al. 1996; North et al. 2002). In zebra fish, *runx1* and c-*myb* are expressed in the AGM as well (Thompson et al. 1998; Burns et al. 2002; Gering and Patient 2005). *runx1* is a member of the runt family of transcriptional regulators involved in many developmental processes including blood and bone development in mammals. In zebra fish, *runx1* is first expressed in the bilateral stripes of the PLM that then migrate to the midline to form the ICM. It subsequently appears during the definitive wave in the ventral wall of the dorsal aorta (Burns et al. 2002). *runx1* overexpression causes HSC expansion in embryos, whereas morpholino knockdown causes defects in definitive hematopoiesis and vasculoangiogenesis (Burns et al. 2005). Furthermore, c-*myb* expression is reduced in *runx1* morphants (Kalev-Zylinska et al. 2002).

runx3 was found to regulate primitive and definitive hematopoietic cells but not vascular cells. Depletion of *runx3* resulted in decreased *runx1* expression in the ventral wall of the dorsal aorta. Conversely, overexpression of *runx3* increased primitive scl^+ cell numbers and $runx1^+$ cells in the aorta, suggesting that *runx3* regulates hematopoietic progenitor numbers and cooperates with *runx1* to regulate HSC formation in the AGM (Kalev-Zylinska et al. 2003).

c-*myb* encodes a proto-oncogene that marks the initiation of HSCs in the ventral wall of the dorsal aorta. In zebra fish, it is expressed in primitive erythroid cells in the ICM region, but it is not required for the primitive wave (Thompson et al. 1998). Expression then shifts to the ventral wall of the dorsal aorta, presumably marking the definitive HSCs in the AGM region. Although these c-myb^+ cells have not been transplanted, the lack of c-*myb* expression in *clo* and *spt* mutants provides further evidence for c-*myb* as a marker of definitive HSCs (Thompson et al. 1998).

The contribution of the *cdx-hox* pathway to specification of hematopoietic cell fate has been elucidated in zebra fish. *cdx* genes belong to the *caudal* family of homeobox transcription factors implicated in the regulation of *hox* gene expression and in AP patterning. Both *cdx1a* and *cdx4* establish the correct *hox* expression domains necessary for blood development in zebra fish (Davidson and Zon 2006). Loss of *cdx4* gene function in homozygous *kugelig* (*kgg*) mutants results in severe anemia with embryos having few scl^+ and $gata1^+$ cells, although the number of $flk1^+$ angioblasts appears to be normal. All *hox* genes examined (*hoxb4*, *hoxb5a*, *hoxb6b*, *hoxb7a*, *hoxb8a*, *hoxb8b*, and *hoxa9a*) displayed altered expression patterns in *kgg* mutants, but overexpression of *hoxb7a* and *hox9a* could rescue erythropoiesis (Davidson et al. 2003). This pathway regulating blood specification was recently found to be conserved in mouse embryonic stem (ES) cells (Lengerke et al. 2008).

Additional transcription factors important for definitive hematopoiesis include *fli1a*, *hhex*, and *tbx16*. *fli1a* is an ETS-domain transcription factor implicated in proliferation or differentiation of hematopoietic precursors. It is coexpressed in the hemangioblasts of the PLM with *gata2*, diverging later to mark only the endothelial cells (Brown et al. 2000). Given that its initial expression is normal in *clo* mutants, *fli1a* may be the earliest marker of hemangioblasts. *hhex* encodes a homeobox-containing protein whose expression begins about 12 hpf in the ALM and PLM. Overexpression enhances blood and endothelial markers but is not essential for their development, which can be compensated by *scl* (Liao et al. 2000). *tbx16* encodes a T-box transcription factor that regulates mesodermal cell migration, which is defective in *spt* mutants. As described previously, abnormal somite patterning and accumulation of mesodermal cells perturb vessel formation, which subsequently leads to defective HSC formation as demonstrated by loss of hematopoietic markers *gata2*, *gata1*, and *runx1* in the PLM (Ho and Kane 1990; Thompson et al. 1998). Overexpression of *scl* rescues blood formation in *spt* mutants, indicating that *tbx16* is upstream of *scl* in directing HSC formation (Dooley et al. 2005).

The analogous expression of these different markers in zebra fish and other vertebrate models suggests that the molecular mechanisms are highly conserved. Once the hematopoietic precursors have been specified, additional blood transcription factors such as *gata1*, *pu.1*, and *ikaros* direct the lineage-specific differentiation of these progenitors into erythroid, myeloid, and lymphoid cell types, respectively. Some of the factors required for HSC forma-

tion (*runx1*, *scl*, and *lmo2*) reappear later within the differentiation of individual blood lineages, and conversely, factors that have more lineage-restricted roles (*pu.1*) can also be found in HSCs (Orkin and Zon 2008). How the same transcription factors are used at various stages of hematopoietic development is not well understood, but the fact that many of these genes are mutated or translocated in human hematopoietic malignancies underscores the importance of these transcription factors in blood development throughout the life of an animal.

PATHWAYS IN THE INDUCTION OF HSCS

In addition to transcriptional regulators, signal transduction pathways are also important for modulating blood formation. Although distinct hematopoietic precursors are generated in different anatomical sites, common signaling events at each site are expected to lead to blood formation. How these different signaling pathways are coupled to control stem cell induction and development is a subject of ongoing research.

The family of Hedgehog (Hh) proteins are known to be involved in embryonic patterning and cell-fate specification. Based on murine mutants, there was no role for Hh signaling in hematopoiesis (Dyer et al. 2001; Byrd et al. 2002). In zebra fish, Hh was found to be required for definitive but not primitive hematopoiesis (Gering and Patient 2005). It is secreted by midline structures (floor plate, notochord, and hypochord) in the developing embryo. When Hh signaling is inhibited by chemicals or in genetic mutants, embryos showed normal numbers of β-*globinE1*$^+$ primitive erythrocytes but reduced *runx1*$^+$ definitive stem cells and *rag1*$^+$ thymocytes, suggesting that Hh is required only for induction of definitive HSCs. Impaired medial migration of *flk1*$^+$ angioblasts was also observed, indicating the possibility that improper patterning of the aorta is the cause of HSC loss. These effects were similar to those seen with vascular endothelial growth factor (VEGF) and Notch inhibition (Gering and Patient 2005).

Notch signaling has been previously shown to be required for induction of HSCs during embryogenesis in mice (Okuda et al. 1996). The Notch pathway is highly conserved throughout evolution, regulating cell-fate decisions in a wide range of biological processes. Using zebra fish *mind bomb* mutants that lack an E3 ubiquitin ligase essential for Notch signaling, *runx1* was identified as a downstream effector (Burns et al. 2005). Overexpression of *notch1a* intracellular domain (NICD) expanded the population of c-*myb*$^+$ and *runx1*$^+$ cells in the AGM region, and this increase was not due to proliferation or conversion of vein-to-artery identity. This phenotype was recapitulated in *runx1* overexpressing embryos (Burns et al. 2005). Given that it rescues the *mind bomb* phenotype, *runx1* may be acting in parallel or downstream from Notch signaling. In addition, *runx1* morphants show reduced c-*myb*$^+$ and *ikaros*$^+$ cells at 50 hpf and loss of *rag1*$^+$ thymocytes at 6 days (Gering and Patient 2005).

A new pathway modulating HSC formation by prostaglandins was recently identified in the zebra fish. Prostaglandins are part of the eicosanoid signal transduction pathway, with prostaglandin E2 (PGE2) being the main effector prostanoid produced in the zebra fish. They are regulated by cyclooxygenases Cox1 and Cox2 (Grosser et al. 2002). When treated with PGE2, zebra fish embryos showed increased *runx1*$^+$ and *cmyb*$^+$ cells in the AGM region by in situ hybridization, confocal microscopy, and quantitative polymerase chain reaction (PCR). Chemical or morpholino inhibition of the pathway reduced HSC formation. These results were verified in both colony-forming and -limiting dilution competitive transplantation assays in the mouse, demonstrating a functional conservation of prostaglandin signaling not only in inducing HSCs, but also in adult maintenance (North et al. 2007). 16,16-Dimethyl-PGE2 (dmPGE2), a stable derivative of PGE2, will be tested in a human phase I clinical trial to determine whether it can improve the efficiency of cord blood transplantations (Lord et al. 2007).

MIGRATORY ROUTES OF HSCs TO SECONDARY HEMATOPOIETIC SITES

The ontogeny of HSCs in the AGM region is followed by subsequent colonization of secondary hematopoietic sites, presumably as different niches become available to support HSC growth within the constantly evolving microenvironment of the developing embryo. Lineage tracing in the mouse has been complicated by the inability to stage embryos precisely in utero and to determine the kinetics of conditional recombination activity, making it difficult to identify clearly the anatomic origins of adult HSCs. One advantage of performing in vivo fate mapping in zebra fish is the optical transparency and external development of its embryos.

Live imaging of cells labeled with green fluorescent protein (GFP) driven by HSC-specific promoters, such as *CD41* and c-*myb*, and caged fluorescein-dextran cell-tracing experiments have shown that HSCs from the AGM region migrate to colonize the CHT, thymus, and pronephros (Murayama et al. 2006; Jin et al. 2007; Zhang and Rodaway 2007; Bertrand et al. 2008; Kissa et al. 2008). *CD41* marks HSCs in the mouse (Mitjavila-Garcia et al. 2002; Ferkowicz et al. 2003; Mikkola et al. 2003). In zebra fish, both *CD41*-GFP$^+$ and c-*myb*-GFP$^+$ cells were observed in the AGM region, consistent with *runx1* expression at the same site (North et al. 2007; Kissa et al. 2008). Knockdown of *runx1* suppressed the appearance of *CD41*-GFP$^+$ cells in this region, the CHT, and thymus (Kissa et al. 2008). Transplantation of *CD41*-GFP$^+$ AGM cells into sibling embryonic recipients demonstrated colonization of the thymus and CHT (Bertrand et al. 2008), although assays have yet to be developed in the zebra fish that can support long-term reconstitution of embryonic donor cells.

Unlike chick and mouse, where AGM HSCs presumably bud off into circulation from intra-aortic clusters, AGM cells in zebra fish enter the circulation through the cardinal vein (CV) to seed the CHT (Kissa et al. 2008). Migration to the CHT requires circulation because *CD41*-GFP$^+$ and c-*myb*$^+$ cells were not found in the CHT of *silent heart* (*sih*) morphants (Murayama et al. 2006), which lack blood flow due to disruption of cardiac tropomyosin. Seeding of the thymus occurs by both circulation and

migration through the mesenchyme from either the AGM or the CHT. These cells then proliferate and generate *rag1*$^+$ T-lymphocyte precursors (Murayama et al. 2006; Kissa et al. 2008).

Recently, a novel route was found for HSCs to seed the kidney. Using time-lapse imaging of *CD41*-GFP and c-*myb*-GFP transgenic animals, hematopoietic cells were observed crawling along the pronephric tubules from the AGM toward the anterior glomeruli (Bertrand et al. 2008). The migration appears to be circulation-independent given that it remains intact in *sih* morphants. These migrating cells were found to express *runx1* and the pan-hematopoietic marker *CD45* as well, suggesting that they are stem cells (Bertrand et al. 2008).

ADVANCES IN ZEBRA FISH FOR THE STUDY OF HSCs

The power of the zebra fish model lies in the ability to perform large-scale genetic screens. Both forward genetic screens, using *N*-ethyl-*N*-nitrosourea (ENU) (Haffter et al. 1996; Weinstein et al. 1996) or insertional mutagenesis (Amsterdam et al. 1999), and reverse genetic screens, using targeted induced local lesions in genomes (TILLING) (Wienholds et al. 2002) and morpholinos, have been described. Zebra fish also provide a unique platform for conducting in vivo whole-animal chemical screening to identify novel compounds of therapeutic value. Although a number of hematopoietic mutants have been isolated from previous screens, a small number affect HSCs (Fig. 2); continued screening thus has the potential to generate new mutations that affect other pathways or regulators of HSC development. More precise genetic manipulations in zebra fish can be accomplished with transgenic fish, for example, using the heat shock Cre/*lox* system to induce tissue-specific gene expression (Feng et al. 2007). Recently, zinc finger nucleases have been used successfully for inducing targeted mutations in the germ line (Meng et al. 2008). The combination of these molecular methods makes it feasible to perform very precise genetic manipulations in zebra fish.

Assays that test stem cell function have also been developed in zebra fish. The major blood lineages (erythroid, lymphoid, myeloid, and precursors) can be segregated by flow cytometry using only the forward scatter and side scatter profiles (Traver et al. 2003); thus, multilineage reconstitution can be measured in irradiation-recovery or transplantation assays (Fig. 3, top left and bottom) (Traver et al. 2004). This method was used to determine the contribution of Notch and prostaglandin signaling to adult hematopoiesis, because these were both identified initially as regulators of HSC induction during embryogenesis (Burns et al. 2005; North et al. 2007). A brief dose of Notch activation or treatment with PGE2 enhanced marrow recovery postirradiation by expanding early multilineage precursors. *runx1*, *lmo2*, *scl*, and even *fli1* expression were significantly up-regulated in these cells (Burns et al. 2005; North et al. 2007). The effects of PGE2 were verified by limiting dilution transplantation assays of HSCs in the mouse (North et al. 2007). Although the mechanism by which these pathways enhance recovery remains unknown, they are ideal candidates for clinical use because any chemical that can enhance their signaling may have the potential to improve patient recovery post-transplantation by stimulating hematopoietic stem and progenitor cells.

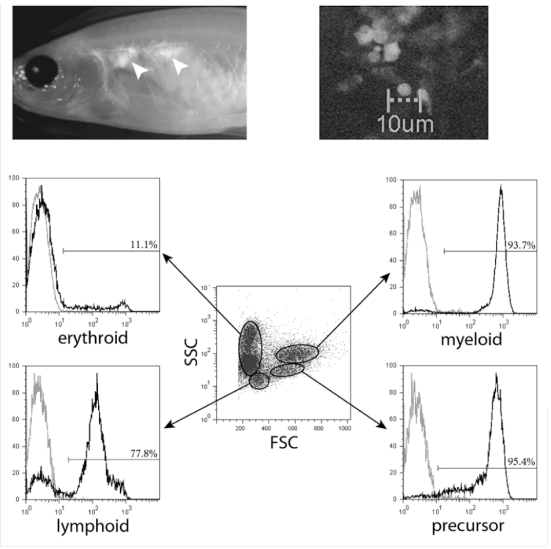

Figure 3. Multilineage reconstitution posttransplantation of transparent *casper* fish. (*Top left*) β-actin:GFP cells transplanted into irradiated *casper* fish show engraftment at 4 weeks post-transplantation. (*White arrowheads*) GFP$^+$ cells observed in the kidney by fluorescent microscopy. (*Top right*) In vivo visualization of recipient kidney marrow by confocal laser scanning shows single GFP$^+$ cells. Bar, 10 μm. (*Bottom*) Whole kidney marrow isolated from transplanted fish can be sorted into erythroid, lymphoid, myeloid, and precursor cells by flow cytometry based on forward scatter (FSC) and side scatter (SSC). Histograms of GFP$^+$ cells show reconstitution in the lymphoid, myeloid, and precuror populations. (*Top right,* Reprinted, with permission, from White et al. 2008 [© *Cell Press*]; *bottom,* images courtesy of J. de Jong.)

Finally, visualization of HSCs in adult fish is now facilitated due to the recent development of a transparent zebra fish called *casper* (White et al. 2008). *casper* fish are doubly mutant for the nacre allele (encoding the *mitfa* gene) and the roy allele (encoding an unknown pigment gene), which blocks the development melanocytes and iridophores, respectively. As a result, the lack of pigmentation allows internal organs such as the heart, intestinal tube, liver, and gallbladder to be observed in vivo with the naked eye (White et al. 2008). HSC homeostasis could be studied in the *casper* fish within the context of the endogenous marrow niche, which has been a traditionally difficult process to observe. The ability to use these fish for examining the kinetics of stem cell homing and engraftment in the transplantation setting with resolution down to the single-cell level is currently unparalleled in other model systems (Fig. 3, top left and right).

CONCLUSIONS

Studies of HSCs in zebra fish have complemented investigations in other model organisms and have advanced our

understanding of hematopoiesis. Much of what has been learned about the signaling pathways and transcription factors involved in the development of HSCs in zebra fish and other vertebrates is highly conserved. Given that zebra fish are amenable to large-scale screens, future genetic screens will continue to uncover new mutants with interesting hematopoietic phenotypes, and whole-animal chemical screening will identify new compounds of clinical value. In vivo screens are feasible using reporter lines and mutant and transgenic strains. As zebra fish methods advance, new opportunities for revealing more details of the molecular mechanisms of stem cell regulation will arise. Finally, the knowledge gained about HSCs will likely be applicable to stem cell biology in general.

ACKNOWLEDGMENTS

We thank X. Bai, J. de Jong, and R.M. White for a critical reading of the manuscript.

REFERENCES

Amsterdam, A., Burgess, S., Golling, G., Chen, W., Sun, Z., Townsend, K., Farrington, S., Haldi, M., and Hopkins, N. 1999. A large-scale insertional mutagenesis screen in zebrafish. *Genes Dev.* **13:** 2713–2724.

Bennett, C.M., Kanki, J.P., Rhodes, J., Liu, T.X., Paw, B.H., Kieran, M.W., Langenau, D.M., Delahaye-Brown, A., Zon, L.I., Fleming, M.D., and Look, A.T. 2001. Myelopoiesis in the zebrafish, *Danio rerio*. *Blood* **98:** 643–651.

Bertrand, J.Y., Kim, A.D., Ten, S., and Traver, D. 2008. $CD41^{+}$ $cmyb^{+}$ precursors colonize the zebrafish pronephros by a novel migration route to initiate adult hematopoiesis. *Development* **135:** 1853–1862.

Bertrand, J.Y., Kim, A.D., Violette, E.P., Stachura, D.L., Cisson, J.L., and Traver, D. 2007. Definitive hematopoiesis initiates through a committed erythromyeloid progenitor in the zebrafish embryo. *Development* **134:** 4147–4156.

Blake, T., Adya, N., Kim, C.H., Oates, A.C., Zon, L., Chitnis, A., Weinstein, B.M., and Liu, P.P. 2000. Zebrafish homolog of the leukemia gene *CBFB:* Its expression during embryogenesis and its relationship to *scl* and *gata-1* in hematopoiesis. *Blood* **96:** 4178–4184.

Brown, L.A., Rodaway, A.R., Schilling, T.F., Jowett, T., Ingham, P.W., Patient, R.K., and Sharrocks, A.D. 2000. Insights into early vasculogenesis revealed by expression of the ETS-domain transcription factor Fli-1 in wild-type and mutant zebrafish embryos. *Mech. Dev.* **90:** 237–252.

Burns, C.E., DeBlasio, T., Zhou, Y., Zon, L.I., and Nimer, S.D. 2002. Isolation and characterization of *runxa* and *runxb,* zebrafish members of the runt family of transcriptional regulators. *Exp. Hematol.* **30:** 1381–1389.

Burns, C.E., Traver, D., Mayhall, E., Shepard, J.L., and Zon, L.I. 2005. Hematopoietic stem cell fate is established by the Notch-Runx pathway. *Genes Dev.* **19:** 2331–2342.

Byrd, N., Becker, S., Maye, P., Narasimhaiah, R., St-Jacques, B., Zhang, X., McMahon, J., McMahon, A., and Grabel, L. 2002. Hedgehog is required for murine yolk sac angiogenesis. *Development* **129:** 361–372.

Carradice, D. and Lieschke, G.J. 2008. Zebrafish in hematology: Sushi or science? *Blood* **111:** 3331–3342.

Cumano, A., Dieterlen-Lièvre, F., and Godin, I. 1996. Lymphoid potential, probed before circulation in mouse, is restricted to caudal intraembryonic splanchnopleura. *Cell* **86:** 907–916.

Davidson, A.J. and Zon, L.I. 2004. The "definitive" (and "primitive") guide to zebrafish hematopoiesis. *Oncogene* **23:** 7233–7246.

Davidson, A.J. and Zon, L.I. 2006. The *caudal*-related homeobox genes *cdx1a* and *cdx4* act redundantly to regulate *hox* gene expression and the formation of putative hematopoietic stem cells during zebrafish embryogenesis. *Dev. Biol.* **292:** 506–518.

Davidson, A.J., Ernst, P., Wang, Y., Dekens, M.P.S., Kingsley, P.D., Palis, J., Korsmeyer, S.J., Daley, G.Q., and Zon, L.I. 2003. *cdx4* mutants fail to specify blood progenitors and can be rescued by multiple *hox* genes. *Nature* **425:** 300–306.

de Bruijn, M.F., Ma, X., Robin, C., Ottersbach, K., Samchez, M.J., and Dzierzak, E. 2002. HSCs localize to the endothelial layer in the midgestation mouse aorta. *Immunity* **16:** 673–683.

Detrich III, H.W., Kieran, M.W., Chan, F.Y., Barone, L.M., Yee, K., Rundstadler, J.A., Pratt, S., Ransom, D., and Zon, L.I. 1995. Intraembryonic hematopoietic cell migration during vertebrate development. *Proc. Natl. Acad. Sci.* **92:** 10713–10717.

Dooley, K.A., Davidson, A.J., and Zon, L.I. 2005. Zebrafish *scl* functions independently in hematopoietic and endothelial development. *Dev. Biol.* **277:** 522–536.

Dyer, M.A., Farrington, S.M., Mohn, D., Munday, J.R., and Baron, M.H. 2001. Indian hedgehog activates hematopoiesis and vasculogenesis and can respecify prospective neuroectodermal cell fate in the mouse embryo. *Development* **128:** 1717–1730.

Feng, H., Langenau, D.M., Madge, J.A., Quinkertz, A., Gutierrez, A., Neuberg, D.S., Kanki, J.P., and Look, T.A. 2007. Heat-shock induction of T-cell lymphoma/leukaemia in conditional Cre/lox-regulated transgenic zebrafish. *Br. J. Haematol.* **138:** 169–175.

Ferkowicz, M.J., Starr, M., Xie, X., Li, W., Johnson, S.A., Shelley, W.C., Morrison, P.R., and Yoder, M.C. 2003. CD41 expression defines the onset of primitive and definitive hematopoiesis in the murine embryo. *Development* **130:** 4393–4403.

Galloway, J.L., Wingert, R.A., Thisse, C., Thisse, B., and Zon, L.I. 2005. Loss of gata1 but not gata2 converts erythropoiesis to myelopoiesis in zebrafish embryos. *Dev. Cell* **8:** 109–116.

Gardiner, M.R., Gongora, M.M., Grimmond, S.M., and Perkins, A.C. 2007. A global role for zebrafish *klf4* in embryonic erythropoiesis. *Mech. Dev.* **124:** 762–774.

Gering, M. and Patient, R. 2005. Hedgehog signaling is required for adult blood stem cell formation in zebrafish embryos. *Dev. Cell* **8:** 389–400.

Gering, M., Yamada, Y., Rabbitts, T.S., and Patient, R.K. 2003. Lmo2 and Scl/Tal1 convert non-axial mesoderm into haemangioblasts which differentiate into endothelial cells in the absence of Gata1. *Development* **130:** 6187–6199.

Gering, M., Rodaway, A.R.F., Gottgens, B., Patient, R.K., and Green, A.R. 1998. The *SCL* gene specifies haemangioblast development from early mesoderm. *EMBO J.* **17:** 4029–4045.

Grosser, T., Yusuff, S., Cheskis, E., Pack, M.A., and FitzGerald, G.A. 2002. Developmental expression of functional cyclooxygenases in zebrafish. *Proc. Natl. Acad. Sci.* **99:** 8418–8423.

Haffter, P., Granato, M., Brand, M., Mullins, M.C., Hammerschmidt, M., Kane, D.A., Odenthal, J., van Eeden, F.J., Jiang, Y.J., Heisenberg, C.P., et al. 1996. The identification of genes with unique and essential functions in the development of the zebrafish, *Danio rerio. Development* **123:** 1–36.

Hart, D.O., Raha, T., Lawson, N.D., and Green, M.R. 2007. Initiation of zebrafish haematopoiesis by the TATA-box-binding protein-related factor Trf3. *Nature* **450:** 1082–1085.

Herbomel, P., Thisse, B., and Thisse, C. 1999. Ontogeny and behavior of early macrophages in the zebrafish embryo. *Development* **126:** 3735–3745.

Ho, R.K. and Kane, D.A. 1990. Cell-autonomous action of zebrafish *spt-1* mutation in specific mesodermal precursors. *Nature* **348:** 728–730.

Jaffredo, T., Gautier, R., Eichmann, A., and Dieterlen-Lièvre, F. 1998. Intraaortic hemopoietic cells are derived from endothelial cells during ontogeny. *Development* **125:** 4575–4583.

Jin, H., Xu, J., and Wen, Z. 2007. Migratory path of definitive hematopoietic stem/progenitor cells during zebrafish development. *Blood* **109:** 5208–5214.

Kalev-Zylinska, M.L., Horsfield, J.A., Flores, M.V.C., Postlethwait, J.H., Vitas, M.R., Baas, A.M., Crosier, P.S., and Crosier,

K.E. 2002. Runx1 is required for zebrafish blood and vessel development and expression of a human RUNX1-CBF2T1 transgene advances a model for studies of leukemogenesis. *Development* **129:** 2015–2030.

Kalev-Zylinska, M.L., Horsfield, J.A., Flores, M.V.C., Postlethwait, J.H., Chau, J.Y.M., Cattin, P.M., Vitas, M.R., Crosier, P.S., and Crosier, K.E. 2003. Runx3 is required for hematopoietic development in zebrafish. *Dev. Dyn.* **228:** 323–336.

Kissa, K., Murayama, E., Zapata, A., Cortes, A., Perret, E., Machu, C., and Herbomel, P. 2008. Live imaging of emerging hermatopoietic stem cells and early thymus colonization. *Blood* **111:** 1147–1156.

Kobayashi, I., Saito, K, Moritomo, T., Araki, K., Takizawa, F., and Nakanishi, T. 2008. Characterization and localization of side population (SP) cells in zebrafish kidney hematopoietic tissue. *Blood* **111:** 1131–1137.

Lengerke, C., Schmitt, S., Bowman, T.V., Jang, I.H., Maouche-Chretien, L., McKinney-Freeman, S., Davidson, A.J., Hammerschmidt, M., Rentzsch, F., Green, J.B.A., Zon, L.I., and Daley, G.Q. 2008. BMP and Wnt specify hematopoietic fate by activation of the *Cdx-Hox* pathway. *Cell Stem Cell* **2:** 72–82.

Li, X., Xiong, J.W., Shelley, C.S., Park, H., and Arnaout, M.A. 2006. The transcription factor ZBP-89 controls generation of the hematopoietic lineage in zebrafish and mouse embryonic stem cells. *Development* **133:** 3641–3650.

Liao, E.C., Paw, B.H., Oates, A.C., Pratt, S.J., Postlethwait, J.H., and Zon, L.I. 1998. SCL/Tal-1 transcription factor acts downstream of *cloche* to specifiy hematopoietic and vascular progenitors in zebrafish. *Genes Dev.* **12:** 621–626.

Liao, W., Ho, C.Y., Yan, Y.L., Postlethwait, J., and Stainier, D.Y. 2000. Hhex and scl function in parallel to regulate early endothelial and blood differentiation in zebrafish. *Development* **127:** 4303–4313.

Lord, A.M., North, T.E., and Zon, L.I. 2007. Prostaglandin E2: Making more of your marrow. *Cell Cycle* **6:** 3054–3057.

Lyons, S.E., Shue, B.C., Lei, L., Oates, A.C., Zon, L.I., and Liu, P.P. 2001. Molecular cloning, genetic mapping, and expression analysis of four zebrafish *c/ebp* genes. *Gene* **281:** 43–51.

Medvinsky, A. and Dzierzak, E. 1996. Definitive hematopoiesis is autonomously initiated by the AGM region. *Cell* **86:** 897–906.

Meng, X., Noyes, M.B., Zhu, L.J., Lawson, N.D., and Wolfe, S.A. 2008. Targeted gene inactivation in zebrafish using engineered zinc-finger nucleases. *Nat. Biotechnol.* **26:** 695–701.

Mikkola, H.K., Fujiwara, Y., Schlaeger, T.M., Traver, D., and Orkin, S.H. 2003. Expression of CD41 marks the initiation of definitive hematopoiesis in the mouse embryo. *Blood* **101:** 508–516.

Mitjavila-Garcia, M.T., Cailleret, M., Godin, I., Nogueira, M.M., Cohen-Solal, K., Schiavon, V., Lecluse, Y., Le Pesteur, F., Lagrue, A.H., and Vainchenker, W. 2002. Expression of CD41 on hematopoietic progenitors derived from embryonic hematopoietic cells. *Development* **129:** 2003–2013.

Murayama, E., Kissa, K., Zapata, A., Mordelet, E., Briolat, V., Lin, H.F., Handin, R.I., and Herbomel, P. 2006. Tracing hematopoietic precursor migration to successive hematopoietic organs during zebrafish development. *Immunity* **25:** 963–975.

Nishikawa, K., Kobayashi, M., Masumi, A., Lyons, S.E., Weinstein, B.M., Liu, P.P., and Yamamoto, M. 2003. Self-association of Gata1 enhances transcriptional activity in vivo in zebra fish embryos. *Mol. Cell Biol.* **23:** 8295–8305.

North, T.E., de Bruijn, M.F., Stacey, T., Talebian, L., Lind, E., Robin, C., Binder, M., Dzierzack, E., and Speck, N.A. 2002. Runx1 expression marks long-term repopulating hematopoietic stem cells in the midgestation mouse embryo. *Immunity* **16:** 661–672.

North, T.E., Goessling, W., Walkley, C.R., Lengerke, C., Kopani, K.R., Lord, A.M., Weber, G.J., Bowman, T.V., Jang, I.H., Grosser, T., et al. 2007. Prostaglandin E2 regulates vertebrate haematopoietic stem cell homeostasis. *Nature* **447:** 1007–1011.

Oates, A.C., Pratt, S.J., Vail, B., Yan, Y.I., Ho, R.K., Johnson, S.L., Postlethwait, J.H., and Zon, L.I. 2001. The zebrafish *klf* gene family. *Blood* **98:**1792–1801.

Okuda, T., van Deursen, J., Hiebert, S.W., Grosveld, G., and Downing, J.R. 1996. AML1, the target of multiple chromosomal translocations in human leukemia, is essential for normal fetal liver hematopoiesis. *Cell* **84:** 321–330.

Orkin, S.H. and Zon, L.I. 2008. Hematopoiesis: An evolving paradigm for stem cell biology. *Cell* **132:** 631–644.

Patterson, L.J., Gering, M., Eckfeldt, C.E., Green, A.R., Verfaillie, C.M., Ekker, S.C., and Patient, R. 2007. The transcription factors Scl and Lmo2 act together during development of the hemangioblast in zebrafish. *Blood* **109:** 2389–2398.

Paffett-Lugassy, N., Hsia, N., Fraenkel, P.G., Paw, B., Leshinsky, I., Barut, B., Bahary, N., Caro, J., Handin, R., and Zon, L.I. 2007. Functional conservation of erythropoietin signaling in zebrafish. *Blood* **110:** 2718–2726.

Pham, V.N., Lawson, N.D., Mugford, J.W., Dye, L., Castranova, D., Lo, B., and Weinstein, B.M. 2007. Combinatorial function of ETS transcription factors in the developing vasculature. *Dev. Biol.* **303:** 772–783.

Pratt, S.J., Drejer, A., Foott, H., Barut, B., Brownlie, A., Postlethwait, J., Kato, Y., Yamamoto, M., and Zon, L.I. 2002. Isolation and characterization of zebrafish NFE2. *Physiol. Genomics* **11:** 91–98.

Ransom, D.G., Bahary, N., Niss, K., Traver, D., Burns, C. Trede, N.S., Paffett-Lugassy, N., Saganic, W.J., Lim, C.A., Hersey, C., et al. 2004. The zebrafish *moonshine* gene encodes transcriptional intermediary factor 1γ, an essential regulator of hematopoiesis. *PloS Biol.* **2:** E237.

Ransom, D.G., Haffter, P., Odenthal, J., Brownlie, A., Vogelsang, E., Kelsh, R.N., Brand, M., van Eeden, F.J., Furutani-Seiki, M., Granato, M., et al. 1996. Characterization of zebrafish mutants with defects in embryonic hematopoiesis. *Development* **123:** 311–319.

Rhodes, J., Hagen, A., Hsu, K., Deng, M., Liu, T.X., Look, A.T., and Kanki, J.P. 2005. Interplay of *pu.1* and *gata1* determines myelo-erythroid progenitor cell fate in zebrafish. *Dev. Cell* **8:** 97–108.

Stainier, D.Y.R., Weinstein, B.M., Detrich III, H.W., Zon, L.I., and Fishman, M.C. 1995. *cloche,* an early acting zebrafish gene, is required by both the endothelial and hematopoietic lineages. *Development* **121:** 3141–3150.

Su, F., Juarez, M.A., Cooke, C.L., Lapointe, L., Shavit, J.A., Yamaoka, J.S., and Lyons, S.E. 2007. Differential regulation of primitive myelopoiesis in the zebrafish by Spi-1/Pu.1 and C/ebp1. *Zebrafish* **4:** 187–199.

Thompson, M.A., Ransom, D.G., Pratt, S.J., MacLennan, H., Kieran, M.W., Detrich III, H.W., Vail, B., Huber, T.L., Paw, B., Brownlie, A.J., et al. 1998. The *cloche* and *spadetail* genes differentially affect hematopoiesis and vasculogenesis. *Dev. Biol.* **197:** 248–269.

Toyama, R., Kobayashi, M., Tomita, T., and Dawid, I.B. 1998. Expression of LIM-domain binding protein (ldb) genes during zebrafish embryogenesis. *Mech. Dev.* **71:** 197–200.

Traver, D., Paw, B.H., Poss, K.D., Penberthy, W.T., Lin, S., and Zon, L.I. 2003. Transplantation and in vivo imaging of multilineage engraftment in zebrafish bloodless mutants. *Nat. Immunol.* **4:** 1238–1246.

Traver, D., Winzeler, A., Stern, H.M., Mayhall, E.A., Langenau, D.M., Kutok, J.L., Look, A.T., and Zon, L.I. 2004. Effects of lethal irradiation in zebrafish and rescue by hematopoietic cell transplantation. *Blood* **104:** 1298–1305.

Vogeli, K.M., Jin, S.W., Martin, G.R., and Stainier, D.Y.R. 2006. A common progenitor for hematopoietic and endothelial lineages in the zebrafish gastrula. *Nature* **443:** 337–339.

Wei, W., Wen, L., Huang, P., Zhang, Z., Chen, Y., Xiao, A., Huang, H., Zhu, Z., Zhang, B., and Lin, S. 2008. Gfi1.1 regulates hematopoietic lineage differentiation zebrafish embryogenesis. *Cell Res.* **18:** 677–685.

Weinstein, B.M., Schier, A.F., Abdelilah, S., Malicki, J., Solnica-Krezel, L., Stemple, D.L., Stainier, D.Y., Zwartkruis, F., Driever, W., and Fishman, M.C. 1996. Hematopoietic mutations in the zebrafish. *Development* **123:** 303–309.

White, R.M., Sessa, A., Burke, C., Bowman, T., LeBlanc, J., Ceol, C., Bourque, C., Dovey, M., Goessling, W., Burns, C.E.,

and Zon, L.I. 2008. Transparent adult zebrafish as a tool for in vivo transplantation analysis. *Cell Stem Cell* **2:** 183–189.
Wienholds, E., Schulte-Merker, S., Walderich, B., and Plasterk, R.H.A. 2002. Targeted-selected inactivation of the zebrafish *rag1* gene. *Science* **297:** 99–102.
Willett, C.E., Kawasaki, H., Amemiya, C.T., Lin, S., and Steiner, L.A. 2001. *Ikaros* expression as a marker for lymphoid progenitors during zebrafish development. *Dev. Dyn.* **222:** 694–698.
Zhang, X.Y. and Rodaway, A.R.F. 2007. *SCL*-GFP transgenic zebrafish: In vivo imaging of blood and endothelial development and identification of the initial site of definitive hematopoiesis. *Dev. Biol.* **307:** 179–194.
Zhu, H., Traver, D., Davidson, A.J., Dibiase, A., Thisse, C., Thisse, B., Nimer, S., and Zon, L.I. 2005. Regulation of the *lmo2* promoter during hematopoietic and vascular development in zebrafish. *Dev. Biol.* **281:** 256–269.

Appendix IV

Direct recruitment of polycomb repressive complex 1 to chromatin by core binding transcription factors

Attributions

I performed all the zebrafish experiments presented in this article. I designed morpholinos to knock down *runx1, bmi1, bmi1b,* and *ring1b.* I did microinjections, performed WISH, and confocal imaging. Katie Kathrein helped with microinjections and confocal imaging.

"Reprinted from *Molecular cell, 45,* Yu, M., Mazor, T., Huang, H., Huang, H.-T., Kathrein, K., Woo, A., Chouinard, C.R., Labadorf, A., Akie, T.E., Moran, T.B., Xie, H., Zacharek, S., Taniuchi, I., Roeder, R.G., Kim, C.F., Zon, L.I., Fraenkel, E., and Cantor, A.B, Direct recruitment of polycomb repressive complex 1 to chromatin by core binding transcription factors, 330-373, 2012, with permission Elsevier."

Direct Recruitment of Polycomb Repressive Complex 1 to Chromatin by Core Binding Transcription Factors

Ming Yu,[1,8,9] Tali Mazor,[2,3,8,10] Hui Huang,[1] Hsuan-Ting Huang,[1] Katie L. Kathrein,[1] Andrew J. Woo,[1] Candace R. Chouinard,[2,3] Adam Labadorf,[2,3] Thomas E. Akie,[1] Tyler B. Moran,[1] Huafeng Xie,[1] Sima Zacharek,[1] Ichiro Taniuchi,[4] Robert G. Roeder,[5] Carla F. Kim,[1,6] Leonard I. Zon,[1,6,7] Ernest Fraenkel,[2,3,*] and Alan B. Cantor[1,6,*]
[1]Children's Hospital Boston and Dana-Farber Cancer Institute, Harvard Medical School, Boston, MA 02115, USA
[2]Department of Biological Engineering
[3]Computer Science and Artificial Intelligence Laboratory
Massachusetts Institute of Technology, Cambridge, MA 02139, USA
[4]Laboratory for Transcriptional Regulation, Research Center for Allergy and Immunology, RIKEN, Yokohoma, Kanagawa 230-0045, Japan
[5]Laboratory of Biochemistry and Molecular Biology, The Rockefeller University, New York, NY 10065, USA
[6]Harvard Stem Cell Institute, Cambridge, MA 02138, USA
[7]Howard Hughes Medical Institute, Boston, MA 02115, USA
[8]These authors contributed equally to this work
[9]Present address: Laboratory of Biochemistry and Molecular Biology, The Rockefeller University, New York, NY 10065, USA
[10]Present address: Brain Tumor Research Center, Department of Neurosurgery, Helen Diller Family Comprehensive Cancer Center, University of California, San Francisco, San Francisco, CA 94115, USA
*Correspondence: fraenkel-admin@mit.edu (E.F.), alan.cantor@childrens.harvard.edu (A.B.C.)
DOI 10.1016/j.molcel.2011.11.032

SUMMARY

Polycomb repressive complexes (PRCs) play key roles in developmental epigenetic regulation. Yet the mechanisms that target PRCs to specific loci in mammalian cells remain incompletely understood. In this study we show that Bmi1, a core component of Polycomb Repressive Complex 1 (PRC1), binds directly to the Runx1/CBFβ transcription factor complex. Genome-wide studies in megakaryocytic cells demonstrate significant chromatin occupancy overlap between the PRC1 core component Ring1b and Runx1/CBFβ and functional regulation of a considerable fraction of commonly bound genes. Bmi1/Ring1b and Runx1/CBFβ deficiencies generate partial phenocopies of one another in vivo. We also show that Ring1b occupies key Runx1 binding sites in primary murine thymocytes and that this occurs via PRC2-independent mechanisms. Genetic depletion of Runx1 results in reduced Ring1b binding at these sites in vivo. These findings provide evidence for site-specific PRC1 chromatin recruitment by core binding transcription factors in mammalian cells.

INTRODUCTION

Polycomb group (PcG) proteins were first identified in homeotic transformation screens in *Drosophila melanogaster* through their silencing of homeobox (Hox) genes (for review see Simon and Kingston, 2009). They are now known to developmentally regulate a large number of genes and play key roles in mammalian stem cell self-renewal, cellular differentiation, and neoplasia. Two phylogenetically conserved PcG complexes have been identified: Polycomb Repressive Complex 1 and 2 (PRC1 and PRC2, respectively). PRC1 is composed of the core proteins Bmi1 (also called Pcgf4) and Ring1b and a variable number of associated components such as Ring1a, CBX proteins, PH1, PH2, and other Pcgf proteins in mammals. It silences genes through histone 2A monoubiquitination (H2Aub) and/or nucleosome compaction. Bmi1 and Ring1b-deficient animals have hematopoietic, neurologic, and skeletal defects and develop stem cell exhaustion due to impaired stem cell self-renewal (Calés et al., 2008; Park et al., 2003; van der Lugt et al., 1994). PRC2 contains the core components EZH2, Suz12, and EED and is also implicated in stem cell maintenance and lymphocyte homeostasis (Margueron and Reinberg, 2011). It catalyzes the methylation of histone 3 at lysine 27 (H3K27me).

Because PRCs do not contain inherent DNA-specific binding activity, additional factors must mediate their site-specific chromatin recruitment. In *Drosophila*, DNA polycomb response elements (PREs) and targeting factors have been defined. However, site-specific targeting mechanisms in mammalian cells remain less well understood.

Core binding transcription factors are heterodimeric complexes composed of a common CBFβ subunit bound to one of three tissue-specific DNA-binding CBFα subunits (now called Runx1, Runx2, and Runx3). Like PRCs, core binding transcription factors play roles in stem cell self-renewal, tissue differentiation, and cancer (for review see Appleford and Woollard, 2009). Runx1 is the predominant hematopoietic-expressed CBFα family member, whereas Runx2 and Runx3 play roles in bone and neural development. Targeted disruption of *Runx1* in mice

leads to complete failure of definitive hematopoiesis during embryogenesis due to defective emergence of the first definitive hematopoietic stem cells (HSCs) from the aorto-gonadal-mesonephros (AGM) region (Chen et al., 2009; Kissa and Herbomel, 2010; North et al., 1999; Wang et al., 1996a). In adult mice, inducible Runx1 deficiency results in blocked megakaryocyte (Mk) maturation, impaired lymphopoiesis, myeloid cell hyperproliferation, and progressive HSC exhaustion (Growney et al., 2005; Ichikawa et al., 2004; Jacob et al., 2010; Sun and Downing, 2004). Similar defects are seen with CBFβ deficiency (Talebian et al., 2007; Wang et al., 1996b).

Runx1 and *CBFβ* are the most common targets of genetic alteration in human leukemia, occurring in ~20%–25% of all cases (Speck and Gilliland, 2002). *Runx1* is also mutated in a subset of myelodysplastic syndrome (MDS) cases and is associated with poor prognosis (Bejar et al., 2011). Germline *Runx1* haploinsufficiency causes familial thrombocytopenia, platelet dysfunction, and increased MDS/leukemia risk (Song et al., 1999).

In order to further understand Runx1 transcriptional mechanisms, we recently purified Runx1-containing multiprotein complexes from megakaryocytic cells (Huang et al., 2009). Here, we report the direct physical and functional association between Runx1/CBFβ and PRC1. Moreover, we provide evidence that Runx1 recruits PRC1 directly to chromatin in a PRC2-independent manner. These findings support a mechanism of site-specific PRC1 chromatin recruitment in mammalian cells and conversely implicate a role for PRC1 in core binding factor-mediated gene regulation.

RESULTS

Runx1 and CBFβ Interact with PRC1 in Megakaryocytic and T Lymphocytic Cells

We previously purified Runx1-containing multiprotein complexes from 12-*O*-tetradecanoylphorbol-13-acetate (TPA)-induced murine L8057 megakaryoblastic cells using metabolic biotin tagging and streptavidin (SA) affinity chromatography and identified associated proteins by liquid chromatography-tandem mass spectrometry (LC-MS/MS) (Huang et al., 2009). In addition to known interacting proteins such as CBFβ, GATA-1, GATA-2, TAL1/SCL, Sin3A, PRMT1, PML, Smad2, CDK6, and the SWI/SNF complex, we identified physical and functional interactions between Runx1 and the Ets transcription factor FLI1 (Huang et al., 2009). From these same preparations we obtained multiple components of PRC1 and TrxG chromatin-remodeling complexes (Figure 1A; Figure S1 and Table S1 available online). Physical association between FLAG-tagged and biotinylated Runx1 ($^{FLAG\text{-}Bio}$Runx1) and the PRC1 core components Ring1b and Bmi1 was confirmed by western blot from independent SA pull-down experiments (Figure 1B). The abundant Mk nuclear protein YAP was not detected, indicating specificity of the assay. No significant difference in interactions was noted using uninduced or TPA-induced L8057 cells (Figure S2). Physical association between CBFβ/Runx1 and Ring1b/Bmi1 was further validated by coimmunoprecipitation (coIP) assays of endogenous proteins in both directions (Figures 1C–1E). Physical interaction between CBFβ and Ring1b/Bmi1 was also observed in human Jurkat T cells (Figure 1F). Glutathione S-transferase (GST) pull-down assays using purified recombinant proteins show that Runx1 and Bmi1 interact directly and that the runt domain of Runx1 is sufficient for Bmi1 binding (Figure 1G). Additional mapping studies indicate that a region involving amino acids 1–57 of Bmi1, which largely contains the Ring domain, contributes significantly to Runx1 binding, although sequences from amino acids 57–167 also participate (Figure 1H).

Runx1/CBFβ and Ring1b Occupy a Large Number of Common Chromatin Sites in L8057 Cells

To assess the association of Runx1/CBFβ and PRC1 at the genomic level, chromatin immunoprecipitation (ChIP) followed by massively parallel sequencing (ChIP-Seq) was performed for Runx1, CBFβ, and Ring1b in TPA-induced L8057 cells. High-quality Bmi1 antibodies are not available for ChIP-Seq. Two biological repeats were performed for each, and the data were compared to control IgG. After aligning sequences to the genome and removing redundant reads and those that mapped to multiple locations, we obtained 44,532,375 filtered reads for Runx1, 48,623,085 for CBFβ, and 56,381,939 for Ring1b (Table S2). This corresponds to a total of 7,073 Runx1, 10,186 CBFβ, and 7,063 Ring1b peaks ($p < 1E\text{-}10$ and false discovery rate [FDR] <5%) using the peak-calling algorithm MACS (Zhang et al., 2008); and 5,595 Runx1, 6,685 CBFβ, and 4,239 Ring1b genes bound between −1 kb upstream of the transcription start site (TSS) to +1 kb downstream of the transcription end site (TES) (see Figure S3A for gene calls using a −10 kb through +10 kb window). As expected, there was considerable overlap between Runx1 and CBFβ occupancy peaks (Figure 2A). Of the Runx1 peaks, 79% were bound by CBFβ, and 55% of the CBFβ peaks were bound by Runx1. There was also significant overlap of Runx1/CBFβ and Ring1b peaks. Of the Runx1 peaks, 57% were bound by Ring1b, and 57% of the Ring1b peaks were bound by Runx1. Of the CBFβ peaks, 48% were bound by Ring1b, and 70% of the Ring1b peaks were bound by CBFβ. A total of 3,688 peaks and 3,097 genes were common to all three factors.

To analyze whether Ring1b was binding at the same sites as Runx1 and CBFβ, we used the Genome Positioning System (GPS) algorithm (Guo et al., 2010), which overcomes the low resolution of ChIP-Seq experiments arising from random DNA fragmentation. Using this method, we found that 61% of Ring1b binding sites have a binding site for CBFβ or Runx1 within 100 bp (Figure 2B).

Examples of gene loci bound by all three factors are shown in Figure 2C (see Figure S3B for additional loci). The high degree of common occupancy between Ring1b and Runx1 was confirmed using a second Ring1b antibody (Figure S4A). Quantitative ChIP (qChIP) assays from independent samples validated commonly occupied peaks for 27 of 28 sites tested (Figure 2D). Each of two sites assayed in purified murine fetal liver-derived Mks also shows occupancy by both CBFβ and Ring1b (Figure 2E).

ChIP-Seq experiments carried out in uninduced L8057 cells also showed a high degree of overlap among Runx1, CBFβ, and Ring1b bound sites, although the total number of peaks (3,310 Runx1, 6,158 CBFβ, and 6,628 Ring1b) and bound genes

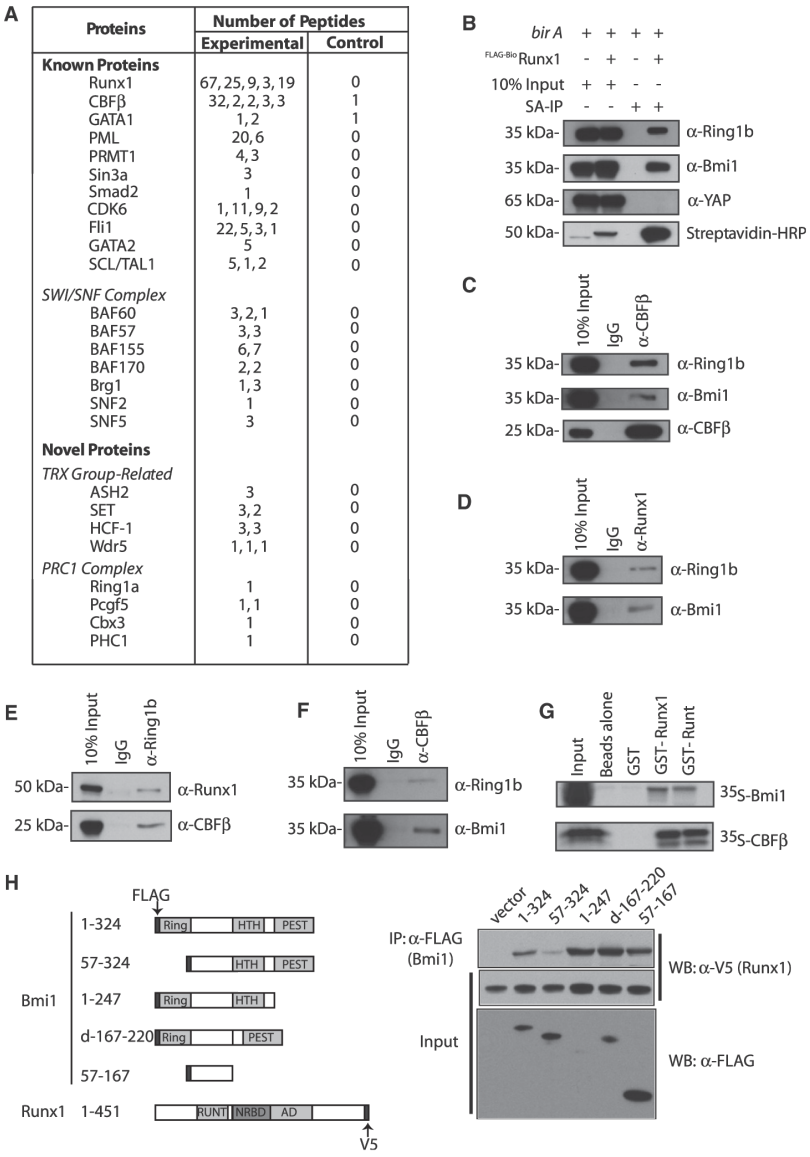

Figure 1. Physical Association between Runx1/CBFβ and Ring1b/Bmi1

(A) Partial list of proteins identified by mass spectrometry following tandem anti-FLAG:SA or single SA affinity chromatography from crude nuclear extracts of $^{FLAG\text{-}Bio}$Runx1 plus biotin ligase *birA* (experimental) or *birA* alone (control) containing L8057 cells treated with TPA for 72 hr (Huang et al., 2009). The number of peptides obtained for each protein from each of five independent experiments is shown. See Figure S1 and Table S1 for additional details.

(B) Western blot for Ring1b, Bmi1, and YAP following SA-IP of $^{FLAG\text{-}Bio}$Runx1 complexes from TPA-induced L8057 cells. Ten percent input is shown.

(C–E) CoIP assays of endogenous proteins from TPA-induced L8057 cells. The immunoprecipitation (IP) antibody is shown on top, and the western blot antibody is shown on the right. Ten percent input is shown. IgG, species-matched control antibody.

(F) Western blot for Ring1b and Bmi1 following IP with α-CBFβ antibody, or control IgG, from Jurkat T cells. Ten percent input is shown.

(G) GST pull-down assay of recombinant Runx1, Bmi1, and CBFβ. In vitro transcribed and translated [^{35}S]methionine-labeled Bmi1 or CBFβ was incubated with uncoupled beads or beads coupled with GST, GST-Runx1, or GST-runt domain fusion proteins as indicated. The beads were washed, and eluted material was separated by SDS-PAGE. An autoradiogram is shown. Ten percent of the input protein is shown.

(H) Mapping of Bmi1 interaction domain. Left view is a schematic diagram of constructs. Right view shows α-FLAG IP followed by α-V5 western blot of constructs coexpressed in COS7 cells. One percent of input is shown.

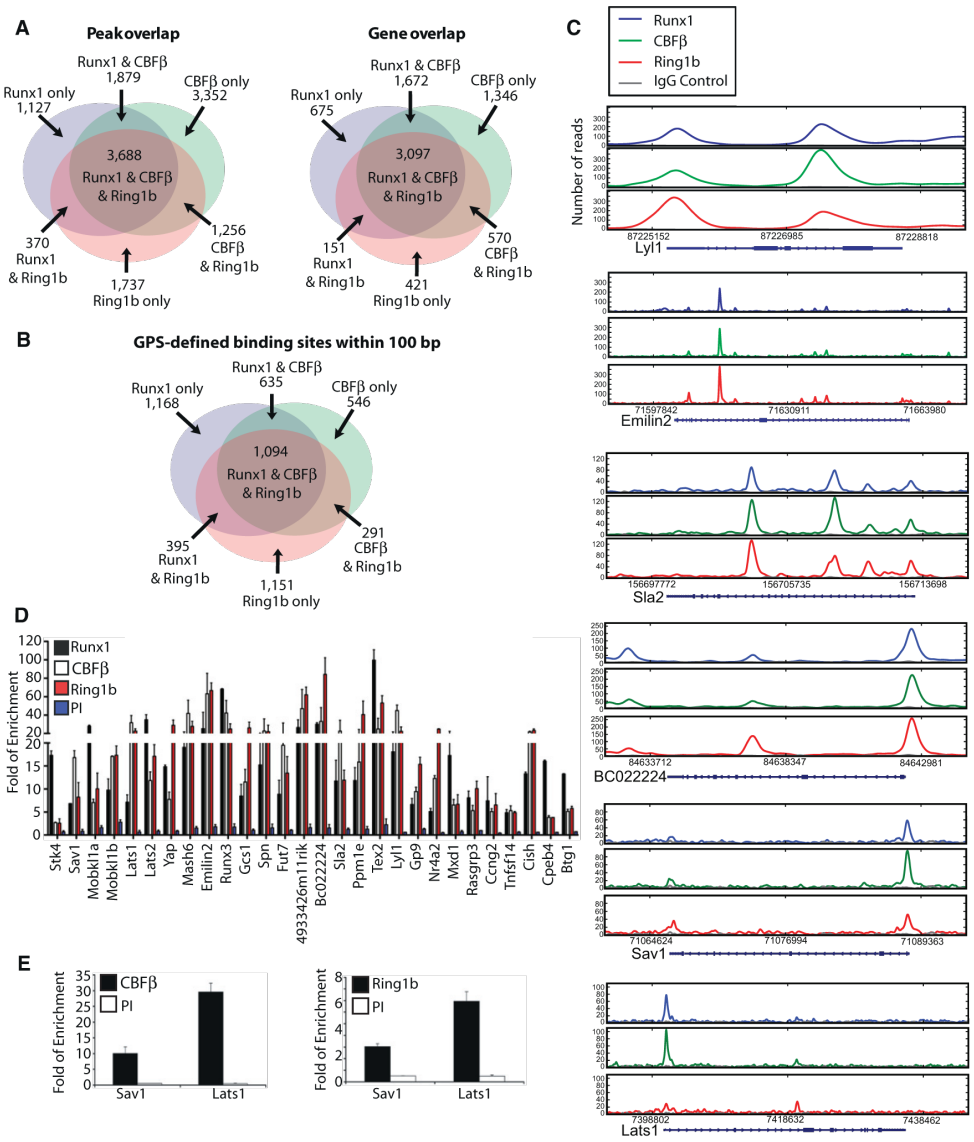

Figure 2. Common Chromatin Site Occupancy by Runx1/CBFβ and Ring1b

(A) Venn diagrams showing overlap of Runx1, CBFβ, and Ring1b occupancy peaks (left) and genes (right) in TPA-induced L8057 cells based on MACS (Zhang et al., 2008). Overlapping peaks are defined as those for which the summits of the peaks are <500 bp from each other. Bound genes are defined as having occupancy peaks between −1 kb of the TSS to +1 kb of the TES.

(B) Venn diagram showing overlap of Runx1, CBFβ, and Ring1b occupancy sites within 100 bp of one another based on GPS (Guo et al., 2010).

(C) Representative Runx1, CBFβ, Ring1b, and control IgG ChIP-Seq profiles of loci occupied by Runx1, CBFβ, and Ring1b. Other genes present in these regions are not shown.

(D) qChIP assays for Runx1, CBFβ, and Ring1b occupancy at the indicated loci in TPA-induced L8057 cells. PI, control antibody. The data are expressed as fold enrichment relative to a negative control region (−2.5 kb 5′ of the *Gapdhs* gene TSS), and represent the mean of three independent experiments ±SD.

(E) qChIP assays for CBFβ and Ring1b occupancy at *Sav1* and *Lats1* gene promoters in primary fetal liver-derived murine Mks. The data are displayed as in (D).

(2,526 Runx1, 4,385 CBFβ, and 4,130 Ring1b) was lower than that observed for the induced cells (Figure S4B). A total of 2,070 peaks and 1,710 genes were bound by all three factors.

As expected, transcription factor binding motif analysis under Runx1 and CBFβ occupancy peaks showed enrichment for the Runx consensus binding sequence (g.w.ACCACAra) ($p = 2.9E-71$ and $p = 1.2E-54$, respectively) (Table S3). Motifs corresponding to Ets and GATA family transcription factors, which physically and functionally interact with Runx proteins (Elagib et al., 2003; Huang et al., 2009; Kim et al., 1999; Wilson et al., 2010), were also highly enriched. Ring1b occupancy sites were likewise enriched for Runx1 ($p = 7.9E-13$), Ets ($p = 2.1E-65$), and GATA ($p = 6.8E-18$) binding sequences.

Ring1b and CBFβ Regulate a Subset of Commonly Bound Genes in Mks

In order to correlate chromatin occupancy with functional gene regulation, CBFβ and Ring1b lentiviral shRNA knockdown was performed in TPA-induced L8057 cells, and gene expression changes were measured by cDNA microarray analysis. A previously characterized CBFβ shRNA construct (Galli et al., 2009) produced marked reduction of CBFβ protein levels (Figure 3A). Runx1 and Ring1b levels were not significantly affected. From three independent experiments, a total of 874 genes changed expression ≥1.5-fold with $p < 0.05$, compared to the empty vector. A total of 595 genes were upregulated, and 279 were downregulated. *CBFβ* was the most downregulated gene, whereas *Ring1b* and *Bmi1* were not significantly altered. Among the 2,782 genes bound by all three factors (Runx1, CBFβ, and Ring1b) ($p < 1E-10$, FDR <5%, binding −1 kb from TSS to +1 kb from TES) and represented by probes on the array that passed quality control, 280 genes changed expression. A total of 217 were upregulated ($p < 3.4E-46$), and 63 were downregulated ($p < 2.9E-5$). Because distal binding events strongly influence gene expression (MacIsaac et al., 2010), we repeated these calculations including genes bound from −10 kb from TSS to +1 kb from TES. Among the 3,530 genes bound by all three factors ($p < 1E-10$, FDR <5%), 341 genes changed expression. A total of 262 were upregulated ($p < 4.0E-54$), and 79 were downregulated ($p < 2.7E-6$). Genes that were bound in multiple regions and those bound only in the distal promoter, introns, or exons were associated with upregulation (Table S4). Bound and upregulated genes were enriched for intracellular signaling (Benjamini $p < 0.009$), regulation of biological process ($p < 0.02$), signal transduction ($p < 0.02$), biological regulation ($p < 0.02$), and regulation of cellular process ($p < 0.03$) (Dennis et al., 2003).

Although knockdown for Ring1b was not as efficient as that for CBFβ, the more potent shRNA construct (shRNA #1) produced significant Ring1b protein reduction (Figure 3B). Runx1 and CBFβ protein levels were not significantly altered. A total of 497 genes changed expression ≥1.5-fold with $p < 0.05$. A total of 152 genes were upregulated, and 345 were downregulated. Among the 3,530 genes bound by all three factors and represented by probes on the array, 65 were upregulated ($p < 1.5E-13$), and 99 were downregulated ($p < 8.3E-8$).

Clustering analysis of genes occupied by Runx1, CBFβ, and/or Ring1b within −1 kb of the TSS to +1 kb of the TES and a heat map of corresponding gene expression changes following CBFβ or Ring1b shRNA knockdown are shown in Figure 3C (see Figure S5 for comparable analysis based on binding −10 kb of TSS to +1 kb of TES). A total of 51 genes that were bound by all three factors changed expression with both CBFβ and Ring1b shRNA knockdown using the high stringency criteria described above (Table S5). Of the genes, 88% changed expression in the same direction (28 genes upregulated, 17 downregulated) (Figure 3D). Quantitative RT-PCR (qRT-PCR) validation studies from independent experiments confirmed the gene expression changes in representatives of each of these classes (Figure 3E). We conclude that CBFβ/Runx1 and Ring1b functionally regulate a set of commonly bound genes.

Deficiency of Ring1b and Bmi1 Impairs Mk Maturation

Runx1 or CBFβ deficiency impairs Mk maturation as evidenced by reduced ploidy and poor platelet production (Growney et al., 2005; Ichikawa et al., 2004; Talebian et al., 2007). To examine the functional role of Ring1b in Mk maturation, we measured the ability of L8057 Ring1b shRNA knockdown cells to undergo TPA-induced endomitosis. As shown in Figure 4A, Ring1b knockdown resulted in reduced ploidy (mean 2.8N ± 0.7N [n = 4] compared to the empty vector control (4.5N ± 1.3N [n = 5]), and was similar to that observed with CBFβ knockdown (mean ploidy 2.5N ± 0.5N [n = 3]).

$Bmi1^{-/-}$ neonatal mice are thrombocytopenic (and lymphopenic) but have normal hemoglobin and granulocyte levels (Park et al., 2003). To probe for a potential Mk defect in these animals, we examined bone marrow histology and cultured Mks from 5- to 6-week-old $Bmi1^{-/-}$ mice. This showed that $Bmi1^{-/-}$ Mks were smaller in size, contained more hypolobulated nuclei, and had reduced ploidy compared to $Bmi1^{+/-}$ littermates (Figure 4B). This is similar to the phenotype of Runx1-deficient Mks (Growney et al., 2005; Ichikawa et al., 2004). These findings are consistent with functional overlap of Runx1/CBFβ and Ring1b/Bmi1 in Mk maturation.

Morpholino Knockdown of Bmi1 or Ring1b Impairs HSC Development in Zebrafish Embryos

Deficiency of either Runx1 or Bmi1/Ring1b leads to HSC exhaustion in adult animals. Runx1/CBFβ deficiency also causes defects in definitive HSC ontogeny during embryogenesis. However, a detailed examination of Bmi1/Ring1b's role in embryonic HSC ontogeny has not been reported to our knowledge. In order to examine this, we knocked down their expression using morpholinos (MOs) in zebrafish embryos. The first definitive HSCs develop in the equivalent AGM region of the developing zebrafish embryo at about 36 hr postfertilization (hpf), and are marked by expression of c-Myb and/or Runx1 (Burns et al., 2002). As previously reported (Burns et al., 2005), Runx1 MO knockdown ablated phenotypic ($c\text{-}Myb^{+}$) definitive HSC formation (Figure 5A, left panel). MO knockdown of Bmi1 and the duplicated zebrafish gene Bmi1b, or Ring1b also resulted in loss of $c\text{-}Myb^{+}/Runx1^{+}$ cells, although not to as full of an extent as Runx1 knockdown (Figure 5A, right panel).

As a complementary approach, knockdown experiments were performed in CD41-eGFP transgenic fish, which express eGFP in HSC/early progenitor cells (HSPCs) and thrombocytes (Lin et al., 2005). Like Runx1, knockdown of Bmi1/Bmi1b and Ring1b

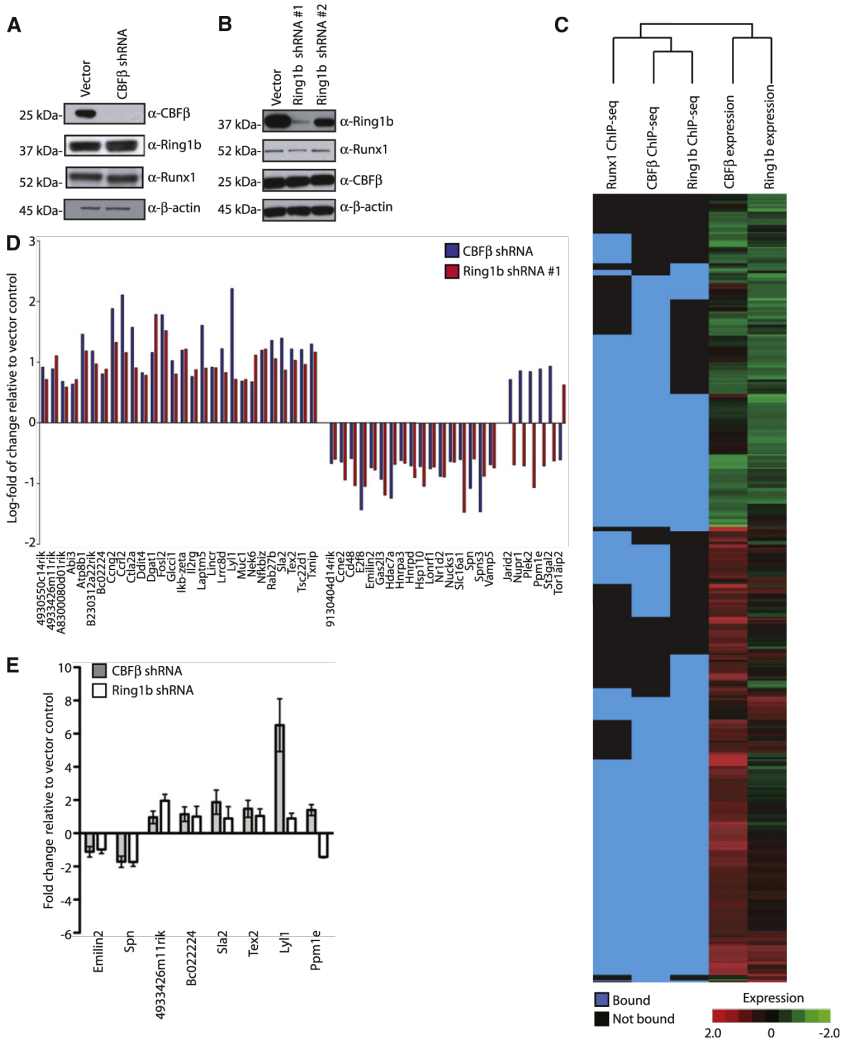

Figure 3. Regulation of a Subset of Commonly Bound CBFβ and Ring1b Direct Target Genes

(A) CBFβ lentiviral shRNA knockdown in TPA-induced L8057 cells. Western blot for CBFβ, Ring1b, Runx1, and β-actin in puromycin selected cells.

(B) Ring1b lentiviral shRNA knockdown in TPA-induced L8057 cells. Western blot for Ring1b, Runx1, CBFβ, and β-actin in puromycin selected cells.

(C) Clustering analysis showing genes occupied by either Runx1, CBFβ and/or Ring1b at −1 kb of TSS to +1 kb of TES, and heat map of corresponding gene expression changes (red, increased; green, decreased; black, no change) following CBFβ or Ring1b shRNA knockdown.

(D) Log-fold gene expression changes based on cDNA microarray analysis for genes bound by all three factors (Runx1, CBFβ, and Ring1b) ($p < 1E-10$, FDR <5%; occupancy −1 kb of the TSS to +1 kb from the TES) that changed expression following both CBFβ and Ring1b shRNA knockdown ≥1.5-fold with $p < 0.05$.

(E) qRT-PCR measurements of gene expression changes of representative commonly occupied genes following CBFβ or Ring1b shRNA knockdown in TPA-induced L8057 cells. Levels are normalized to *Gapdhs*. The mean of four independent experiments is shown ±SD.

resulted in a significant reduction of eGFP$^+$ cells in the AGM region, as well as in the caudal hematopoietic tissue (CHT), which is seeded by AGM HSCs (Figure 5B). Similar to Runx1 deficiency (Wang et al., 1996a), Bmi1/Bmi1b or Ring1b knockdown did not significantly affect primitive erythropoiesis (Figure 5C), or alter overall morphology of the embryos (Figure S6).

Both Bmi1 and Runx1 knockout mice have a block in T cell maturation at the CD4$^-$CD8$^-$ double-negative (DN) to CD4$^+$CD8$^+$ double-positive (DP) transition stage, although Bmi1 loss predominantly impairs the DN3 (CD44$^-$CD25$^+$) to DN4 transition (CD44$^-$CD25$^-$) (Miyazaki et al., 2008), whereas Runx1 loss predominantly impairs the DN2 (CD44$^+$CD25$^+$) to DN3 transition (Ichikawa et al., 2004). Thus, like in Mk

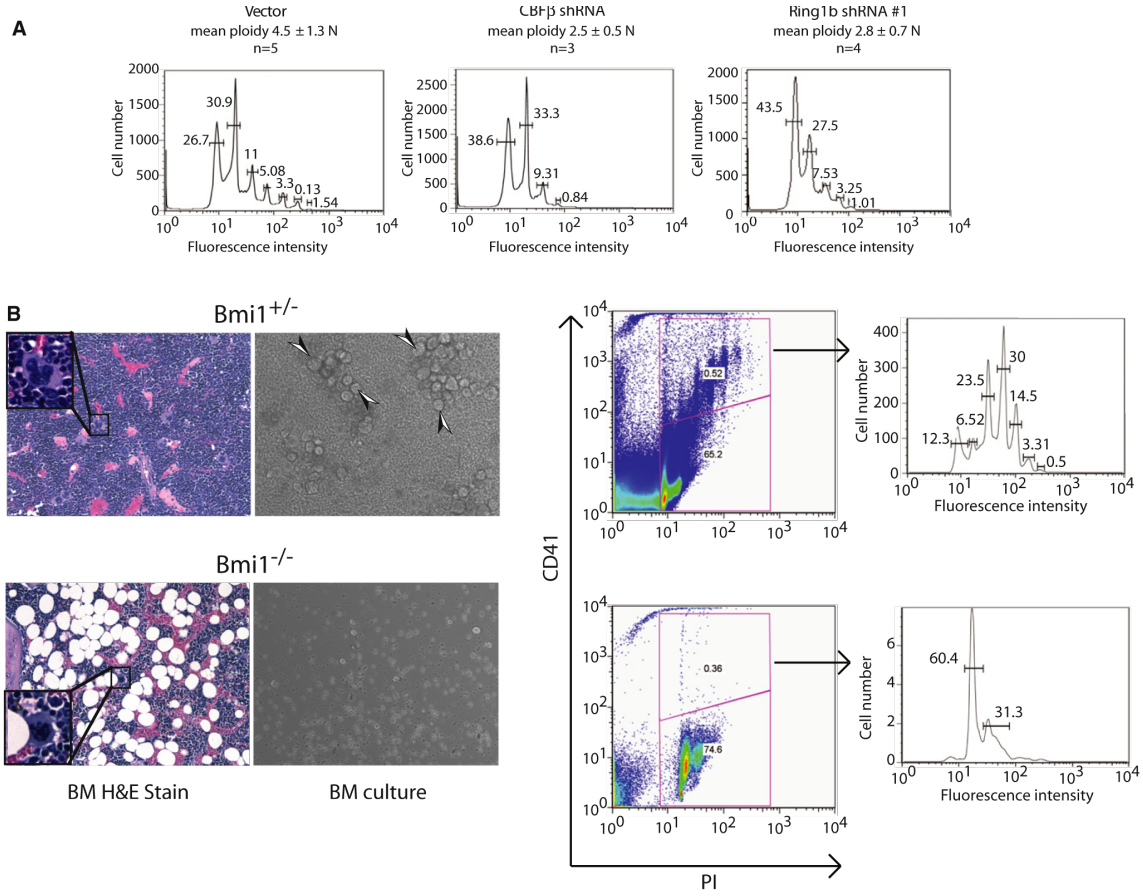

Figure 4. Partial Phenocopies of Ring1b/Bmi1 and Runx1/CBFβ Deficiency in Megakaryopoiesis

(A) Representative flow cytometric plots of propidium iodide (PI) DNA ploidy analysis of TPA-induced L8057 cells transduced with the empty vector, CBFβ shRNA, or Ring1b shRNA #1. The percentages of cells with each DNA ploidy state (2N, 4N, 16N, 32N, 64N, and 128N) and the mean ploidy (vector [n = 5], CBFβ shRNA [n = 3], Ring1b shRNA #1 [n = 4]) are given ±SD.

(B) Phenotype of Bmi1$^{-/-}$ Mks. Left panel shows hematoxylin and eosin-stained histologic sections of bone marrow from Bmi1$^{+/-}$ and Bmi1$^{-/-}$ mice. Inset shows representative Mk at higher magnification (original 600×). Middle panel is a phase-contrast photomicrograph of bone marrow cells cultured from Bm1$^{+/-}$ and Bmi1$^{-/-}$ mice in the presence of Tpo and stem cell factor. Arrowheads indicate large (maturing) Mks. Right panel shows flow cytometric plots of cultured bone marrow cells for CD41 expression and DNA content (PI). Histogram plots for different ploidy classes are shown to the right for CD41^{+}-gated cells. Gates were set using control IgG-stained cells.

development and HSC ontogeny, Ring1b/Bmi1 or Runx1/CBFβ deficiencies generate partial phenocopies of one another with respect to T lymphocyte development. In total these findings argue for functional cooperation between Runx1 and PRC1 components in development.

Runx1 Recruits Ring1b to Runx1 Binding Sites in Primary Murine Thymocytes

To examine whether Runx1 participates in Ring1b recruitment at selected chromatin sites, we performed qChIP assays for Runx1, CBFβ, and Ring1b in primary thymocytes from Runx1$^{fl/fl}$, Vav1-Cre mice, which have pan-hematopoietic deletion of Runx1 (Chen et al., 2009). In control mice (Runx1$^{fl/fl}$) we observed significant enrichment for Runx1 and CBFβ at the previously described Runx1 binding sites in the *CD4* silencer (Yu et al., 2008), *Th-POK* regulatory regions (Th-POK RBS1 and 2) (Setoguchi et al., 2008), and *TCRβ* enhancer (Setoguchi et al., 2008), as well as several sites inferred from our Mk ChIP-Seq data set (*Top2b*, *Stat1*, and *Stat3* promoters) (Figure 6A). Only low levels of Runx1/CBFβ were found at the *Th-POK* promoter, consistent with our previous report (Setoguchi et al., 2008). Ring1b was significantly enriched at each of the Runx1/CBFβ occupied sites.

In the knockout mice, Runx1 and CBFβ enrichment levels were markedly reduced at these sites, as expected (Figure 6A). Low levels of residual Runx1 are likely due to incomplete conditional

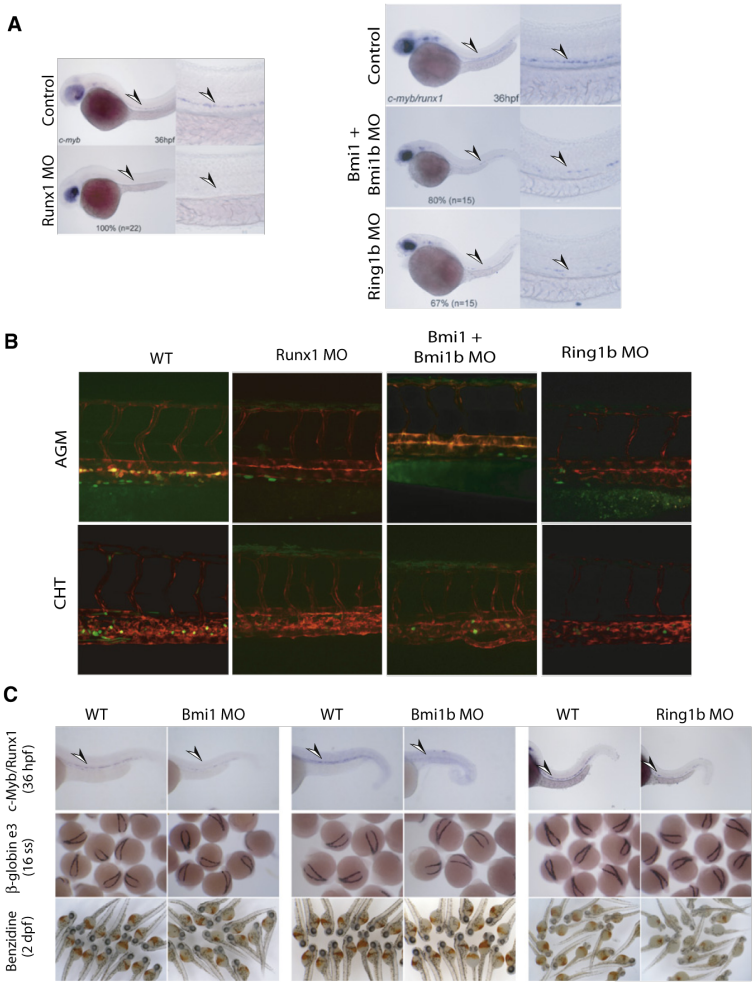

Figure 5. Partial Phenocopies of Ring1b/Bmi1 and Runx1/CBFβ Deficiency in Definitive HSC Ontogeny

(A) Left panel shows in situ hybridization for c-Myb in 36 hpf uninjected control and *Runx1* morphant zebrafish embryos. Low-magnification (10×) (left) and high-magnification (40×) images of the trunk region (right) are shown. The percentage of embryos with the represented phenotype is indicated. Right panel shows in situ hybridization for c-Myb/Runx1 in 36 hpf uninjected control or embryos injected at the single-cell stage with Bmi1, Bmi1b, and/or Ring1b translation blocking MOs. Arrowheads indicate phenotypic HSCs.

(B) MO injection into transgenic CD41-eGFP:flk1-RFP double-transgenic embryos. eGFP^{+} cells (green) represent HSPCs and thrombocytes; RFP^{+} cells (red) represent vasculature. The AGM region was visualized at 36 hpf, and the CHT was visualized 3 days later.

(C) Upper row shows in situ hybridization for c-Myb and Runx1 at 36 hpf in zebrafish embryos injected with Bmi1, Bmi1b, or Ring1b MOs, compared to wild-type (WT) embryos. Middle row illustrates ε3-globin in situ hybridization at the 16-somite stage (ss). Lower row shows o-dianisidine (benzidine) stains of 2 days postfertilization (dpf) embryos. Hemoglobinized cells stain orange/brown. Arrowheads indicate phenotypic HSCs.

allele excision. Importantly, Ring1b is also markedly depleted at these sites. H2Aub enrichment was found at a subset of Runx1, CBFβ, and Ring1b commonly occupied sites in control mice, and was also markedly depleted upon Runx1 deletion (Figure 6B). Control experiments validated the chromatin integrity of the knockout animal samples (Figure S7).

To examine these effects in a more global manner, we performed ChIP-Seq for Runx1, CBFβ, and Ring1b in primary thymocytes from Runx1$^{fl/fl}$ and Runx1$^{fl/fl}$, Vav1-Cre 5- to 8-week-old mice.

From the Runx1$^{fl/fl}$ mice we obtained 1,898,522 Runx1, 2,109,935 CBFβ, and 1,543,887 Ring1b aligned and filtered reads (Table S2). This corresponds to 1,507 Runx1, 4,033 CBFβ, and 712 Ring1b peaks ($p < 1E-10$, FDR <5%), and 1,364 Runx1, 3,369 CBFβ, and 665 Ring1b bound genes (binding between −1 kb of TSS to +1 kb of TES). Similar to our findings in L8057 cells, there was considerable overlap of the occupancy peaks and genes of all three factors (Figure 6C). Of the Ring1b bound genes, 46% were also bound by Runx1, and 71% were bound by CBFβ. A total of 292 genes were bound by all three factors (Table S6).

From the Runx1$^{fl/fl}$, Vav1-Cre mice, we obtained 1,597,571 Runx1, 2,571,167 CBFβ, and 2,197,463 Ring1b aligned and filtered reads (Table S2). None of the Runx1 or CBFβ peaks met the statistical cutoff of a p value of <1E-10 and FDR <5%. Although 23 Ring1b peaks remained in the Runx1-deficient thymocytes, only one of these corresponds to a Runx1/CBFβ commonly bound site from the control mice. A more detailed analysis of the binding data revealed that even in the Runx1 knockout animals, some residual Runx1 binding could be detected, reflecting incomplete excision of the floxed allele. To quantify this, we counted the number of unique reads associated with peaks bound by all three proteins in the control animal and at the same loci in the knockout animal (Figure 6D). For Ring1b, 7% of the regions had no reads at all in the knockout animals (compared to 8% for Runx1 and 2% for CBFβ). At the remaining sites, the median ratio of reads at these locations in the control to knockout was 4.1 for Runx1, 5.2 for CBFβ, and 1.3 for Ring1b. The reduced read numbers in the Runx1-deficient thymocytes occur despite the fact that the libraries for Ring1b and CBFβ were sequenced more deeply in these mice. (The expected ratios based on the number of uniquely mapped reads would be 1.2 for Runx1, 0.8 for CBFβ, and 0.7 for Ring1b.) Examples

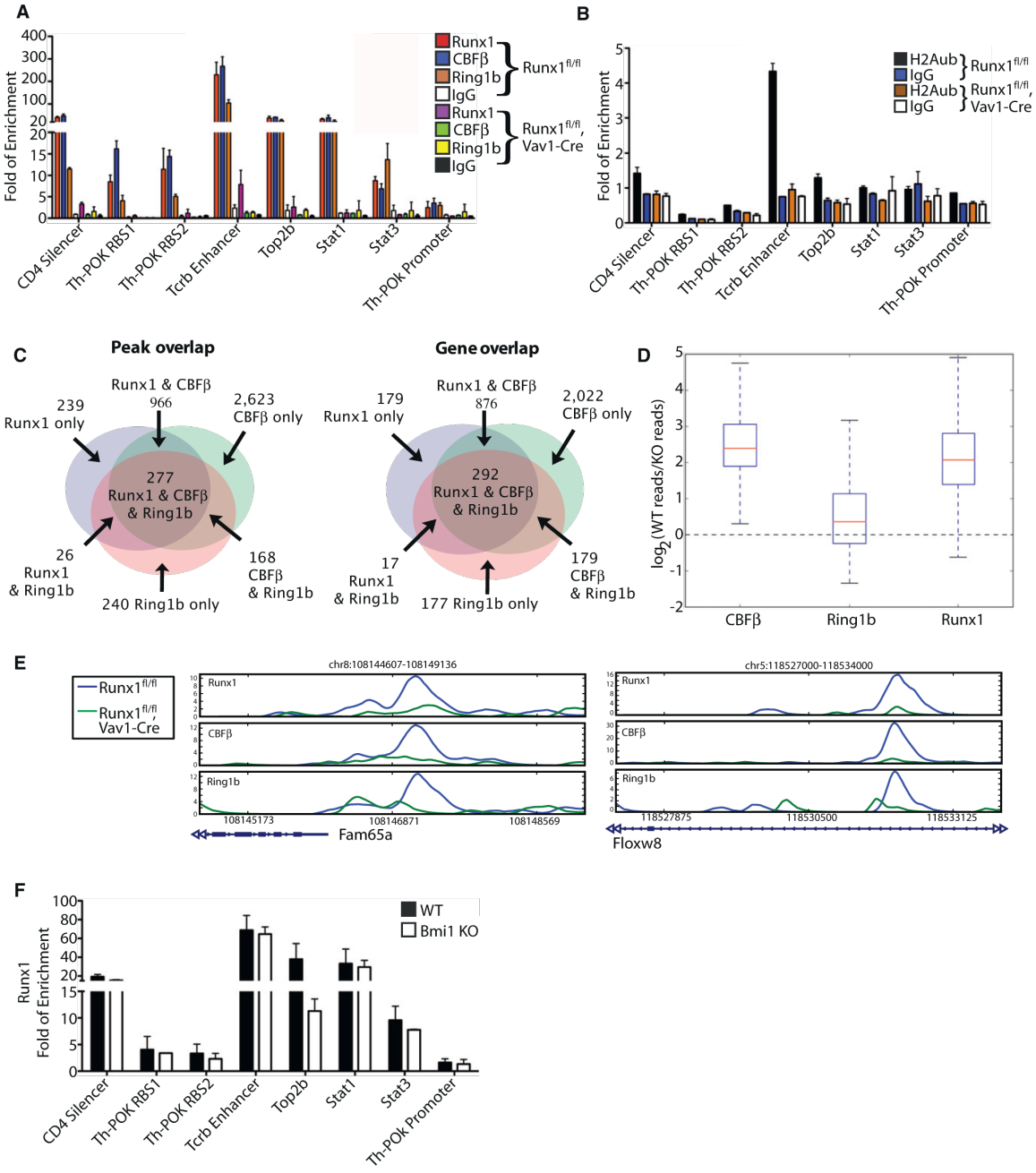

Figure 6. Runx1 Dependency of Ring1b Chromatin Occupancy at Commonly Bound Sites in Primary Murine Thymocytes

(A) qChIP assays for Runx1, CBFβ, and Ring1b in primary thymocytes from either Runx1$^{fl/fl}$ or Runx1$^{fl/fl}$, Vav1-Cre 6-week-old mice. Fold of enrichment is shown relative to a negative control region (see Experimental Procedures). The mean of three independent assays is shown ±SD.

(B) qChIP assay for H2Aub at each of the individual sites tested in (A).

(C) Venn diagrams showing overlap of Runx1, CBFβ, and Ring1b peaks and bound genes from primary thymocytes of 5- to 8-week-old Runx1$^{fl/fl}$ mice. Peaks are filtered for p < 1E-10, FDR <5%, and overlaps are defined as MACS summits within 500 bp of each other. Bound genes contain occupancy peaks within −1 kb of the TSS to + 1 kb of the TES.

of ChIP-Seq profiles showing the concomitant decrease in Runx1, CBFβ, and Ring1b reads upon Runx1 depletion are shown in Figure 6E. We conclude that Runx1/CBFβ participates in Ring1b recruitment at some commonly bound sites.

To examine the possibility that PRC1 may recruit or stabilize Runx1, qChIP assays were performed from primary thymocytes of 5- to 6-week-old Bmi1$^{-/-}$ mice. With the exception of the *TOP2b* promoter, we observed no significant difference of Runx1 enrichment at the sites tested (Figure 6F). These data are consistent with Runx1-mediated recruitment of PRC1, rather than PRC1-mediated recruitment or stabilization of Runx1.

Ring1b Occupancy at Commonly Bound Runx1/CBFβ Sites Occurs Independent of PRC2

A proposed model of PRC1 chromatin recruitment involves its direct binding to H3K27me3 residues, which are first generated by the action of PRC2 (Simon and Kingston, 2009). In order to examine whether H3K27me3 is involved in PRC1 recruitment at sites commonly occupied by Runx1/CBFβ, we measured H3K27me3 enrichment levels at each of the tested sites in wild-type primary thymocytes. Although significant H3K27me3 enrichment was observed at the *Th-POK* RBS1, RBS2, and promoter regions, all of the other sites had only background levels (Figure 7A).

To test this further, we examined Runx1, CBFβ, and Ring1b chromatin occupancy in thymocytes from EZH2$^{fl/fl}$, Vav1-Cre, Rosa26-flox-stopper-flox-EYFP mice (Wilson et al., 2011). Flow cytometry of thymocytes and splenocytes showed that 91.2% and 95.9% of the total cells expressed EYFP, respectively, indicating efficient activation of Cre in these tissues. Of the CD3^{+} populations (T cells), 96.3% and 98.4% were EYFP positive and had 12- and 29-fold decreases in EZH2 mRNA levels compared to control mice for spleen and thymus, respectively (Figure 7B). Despite this marked EZH2 depletion, qChIP assays from the thymocytes of these animals demonstrated no significant loss of Ring1b, Runx1, or CBFβ chromatin occupancy at the sites tested (Figure 7C). This strongly suggests that recruitment of Ring1b to these Runx1/CBFβ occupied sites occurs independent of PRC2 activity.

DISCUSSION

In this study we provide evidence that core binding transcription factors contribute to site-selective physical and functional recruitment of PRC1 in mammalian cells. In *Drosophila*, PREs have been defined based on functional assays and consist of several hundred base pair sequences (Simon and Kingston, 2009). These regions contain binding sites for the transcription factor PHO (ortholog of the mammalian transcription factor YY1), which participates in PcG recruitment in some cases. Less is known about PcG recruitment in mammalian cells. Several examples of noncoding RNA-mediated recruitment have been uncovered, particularly in X chromosome inactivation (Zhao et al., 2008). Woo et al. recently defined a PRC recruitment site within the human HOXD cluster (Woo et al., 2010). We recently showed that the lineage-specific transcription factor GATA-1 physically and functionally associates with PRC2 during erythroid terminal maturation (Yu et al., 2009). The findings in the current study indicate that Runx1 and CBFβ contribute to direct PRC1 recruitment at some sites in Mks and lymphocytes. It is of interest to note that both YY1 and Runx factors share a common central TGG core element in their DNA consensus binding sites.

There is prior evidence that PRC1 can be recruited to chromatin independent of PRC2 (Pasini et al., 2007; Schoeftner et al., 2006; Vincenz and Kerppola, 2008). Our data are consistent with the existence of PRC2-independent mechanisms and suggest that direct interactions with DNA-binding proteins, such as core binding transcription factors, may be responsible in some cases. Similar to our findings, direct interaction between PRC1 and PHO has been described in *Drosophila* (Mohd-Sarip et al., 2006).

Like many transcription factors, Runx proteins both activate and repress transcription in a gene and developmental context-dependent manner. For example, Runx1 activates the *PU.1* gene in myeloid and B cells, but represses it in T lymphocytes and Mks (Huang et al., 2008). Some Runx-associated repressive events are mediated by Groucho/TLE family proteins. However, there is also evidence that Groucho-independent mechanisms exist (Walrad et al., 2010). The findings from the current study suggest that PRC1 may be involved in some of these alternate repressive pathways.

Genetic suppressor screens in *Drosophila* indicate that SWI/SNF and TrxG chromatin remodeling factors play antagonistic roles to PcG-mediated gene silencing (Simon and Kingston, 2009). Interestingly, we identified multiple components of the SWI/SNF and TrxG (ASH2/SET complex) complexes in our Runx1-containing multiprotein complex purifications. Bakshi et al. recently reported that SWI/SNF physically interacts with Runx1 and controls hematopoietic target genes (Bakshi et al., 2010). Moreover, they showed that reduced Runx1 levels correlate with impaired SWI/SNF chromatin occupancy at several common loci. Collectively, these findings suggest that Runx proteins may differentially recruit PcG and SWI-SNF/TrxG complexes in a gene- and developmental-specific context.

Adult HSC self-renewal is impaired in both Bmi1/Ring1b and Runx1-deficient animals (Calés et al., 2008; Jacob et al., 2010; Park et al., 2003; Sun and Downing, 2004; van der Lugt et al., 1994). Our data in zebrafish embryos indicate that Ring1b and Bmi1, like Runx1/CBFβ, are also involved in definitive HSC ontogeny (Figure 5). However, the fact that Bmi1$^{-/-}$ mice (Park

(D) Ratio of the number of reads obtained from ChIP-Seq for CBFβ, Ring1b, and Runx1 at commonly occupied sites in thymocytes from Runx1$^{fl/fl}$ versus Runx1$^{fl/fl}$, Vav1-Cre mice in log-base-2. The red horizontal bars represent the median value, the boxes represent the 25th–75th percentile (%) range, and the whiskers extend to the most extreme data point within 1.5× of the interquartile range. The expected log ratios based on the number of reads in each experiment are −0.29 for CBFβ, −0.51 for Ring1b, and 0.25 for Runx1.

(E) Examples of ChIP-Seq profiles showing concomitant reduction of Runx1, CBFβ, and Ring1b occupancy at commonly occupied sites.

(F) qChIP assays for Runx1 in primary thymocytes from 5- to 6-week-old Bmi1$^{-/-}$ or wild-type littermate controls. The mean of three independent assays is shown ±SD.

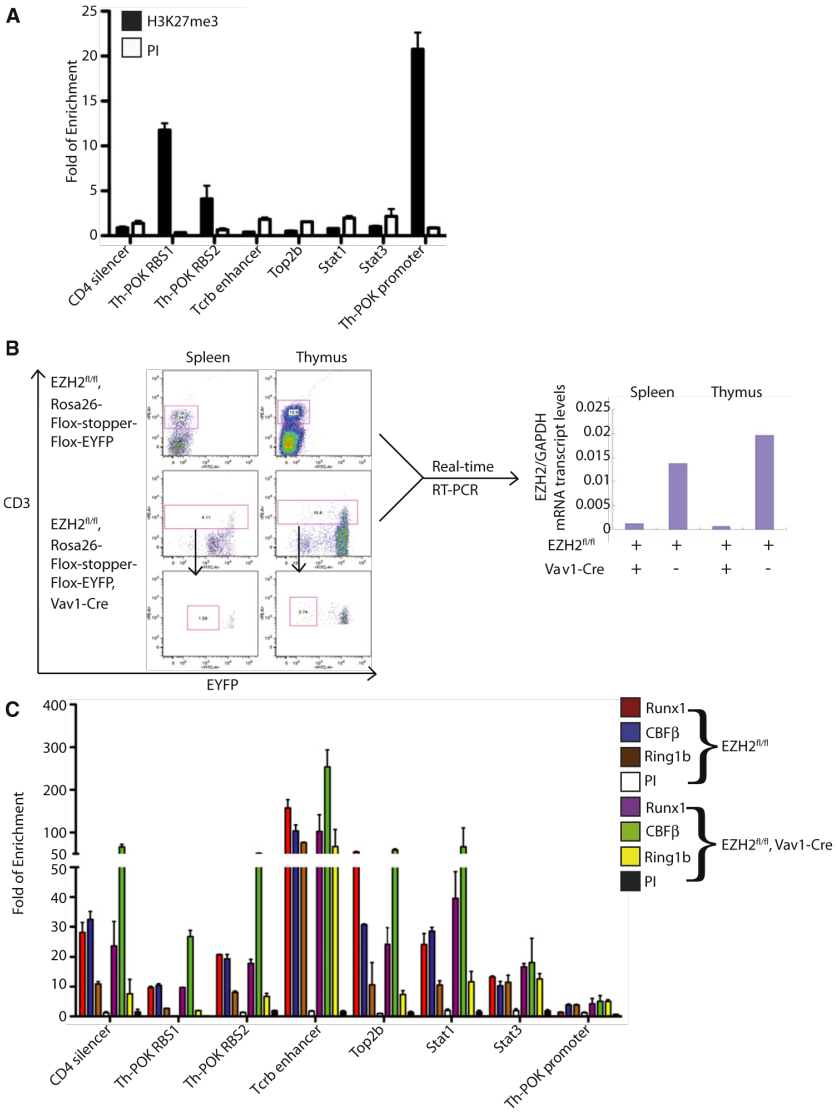

Figure 7. PRC2-Independent Occupancy of Ring1b at Runx1/CBFβ Commonly Occupied Genes

(A) qChIP assays for H3K27me3 at each of the indicated sites in wild-type murine primary thymocytes. The mean of three independent assays is shown ±SD.

(B) Left panel shows flow cytometry for CD3 and EYFP expression from spleen or thymus of EZH2$^{fl/fl}$, Rosa26-flox-stopper-flox-EYFP and EZH2$^{fl/fl}$, Rosa26-flox-stopper-flox-EYFP, Vav1-Cre mice. Right panels illustrate qRT-PCR analysis for EZH2 mRNA transcript levels in corresponding splenic or thymic CD3^{+} cells.

(C) qChIP assays for Runx1, CBFβ, and Ring1b in primary thymocytes from 6- to 8-week-old EZH2$^{fl/fl}$, Rosa26-flox-stopper-flox-EYFP or EZH2$^{fl/fl}$, Rosa26-flox-stopper-flox-EYFP, Vav1-Cre littermates. The data are expressed as fold enrichment relative to a negative control region (see Experimental Procedures). The data represent the mean of three independent experiments for Ring1b, and two independent experiments for Runx1 and CBFβ ±SD.

et al., 2003; van der Lugt et al., 1994) lack the complete failure of HSC development seen in Runx1$^{-/-}$ mouse embryos (Wang et al., 1996a) indicates that either PRC1 is not absolutely required for Runx1 function in HSC ontogeny or that compensatory mechanisms exist. Runx1 is also an upstream regulator of *Bmi1* in HSCs (Motoda et al., 2007), which could explain some of the HSC phenotypic overlap.

How dysregulation of Runx proteins predisposes to cancer is not fully understood. All of the human leukemia-associated *Runx1* chromosomal translocations generate fusion proteins

that retain the runt domain. Moreover, many malignancy-related *Runx1* somatic and germline point mutations affect the runt domain. It will be of interest to determine if any of these abnormal products lead to altered PRC1 chromatin recruitment and epigenetic changes and whether this plays a role in Runx1-related malignancies.

In summary the data presented in this study provide evidence that core binding transcription factors contribute to chromatin recruitment of PRC1 at site-specific loci in megakaryocytic and lymphocytic cells. Future studies will be needed to determine if other lineage-specific transcription factors also play a direct role in recruiting PRC1 in different tissue contexts.

EXPERIMENTAL PROCEDURES

See Supplemental Experimental Procedures for more details.

Cells and Cell Culture

The L8057-*birA* and L8057-$^{FLAG\text{-}bio}$Runx-1 cell lines were generated and cultured as previously described (Huang et al., 2009). Cell maturation was induced by adding 50 nM (final concentration) TPA to the medium for 3 days.

Conditional Knockout Mice

Runx1$^{fl/fl}$ mice were kindly provided by D. Gary Gilliland (Growney et al., 2005) and interbred with Vav1-Cre mice (Georgiades et al., 2002). EZH2$^{fl/fl}$, flox-stopper-flox Rosa26-EYFP, Vav1-Cre mice (Wilson et al., 2011) were kindly provided by Stuart Orkin. Bmi1$^{-/-}$ mice were kindly provided by Maarten van Lohuizen (van der Lugt et al., 1994). All animal procedures were approved by the Children's Hospital Institutional Animal Care and Use Committee.

Runx1 Multiprotein Complex Purification and Proteomic Analysis

Runx1-containing multiprotein complexes were purified and characterized as previously described (Huang et al., 2009). Copurified proteins were separated by SDS-PAGE, and the entire lane was analyzed by LC-MS/MS using an LTQ linear ion-trap mass spectrometer (Thermo Scientific). Peptide sequences were determined by matching protein or translated nucleotide databases with the acquired fragmentation pattern by the software program SEQUEST (Thermo Scientific) (Eng et al., 1994).

CoIP Assays

CoIP assays were performed as previously described (Yu et al., 2009). See Supplemental Experimental Procedures for more details.

GST Pull-Down Assays

See Supplemental Experimental Procedures.

ChIP and ChIP-Seq

Cells were fixed with 0.4% formaldehyde at room temperature for 10 min. For primary Mk studies, fetal liver cells were harvested from embryonic day 13.5 C57BL/6 murine embryos, cultured in the presence of 1% thrombopoietin (Tpo)-conditioned medium (Villeval et al., 1997) for 4 days, and mature Mks were enriched by discontinuous BSA density gradient as previously described (Drachman et al., 1997). For primary thymocyte studies, whole thymuses from 5- to 8-week-old mice were dissected, and single-cell suspensions were generated by gentle grinding of the tissue and passage through a 100 μm cell strainer in RPMI 1640 medium containing 10% heat-inactivated fetal calf serum. Thymocytes were crosslinked with 1% formaldehyde (final concentration) for 5 min at room temperature.

qChIP assays were performed as previously described (Yu et al., 2009). A site 2.5 kb upstream from the *Gapdhs* gene TSS was used as the internal control, and fold of enrichment was calculated using the $2^{\Delta Ct}$ method. The real-time PCR primers are listed in Table S7.

For ChIP-Seq, purified DNA was prepared for sequencing on a Beckman Coulter SPRI-TE following manufacturer's instructions. The seq-prepped DNA was PCR amplified using Illumina primers for 18 cycles. Samples were sequenced on either the Illumina Genome Analyzer II or Illumina Hi-Seq 2000 following the manufacturer's protocols. Raw ChIP-Seq data were processed using the Illumina software pipeline. Only ChIP-Seq reads that aligned to exactly one location in the reference mouse genome (UCSC, mm9) were retained. See Supplemental Experimental Procedures for data analysis details.

RNA Interference, qRT-PCR, and cDNA Microarray Analysis

Validated shRNA clones in the pLKO.1-puro vector (TRCN0000084942 [CBFβ], TRCN0000040581 [Ring1b], and TRCN00000257390 [Ring1b]) were obtained from Sigma-Aldrich, and the empty vector was used as control. Twenty-four hours after infection, cells were washed twice with PBS and fresh medium was added. Forty-eight hours after transduction, puromycin (2 μg/ml final concentration) and TPA (50 nM final concentration) were added. The cells were cultured for another 72 hr before harvest and analyzed by qRT-PCR or cDNA microarray. The qRT-PCR primers are listed in Figure S7.

Zebrafish Maintenance and MO Microinjection

All animal procedures were approved by the Children's Hospital Institutional Animal Care and Use Committee. See Supplemental Experimental Procedures.

ACCESSION NUMBERS

The ChIP-Seq and cDNA microarray data have been deposited in the Gene Expression Omnibus public database under accession numbers GSE33653 and GSE33659, respectively.

SUPPLEMENTAL INFORMATION

Supplemental Information includes seven figures, seven tables, and Supplemental Experimental Procedures and can be found with this article online at doi:10.1016/j.molcel.2011.11.032.

ACKNOWLEDGMENTS

M.Y. is supported by a grant from the Wendy Will Case Cancer Fund and an American Heart Association postdoctoral fellowship award. A.B.C. is supported by a grant from the NIH (R01-HL082952). E.F. is the recipient of the Eugene Bell Career Development Chair and is supported by NIH Grants U54-CA112967 and R01-GM089903. This work used computing resources funded by the National Science Foundation under Award No. DB1-0821391, and sequencing support from the NIH (P30-ES002109). The authors would like to thank D. Gary Gilliland, Stuart Orkin, and Maarten van Lohuizen for providing knockout mouse strains and Ross Tomaino and Steven Gygi at the Taplin Mass Spectrometry Facility for assistance with protein identification.

Received: February 28, 2011
Revised: September 15, 2011
Accepted: November 23, 2011
Published online: February 9, 2012

REFERENCES

Appleford, P.J., and Woollard, A. (2009). RUNX genes find a niche in stem cell biology. J. Cell. Biochem. *108*, 14–21.

Bakshi, R., Hassan, M.Q., Pratap, J., Lian, J.B., Montecino, M.A., van Wijnen, A.J., Stein, J.L., Imbalzano, A.N., and Stein, G.S. (2010). The human SWI/SNF complex associates with RUNX1 to control transcription of hematopoietic target genes. J. Cell. Physiol. *225*, 569–576.

Bejar, R., Stevenson, K., Abdel-Wahab, O., Galili, N., Nilsson, B., Garcia-Manero, G., Kantarjian, H., Raza, A., Levine, R.L., Neuberg, D., and Ebert, B.L. (2011). Clinical effect of point mutations in myelodysplastic syndromes. N. Engl. J. Med. *364*, 2496–2506.

Burns, C.E., DeBlasio, T., Zhou, Y., Zhang, J., Zon, L., and Nimer, S.D. (2002). Isolation and characterization of runxa and runxb, zebrafish

members of the runt family of transcriptional regulators. Exp. Hematol. *30*, 1381–1389.

Burns, C.E., Traver, D., Mayhall, E., Shepard, J.L., and Zon, L.I. (2005). Hematopoietic stem cell fate is established by the Notch-Runx pathway. Genes Dev. *19*, 2331–2342.

Calés, C., Román-Trufero, M., Pavón, L., Serrano, I., Melgar, T., Endoh, M., Pérez, C., Koseki, H., and Vidal, M. (2008). Inactivation of the polycomb group protein Ring1B unveils an antiproliferative role in hematopoietic cell expansion and cooperation with tumorigenesis associated with Ink4a deletion. Mol. Cell. Biol. *28*, 1018–1028.

Chen, M.J., Yokomizo, T., Zeigler, B.M., Dzierzak, E., and Speck, N.A. (2009). Runx1 is required for the endothelial to haematopoietic cell transition but not thereafter. Nature *457*, 887–891.

Dennis, G., Jr., Sherman, B.T., Hosack, D.A., Yang, J., Gao, W., Lane, H.C., and Lempicki, R.A. (2003). DAVID: Database for Annotation, Visualization, and Integrated Discovery. Genome Biol. *4*, P3.

Drachman, J.G., Sabath, D.F., Fox, N.E., and Kaushansky, K. (1997). Thrombopoietin signal transduction in purified murine megakaryocytes. Blood *89*, 483–492.

Elagib, K.E., Racke, F.K., Mogass, M., Khetawat, R., Delehanty, L.L., and Goldfarb, A.N. (2003). RUNX1 and GATA-1 coexpression and cooperation in megakaryocytic differentiation. Blood *101*, 4333–4341.

Eng, J.K., McCormack, A.L., and Yates, J.R., III. (1994). An approach to correlate tandem mass spectral data of peptides with amino acid sequences in a protein database. J. Am. Soc. Mass Spectrom. *5*, 976–989.

Galli, C., Fu, Q., Wang, W., Olsen, B.R., Manolagas, S.C., Jilka, R.L., and O'Brien, C.A. (2009). Commitment to the osteoblast lineage is not required for RANKL gene expression. J. Biol. Chem. *284*, 12654–12662.

Georgiades, P., Ogilvy, S., Duval, H., Licence, D.R., Charnock-Jones, D.S., Smith, S.K., and Print, C.G. (2002). VavCre transgenic mice: a tool for mutagenesis in hematopoietic and endothelial lineages. Genesis *34*, 251–256.

Growney, J.D., Shigematsu, H., Li, Z., Lee, B.H., Adelsperger, J., Rowan, R., Curley, D.P., Kutok, J.L., Akashi, K., Williams, I.R., et al. (2005). Loss of Runx1 perturbs adult hematopoiesis and is associated with a myeloproliferative phenotype. Blood *106*, 494–504.

Guo, Y., Papachristoudis, G., Altshuler, R.C., Gerber, G.K., Jaakkola, T.S., Gifford, D.K., and Mahony, S. (2010). Discovering homotypic binding events at high spatial resolution. Bioinformatics *26*, 3028–3034.

Huang, G., Zhang, P., Hirai, H., Elf, S., Yan, X., Chen, Z., Koschmieder, S., Okuno, Y., Dayaram, T., Growney, J.D., et al. (2008). PU.1 is a major downstream target of AML1 (RUNX1) in adult mouse hematopoiesis. Nat. Genet. *40*, 51–60.

Huang, H., Yu, M., Akie, T.E., Moran, T.B., Woo, A.J., Tu, N., Waldon, Z., Lin, Y.Y., Steen, H., and Cantor, A.B. (2009). Differentiation-dependent interactions between RUNX-1 and FLI-1 during megakaryocyte development. Mol. Cell. Biol. *29*, 4103–4115.

Ichikawa, M., Asai, T., Saito, T., Seo, S., Yamazaki, I., Yamagata, T., Mitani, K., Chiba, S., Ogawa, S., Kurokawa, M., and Hirai, H. (2004). AML-1 is required for megakaryocytic maturation and lymphocytic differentiation, but not for maintenance of hematopoietic stem cells in adult hematopoiesis. Nat. Med. *10*, 299–304.

Jacob, B., Osato, M., Yamashita, N., Wang, C.Q., Taniuchi, I., Littman, D.R., Asou, N., and Ito, Y. (2010). Stem cell exhaustion due to Runx1 deficiency is prevented by Evi5 activation in leukemogenesis. Blood *115*, 1610–1620.

Kim, W.Y., Sieweke, M., Ogawa, E., Wee, H.J., Englmeier, U., Graf, T., and Ito, Y. (1999). Mutual activation of Ets-1 and AML1 DNA binding by direct interaction of their autoinhibitory domains. EMBO J. *18*, 1609–1620.

Kissa, K., and Herbomel, P. (2010). Blood stem cells emerge from aortic endothelium by a novel type of cell transition. Nature *464*, 112–115.

Lin, H.F., Traver, D., Zhu, H., Dooley, K., Paw, B.H., Zon, L.I., and Handin, R.I. (2005). Analysis of thrombocyte development in CD41-GFP transgenic zebrafish. Blood *106*, 3803–3810.

MacIsaac, K.D., Lo, K.A., Gordon, W., Motola, S., Mazor, T., and Fraenkel, E. (2010). A quantitative model of transcriptional regulation reveals the influence of binding location on expression. PLoS Comput. Biol. *6*, e1000773.

Margueron, R., and Reinberg, D. (2011). The Polycomb complex PRC2 and its mark in life. Nature *469*, 343–349.

Miyazaki, M., Miyazaki, K., Itoi, M., Katoh, Y., Guo, Y., Kanno, R., Katoh-Fukui, Y., Honda, H., Amagai, T., van Lohuizen, M., et al. (2008). Thymocyte proliferation induced by pre-T cell receptor signaling is maintained through polycomb gene product Bmi-1-mediated Cdkn2a repression. Immunity *28*, 231–245.

Mohd-Sarip, A., van der Knaap, J.A., Wyman, C., Kanaar, R., Schedl, P., and Verrijzer, C.P. (2006). Architecture of a polycomb nucleoprotein complex. Mol. Cell *24*, 91–100.

Motoda, L., Osato, M., Yamashita, N., Jacob, B., Chen, L.Q., Yanagida, M., Ida, H., Wee, H.J., Sun, A.X., Taniuchi, I., et al. (2007). Runx1 protects hematopoietic stem/progenitor cells from oncogenic insult. Stem Cells *25*, 2976–2986.

North, T., Gu, T.L., Stacy, T., Wang, Q., Howard, L., Binder, M., Marín-Padilla, M., and Speck, N.A. (1999). Cbfa2 is required for the formation of intra-aortic hematopoietic clusters. Development *126*, 2563–2575.

Park, I.K., Qian, D., Kiel, M., Becker, M.W., Pihalja, M., Weissman, I.L., Morrison, S.J., and Clarke, M.F. (2003). Bmi-1 is required for maintenance of adult self-renewing haematopoietic stem cells. Nature *423*, 302–305.

Pasini, D., Bracken, A.P., Hansen, J.B., Capillo, M., and Helin, K. (2007). The polycomb group protein Suz12 is required for embryonic stem cell differentiation. Mol. Cell. Biol. *27*, 3769–3779.

Schoeftner, S., Sengupta, A.K., Kubicek, S., Mechtler, K., Spahn, L., Koseki, H., Jenuwein, T., and Wutz, A. (2006). Recruitment of PRC1 function at the initiation of X inactivation independent of PRC2 and silencing. EMBO J. *25*, 3110–3122.

Setoguchi, R., Tachibana, M., Naoe, Y., Muroi, S., Akiyama, K., Tezuka, C., Okuda, T., and Taniuchi, I. (2008). Repression of the transcription factor Th-POK by Runx complexes in cytotoxic T cell development. Science *319*, 822–825.

Simon, J.A., and Kingston, R.E. (2009). Mechanisms of polycomb gene silencing: knowns and unknowns. Nat. Rev. Mol. Cell Biol. *10*, 697–708.

Song, W.J., Sullivan, M.G., Legare, R.D., Hutchings, S., Tan, X., Kufrin, D., Ratajczak, J., Resende, I.C., Haworth, C., Hock, R., et al. (1999). Haploinsufficiency of CBFA2 causes familial thrombocytopenia with propensity to develop acute myelogenous leukaemia. Nat. Genet. *23*, 166–175.

Speck, N.A., and Gilliland, D.G. (2002). Core-binding factors in haematopoiesis and leukaemia. Nat. Rev. Cancer *2*, 502–513.

Sun, W., and Downing, J.R. (2004). Haploinsufficiency of AML1 results in a decrease in the number of LTR-HSCs while simultaneously inducing an increase in more mature progenitors. Blood *104*, 3565–3572.

Talebian, L., Li, Z., Guo, Y., Gaudet, J., Speck, M.E., Sugiyama, D., Kaur, P., Pear, W.S., Maillard, I., and Speck, N.A. (2007). T-lymphoid, megakaryocyte, and granulocyte development are sensitive to decreases in CBFbeta dosage. Blood *109*, 11–21.

van der Lugt, N.M., Domen, J., Linders, K., van Roon, M., Robanus-Maandag, E., te Riele, H., van der Valk, M., Deschamps, J., Sofroniew, M., van Lohuizen, M., et al. (1994). Posterior transformation, neurological abnormalities, and severe hematopoietic defects in mice with a targeted deletion of the bmi-1 proto-oncogene. Genes Dev. *8*, 757–769.

Villeval, J.L., Cohen-Solal, K., Tulliez, M., Giraudier, S., Guichard, J., Burstein, S.A., Cramer, E.M., Vainchenker, W., and Wendling, F. (1997). High thrombopoietin production by hematopoietic cells induces a fatal myeloproliferative syndrome in mice. Blood *90*, 4369–4383.

Vincenz, C., and Kerppola, T.K. (2008). Different polycomb group CBX family proteins associate with distinct regions of chromatin using nonhomologous protein sequences. Proc. Natl. Acad. Sci. USA *105*, 16572–16577.

Walrad, P.B., Hang, S., Joseph, G.S., Salas, J., and Gergen, J.P. (2010). Distinct contributions of conserved modules to Runt transcription factor activity. Mol. Biol. Cell *21*, 2315–2326.

Wang, Q., Stacy, T., Binder, M., Marin-Padilla, M., Sharpe, A.H., and Speck, N.A. (1996a). Disruption of the Cbfa2 gene causes necrosis and hemorrhaging in the central nervous system and blocks definitive hematopoiesis. Proc. Natl. Acad. Sci. USA *93*, 3444–3449.

Wang, Q., Stacy, T., Miller, J.D., Lewis, A.F., Gu, T.L., Huang, X., Bushweller, J.H., Bories, J.C., Alt, F.W., Ryan, G., et al. (1996b). The CBFbeta subunit is essential for CBFalpha2 (AML1) function in vivo. Cell *87*, 697–708.

Wilson, B.G., Wang, X., Shen, X., McKenna, E.S., Lemieux, M.E., Cho, Y.J., Koellhoffer, E.C., Pomeroy, S.L., Orkin, S.H., and Roberts, C.W. (2010). Epigenetic antagonism between polycomb and SWI/SNF complexes during oncogenic transformation. Cancer Cell *18*, 316–328.

Wilson, N.K., Foster, S.D., Wang, X., Knezevic, K., Schütte, J., Kaimakis, P., Chilarska, P.M., Kinston, S., Ouwehand, W.H., Dzierzak, E., et al. (2011). Combinatorial transcriptional control in blood stem/progenitor cells: genome-wide analysis of ten major transcriptional regulators. Cell Stem Cell *7*, 532–544.

Woo, C.J., Kharchenko, P.V., Daheron, L., Park, P.J., and Kingston, R.E. (2010). A region of the human HOXD cluster that confers polycomb-group responsiveness. Cell *140*, 99–110.

Yu, M., Wan, M., Zhang, J., Wu, J., Khatri, R., and Chi, T. (2008). Nucleoprotein structure of the CD4 locus: implications for the mechanisms underlying CD4 regulation during T cell development. Proc. Natl. Acad. Sci. USA *105*, 3873–3878.

Yu, M., Riva, L., Xie, H., Schindler, Y., Moran, T.B., Cheng, Y., Yu, D., Hardison, R., Weiss, M.J., Orkin, S.H., et al. (2009). Insights into GATA-1-mediated gene activation versus repression via genome-wide chromatin occupancy analysis. Mol. Cell *36*, 682–695.

Zhang, Y., Liu, T., Meyer, C.A., Eeckhoute, J., Johnson, D.S., Bernstein, B.E., Nusbaum, C., Myers, R.M., Brown, M., Li, W., and Liu, X.S. (2008). Model-based analysis of ChIP-Seq (MACS). Genome Biol. *9*, R137.

Zhao, J., Sun, B.K., Erwin, J.A., Song, J.J., and Lee, J.T. (2008). Polycomb proteins targeted by a short repeat RNA to the mouse X chromosome. Science *322*, 750–756.

Bibliography

Abdelilah, S., Mountcastle-Shah, E., Harvey, M., Solnica-Krezel, L., Schier, A., Stemple, D., et al. (1996). Mutations affecting neural survival in the zebrafish Danio rerio. *Development (Cambridge, England), 123,* 217-244.

Aguilo, F., Avagyan, S., Labar, A., Sevilla, A., Lee, D.-F., Kumar, P., et al. (2011). Prdm16 is a physiologic regulator of hematopoietic stem cells. *Blood, 117*(19), 5057-5123.

Amatruda, J., & Zon, L. (1999). Dissecting hematopoiesis and disease using the zebrafish. *Developmental biology, 216*(1), 1-16.

Antonchuk, J., Sauvageau, G., & Humphries, R. (2001). HOXB4 overexpression mediates very rapid stem cell regeneration and competitive hematopoietic repopulation. *Experimental hematology, 29*(9), 1125-1159.

Avery, O. T., MacLeod, C. M., & McCarty, M. (1944). Induction of transformation by a desoxyribonucleic acid fraction isolated from pneumococcus type III. *J Exp Med, 79*, 137-295.

Bagchi, A., Papazoglu, C., Wu, Y., Capurso, D., Brodt, M., Francis, D., et al. (2007). CHD5 is a tumor suppressor at human 1p36. *Cell, 128*(3), 459-534.

Bai, X., Kim, J., Yang, Z., Jurynec, M., Akie, T., Lee, J., et al. (2010). TIF1gamma controls erythroid cell fate by regulating transcription elongation. *Cell, 142*(1), 133-176.

Bajpai, R., Chen, D., Rada-Iglesias, A., Zhang, J., Xiong, Y., Helms, J., et al. (2010). CHD7 cooperates with PBAF to control multipotent neural crest formation. *Nature, 463*(7283), 958-1020.

Bakshi, R., Hassan, M., Pratap, J., Lian, J., Montecino, M., van Wijnen, A., et al. (2010). The human SWI/SNF complex associates with RUNX1 to control transcription of hematopoietic target genes. *Journal of cellular physiology, 225*(2), 569-645.

Banères, J., Martin, A., & Parello, J. (1997). The N tails of histones H3 and H4 adopt a highly structured conformation in the nucleosome. *Journal of molecular biology, 273(3)*, 503-511.

Bannister, A., & Kouzarides, T. The CBP co-activator is a histone acetyltransferase. *Nature, 384*(6610), 641-644.

Barresi, M., Burton, S., Dipietrantonio, K., Amsterdam, A., Hopkins, N., & Karlstrom, R. (2010). Essential genes for astroglial development and axon pathfinding during zebrafish embryogenesis. *Developmental dynamics : an official publication of the American Association of Anatomists, 239*(10), 2603-2621.

Barski, A., Cuddapah, S., Cui, K., Roh, T.-Y., Schones, D., Wang, Z., et al. (2007). High-resolution profiling of histone methylations in the human genome. *Cell, 129*(4), 823-860.

Beerman, I., Bhattacharya, D., Zandi, S., Sigvardsson, M., Weissman, I., Bryder, D., et al. (2010). Functionally distinct hematopoietic stem cells modulate hematopoietic lineage potential during aging by a mechanism of clonal expansion. *Proceedings of the National Academy of Sciences of the United States of America, 107*(12), 5465-5535.

Bennett, C., Kanki, J., Rhodes, J., Liu, T., Paw, B., Kieran, M., et al. (2001). Myelopoiesis in the zebrafish, Danio rerio. *Blood, 98*(3), 643-694.

Bergman, J., Bosman, E., van Ravenswaaij-Arts, C., & Steel, K. (2010). Study of smell and reproductive organs in a mouse model for CHARGE syndrome. *European journal of human genetics : EJHG, 18*(2), 171-178.

Bernardos, R., & Raymond, P. (2006). GFAP transgenic zebrafish. *Gene expression patterns : GEP, 6*(8), 1007-1020.

Bernstein, B., Kamal, M., Lindblad-Toh, K., Bekiranov, S., Bailey, D., Huebert, D., et al. (2005). Genomic maps and comparative analysis of histone modifications in human and mouse. *Cell, 120*(2), 169-250.

Bernstein, B., Meissner, A., & Lander, E. (2007). The mammalian epigenome. *Cell, 128*(4), 669-750.

Bertrand, J., Chi, N., Santoso, B., Teng, S., Stainier, D., & Traver, D. (2010).

Haematopoietic stem cells derive directly from aortic endothelium during development. *Nature, 464*(7285), 108-119.

Bertrand, J., Giroux, S. b., Golub, R., Klaine, M. l., Jalil, A., Boucontet, L., et al. (2005). Characterization of purified intraembryonic hematopoietic stem cells as a tool to define their site of origin. *Proceedings of the National Academy of Sciences of the United States of America, 102*(1), 134-143.

Bertrand, J., Kim, A., Violette, E., Stachura, D., Cisson, J., & Traver, D. (2007). Definitive hematopoiesis initiates through a committed erythromyeloid progenitor in the zebrafish embryo. *Development (Cambridge, England), 134*(23), 4147-4203.

Blobel, G. (2000). CREB-binding protein and p300: molecular integrators of hematopoietic transcription. *Blood, 95*(3), 745-800.

Blobel, G., Nakajima, T., Eckner, R., Montminy, M., & Orkin, S. (1998). CREB-binding protein cooperates with transcription factor GATA-1 and is required for erythroid differentiation. *Proceedings of the National Academy of Sciences of the United States of America, 95*(5), 2061-2067.

Bosman, E., Penn, A., Ambrose, J., Kettleborough, R., Stemple, D., & Steel, K. (2005). Multiple mutations in mouse Chd7 provide models for CHARGE syndrome. *Human molecular genetics, 14*(22), 3463-3539.

Brehm, A., Miska, E., McCance, D., Reid, J., Bannister, A., & Kouzarides, T. (1998). Retinoblastoma protein recruits histone deacetylase to repress transcription. *Nature, 391*(6667), 597-1198.

Bröske, A.-M., Vockentanz, L., Kharazi, S., Huska, M., Mancini, E., Scheller, M., et al. (2009). DNA methylation protects hematopoietic stem cell multipotency from myeloerythroid restriction. *Nature genetics, 41*(11), 1207-1222.

Brownell, J., Zhou, J., Ranalli, T., Kobayashi, R., Edmondson, D., Roth, S., et al. (1996). Tetrahymena histone acetyltransferase A: a homolog to yeast Gcn5p linking histone acetylation to gene activation. *Cell, 84*(6), 843-894.

Brownlie, A., Hersey, C., Oates, A., Paw, B., Falick, A., Witkowska, H., et al. (2003).

Characterization of embryonic globin genes of the zebrafish. *Developmental biology, 255*(1), 48-109.

Bultman, S., Gebuhr, T., Yee, D., La Mantia, C., Nicholson, J., Gilliam, A., et al. (2000). A Brg1 null mutation in the mouse reveals functional differences among mammalian SWI/SNF complexes. *Molecular cell, 6*(6), 1287-1382.

Burns, C., Galloway, J., Smith, A., Keefe, M., Cashman, T., Paik, E., et al. (2009). A genetic screen in zebrafish defines a hierarchical network of pathways required for hematopoietic stem cell emergence. *Blood, 113*(23), 5776-5858.

Cao, R., Wang, L., Wang, H., Xia, L., Erdjument-Bromage, H., Tempst, P., et al. (2002). Role of histone H3 lysine 27 methylation in Polycomb-group silencing. *Science (New York, N.Y.), 298*(5595), 1039-1082.

Chakraborty, S., Sinha, K., Senyuk, V., & Nucifora, G. (2003). SUV39H1 interacts with AML1 and abrogates AML1 transactivity. AML1 is methylated in vivo. *Oncogene, 22*(34), 5229-5266.

Chandor-Proust, A., Berteau, O., Douki, T., Gasparutto, D., Ollagnier-de-Choudens, S., Fontecave, M., et al. (2008). DNA repair and free radicals, new insights into the mechanism of spore photoproduct lyase revealed by single amino acid substitution. *The Journal of biological chemistry, 283*(52), 36361-36369.

Chen, T., & Allfrey, V. (1987). Rapid and reversible changes in nucleosome structure accompany the activation, repression, and superinduction of murine fibroblast protooncogenes c-fos and c-myc. *Proceedings of the National Academy of Sciences of the United States of America, 84*(15), 5252-5258.

Chen, T., Sterner, R., Cozzolino, A., & Allfrey, V. (1990). Reversible and irreversible changes in nucleosome structure along the c-fos and c-myc oncogenes following inhibition of transcription. *Journal of molecular biology, 212*(3), 481-574.

Chen, Z., Zang, J., Whetstine, J., Hong, X., Davrazou, F., Kutateladze, T., et al.

(2006). Structural insights into histone demethylation by JMJD2 family members. *Cell, 125*(4), 691-1393.

Choi, K., Kennedy, M., Kazarov, A., Papadimitriou, J., & Keller, G. (1998). A common precursor for hematopoietic and endothelial cells. *Development (Cambridge, England), 125*(4), 725-757.

Chuikov, S., Levi, B., Smith, M., & Morrison, S. (2010). Prdm16 promotes stem cell maintenance in multiple tissues, partly by regulating oxidative stress. *Nature cell biology, 12*(10), 999-2005.

Corbel, C., Salaün, J., Belo-Diabangouaya, P., & Dieterlen-Li√®vre, F. o. (2007). Hematopoietic potential of the pre-fusion allantois. *Developmental biology, 301*(2), 478-566.

Côté, J., Quinn, J., Workman, J., & Peterson, C. (1994). Stimulation of GAL4 derivative binding to nucleosomal DNA by the yeast SWI/SNF complex. *Science (New York, N.Y.), 265*(5168), 53-113.

Crosier, P., Kalev-Zylinska, M., Hall, C., Flores, M., Horsfield, J., & Crosier, K. (2002). Pathways in blood and vessel development revealed through zebrafish genetics. *The International journal of developmental biology, 46*(4), 493-995.

Cumano, A., Dieterlen-Lievre, F., & Godin, I. (1996). Lymphoid potential, probed before circulation in mouse, is restricted to caudal intraembryonic splanchnopleura. *Cell, 86*(6), 907-923.

Cumano, A., Ferraz, J., Klaine, M., Di Santo, J., & Godin, I. (2001). Intraembryonic, but not yolk sac hematopoietic precursors, isolated before circulation, provide long-term multilineage reconstitution. *Immunity, 15*(3), 477-562.

Cuthbert, G., Daujat, S., Snowden, A., Erdjument-Bromage, H., Hagiwara, T., Yamada, M., et al. (2004). Histone deimination antagonizes arginine methylation. *Cell, 118*(5), 545-598.

Dai, G., Sakamoto, H., Shimoda, Y., Fujimoto, T., Nishikawa, S.-I., & Ogawa, M. (2006). Over-expression of c-Myb increases the frequency of hemogenic

precursors in the endothelial cell population. *Genes to cells : devoted to molecular & cellular mechanisms, 11*(8), 859-929.

Davidson, A., & Zon, L. (2004). The 'definitive' (and 'primitive') guide to zebrafish hematopoiesis. *Oncogene, 23*(43), 7233-7279.

de Bruijn, M., Speck, N., Peeters, M., & Dzierzak, E. (2000). Definitive hematopoietic stem cells first develop within the major arterial regions of the mouse embryo. *The EMBO journal, 19*(11), 2465-2539.

Detrich, H., Kieran, M., Chan, F., Barone, L., Yee, K., Rundstadler, J., et al. (1995). Intraembryonic hematopoietic cell migration during vertebrate development. *Proceedings of the National Academy of Sciences of the United States of America, 92*(23), 10713-10720.

Dixon, J., Trainor, P., & Dixon, M. (2007). Treacher Collins syndrome. *Orthodontics & craniofacial research, 10*(2), 88-183.

Dooley, K., Davidson, A., & Zon, L. (2005). Zebrafish scl functions independently in hematopoietic and endothelial development. *Developmental biology, 277*(2), 522-558.

Durrin, L., Mann, R., Kayne, P., & Grunstein, M. (1991). Yeast histone H4 N-terminal sequence is required for promoter activation in vivo. *Cell, 65*(6), 1023-1054.

Dzierzak, E., & Speck, N. (2008). Of lineage and legacy: the development of mammalian hematopoietic stem cells. *Nature immunology, 9*(2), 129-165.

Fazzio, T., Huff, J., & Panning, B. (2008). An RNAi screen of chromatin proteins identifies Tip60-p400 as a regulator of embryonic stem cell identity. *Cell, 134*(1), 162-236.

Fehling, H., Lacaud, G., Kubo, A., Kennedy, M., Robertson, S., Keller, G., et al. (2003). Tracking mesoderm induction and its specification to the hemangioblast during embryonic stem cell differentiation. *Development (Cambridge, England), 130*(17), 4217-4244.

Ferkowicz, M., Starr, M., Xie, X., Li, W., Johnson, S., Shelley, W., et al. (2003). CD41 expression defines the onset of primitive and definitive hematopoiesis in the murine embryo. *Development (Cambridge, England), 130*(18), 4393-4796.

Fisher-Adams, G., & Grunstein, M. (1995). Yeast histone H4 and H3 N-termini have different effects on the chromatin structure of the GAL1 promoter. *The EMBO journal, 14*(7), 1468-1545.

Fujiwara, Y., Browne, C., Cunniff, K., Goff, S., & Orkin, S. (1996). Arrested development of embryonic red cell precursors in mouse embryos lacking transcription factor GATA-1. *Proceedings of the National Academy of Sciences of the United States of America, 93*(22), 12355-12363.

Furutani-Seiki, M., Jiang, Y., Brand, M., Heisenberg, C., Houart, C., Beuchle, D., et al. (1996). Neural degeneration mutants in the zebrafish, Danio rerio. *Development (Cambridge, England), 123*, 229-268.

Galloway, J., Wingert, R., Thisse, C., Thisse, B., & Zon, L. (2005). Loss of gata1 but not gata2 converts erythropoiesis to myelopoiesis in zebrafish embryos. *Developmental cell, 8*(1), 109-125.

Garcia-Ramirez, M., Rocchini, C., & Ausio, J. (1995). Modulation of chromatin folding by histone acetylation. *The Journal of biological chemistry, 270*(30), 17923-17931.

Gaspar-Maia, A., Alajem, A., Polesso, F., Sridharan, R., Mason, M., Heidersbach, A., et al. (2009). Chd1 regulates open chromatin and pluripotency of embryonic stem cells. *Nature, 460*(7257), 863-871.

Gekas, C., Dieterlen-Liévre, F., Orkin, S., & Mikkola, H. (2005). The placenta is a niche for hematopoietic stem cells. *Developmental cell, 8*(3), 365-440.

Gennery, A., Slatter, M., Rice, J., Hoefsloot, L., Barge, D., McLean-Tooke, A., et al. (2008). Mutations in CHD7 in patients with CHARGE syndrome cause T-B + natural killer cell + severe combined immune deficiency and may cause Omenn-like syndrome. *Clinical and experimental immunology, 153*(1), 75-155.

Gering, M., & Patient, R. (2005). Hedgehog signaling is required for adult blood stem cell formation in zebrafish embryos. *Developmental cell, 8*(3), 389-789.

Gering, M., Rodaway, A., G√∂ttgens, B., Patient, R., & Green, A. (1998). The SCL gene specifies haemangioblast development from early mesoderm. *The EMBO journal, 17*(14), 4029-4074.

Gering, M., Yamada, Y., Rabbitts, T., & Patient, R. (2003). Lmo2 and Scl/Tal1 convert non-axial mesoderm into haemangioblasts which differentiate into endothelial cells in the absence of Gata1. *Development (Cambridge, England), 130*(25), 6187-6286.

Giraldez, A., Mishima, Y., Rihel, J., Grocock, R., Van Dongen, S., Inoue, K., et al. (2006). Zebrafish MiR-430 promotes deadenylation and clearance of maternal mRNAs. *Science (New York, N.Y.), 312*(5770), 75-84.

Goessling, W., Allen, R., Guan, X., Jin, P., Uchida, N., Dovey, M., et al. (2011). Prostaglandin E2 enhances human cord blood stem cell xenotransplants and shows long-term safety in preclinical nonhuman primate transplant models. *Cell stem cell, 8*(4), 445-503.

Gupta, S., Zhu, H., Zon, L., & Evans, T. (2006). BMP signaling restricts hemato-vascular development from lateral mesoderm during somitogenesis. *Development (Cambridge, England), 133*(11), 2177-2264.

Hammerschmidt, M., & Mullins, M. (2002). Dorsoventral patterning in the zebrafish: bone morphogenetic proteins and beyond. *Results and problems in cell differentiation, 40*, 72-167.

Han, M., & Grunstein, M. (1988). Nucleosome loss activates yeast downstream promoters in vivo. *Cell, 55*(6), 1137-1182.

Hassa, P., Haenni, S., Elser, M., & Hottiger, M. (2006). Nuclear ADP-ribosylation reactions in mammalian cells: where are we today and where are we going? *Microbiology and molecular biology reviews : MMBR, 70*(3), 789-1618.

Hawker, K., Fuchs, H., Angelis, M., & Steel, K. (2005). Two new mouse mutants with vestibular defects that map to the highly mutable locus on chromosome 4. *International journal of audiology, 44*(3), 171-178.

Hendzel, M., Wei, Y., Mancini, M., Van Hooser, A., Ranalli, T., Brinkley, B., et al. (1997). Mitosis-specific phosphorylation of histone H3 initiates primarily within pericentromeric heterochromatin during G2 and spreads in an ordered fashion coincident with mitotic chromosome condensation. *Chromosoma, 106*(6), 348-408.

Herbomel, P., Thisse, B., & Thisse, C. (1999). Ontogeny and behaviour of early macrophages in the zebrafish embryo. *Development (Cambridge, England), 126*(17), 3735-3780.

Ho, L., & Crabtree, G. (2010). Chromatin remodelling during development. *Nature, 463*(7280), 474-558.

Ho, L., Jothi, R., Ronan, J., Cui, K., Zhao, K., & Crabtree, G. (2009). An embryonic stem cell chromatin remodeling complex, esBAF, is an essential component of the core pluripotency transcriptional network. *Proceedings of the National Academy of Sciences of the United States of America, 106*(13), 5187-5278.

Hock, H., Hamblen, M., Rooke, H., Schindler, J., Saleque, S., Fujiwara, Y., et al. (2004). Gfi-1 restricts proliferation and preserves functional integrity of haematopoietic stem cells. *Nature, 431*(7011), 1002-1009.

Holliday, R., & Pugh, J. (1975). DNA modification mechanisms and gene activity during development. *Science (New York, N.Y.), 187*(4173), 226-258.

Holloway, B., Gomez de la Torre Canny, S., Ye, Y., Slusarski, D., Freisinger, C., Dosch, R., et al. (2009). A novel role for MAPKAPK2 in morphogenesis during zebrafish development. *PLoS genetics, 5*(3).

Hong, L., Schroth, G., Matthews, H., Yau, P., & Bradbury, E. (1993). Studies of the DNA binding properties of histone H4 amino terminus. Thermal denaturation studies reveal that acetylation markedly reduces the

binding constant of the H4 "tail" to DNA. *The Journal of biological chemistry, 268*(1), 305-319.

Hong, W., Nakazawa, M., Chen, Y.-Y., Kori, R., Vakoc, C., Rakowski, C., et al. (2005). FOG-1 recruits the NuRD repressor complex to mediate transcriptional repression by GATA-1. *The EMBO journal, 24*(13), 2367-2445.

Hoover-Fong, J., Savage, W., Lisi, E., Winkelstein, J., Thomas, G., Hoefsloot, L., et al. (2009). Congenital T cell deficiency in a patient with CHARGE syndrome. *The Journal of pediatrics, 154*(1), 140-142.

Hsu, J., Lee, C-T., Gerber, S., Yu, S., & Speck, N. (2011). Runx1-Cbfb interacts with CHD7, a chromatin modifying enzyme with a potential role in hematopoiesis. Blood (ASH Annual Meeting Abstracts), Nov 2011; 118: 1300.

Hu, X., Li, X., Valverde, K., Fu, X., Noguchi, C., Qiu, Y., et al. (2009). LSD1-mediated epigenetic modification is required for TAL1 function and hematopoiesis. *Proceedings of the National Academy of Sciences of the United States of America, 106*(25), 10141-10147.

Huang, H., Zhang, B., Hartenstein, P., Chen, J.-n., & Lin, S. (2005). NXT2 is required for embryonic heart development in zebrafish. *BMC developmental biology, 5*, 7.

Huber, T., Kouskoff, V., Fehling, H., Palis, J., & Keller, G. (2004). Haemangioblast commitment is initiated in the primitive streak of the mouse embryo. *Nature, 432*(7017), 625-655.

Hurd, E., Capers, P., Blauwkamp, M., Adams, M., Raphael, Y., Poucher, H., et al. (2007). Loss of Chd7 function in gene-trapped reporter mice is embryonic lethal and associated with severe defects in multiple developing tissues. *Mammalian genome : official journal of the International Mammalian Genome Society, 18*(2), 94-198.

Hurd, E., Poucher, H., Cheng, K., Raphael, Y., & Martin, D. (2010). The ATP-dependent chromatin remodeling enzyme CHD7 regulates pro-neural gene expression and neurogenesis in the inner ear. *Development*

(Cambridge, England), 137(18), 3139-3189.

Imbalzano, A., Kwon, H., Green, M., & Kingston, R. (1994). Facilitated binding of TATA-binding protein to nucleosomal DNA. *Nature, 370*(6489), 481-486.

Inoue, H., Takada, H., Kusuda, T., Goto, T., Ochiai, M., Kinjo, T., et al. (2010). Successful cord blood transplantation for a CHARGE syndrome with CHD7 mutation showing DiGeorge sequence including hypoparathyroidism. *European journal of pediatrics, 169*(7), 839-883.

Jaffredo, T., Bollerot, K., Sugiyama, D., Gautier, R., & Drevon, C. c. (2005). Tracing the hemangioblast during embryogenesis: developmental relationships between endothelial and hematopoietic cells. *The International journal of developmental biology, 49*(2-3), 269-346.

Jin, H., Sood, R., Xu, J., Zhen, F., English, M., Liu, P., et al. (2009). Definitive hematopoietic stem/progenitor cells manifest distinct differentiation output in the zebrafish VDA and PBI. *Development (Cambridge, England), 136*(4), 647-701.

Jin, H., Xu, J., & Wen, Z. (2007). Migratory path of definitive hematopoietic stem/progenitor cells during zebrafish development. *Blood, 109*(12), 5208-5222.

Ju, B.-G., Lunyak, V., Perissi, V., Garcia-Bassets, I., Rose, D., Glass, C., et al. (2006). A topoisomerase IIbeta-mediated dsDNA break required for regulated transcription. *Science (New York, N.Y.), 312*(5781), 1798-2600.

Jude, C., Climer, L., Xu, D., Artinger, E., Fisher, J., & Ernst, P. (2007). Unique and independent roles for MLL in adult hematopoietic stem cells and progenitors. *Cell stem cell, 1*(3), 324-361.

Kadam, S., & Emerson, B. (2003). Transcriptional specificity of human SWI/SNF BRG1 and BRM chromatin remodeling complexes. *Molecular cell, 11*(2), 377-466.

Kalev-Zylinska, M., Horsfield, J., Flores, M., Postlethwait, J., Vitas, M., Baas, A., et al. (2002). Runx1 is required for zebrafish blood and vessel development

and expression of a human RUNX1-CBF2T1 transgene advances a model for studies of leukemogenesis. *Development (Cambridge, England), 129*(8), 2015-2045.

Kalkhoven, E. (2004). CBP and p300: HATs for different occasions. *Biochemical pharmacology, 68*(6), 1145-1200.

Kasten, M., Clapier, C., & Cairns, B. (2011). SnapShot: Chromatin remodeling: SWI/SNF. *Cell, 144*(2), 3100.

Kemp, H., Carmany-Rampey, A., & Moens, C. (2009). Generating chimeric zebrafish embryos by transplantation. *Journal of visualized experiments : JoVE*(29).

Keogh, M.-C., Kurdistani, S., Morris, S., Ahn, S., Podolny, V., Collins, S., et al. (2005). Cotranscriptional set2 methylation of histone H3 lysine 36 recruits a repressive Rpd3 complex. *Cell, 123*(4), 593-1198.

Kim, J., Chu, J., Shen, X., Wang, J., & Orkin, S. (2008). An extended transcriptional network for pluripotency of embryonic stem cells. *Cell, 132*(6), 1049-1110.

Kim, J., Guermah, M., McGinty, R., Lee, J.-S., Tang, Z., Milne, T., et al. (2009). RAD6-Mediated transcription-coupled H2B ubiquitylation directly stimulates H3K4 methylation in human cells. *Cell, 137*(3), 459-530.

Kimmel, C., Ballard, W., Kimmel, S., Ullmann, B., & Schilling, T. (1995). Stages of embryonic development of the zebrafish. *Developmental dynamics : an official publication of the American Association of Anatomists, 203*(3), 253-563.

Kissa, K., Murayama, E., Zapata, A., Cort√©s, A., Perret, E., Machu, C., et al. (2008). Live imaging of emerging hematopoietic stem cells and early thymus colonization. *Blood, 111*(3), 1147-1203.

Knezetic, J., & Luse, D. (1986). The presence of nucleosomes on a DNA template prevents initiation by RNA polymerase II in vitro. *Cell, 45*(1), 95-199.

Kornberg, R., & Thomas, J. (1974). Chromatin structure; oligomers of the histones. *Science (New York, N.Y.), 184*(4139), 865-873.

Kouzarides, T. (2007). Chromatin modifications and their function. *Cell, 128*(4), 693-1398.

Kwon, H., Imbalzano, A., Khavari, P., Kingston, R., & Green, M. (1994). Nucleosome disruption and enhancement of activator binding by a human SW1/SNF complex. *Nature, 370*(6489), 477-558.

Lancrin, C., Sroczynska, P., Stephenson, C., Allen, T., Kouskoff, V., & Lacaud, G. (2009). The haemangioblast generates haematopoietic cells through a haemogenic endothelium stage. *Nature, 457*(7231), 892-897.

Latham, J., & Dent, S. (2007). Cross-regulation of histone modifications. *Nature structural & molecular biology, 14*(11), 1017-1041.

Laurenti, E., Varnum-Finney, B., Wilson, A., Ferrero, I., Blanco-Bose, W., Ehninger, A., et al. (2008). Hematopoietic stem cell function and survival depend on c-Myc and N-Myc activity. *Cell stem cell, 3*(6), 611-635.

Lawson, N., Mugford, J., Diamond, B., & Weinstein, B. (2003). phospholipase C gamma-1 is required downstream of vascular endothelial growth factor during arterial development. *Genes & development, 17*(11), 1346-1397.

Layman, W., McEwen, D., Beyer, L., Lalani, S., Fernbach, S., Oh, E., et al. (2009). Defects in neural stem cell proliferation and olfaction in Chd7 deficient mice indicate a mechanism for hyposmia in human CHARGE syndrome. *Human molecular genetics, 18*(11), 1909-1932.

Lee, D., Hayes, J., Pruss, D., & Wolffe, A. (1993). A positive role for histone acetylation in transcription factor access to nucleosomal DNA. *Cell, 72*(1), 73-157.

Lee, D., Teyssier, C., Strahl, B., & Stallcup, M. (2005). Role of protein methylation in regulation of transcription. *Endocrine reviews, 26*(2), 147-217.

Lee, M., Villa, R., Trojer, P., Norman, J., Yan, K.-P., Reinberg, D., et al. (2007).

Demethylation of H3K27 regulates polycomb recruitment and H2A ubiquitination. *Science (New York, N.Y.), 318*(5849), 447-497.

Lefebvre, P., Mouchon, A., Lefebvre, B., & Formstecher, P. (1998). Binding of retinoic acid receptor heterodimers to DNA. A role for histones NH2 termini. *The Journal of biological chemistry, 273*(20), 12288-12383.

Lenfant, F., Mann, R., Thomsen, B., Ling, X., & Grunstein, M. (1996). All four core histone N-termini contain sequences required for the repression of basal transcription in yeast. *The EMBO journal, 15*(15), 3974-4059.

Lengerke, C., Schmitt, S., Bowman, T., Jang, I., Maouche-Chretien, L., McKinney-Freeman, S., et al. (2008). BMP and Wnt specify hematopoietic fate by activation of the Cdx-Hox pathway. *Cell stem cell, 2*(1), 72-154.

Lessard, J., & Sauvageau, G. (2003). Bmi-1 determines the proliferative capacity of normal and leukaemic stem cells. *Nature, 423*(6937), 255-315.

Lessard, J., Wu, J., Ranish, J., Wan, M., Winslow, M., Staahl, B., et al. (2007). An essential switch in subunit composition of a chromatin remodeling complex during neural development. *Neuron, 55*(2), 201-216.

Li, B., Carey, M., & Workman, J. (2007). The role of chromatin during transcription. *Cell, 128*(4), 707-726.

Li, Z., Chen, M., Stacy, T., & Speck, N. (2006). Runx1 function in hematopoiesis is required in cells that express Tek. *Blood, 107*(1), 106-116.

Liao, E., Paw, B., Oates, A., Pratt, S., Postlethwait, J., & Zon, L. (1998). SCL/Tal-1 transcription factor acts downstream of cloche to specify hematopoietic and vascular progenitors in zebrafish. *Genes & development, 12*(5), 621-627.

Lieschke, G., Oates, A., Paw, B., Thompson, M., Hall, N., Ward, A., et al. (2002). Zebrafish SPI-1 (PU.1) marks a site of myeloid development independent of primitive erythropoiesis: implications for axial patterning. *Developmental biology, 246*(2), 274-369.

Lieu, Y., & Reddy, E. (2009). Conditional c-myb knockout in adult hematopoietic stem cells leads to loss of self-renewal due to impaired proliferation and accelerated differentiation. *Proceedings of the National Academy of Sciences of the United States of America, 106*(51), 21689-21783.

Lorès, P., Visvikis, O., Luna, R., Lemichez, E., & Gacon, G. r. (2010). The SWI/SNF protein BAF60b is ubiquitinated through a signalling process involving Rac GTPase and the RING finger protein Unkempt. *The FEBS journal, 277*(6), 1453-1517.

Luger, K., Mäder, A., Richmond, R., Sargent, D., & Richmond, T. (1997). Crystal structure of the nucleosome core particle at 2.8 A resolution. *Nature, 389*(6648), 251-311.

Maeder, M., Thibodeau-Beganny, S., Osiak, A., Wright, D., Anthony, R., Eichtinger, M., et al. (2008). Rapid "open-source" engineering of customized zinc-finger nucleases for highly efficient gene modification. *Molecular cell, 31*(2), 294-595.

McDaniel, I., Lee, J., Berger, M., Hanagami, C., & Armstrong, J. (2008). Investigations of CHD1 function in transcription and development of Drosophila melanogaster. *Genetics, 178*(1), 583-590.

McMahon, K., Hiew, S., Hadjur, S., Veiga-Fernandes, H., Menzel, U., Price, A., et al. (2007). Mll has a critical role in fetal and adult hematopoietic stem cell self-renewal. *Cell stem cell, 1*(3), 338-383.

Medvinsky, A., & Dzierzak, E. (1996). Definitive hematopoiesis is autonomously initiated by the AGM region. *Cell, 86*(6), 897-1803.

Megee, P., Morgan, B., & Smith, M. (1995). Histone H4 and the maintenance of genome integrity. *Genes & development, 9*(14), 1716-1743.

Meng, X., Noyes, M., Zhu, L., Lawson, N., & Wolfe, S. (2008). Targeted gene inactivation in zebrafish using engineered zinc-finger nucleases. *Nature biotechnology, 26*(6), 695-1396.

Mikkelsen, T., Ku, M., Jaffe, D., Issac, B., Lieberman, E., Giannoukos, G., et al.

(2007). Genome-wide maps of chromatin state in pluripotent and lineage-committed cells. *Nature, 448*(7153), 553-613.

Mikkola, H., Fujiwara, Y., Schlaeger, T., Traver, D., & Orkin, S. (2003). Expression of CD41 marks the initiation of definitive hematopoiesis in the mouse embryo. *Blood, 101*(2), 508-524.

Mikkola, H., Klintman, J., Yang, H., Hock, H., Schlaeger, T., Fujiwara, Y., et al. (2003). Haematopoietic stem cells retain long-term repopulating activity and multipotency in the absence of stem-cell leukaemia SCL/tal-1 gene. *Nature, 421*(6922), 547-598.

Mohler, J., Weiss, N., Murli, S., Mohammadi, S., Vani, K., Vasilakis, G., et al. (1992). The embryonically active gene, unkempt, of Drosophila encodes a Cys3His finger protein. *Genetics, 131*(2), 377-465.

Morrison, S., Hemmati, H., Wandycz, A., & Weissman, I. (1995). The purification and characterization of fetal liver hematopoietic stem cells. *Proceedings of the National Academy of Sciences of the United States of America, 92*(22), 10302-10308.

Mosimann, C., Kaufman, C., Li, P., Pugach, E., Tamplin, O., & Zon, L. (2011). Ubiquitous transgene expression and Cre-based recombination driven by the ubiquitin promoter in zebrafish. *Development (Cambridge, England), 138*(1), 169-246.

Mucenski, M., McLain, K., Kier, A., Swerdlow, S., Schreiner, C., Miller, T., et al. (1991). A functional c-myb gene is required for normal murine fetal hepatic hematopoiesis. *Cell, 65*(4), 677-766.

Müller, A., Medvinsky, A., Strouboulis, J., Grosveld, F., & Dzierzak, E. (1994). Development of hematopoietic stem cell activity in the mouse embryo. *Immunity, 1*(4), 291-592.

Murayama, E., Kissa, K., Zapata, A., Mordelet, E., Briolat, V. r., Lin, H.-F., et al. (2006). Tracing hematopoietic precursor migration to successive hematopoietic organs during zebrafish development. *Immunity, 25*(6), 963-1038.

Nasevicius, A., & Ekker, S. (2000). Effective targeted gene 'knockdown' in zebrafish. *Nature genetics, 26*(2), 216-236.

Nathan, D., Ingvarsdottir, K., Sterner, D., Bylebyl, G., Dokmanovic, M., Dorsey, J., et al. (2006). Histone sumoylation is a negative regulator in Saccharomyces cerevisiae and shows dynamic interplay with positive-acting histone modifications. *Genes & development, 20*(8), 966-1042.

Neave, B., Holder, N., & Patient, R. (1997). A graded response to BMP-4 spatially coordinates patterning of the mesoderm and ectoderm in the zebrafish. *Mechanisms of development, 62*(2), 183-278.

Nelson, C., Santos-Rosa, H., & Kouzarides, T. (2006). Proline isomerization of histone H3 regulates lysine methylation and gene expression. *Cell, 126*(5), 905-921.

Ness, S., Kowenz-Leutz, E., Casini, T., Graf, T., & Leutz, A. (1993). Myb and NF-M: combinatorial activators of myeloid genes in heterologous cell types. *Genes & development, 7*(5), 749-808.

North, T., Goessling, W., Peeters, M., Li, P., Ceol, C., Lord, A., et al. (2009). Hematopoietic stem cell development is dependent on blood flow. *Cell, 137*(4), 736-784.

North, T., Goessling, W., Walkley, C., Lengerke, C., Kopani, K., Lord, A., et al. (2007). Prostaglandin E2 regulates vertebrate haematopoietic stem cell homeostasis. *Nature, 447*(7147), 1007-1018.

North, T., Gu, T., Stacy, T., Wang, Q., Howard, L., Binder, M., et al. (1999). Cbfa2 is required for the formation of intra-aortic hematopoietic clusters. *Development (Cambridge, England), 126*(11), 2563-2638.

Nowak, S., & Corces, V. (2004). Phosphorylation of histone H3: a balancing act between chromosome condensation and transcriptional activation. *Trends in genetics : TIG, 20*(4), 214-234.

O'Boyle, S., Bree, R., McLoughlin, S., Grealy, M., & Byrnes, L. (2007). Identification

of zygotic genes expressed at the midblastula transition in zebrafish. *Biochemical and biophysical research communications, 358*(2), 462-470.

Ogryzko, V., Schiltz, R., Russanova, V., Howard, B., & Nakatani, Y. (1996). The transcriptional coactivators p300 and CBP are histone acetyltransferases. *Cell, 87*(5), 953-962.

Oguro, H., Yuan, J., Ichikawa, H., Ikawa, T., Yamazaki, S., Kawamoto, H., et al. (2010). Poised lineage specification in multipotential hematopoietic stem and progenitor cells by the polycomb protein Bmi1. *Cell stem cell, 6*(3), 279-365.

Okada, Y., Yamagata, K., Hong, K., Wakayama, T., & Zhang, Y. (2010). A role for the elongator complex in zygotic paternal genome demethylation. *Nature, 463*(7280), 554-562.

Okuda, T., van Deursen, J., Hiebert, S., Grosveld, G., & Downing, J. (1996). AML1, the target of multiple chromosomal translocations in human leukemia, is essential for normal fetal liver hematopoiesis. *Cell, 84*(2), 321-351.

Orkin, S., & Zon, L. (2008). Hematopoiesis: an evolving paradigm for stem cell biology. *Cell, 132*(4), 631-675.

Ottersbach, K., & Dzierzak, E. (2005). The murine placenta contains hematopoietic stem cells within the vascular labyrinth region. *Developmental cell, 8*(3), 377-464.

Owen, D., Ornaghi, P., Yang, J., Lowe, N., Evans, P., Ballario, P., et al. (2000). The structural basis for the recognition of acetylated histone H4 by the bromodomain of histone acetyltransferase gcn5p. *The EMBO journal, 19*(22), 6141-6150.

Pagon, R., Graham, J., Zonana, J., & Yong, S. (1981). Coloboma, congenital heart disease, and choanal atresia with multiple anomalies: CHARGE association. *The Journal of pediatrics, 99*(2), 223-230.

Palis, J., Robertson, S., Kennedy, M., Wall, C., & Keller, G. (1999). Development of erythroid and myeloid progenitors in the yolk sac and embryo proper of

the mouse. *Development (Cambridge, England), 126*(22), 5073-5157.

Park, I.-k., Qian, D., Kiel, M., Becker, M., Pihalja, M., Weissman, I., et al. (2003). Bmi-1 is required for maintenance of adult self-renewing haematopoietic stem cells. *Nature, 423*(6937), 302-307.

Patten, S., Jacobs-McDaniels, N., Zaouter, C., Drapeau, P., Albertson, R., & Moldovan, F. (2012). Role of Chd7 in Zebrafish: A Model for CHARGE Syndrome. *PloS one, 7*(2), e31650.

Patterson, L., Gering, M., & Patient, R. (2005). Scl is required for dorsal aorta as well as blood formation in zebrafish embryos. *Blood, 105*(9), 3502-3513.

Patton, E., & Zon, L. (2001). The art and design of genetic screens: zebrafish. *Nature reviews. Genetics, 2*(12), 956-1022.

Pavri, R., Zhu, B., Li, G., Trojer, P., Mandal, S., Shilatifard, A., et al. (2006). Histone H2B monoubiquitination functions cooperatively with FACT to regulate elongation by RNA polymerase II. *Cell, 125*(4), 703-720.

Pevny, L., Simon, M., Robertson, E., Klein, W., Tsai, S., D'Agati, V., et al. (1991). Erythroid differentiation in chimaeric mice blocked by a targeted mutation in the gene for transcription factor GATA-1. *Nature, 349*(6306), 257-317.

Puig, O., Bellés, E., López-Rodas, G., Sendra, R., & Tordera, V. (1998). Interaction between N-terminal domain of H4 and DNA is regulated by the acetylation degree. *Biochimica et biophysica acta, 1397*(1), 79-169.

Ram, O., Goren, A., Amit, I., Shoresh, N., Yosef, N., Ernst, J., et al. (2011). Combinatorial patterning of chromatin regulators uncovered by genome-wide location analysis in human cells. *Cell, 147*(7), 1628-1667.

Ramos, Y., Hestand, M., Verlaan, M., Krabbendam, E., Ariyurek, Y., van Galen, M., et al. (2010). Genome-wide assessment of differential roles for p300 and CBP in transcription regulation. *Nucleic acids research, 38*(16), 5396-5804.

Rea, S., Eisenhaber, F., O'Carroll, D., Strahl, B., Sun, Z., Schmid, M., et al. (2000). Regulation of chromatin structure by site-specific histone H3 methyltransferases. *Nature, 406*(6796), 593-602.

Rebel, V., Kung, A., Tanner, E., Yang, H., Bronson, R., & Livingston, D. (2002). Distinct roles for CREB-binding protein and p300 in hematopoietic stem cell self-renewal. *Proceedings of the National Academy of Sciences of the United States of America, 99*(23), 14789-14883.

Reyes, J., Barra, J., Muchardt, C., Camus, A., Babinet, C., & Yaniv, M. (1998). Altered control of cellular proliferation in the absence of mammalian brahma (SNF2alpha). *The EMBO journal, 17*(23), 6979-7070.

Rice, K., Hormaeche, I., & Licht, J. (2007). Epigenetic regulation of normal and malignant hematopoiesis. *Oncogene, 26*(47), 6697-7411.

Riggs, A. (1975). X inactivation, differentiation, and DNA methylation. *Cytogenetics and cell genetics, 14*(1), 9-34.

Robb, L., Lyons, I., Li, R., Hartley, L., Köntgen, F., Harvey, R., et al. (1995). Absence of yolk sac hematopoiesis from mice with a targeted disruption of the scl gene. *Proceedings of the National Academy of Sciences of the United States of America, 92*(15), 7075-7084.

Rodríguez-Paredes, M., Ceballos-Chávez, M., Esteller, M., García-Domínguez, M., & Reyes, J. (2009). The chromatin remodeling factor CHD8 interacts with elongating RNA polymerase II and controls expression of the cyclin E2 gene. *Nucleic acids research, 37*(8), 2449-2509.

Rodrigues, N., Janzen, V., Forkert, R., Dombkowski, D., Boyd, A., Orkin, S., et al. (2005). Haploinsufficiency of GATA-2 perturbs adult hematopoietic stem-cell homeostasis. *Blood, 106*(2), 477-561.

Rodriguez, P., Bonte, E., Krijgsveld, J., Kolodziej, K., Guyot, B., Heck, A., et al. (2005). GATA-1 forms distinct activating and repressive complexes in erythroid cells. *The EMBO journal, 24*(13), 2354-2420.

Sánchez, M., Holmes, A., Miles, C., & Dzierzak, E. (1996). Characterization of the

first definitive hematopoietic stem cells in the AGM and liver of the mouse embryo. *Immunity, 5*(6), 513-538.

Sabin, F. R. (1920). Studies on the origin of blood vessels and of red corpuscles as seen in the living blastoderm of the chick during the second day of incubation. *Contributions to embryology, 9*, 213-475.

Schübeler, D., MacAlpine, D., Scalzo, D., Wirbelauer, C., Kooperberg, C., van Leeuwen, F., et al. (2004). The histone modification pattern of active genes revealed through genome-wide chromatin analysis of a higher eukaryote. *Genes & development, 18*(11), 1263-1334.

Schaniel, C., Ang, Y.-S., Ratnakumar, K., Cormier, C., James, T., Bernstein, E., et al. (2009). Smarcc1/Baf155 couples self-renewal gene repression with changes in chromatin structure in mouse embryonic stem cells. *Stem cells (Dayton, Ohio), 27*(12), 2979-3070.

Schnetz, M., Bartels, C., Shastri, K., Balasubramanian, D., Zentner, G., Balaji, R., et al. (2009). Genomic distribution of CHD7 on chromatin tracks H3K4 methylation patterns. *Genome research, 19*(4), 590-1191.

Schnetz, M., Handoko, L., Akhtar-Zaidi, B., Bartels, C., Pereira, C., Fisher, A., et al. (2010). CHD7 targets active gene enhancer elements to modulate ES cell-specific gene expression. *PLoS genetics, 6*(7), e1001023.

Schones, D., Cui, K., Cuddapah, S., Roh, T.-Y., Barski, A., Wang, Z., et al. (2008). Dynamic regulation of nucleosome positioning in the human genome. *Cell, 132*(5), 887-985.

Schotta, G., Ebert, A., Krauss, V., Fischer, A., Hoffmann, J., Rea, S., et al. (2002). Central role of Drosophila SU(VAR)3-9 in histone H3-K9 methylation and heterochromatic gene silencing. *The EMBO journal, 21*(5), 1121-1152.

Schotta, G., Lachner, M., Sarma, K., Ebert, A., Sengupta, R., Reuter, G., et al. (2004). A silencing pathway to induce H3-K9 and H4-K20 trimethylation at constitutive heterochromatin. *Genes & development, 18*(11), 1251-1313.

Scott, E., Simon, M., Anastasi, J., & Singh, H. (1994). Requirement of transcription

factor PU.1 in the development of multiple hematopoietic lineages. *Science (New York, N.Y.), 265*(5178), 1573-1580.

Shapiro, L. (1995). Myb and Ets proteins cooperate to transactivate an early myeloid gene. *The Journal of biological chemistry, 270*(15), 8763-8834.

Shepard, J., Amatruda, J., Stern, H., Subramanian, A., Finkelstein, D., Ziai, J., et al. (2005). A zebrafish bmyb mutation causes genome instability and increased cancer susceptibility. *Proceedings of the National Academy of Sciences of the United States of America, 102*(37), 13194-13203.

Shi, Y., Lan, F., Matson, C., Mulligan, P., Whetstine, J., Cole, P., et al. (2004). Histone demethylation mediated by the nuclear amine oxidase homolog LSD1. *Cell, 119*(7), 941-994.

Shilatifard, A. (2006). Chromatin modifications by methylation and ubiquitination: implications in the regulation of gene expression. *Annual review of biochemistry, 75*, 243-312.

Shimoda, N., Yamakoshi, K., Miyake, A., & Takeda, H. (2005). Identification of a gene required for de novo DNA methylation of the zebrafish no tail gene. *Developmental dynamics : an official publication of the American Association of Anatomists, 233*(4), 1509-1525.

Shivdasani, R., Mayer, E., & Orkin, S. (1995). Absence of blood formation in mice lacking the T-cell leukaemia oncoprotein tal-1/SCL. *Nature, 373*(6513), 432-436.

Sofia, H., Chen, G., Hetzler, B., Reyes-Spindola, J., & Miller, N. (2001). Radical SAM, a novel protein superfamily linking unresolved steps in familiar biosynthetic pathways with radical mechanisms: functional characterization using new analysis and information visualization methods. *Nucleic acids research, 29*(5), 1097-1203.

Soza-Ried, C., Hess, I., Netuschil, N., Schorpp, M., & Boehm, T. (2010). Essential role of c-myb in definitive hematopoiesis is evolutionarily conserved. *Proceedings of the National Academy of Sciences of the United States of America, 107*(40), 17304-17312.

Srinivasan, S., Dorighi, K., & Tamkun, J. (2008). Drosophila Kismet regulates histone H3 lysine 27 methylation and early elongation by RNA polymerase II. *PLoS genetics, 4*(10), e1000217.

Stainier, D., Weinstein, B., Detrich, H., Zon, L., & Fishman, M. (1995). Cloche, an early acting zebrafish gene, is required by both the endothelial and hematopoietic lineages. *Development (Cambridge, England), 121*(10), 3141-3191.

Sterner, D., & Berger, S. (2000). Acetylation of histones and transcription-related factors. *Microbiology and molecular biology reviews : MMBR, 64*(2), 435-494.

Stickney, H., Imai, Y., Draper, B., Moens, C., & Talbot, W. (2007). Zebrafish bmp4 functions during late gastrulation to specify ventroposterior cell fates. *Developmental biology, 310*(1), 71-155.

Stopka, T., Amanatullah, D., Papetti, M., & Skoultchi, A. (2005). PU.1 inhibits the erythroid program by binding to GATA-1 on DNA and creating a repressive chromatin structure. *The EMBO journal, 24*(21), 3712-3735.

Stopka, T., & Skoultchi, A. (2003). The ISWI ATPase Snf2h is required for early mouse development. *Proceedings of the National Academy of Sciences of the United States of America, 100*(24), 14097-14199.

Strahl, B., & Allis, C. (2000). The language of covalent histone modifications. *Nature, 403*(6765), 41-46.

Sun, X.-J., Xu, P.-F., Zhou, T., Hu, M., Fu, C.-T., Zhang, Y., et al. (2008). Genome-wide survey and developmental expression mapping of zebrafish SET domain-containing genes. *PloS one, 3*(1), e1499.

Takada, I., Mihara, M., Suzawa, M., Ohtake, F., Kobayashi, S., Igarashi, M., et al. (2007). A histone lysine methyltransferase activated by non-canonical Wnt signalling suppresses PPAR-gamma transactivation. *Nature cell biology, 9*(11), 1273-1358.

Tan, M., Luo, H., Lee, S., Jin, F., Yang, J., Montellier, E., et al. (2011). Identification of 67 histone marks and histone lysine crotonylation as a new type of histone modification. *Cell, 146*(6), 1016-1044.

Thisse, B., Heyer, V., Lux, A., Alunni, V., Degrave, A. s., Seiliez, I., et al. (2004). Spatial and temporal expression of the zebrafish genome by large-scale in situ hybridization screening. *Methods in cell biology, 77*, 505-524.

Thisse, C., & Thisse, B. (2008). High-resolution in situ hybridization to whole-mount zebrafish embryos. *Nature protocols, 3*(1), 59-128.

Thompson, B., Tremblay, V. r., Lin, G., & Bochar, D. (2008). CHD8 is an ATP-dependent chromatin remodeling factor that regulates beta-catenin target genes. *Molecular and cellular biology, 28*(12), 3894-4798.

Thompson, M., Ransom, D., Pratt, S., MacLennan, H., Kieran, M., Detrich, H., et al. (1998). The cloche and spadetail genes differentially affect hematopoiesis and vasculogenesis. *Developmental biology, 197*(2), 248-317.

Traver, D., Paw, B., Poss, K., Penberthy, W., Lin, S., & Zon, L. (2003). Transplantation and in vivo imaging of multilineage engraftment in zebrafish bloodless mutants. *Nature immunology, 4*(12), 1238-1284.

Trompouki, E., Bowman, T., Lawton, L., Fan, Z., Wu, D.-C., DiBiase, A., et al. (2011). Lineage regulators direct BMP and Wnt pathways to cell-specific programs during differentiation and regeneration. *Cell, 147*(3), 577-666.

Trowbridge, J., Snow, J., Kim, J., & Orkin, S. (2009). DNA methyltransferase 1 is essential for and uniquely regulates hematopoietic stem and progenitor cells. *Cell stem cell, 5*(4), 442-451.

Tse, C., Sera, T., Wolffe, A., & Hansen, J. (1998). Disruption of higher-order folding by core histone acetylation dramatically enhances transcription of nucleosomal arrays by RNA polymerase III. *Molecular and cellular biology, 18*(8), 4629-4667.

Tsukada, Y.-i., Fang, J., Erdjument-Bromage, H., Warren, M., Borchers, C., Tempst, P., et al. (2006). Histone demethylation by a family of JmjC domain-

containing proteins. *Nature, 439*(7078), 811-817.

Ueno, H., & Weissman, I. (2006). Clonal analysis of mouse development reveals a polyclonal origin for yolk sac blood islands. *Developmental cell, 11*(4), 519-552.

Usachenko, S., Gavin, I., & Bavykin, S. (1996). Alterations in nucleosome core structure in linker histone-depleted chromatin. *The Journal of biological chemistry, 271*(7), 3831-3837.

Utley, R., Côté, J., Owen-Hughes, T., & Workman, J. (1997). SWI/SNF stimulates the formation of disparate activator-nucleosome complexes but is partially redundant with cooperative binding. *The Journal of biological chemistry, 272*(9), 12642-12651.

Varga-Weisz, P., & Becker, P. (1998). Chromatin-remodeling factors: machines that regulate? *Current opinion in cell biology, 10*(3), 346-399.

Varshavsky, A., Levinger, L., Sundin, O., Barsoum, J., Ozkaynak, E., Swerdlow, P., et al. (1983). Cellular and SV40 chromatin: replication, segregation, ubiquitination, nuclease-hypersensitive sites, HMG-containing nucleosomes, and heterochromatin-specific protein. *Cold Spring Harbor symposia on quantitative biology, 47 Pt 1*, 511-539.

Vastenhouw, N., Zhang, Y., Woods, I., Imam, F., Regev, A., Liu, X., et al. (2010). Chromatin signature of embryonic pluripotency is established during genome activation. *Nature, 464*(7290), 922-928.

Vermeulen, M., Eberl, H., Matarese, F., Marks, H., Denissov, S., Butter, F., et al. (2010). Quantitative interaction proteomics and genome-wide profiling of epigenetic histone marks and their readers. *Cell, 142*(6), 967-1047.

Vettese-Dadey, M., Grant, P., Hebbes, T., Crane- Robinson, C., Allis, C., & Workman, J. (1996). Acetylation of histone H4 plays a primary role in enhancing transcription factor binding to nucleosomal DNA in vitro. *The EMBO journal, 15*(10), 2508-2526.

Vissers, L., van Ravenswaaij, C., Admiraal, R., Hurst, J., de Vries, B., Janssen, I., et

al. (2004). Mutations in a new member of the chromodomain gene family cause CHARGE syndrome. *Nature genetics, 36*(9), 955-962.

Wang, H., Wang, L., Erdjument-Bromage, H., Vidal, M., Tempst, P., Jones, R., et al. (2004). Role of histone H2A ubiquitination in Polycomb silencing. *Nature, 431*(7010), 873-881.

Wang, L., Zhang, P., Wei, Y., Gao, Y., Patient, R., & Liu, F. (2011). A blood flow-dependent klf2a-NO signaling cascade is required for stabilization of hematopoietic stem cell programming in zebrafish embryos. *Blood, 118*(15), 4102-4112.

Warga, R., Kane, D., & Ho, R. (2009). Fate mapping embryonic blood in zebrafish: multi- and unipotential lineages are segregated at gastrulation. *Developmental cell, 16*(5), 744-799.

Willett, C., Kawasaki, H., Amemiya, C., Lin, S., & Steiner, L. (2001). Ikaros expression as a marker for lymphoid progenitors during zebrafish development. *Developmental dynamics : an official publication of the American Association of Anatomists, 222*(4), 694-702.

Wittschieben, B., Otero, G., de Bizemont, T., Fellows, J., Erdjument-Bromage, H., Ohba, R., et al. (1999). A novel histone acetyltransferase is an integral subunit of elongating RNA polymerase II holoenzyme. *Molecular cell, 4*(1), 123-131.

Wolffe, A., & Hayes, J. (1999). Chromatin disruption and modification. *Nucleic acids research, 27*(3), 711-731.

Wong, P., Hattangadi, S., Cheng, A., Frampton, G., Young, R., & Lodish, H. (2011). Gene induction and repression during terminal erythropoiesis are mediated by distinct epigenetic changes. *Blood, 118*(16), e128-38.

Woodage, T., Basrai, M., Baxevanis, A., Hieter, P., & Collins, F. (1997). Characterization of the CHD family of proteins. *Proceedings of the National Academy of Sciences of the United States of America, 94*(21), 11472-11479.

Xu, C., Fan, Z., Müller, P., Fogley, R., Dibiase, A., Trompouki, E., et al. (2012). Nanog-like Regulates Endoderm Formation through the Mxtx2-Nodal Pathway. *Developmental cell, 22*(3), 625-663.

Xue, Y., Wong, J., Moreno, G., Young, M., Côté, J., & Wang, W. (1998). NURD, a novel complex with both ATP-dependent chromatin-remodeling and histone deacetylase activities. *Molecular cell, 2*(6), 851-912.

Yao, T., Oh, S., Fuchs, M., Zhou, N., Ch'ng, L., Newsome, D., et al. (1998). Gene dosage-dependent embryonic development and proliferation defects in mice lacking the transcriptional integrator p300. *Cell, 93*(3), 361-433.

Yoder, M., Hiatt, K., Dutt, P., Mukherjee, P., Bodine, D., & Orlic, D. (1997). Characterization of definitive lymphohematopoietic stem cells in the day 9 murine yolk sac. *Immunity, 7*(3), 335-379.

Yokomizo, T., Ogawa, M., Osato, M., Kanno, T., Yoshida, H., Fujimoto, T., et al. (2001). Requirement of Runx1/AML1/PEBP2alphaB for the generation of haematopoietic cells from endothelial cells. *Genes to cells : devoted to molecular & cellular mechanisms, 6*(1), 13-36.

Yokota, T., Huang, J., Tavian, M., Nagai, Y., Hirose, J., Zúñiga-Plücker, J.-C., et al. (2006). Tracing the first waves of lymphopoiesis in mice. *Development (Cambridge, England), 133*(10), 2041-2092.

Yoshida, T., Ng, S., Zuniga-Pflucker, J., & Georgopoulos, K. (2006). Early hematopoietic lineage restrictions directed by Ikaros. *Nature immunology, 7*(4), 382-473.

Young, J., Wu, S., Hansteen, G., Du, C., Sambucetti, L., Remiszewski, S., et al. (2004). Inhibitors of histone deacetylases promote hematopoietic stem cell self-renewal. *Cytotherapy, 6*(4), 328-364.

Yu, M., Mazor, T., Huang, H., Huang, H.-T., Kathrein, K., Woo, A., et al. (2012). Direct recruitment of polycomb repressive complex 1 to chromatin by core binding transcription factors. *Molecular cell, 45*(3), 330-373.

Yuasa, H., Oike, Y., Iwama, A., Nishikata, I., Sugiyama, D., Perkins, A., et al. (2005).

Oncogenic transcription factor Evi1 regulates hematopoietic stem cell proliferation through GATA-2 expression. *The EMBO journal, 24*(11), 1976-2063.

Zeigler, B., Sugiyama, D., Chen, M., Guo, Y., Downs, K., & Speck, N. (2006). The allantois and chorion, when isolated before circulation or chorio-allantoic fusion, have hematopoietic potential. *Development (Cambridge, England), 133*(21), 4183-4275.

Zentner, G., Hurd, E., Schnetz, M., Handoko, L., Wang, C., Wang, Z., et al. (2010). CHD7 functions in the nucleolus as a positive regulator of ribosomal RNA biogenesis. *Human molecular genetics, 19*(18), 3491-3992.

Zentner, G., Layman, W., Martin, D., & Scacheri, P. (2010). Molecular and phenotypic aspects of CHD7 mutation in CHARGE syndrome. *American journal of medical genetics. Part A, 152A*(3), 674-760.

Zhang, X., & Rodaway, A. (2007). SCL-GFP transgenic zebrafish: in vivo imaging of blood and endothelial development and identification of the initial site of definitive hematopoiesis. *Developmental biology, 307*(2), 179-273.

Zhang, Y., LeRoy, G., Seelig, H., Lane, W., & Reinberg, D. (1998). The dermatomyositis-specific autoantigen Mi2 is a component of a complex containing histone deacetylase and nucleosome remodeling activities. *Cell, 95*(2), 279-368.

Zovein, A., Hofmann, J., Lynch, M., French, W., Turlo, K., Yang, Y., et al. (2008). Fate tracing reveals the endothelial origin of hematopoietic stem cells. *Cell stem cell, 3*(6), 625-661.